ZINC IS AN INTRACELLULAR SECONDARY MESSENGER IN PLATELETS

Thesis submitted for the degree of

Doctor of Philosophy

at Anglia Ruskin University

by

Niaz Shahed Ahmed

Department of Biomedical and Forensic Sciences

Anglia Ruskin University

Submitted: January 2019

Acknowledgements

I would firstly like to thank my first supervisor Dr Nicholas Pugh for providing me with the opportunity to carry out this project and for all his help and support throughout the entirety of my PhD as I could not have asked for a better supervisor. I will also like to thank Dr Kirk Taylor and Dr Maria Lopes-Pires for all their help and providing me with invaluable advice to succeed in research. I will also like to thank my second and third supervisor's Dr Linda King and Dr Havovi Chichger for all their help and support and guiding me through my time as a PhD student. Finally, I would like to thank my family and in particular my parents Iqbal and Dilara Ahmed for all their love and support which has pushed me on and driven me to complete this project to the best of my ability.

Abstract

ANGLIA RUSKIN UNIVERSITY

ABSTRACT

FACULTY OF SCIENCE AND TECHNOLOGY

DOCTOR OF PHILOSOPHY

ZINC IS AN INTRACELLULAR SECONDARY MESSENGER IN PLATELETS

NIAZ SHAHED AHMED

JANUARY 2019

Zinc (Zn^{2+}) is an essential trace element which regulates intracellular processes in multiple cell types. Whilst Zn^{2+} has been shown to be released from intracellular compartments of a variety of cell types in response to external stimuli, its role in platelets has yet to be confirmed. This work aimed to determine whether agonist-evoked activation of platelets induced changes in cytosolic zinc concentrations ($[Zn^{2+}]_i$) contributing to modulation of activatory processes in platelets, in a manner consistent with a secondary messenger.

Fluorometry was used to assess intracellular Zn^{2+} $[Zn^{2+}]_i$ changes via zinc-specific fluorophores. Fluctuations in $[Zn^{2+}]_i$ were modulated using Zn^{2+}-specific chelators and ionophores. Light transmission aggregometry, flow cytometry and western blotting were employed to assess the influence of $[Zn^{2+}]_i$ on platelet function.

Stimulation by CRP-XL or U46619 evoked increases in intraplatelet Fluozin-3 (FZ-3) fluorescence consistent with $[Zn^{2+}]_i$ elevation. Increases in FZ-3 fluorescence were abrogated by Zn^{2+} chelators and were distinct from agonist-evoked $[Ca^{2+}]_i$ signals. Fluctuations of $[Zn^{2+}]_i$ induced by CRP-XL or U46619 were sensitive to changes in platelet redox states. Sustained increases of $[Zn^{2+}]_i$ were induced by the Zn^{2+} ionophores, Clioquinol or Pyrithione, which resulted in significant platelet shape change, integrin $\alpha_{IIb}\beta_3$ upregulation, dense granule but not α granule secretion and phosphatidylserine exposure. Chelation of $[Zn^{2+}]_i$ also resulted in the inhibition of agonist-induced platelet activity. Furthermore, elevation of $[Zn^{2+}]_i$ was also found to occur in a similar manner to $[Ca^{2+}]_i$ elevation from stores within platelets in addition to redox state modulation.

In conclusion, this is the first description of agonist-dependent increases in platelet $[Zn^{2+}]_i$, indicative of a role as a secondary messenger. The Zn^{2+} release is sensitive to mediators of the platelet redox state, and so may be attributable to release from oxidised thiol groups on Zn^{2+} -binding proteins. Modulation of $[Zn^{2+}]_i$ indicated a role for Zn^{2+} in platelet activatory processes. The rise in $[Zn^{2+}]_i$ in response to CRP-XL and U46619 demonstrates the physiological importance of Zn^{2+}, implying the importance to Zn^{2+} in platelet activation during thrombus formation.

Keywords: Platelets, zinc, intracellular, redox-sensitive, ionophores, platelet activation

Publications:

Articles

Ahmed NS, Lopes Pires ME, Taylor KA, Pugh N. 2019.

Agonist-Evoked Increases in Intra-Platelet Zinc Couple to Functional Responses.

Thrombosis and Haemostasis,119(1):128-139

Iegre J, **Ahmed NS**, Gaynord JS, Wu Y, Herlihy KM, Tan YS, Lopes-Pires ME, Jha R, Lau YH, Sore HF, Verma C, O' Donovan DH, Pugh N, Spring DR. 2018

Stapled peptides as a new technology to investigate protein-protein interactions in human platelets.

Chemical Science,9(20):4638-4643

Oral Communications

Ahmed NS. Pugh N. Functional role of intracellular Zn^{2+} in platelets. 10th Annual student research conference, Anglia Ruskin University, Cambridge, UK, July 2016.

Ahmed NS. Pugh N. The role of Zn^{2+} in platelets. Research Seminar, Anglia Ruskin University, Cambridge, UK, May 2017

Poster Communications

Ahmed NS, Taylor KA, Pugh N. Modelling intracellular Zn^{2+} in platelets. 3rd European platelet network (EUPLAN) conference. Bad Homburg vor der Höhe, Germany, September 2016

Ahmed NS, Pugh N. Zn^{2+} is an intracellular secondary messenger in platelets. Cambridge cardiovascular 5th annual research symposium. Cambridge, April 2018

Ahmed NS. Pugh N. Zn^{2+} regulates platelet shape change. 11th Annual student research conference, Anglia Ruskin University, Cambridge, UK, July 2017

Ahmed NS. Pugh N. Redox dependent intracellular Zn^{2+} elevation in platelets. 12th Annual student research conference, Anglia Ruskin University, Cambridge, UK, July 2018.

Declaration

I declare that this work has not previously been submitted for the acceptance of any other degree or diploma.

Commonly used abbreviations

ADP Adenosine diphosphate

BAPTA 1,2-Bis(2-aminophenoxy)ethane-N,N,N',N'-tetraacetic acid tetrakis

Ca^{2+} Calcium

$[Ca^{2+}]_i$ Intracellular Calcium

CAT Catalase

Cq Clioquinol

CRP Collagen related peptide

CRP-XL Crosslinked Collagen related peptide

Cyt D Cytochalasin D

DMSO Dimethyl sulphoxide

DTS Dense tubular system

EGTA Ethylene glycol-bis (β-aminoethylether)-N,N,N',N'-tetraacetic acid

FZ-3 Fluozin-3

GPCR G protein-coupled receptor

GR GR144053

IP3R Inositol trisphosphate receptor

NO Nitric oxide

NOX Nicotinamide adenine dinucleotide phosphate oxidase

MEF Mouse embryonic fibroblasts

MLC Myosin light chain

MLCK Myosin light chain kinase

MLC-P Myosin light change phosphatase

PAR Protease-activated receptor

PEG-CAT Polyethylene glycol-Catalyse

PEG-SOD Polyethylene glycol-Superoxide dismutase

PGI_2 Prostacyclin

PKC Protein kinase C

PLC Phospholipase C

PRP Platelet Rich Plasma

PS Phosphatidylserine

Py Pyrithione

ROCK Rho-associated coiled-coil-containing protein kinase

SOCE Store-operated Ca^{2+} entry

SOD Superoxide dismutase

SOZE Store-operated Zn^{2+} entry

TG Thapsigargin

TPEN N,N,N′,N′-Tetrakis(2-pyridylmethyl)ethylenediamine

TxA_2 Thromboxane A_2

VWF Von Willebrand factor

ZIP7 Zrt-Irt(Zinc transporter)-like protein 7

Zn^{2+} Zinc

$[Zn^{2+}]_i$ Intracellular Zinc

Table of Contents

Figures

Chapter 1

Chapter 2

Chapter 3

Chapter 4

Chapter 5

Chapter 6

Chapter 7

Tables

Chapter 1

1.0 Introduction

Cardiovascular diseases (CVD) including coronary heart disease, stroke and myocardial infarction, are the leading causes of mortality in the UK (GBD 2013 Mortality and Causes of Death Collaborators, 2015). However, as a result of extensive cardiovascular research and public awareness, the mortality rates due to CVD have declined over the past 30 years (Bhatnagar et al., 2016; Smolina et al., 2012). For example, mortality rates as a result of myocardial infarctions have dropped by approximately 4.8% in men and 9.1% in women on average annually since 2002 (Smolina et al., 2012). CVD is attributable to inappropriate haemostasis, which is the physiological process whereby elements of the circulatory system interact with damaged endothelium to form a stable thrombus to stop bleeding and maintain the integrity of the circulatory system (Berndt et al., 2014; Clemetson, 2012; Reininger, 2008a, Faure et al., 1995, Asselin et al., 1997). Inappropriate activation of the haemostatic response can occur leading to cardiovascular diseases such as myocardial infarctions and stroke (Kowalska et al., 1994).

1.1 Haemostasis and Thrombosis

Vascular injury exposes sub-endothelial matrix proteins including collagen, and von Willebrand factor (VWF) within the vessel to the circulation (Ferhat-Hamida et al., 2015). These proteins initiate a series of reactions known as the 'haemostatic response' that culminates in clot formation and the cessation of bleeding, resulting in the formation of a thrombosis (Gogia and Neelamegham, 2015).

Haemostasis is dependent on the vessel wall, protein components in the blood (coagulation factors) and blood cells known as platelets (Li et al., 2010). Platelets adhere to sites of vascular injury, which become exposed as a result of damage to the endothelium. Platelets interact with these regions via membrane receptors and undergo a process of activation which results in many cellular responses (Mammadova-Bach et al., 2015). These include upregulation of the fibrinogen-binding receptor, integrin $\alpha_{IIb}\beta_3$, which upregulates platelet-platelet interactions leading to thrombus formation (Chari-Turaga and Naik, 2011). Activation also results in the release of α-and dense-granules (Cai et al., 2016, Asselin et al., 1997) which contain adhesive proteins, coagulation factors and soluble platelet agonists. These include ADP andATP which mediate further platelet activation as well as recruiting circulatory

platelets and enhancing stable adhesion of the subendothelium (Kuwahara et al., 2002; Rahman et al., 2016; Watson et al., 2016).

The haemostatic process is subdivided into several stages. Following vascular injury, myogenic reflexes induce vasoconstriction which results in the narrowing of the lumen of the blood vessel. This vasoconstriction is an immediate effect to minimise blood flow to the area of injury, thus reducing blood loss (Clemetson, 2012). Following vasoconstriction, platelets are recruited and undergo activation, which leads to platelet aggregation and formation of a platelet plug to stop blood loss (Berndt et al., 2014; Clemetson, 2012). Subsequently, the coagulation phase is initiated, which reinforces the stable platelet plug allowing a stable long lasting clot to form (Abdollahi et al., 2013). Once the clot has formed, and the healing process is complete, fibrinolysis occurs which dissolves the clot via enzymatic reactions (Palta et al., 2014).

1.2 Platelet physiology

Platelets are small (typically 2-3µm in diameter) discoid anuclear blood cells that are central to haemostasis and thrombus formation. Platelets circulate in a resting state and become activated following vascular injury to form a platelet plug to prevent excessive bleeding. Platelet activation in the context of a ruptured atherosclerotic plaque or narrowed arteries may result in an occlusive thrombus causing a myocardial infarction or ischaemic stroke. Platelets are generated from megakaryocytes (MKs) in the bone marrow (Machlus and Italiano, 2013). As megakaryocytes mature they migrate from the osteoblastic to the vascular niche in the bone marrow. MKs align with the venous sinusoid, where they project pro-platelet extensions into the circulation where platelets are released (Harker and Finch, 1969; Italiano et al., 1999; Jackson and Edwards, 1977; Nakeff and Maat, 1974; Pease, 1956; Richardson et al., 2005). The lifespan of human platelets once released into the bloodstream generally ranges from 7-10 days (Aster, 1967). The normal circulating level of platelets ranges from $150x10^9$/L to $400x10^9$/L (Daly, 2011).

Platelets undergo activation in response to several agonists such as collagen, thrombin, thromboxane A_2 and ADP. These agonists induce downstream intracellular signalling via stimulation of specific platelet receptors. Figure 1.1 below illustrates a general overview of platelet activation via the major platelet agonists. A hallmark of platelet activation is phospholipase C-mediated elevation of intracellular Ca^{2+} ($[Ca^{2+}]_i$) via mobilisation from intracellular stores.

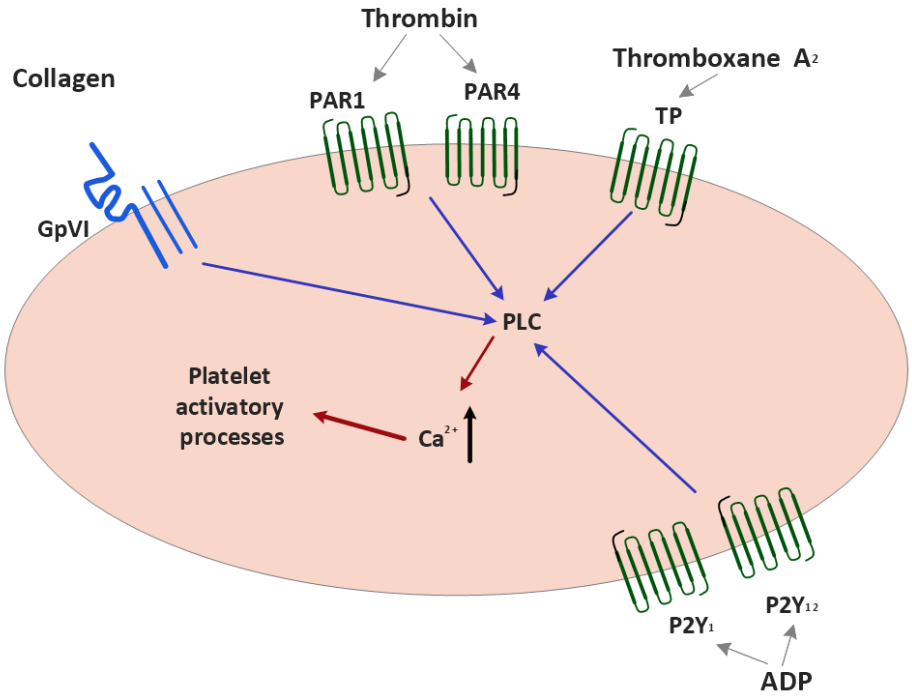

Figure 1.1. Schematic illustrating general overview of agonist evoked platelet activation. Major platelet agonists including collagen, thrombin, thromboxane A2 and adenosine diphosphate (ADP) induce activation via stimulation of their cognate receptors. The primary platelet collagen receptor is glycoprotein VI (GpVI), whereas thrombin, thromboxane A2 and ADP stimulate G protein-coupled receptors (GPCRs). Thrombin stimulates protease-activated receptor (PAR) 1 and 4; thromboxane A2 stimulates the thromboxane receptor (TP); ADP stimulates the Purinergic (P2Y) receptors P2Y1 and P2Y12. Activation by these agonists results in the mobilisation of Ca^{2+} from its store via the activation of phospholipase C. Elevation of $[Ca^{2+}]i$ is well documented as a hallmark of platelet activation. Many activatory processes are thought to be regulated by $[Ca^{2+}]I$ elevated in response to agonists.

1.2.1 Initiation of platelet activation

Platelet activation is a progressive process which is initiated by interactions with VWF, followed by collagen-induced activation via the GpVI receptor as illustrated by Figure 1.2 below. Platelet activation can also be evoked upon stimulation of G protein-coupled receptors (GPCRs) found on platelets such as protease-activated receptors (PAR) 1 and 4, thromboxane receptor (TP) and the Purinergic (P2Y) receptors $P2Y_1$ and $P2Y_{12}$.

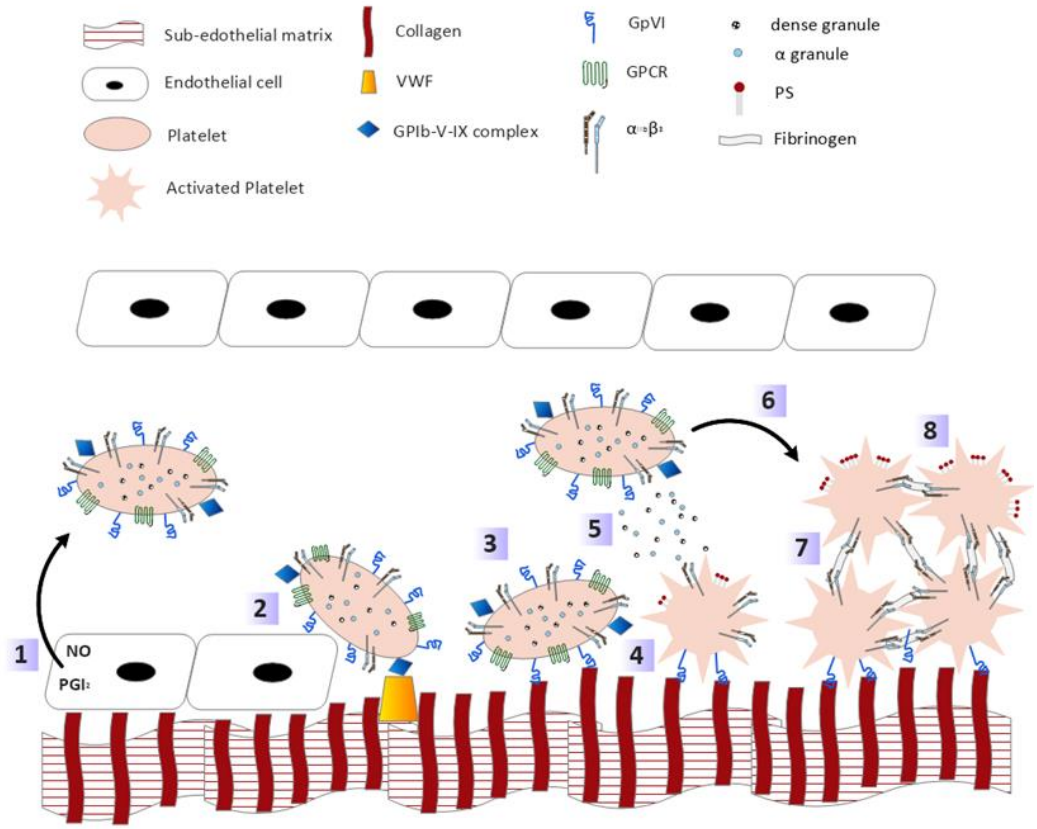

Figure 1.2. Representation of platelet activation during haemostasis. 1) Circulating platelets are maintained in their resting state by the actions of nitric oxide (NO) and Prostacyclin (PGI_2) which are released from the endothelial cells. 2) Vascular injury to blood vessel results in the exposure of the subendothelial matrix, where Von Willebrand factor (VWF) and collagen are present. Circulating platelets interact with the VWF via the membrane receptor complex, glycoprotein Ib/V/IX (GPIb-V-IX). 3) Platelets become tethered to VWF, resulting in platelets transiently interacting (rolling) along the sub-endothelium. GpVI receptors on the platelet surface bind to the exposed collagen initiate intracellular signalling pathways leading to platelet activation. 4) Activated platelets undergo a shape change and granule release and begin externalising phosphatidyl-serine (PS) on their surfaces. 5) The contents of the alpha and dense granules activate surrounding platelets. 6) Activated platelets are recruited to enable platelet aggregation. 7) Integrin $\alpha_{IIb}\beta_3$ becomes activated as a result of inside-out signalling, enabling fibrinogen to crosslink the activated platelets, culminating in platelet aggregation. 8) Coagulation then occurs, as thrombin formation is promoted from the coagulation factors which assemble on PS-rich platelet surface. Thrombin then cleaves fibrinogen to form fibrin which associates to form fibrin meshwork. This results in the generation of a stable thrombus.

1.2.2 Primary platelet adhesion to collagen

Vascular injury results in damage to endothelial cells, which results in exposure of the subendothelial extracellular matrix (Stalker et al., 2012). Platelets subsequently recognise and bind to exposed sub-endothelial matrix proteins. VWF is an adhesive glycoprotein which is released from activated endothelial cells or is exposed upon injury to become immobilised on fibrillar collagen within

the matrix via its A3 domain (Reininger, 2008). Shear stress which regulates VWF activity is the result of tangential forces in the direction of the blood flow, which occurs due to the occurrence of a pressure gradient that occurs when blood flows through vessels (Gogia and Neelamegham, 2015). Shear stress induces structural changes of the VWF domains, enabling activation of these domains (O'Brien and Salmon, 1987). The binding of VWF to platelet receptors and proteins and endothelial cells is also regulated by shear stress (Dayananda et al., 2010; Gogia and Neelamegham, 2015; Kroll et al., 1996).

VWF regulates the initial adherence of platelets to the damaged vessel in the initial stages of platelet plug formation. VWF crosslinks collagen to platelets via the platelet glycoprotein Ib/V/IX (GPIb/V/IX) (Peyvandi et al., 2011) which, unlike other platelet receptors, does not require pre-activation for binding. Binding of GPIbα to VWF is transient. However, this transient interaction enables lower affinity platelet receptors to engage their cognate ligands, resulting in a stronger adhesion reaction, and the initiation of intracellular signalling (Hoylaerts, 1997; Wu et al., 2000).

The adhesion of platelets to collagen is a critical step for inducing the formation of a thrombus. There are different types of collagen on the vessel wall. Types I, III and V are crucial in regulating platelet adhesion to the damaged vessel wall and have high affinity to VWF (Marjoram et al., 2014). Collagen type IV is a sheet-forming collagen and has also been found to regulate adhesion of platelets to the damaged vessel wall (Henrita van Zanten et al., 1996). The A3 domain is the major binding domain of VWF which binds to collagen. However, Collagen type IV has also been found to bind the A1 domain of VWF under high shear stress, indicating the importance of the other domains of VWF for collagen binding (Flood et al., 2015; Ferhat-Hamida et al., 2015; Brondijk et al., 2012). The activity of collagen type IV is modulated by cations such as Mg^{2+} in platelets (Henrita van Zanten et al., 1996). Although the exact mechanism by which cations influence collagen type IV is yet to be confirmed, this provides scope for investigating possible roles of Zn^{2+} in this process. Collagen binds to collagen receptors on the platelet surface, of which two have been characterised: GpVI and integrin $\alpha_2\beta_1$. Engagement through these receptors ensures platelet activation and subsequent stable adhesion (Gardiner and Andrews, 2014). The interaction between $\alpha_2\beta_1$ and GpVI and their cognate ligands are synergistic and dependent on the presence of high-affinity binding motifs in the exposed collagen molecule (Pugh et al., 2010). Engagement of GpVI results in the initiation of downstream signals that result in a number of cellular effects that constitute platelet activation (Carrim et al., 2014).

1.2.3 Platelet activation via Glycoprotein VI signalling

A member of the immunoglobulin superfamily member, Glycoprotein VI (GpVI) consists of a C terminus, a single transmembrane domain and two immunoglobulin domains located on its extracellular face (Asselin et al., 1997; Diaz-Ricart et al., 2008). GpVI couples to the Fc receptor γ chain (FcγR) via a salt bridge. The FcγR is a receptor for the fragment crystallizable region of immunoglobulins (Arman and Krauel, 2015; Hayes et al., 2016; Poole et al., 1997). FcγR contains an immunoreceptor tyrosine-based activation motif (ITAM) in the cytoplasmic domain (Gibbins et al., 1996; Poole et al., 1997; Watson et al., 2005). Collagen motifs consisting of glycine-proline-hydroxyproline repeats bind to the immunoglobulin domains of GpVI, resulting in receptor dimerisation (evoking clustering of the receptor) and the initiation of a downstream signalling cascade (Figure 1.3, Bella and Hulmes, 2017; Gibbins et al., 1996, 1997; Nieswandt and Watson, 2003). Following adhesion, members of the Src family kinases (SFK, predominantly Fyn and Lyn, which are bound to the proline-rich region of the GpVI cytoplasmic tail) are able to interact with Src homology 3 (SH3) domains and come into proximity with the ITAM motif where phosphorylation of tyrosine residues of this motif takes place (Gambaryan et al., 2010; Li et al., 2010). ITAM phosphorylation results in the binding and activation of the tyrosine kinase, Syk. Syk activation occurs via autophosphorylation following interaction with SH2 domains which enables Syk to be recruited to the ITAM motif. The transmembrane adapter linker for activated T-cells (LAT) then associates with the developing signalling complex (a signalosome), resulting in the recruitment and activation of other signalling proteins, most significantly PLCγ2 which result in the mobilisation of Ca^{2+} from its store in platelets which as stated earlier is e hallmark of platelet activation (Asselin et al., 1997; Li et al., 2010; Smith et al., 1992). The cytosolic adaptor proteins Mona/Grap2,GrpL/Grf40 (GADs) and SH2 domain containing leukocyte protein of 76kDa (SLP76) have also been found be within the core (alongside LAT) of the signalosome induced following Syk activation which mediate activation of PLCγ2 (Judd et al., 2002; Pasquet et al., 1999).

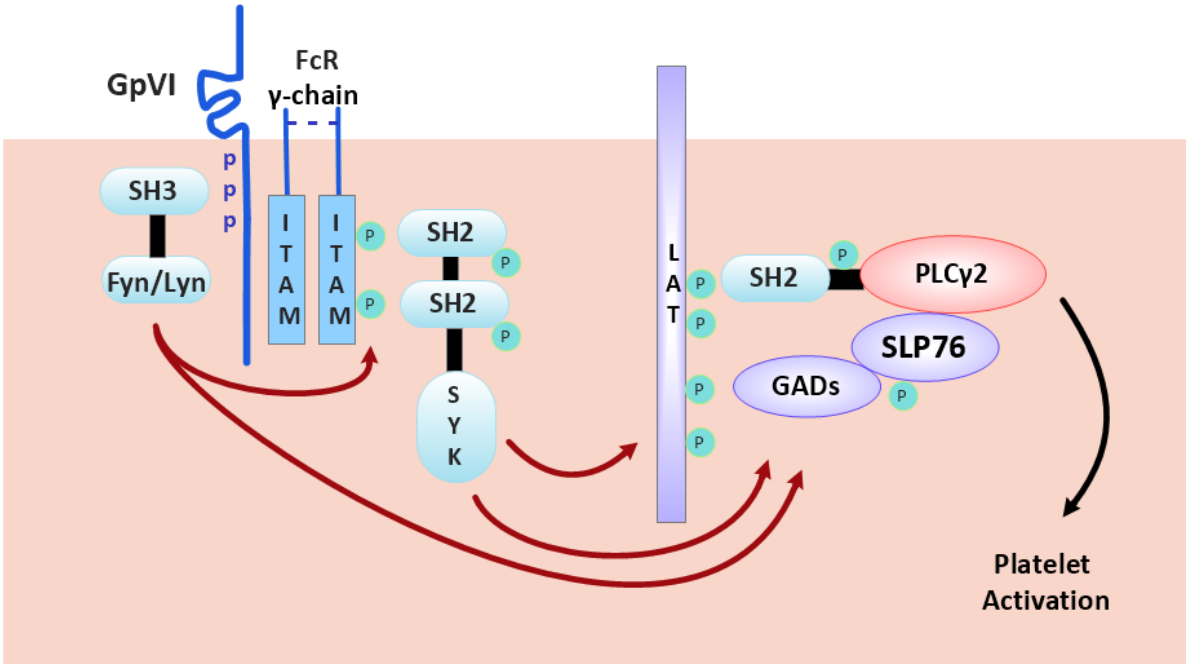

Figure 1.3. Glycoprotein VI (GpVI) signalling. Engagement of GpVI evokes tyrosine phosphorylation of ITAM motifs of FcγR. The Src family kinases, Fyn and Lyn which are bound to the proline-rich tail of GpVI and recruited to the ITAM via interaction by SH3 domains, induce the phosphorylation of the ITAM. This is followed by phosphorylation of Syk, which is recruited to the ITAM via interactions with SH2 domains. Syk-induced signalling is initiated, resulting in the formation of a signalosome which consists of adaptor and effector proteins. Within this signalosome, the transmembrane adapter linker for activated T-cells (LAT) and cytosolic adapter proteins Mona/Grap2, GrpL/Grf40 (GADs) and SH2 domain containing leukocyte protein of 76kDa (SLP76) induce the activation of PLCγ2, which enables Ca^{2+} mobilisations from its store and thereby inducing platelet activation.

Due to its importance in platelet activation, GpVI has been identified as an antithrombotic target. Fibrillar collagen strands commonly consist of proline and hydroxyproline repeats, with glycine at every third residue to enable folding and a triple helix conformation of the strand (Prockop and Kivirikko, 1995). Potent agonists identified as crosslinked collagen-related peptide (CRP-XL) that adopt the collagen conformation have been synthesised to activate the GpVI receptors (Smethurst et al., 2007). Collagen-related peptides (CRP) mimic the triple helix structure of collagen strands. The crosslinking of CRP (CRP-XL) enables conformational changes by bestowing a quaternary structure on this peptide, which enables this peptide to be a potent GpVI activation agonist (Achison et al., 1996; Asselin et al., 1997, 1997). Collagen exists in a tertiary confirmation (triple helical) and can spontaneously assemble into the highly organised quaternary (polymeric) conformation (Bella and Hulmes, 2017; Smethurst et al., 2007). Quaternary conformations are potent in inducing platelet activation and are essential for collagen-induced platelet activation (Kehrel et al., 1998).

1.2.4 Platelet activation via G protein-coupled receptors

In addition to collagen-mediated signalling, platelets also become activated via the action of soluble mediators, some of which are generated during the haemostatic response and others released from activated platelets (Stalker et al., 2012). Signalling via soluble activators predominantly occurs via GPCRs, of which several subtypes are present on platelets. Following receptor engagement, conformational changes in GCPRs result in the exposure of an intracellular domain, which is then able to couple to cytosolic heterotrimeric G proteins which transmit signals following agonist stimulation (Gavi et al., 2006). G proteins act as molecular switches, and can be in their inactive states when they are bound to GDP (Guanosine diphosphate) and in their active state when they are bound to GTP (Guanosine triphosphate, Figure 1.4 (Rosenbaum et al., 2009).

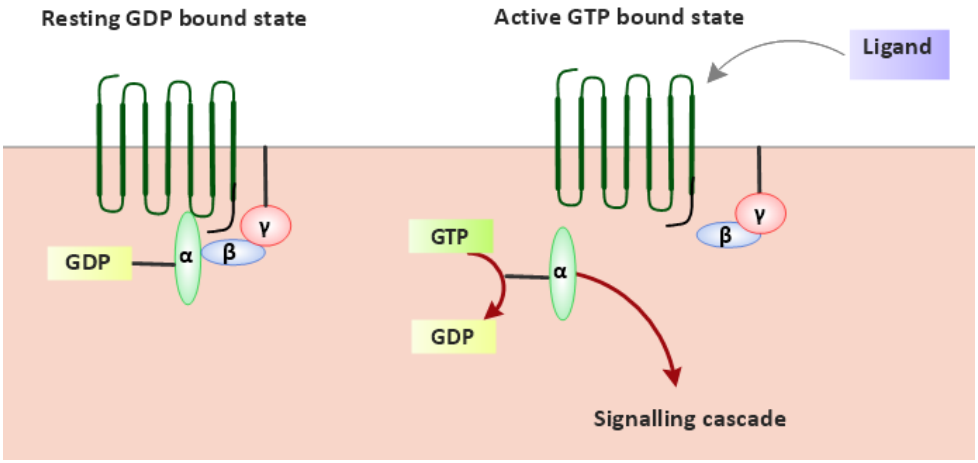

Figure 1.4. Schematic illustrating G protein-coupled receptor activation. Heterotrimeric G proteins consist of α,β and γ subunits. The β and γ can form a stable dimeric complex ($G_{\beta\gamma}$). Conformational changes that occur to the GPCR following ligand engagement result in binding of the G protein, and exchange of GDP to GTP within the nucleotide binding pocket. Following activation, the α subunit (G_{α}) of heterotrimeric G proteins dissociates from the βγ dimeric complex and can activate downstream signalling cascades. The Gα subunit can eventually re-associate with the $G_{\beta\gamma}$ dimeric complex following hydrolysis of GTP to GDP, thus reforming the heterotrimeric G -protein, resetting the signalling cascade cycle)

A number of G_{α} isoforms are expressed in platelets where they exert differing signalling cascades (Brass et al., 1993b). The activation of platelets via GPCR involves $G_{\alpha}12/13$, $G_{\alpha}i$ or $G_{\alpha}q$ which are coupled to agonist-dependent receptors (Capote et al., 2015; Offermanns, 2006). Receptor engagement couples to differential signalling via different G proteins. $G_{\alpha}12/13$-mediated signalling

induces activation of the small monomeric G-protein, RhoA, which in turn activates Rho Kinases. Rho Kinases primarily induce platelet shape change during activation (Kureishi et al., 1997). $G_{\alpha}i$-induced signalling inhibits the activity of adenylyl cyclase, which in turn inhibits cAMP signalling (cAMP signalling induces activation of PKA which inhibits platelet aggregation and granule release) (Beck et al., 2014; Pulcinelli et al., 1998). $G_{\alpha}q$ primarily induces PLCβ-induced Ca^{2+} mobilisation. The major GPCRs found in platelets include the thrombin-activated protease actives receptors (PARs), the TxA_2-activated TP receptors and the ADP-activated P2Y receptors(Brass et al., 1993a).

Platelet activation via PAR receptors

Thrombin is one of the most potent agonists of platelet activation. Thrombin induces activatory processes such as $[Ca^{2+}]_i$ elevation, shape change, degranulation and phosphatidylserine (PS) exposure (Lever et al., 2015). Protease-activated receptors (PARs) are activated by thrombin, which is generated via the coagulation pathway. PARs operate in a dual system, with PAR1 and PAR4 expressed in human platelets, and PAR3 and PAR4 in mouse platelets (Jakobsche-Policht et al., 2014). PAR1 has a higher sensitivity to thrombin than PAR4, although PAR4 stimulation results in a more prolonged response compared to that of PAR1 (Reséndiz et al., 2007). Thrombin is a serine protease and can recognise and cleave the extracellular N-terminus of PAR. This results in the exposure of a new N-terminus which serves as a 'tethered ligand'. This newly unveiled N-terminus acts as a receptor agonist to induce transmembrane signalling and platelet activation (Jakobsche-Policht et al., 2014; Li et al., 2010; Monroe et al., 2002), The PAR receptors in platelets are coupled to $G_{\alpha}q$ and $G_{\alpha}12/13$ which induce PLCβ induced Ca^{2+} mobilisation and platelet shape change (Offermanns, 2006).

PARs in platelets serve as an antithrombotic target, due to the potency of thrombin on platelet activation (Gryka et al., 2017). The drugs, Vorapaxar and Atopaxar, are PAR-1 antagonists that have undergone extensive clinical testing (Lam and Tran, 2015; Wurster and May, 2012). Vorapaxar has undergone phase 3 of clinical trials whereas Atopaxar has undergone phase 2 (Makris et al., 2013; Oestreich et al., 2013). The significant issues with the use of these drugs are the high bleeding risks they impose. This warrants the development of safer antithrombotics which are can target PARs (O'Donoghue et al., 2011).

Platelet activation via TP receptors

The thromboxane A2-activated TP receptor (TxA2) is an important platelet GPCR (Offermanns, 2006). Upon agonist-induced stimulation, phospholipase A_2 (PLA_2) is activated, which enables the

activation of arachidonic acids which are liberated from membrane phospholipids. TxA_2 is formed from arachidonic acids via enzymatic activation of cyclooxygenase-1 (COX-1) and thromboxane synthase (Smith et al., 1980). COX-1 regulates the formation of prostaglandin G_2 (PGG_2) from arachidonic acid, which is then converted to prostaglandin H_2 (PGH_2) (Moncada and Vane, 1980). PGH_2 is a substrate for many types of prostacyclins including $PG1_2$, a potent platelet antagonist via the activation of PKA. Thromboxane synthase, a microsomal enzyme which is present in platelets, catalyses the conversion of PGH_2 to TxA_2 (Ornelas et al., 2017; Schrör, 1997).

TxA_2 synthesis is inhibited by aspirin (Gryglewski et al., 1978)., which is a widely used analgesic and has been used as an antithrombotic and principal antiplatelet agent (Smith and Willis, 1971). Aspirin inhibits TxA_2 synthesis by inducing acetylation of the functionally important $serine_{529}$ in COX-1 (Gryglewski, 1980). Acetylation inhibits arachidonic acids from interacting with the catalytic site of COX-1, resulting in the irreversible inhibition of TxA_2 synthesis. Inhibition of COX-1 by aspirin inhibits production of prostacyclins such as $PG1_2$.

Upon synthesis, TxA_2 diffuses out of the platelet. TxA_2 is unstable with a short half-life of approximately 30 seconds (Higuchi et al., 1999). However, during this time period, TxA2 can bind to and activate TP receptors, which couple to $G_\alpha q$ and $G_\alpha 12/13$, initiating the signalling cascade induced by these G-proteins (Fontana et al., 2014). The unstable nature of TxA_2 makes it difficult to investigate its signalling mechanism. Therefore the stable TxA_2 analogue, U46619, is commonly employed to assess TxA_2 activity in platelets (Rotondo et al., 1995). U46619 can bind to the TP receptor on platelets and induces many platelet activatory processes such as $[Ca^{2+}]_i$ elevation, shape change and degranulation and aggregation (Kim et al., 2009). These activatory processes are mediated by downstream signalling of $G_\alpha q$ and $G_\alpha 12/13$.

Platelet activation via P2Y receptors

Other GPCRs present on the platelet surface that are important in platelet function include the ADP-activated receptors, $P2Y_1$ and $P2Y_{12}$ (Brass et al., 1993a). ADP (adenosine diphosphate) is released from dense granules upon platelet activation. The activation of both $P2Y_1$ and $P2Y_{12}$ are required to enable a full ADP-dependent response (Vaduganathan and Bhatt, 2016). ADP is utilised in platelets to activate other pathways and to amplify platelet activation. (Oestreich et al., 2013; Woulfe et al., 2001).

$P2Y_1$ receptors couple to $G_\alpha q$, whereas $P2Y_{12}$ couple to $G_\alpha i$ (Offermanns, 2006). Inhibition of $P2Y_1$ impairs $[Ca^{2+}]_i$ elevation, shape change and aggregation (Hechler et al., 1998). Platelets from mouse $P2Y_1$ knockout models are still sensitive to ADP-induced aggregation (Savi et al., 1998). $P2Y_1$ couples to $G_\alpha q$ to mediate PLC activation but does not couple to $G_\alpha i$ (Offermanns, 2006). The knockout of $P2Y_{12}$ results in impaired ADP induced aggregation; however, responses such as shape change and PLC activation which are responses mediated by the $P2Y_1$ receptor remained unaffected (Andre et al., 2003; Vaduganathan and Bhatt, 2016). The impaired ADP-induced aggregation coincides with the redundancy of cAMP signalling inhibition (Gachet, 2012), indicating that $P2Y_{12}$ couples to $G_\alpha i$ and not $G_\alpha q$. Thus these studies demonstrate that both $P2Y_1$ and $P2Y_{12}$ activation enable optimal ADP-induced platelet activation (Vaduganathan and Bhatt, 2016).

The importance of the P2Y receptors in platelet activation makes them an attractive antithrombotic target. Current antithrombotics that target P2Y receptors include clopidogrel which is a $P2Y_{12}$ antagonist (Oestreich et al., 2013). Clopidogrel is relatively safe to use, although has associated increased bleeding as is the case with many antithrombotics. The restoration of platelet activity after discontinuation of clopidogrel usage has raised concerns due to the irreversible effect of clopidogrel on $P2Y_{12}$. However, this effect has not been observed in humans, as full platelet restoration occurs approximately seven days after discontinuation of the treatment (Weber et al., 2001). Further clinical work is to be carried out to develop further P2Y antagonists which could also target the $P2Y_1$ receptor.

1.2.5 Platelet activation leads to Integrin activation

The primary outcome of platelet activation is the upregulation of the activity of integrins on the platelet surface (Li et al., 2010). Integrins are a family of heterodimeric receptors consisting of α and β subunits which interact with the platelet cytoskeleton (Bennett et al., 1999). Platelets express many integrins that play a crucial role in mediating the interaction between platelets to the exposed extracellular matrix as well as to another platelet, as integrins are highly important for enabling platelet aggregation (Stalker et al., 2012). The most abundant and major integrins found on platelets are $\alpha_2\beta_1$ (approximately 2000 to 4000 per platelet) which bind collagen, and $\alpha_{IIb}\beta_3$ (approximately 80,000 per platelet) which bind fibrinogen (Chari-Turaga and Naik, 2011; Reininger, 2008). Other integrins such as $\alpha_5\beta_1$ and $\alpha_6\beta_1$ bind other sub-endothelial matrix proteins including laminin and fibronectin to enhance the adhesion strength (Huynh et al., 2013; Kunicki et al., 1993).

Integrin $\alpha_2\beta_1$ contributes to the binding of platelets to collagen as well as aiding in thrombus stabilisation (Marjoram et al., 2014). In contrast to GpVI signalling, $\alpha_2\beta_1$ does not induce tyrosine

kinase activity (Gibbins, 2004; Gofer-Dadosh et al., 1997). Due to this, previous work has suggested that upon collagen-induced activation, $\alpha_2\beta_1$ initially stabilises platelet interaction with collagen, which is followed by GpVI signalling (Kirchhofer et al., 1990; Santoro et al., 1991). Inside-out signalling enables activation of $\alpha_2\beta_1$ via GpVI signalling (Asselin et al., 1997; Marjoram et al., 2014).

Integrin $\alpha_{IIb}\beta_3$, the most abundantly expressed platelet receptor, acts as a receptor for fibrinogen, which is found in plasma and platelet α-granules. $\alpha_{IIb}\beta_3$ is maintained at a low-affinity state in resting platelets (Chari-Turaga and Naik, 2011; Kunicki et al., 1993). The importance of $\alpha_{IIb}\beta_3$ is demonstrated by the occurrence of the rare inherited autosomal recessive bleeding disorder known as Glanzmann Thrombasthenia (GT) which is caused by a defect of $\alpha_{IIb}\beta_3$ (Nurden, 2006). GT results in unpredictable and severe bleeding tendencies (Nurden, 2006). Platelet transfusion is the primary treatment for GT, although this may evoke the development of platelet antibodies to $\alpha_{IIb}\beta_3$ which in turn could potentially result in platelet refractoriness (Poon et al., 2016). In the case of platelet refractoriness, recombinant activated factor VII (rFVIIa) is employed to induce fibrinogen formation which results in platelet aggregation and adhesion to prevent bleeding and induced primary haemostasis (Rajpurkar et al., 2014). However, the mechanism of action of rFVIIa is poorly understood and requires further investigation and is not safe to employ as of yet as a regular therapeutic agent (Poon, 2007; Poon et al., 2006; Rajpurkar et al., 2014).

Upon upregulation, $\alpha_{IIb}\beta_3$ can bind to the arginine-glycine-aspartate (RGD) tripeptide sequence, enabling platelet crosslinking and leading to aggregation (Bernardi et al., 2006; Brass et al., 1997). The α and β subunits of $\alpha_{IIb}\beta_3$ contain cation binding sites (Zhang and Chen, 2012). Cations are essential for integrin functions such as ligand binding, as well as inducing stabilisation of the integrin structure upon ligand binding. Two cation-specific binding sites are present in $\alpha_{IIb}\beta_3$ and must be occupied by cations to enable ligand binding. One of these sites binds Ca^{2+} (being saturated at 10^{-6} M) whereas the other site is less specific and binds to Mg^{2+} or Ca^{2+} (with an affinity of 10^{-3} M) (Zhang and Chen, 2012). Direct activation of $\alpha_{IIb}\beta_3$ occurs in response to exogenous treatment with Mg^{2+} (Gailit and Ruoslahti, 1988; Phillips and Baughan, 1983; Taylor and Pugh, 2016; Zhang and Chen, 2012). Excessive cation concentrations may saturate the cation binding sites and induce inappropriate $\alpha_{IIb}\beta_3$ activation; thus high cation concentrations may be problematic as they may interfere with platelet aggregation and induce agglutination instead (Gowland et al., 1969; Phillips and Baughan, 1983; Zhang and Chen, 2012).

As $\alpha_{IIb}\beta_3$ is crucial for platelet activity and thrombus formation, it is a candidate for anti-thrombotic therapy. Current anti-thrombotic drugs that target $\alpha_{IIb}\beta_3$ such as the $\alpha_{IIb}\beta_3$ antagonist Abciximab, and are commonly used during surgical interventions but is a high-risk strategy due to

associated high bleeding risks. (Makris et al., 2013). Studies have found that thrombocytopenia (platelet deficiency) occur as a side effect of Abciximab treatment in patients who have undergone CVD-related surgery such as coronary stenting and coronary angioplasty, outlining the risks involved with Abciximab (Gammie et al., 1998; Merlini et al., 2004). Severe thrombocytopenia requires platelet transfusion (Madan and Berkowitz, 1999). Repeated treatment with Abciximab induces severe thrombocytopenia and induces high bleeding risks which could be fatal (Tcheng et al., 2001, 1994). Thus further the development of safer anti-thrombotic which does not impose bleeding risks is required (Orford and Holmes, 2002).

Signalling via $\alpha_{IIb}\beta_3$

Upon agonist-dependent stimulation, the affinity of $\alpha_{IIb}\beta_3$ for fibrinogen is amplified via 'inside-out' signalling (Li et al., 2010). Signalling via multiple pathways (including GpVI and Gα proteins, GPCRs) upon agonist evoked stimulation induces inside-out activation of the integrin, as a result of activation of the small GTPase, Rap1b (Figure 1.5. Nieswandt and Watson, 2003). Activation of Ras-related protein 1B (Rap1b) is induced by P13K. However, Ca^{2+} and diacylglycerol (DAG) regulated guanine nucleotide exchange factor 1 (CalDAG-GEF1) is also vital for Rap1b activation as it mediates the conversion of Rap1b from its inactive state (GDP-bound) to its activated state (GTP-bound) (Bernardi et al., 2006). Active Rap1b interacts with talin, an integrin-associated cytoskeletal protein . (Nieswandt et al., 2011). These interactions upregulate the affinity of $\alpha_{IIb}\beta_3$ to its ligand by allowing interactions of the β_3 subunit with its cytoplasmic domain, thus enabling integrin activation to a high-affinity state (Peyvandi et al., 2011).

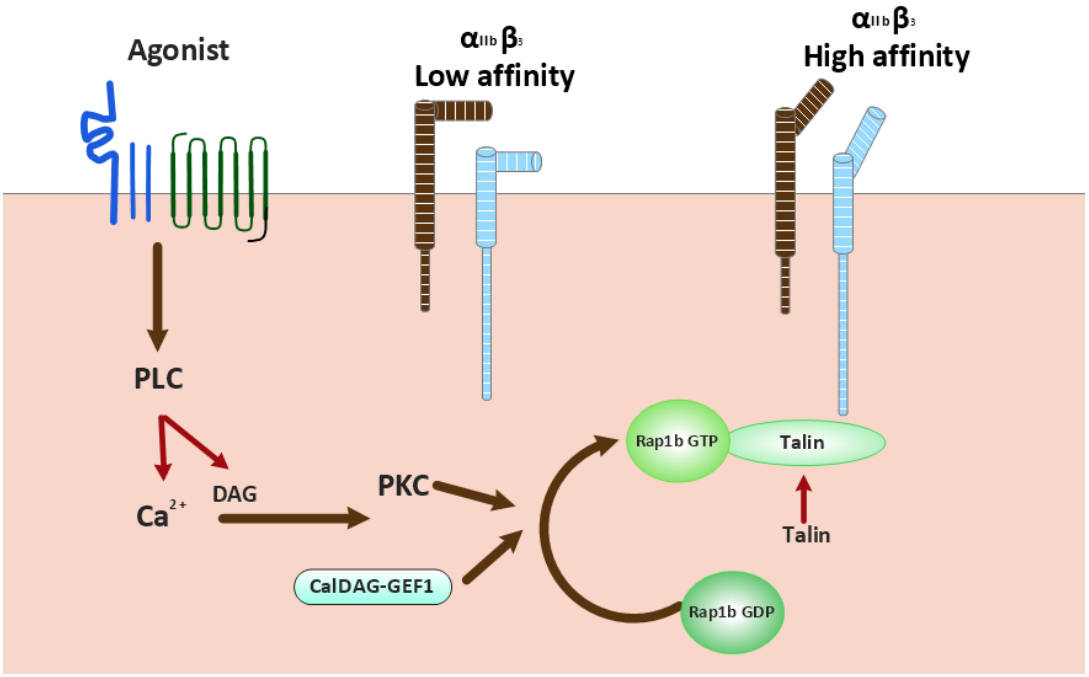

Figure 1.5. Inside-out activation of integrin $\alpha_{IIb}\beta_3$. Agonist induced stimulation results in the activation of phospholipase C (PLC) which induces the formation of the secondary messenger diacylglycerol (DAG) as well as mobilisation of Ca^{2+} from its store. DAG and Ca^{2+} evoke activation of protein kinase C (PKC) and CalDAG-GEF1, which mediate GDP/GTP exchange and the activation of Rap1b. Rap-1b and talin interact resulting in the exposure of integrin binding. Talin binds to and disrupts the salt bridge between the cytoplasmic tails of the α_{IIb} and β_3 subunits. This results in conformation changes of these subunits which change the integrin from its low-affinity state to its high-affinity state

'Outside-in' signalling occurs following ligand binding to $\alpha_{IIb}\beta_3$ resulting in the clustering of this integrin (Stalker et al., 2012). Ligand binding (which in physiological cases would be fibrinogen and VWF)-dependent outside-in signalling initiates intracellular signalling (Bennett et al., 1988), and activation of many major processes, including cytoskeletal rearrangement, PKC activation and Ca^{2+} mobilisation (Hammond et al., 2015; Lever et al., 2015; Murugappan et al., 2005; Wee and Jackson, 2006). Outside-in signalling results in SFK-dependent tyrosine phosphorylation of the β_3 cytoplasmic domain (Senis et al., 2014). Following phosphorylation, Syk is recruited and activated during outside-in signalling, mediating activation of PLCγ2(Ozaki et al., 2000). The resulting downstream signalling cascade is similar to that mediated by GpVI signalling (Figure 1.6. Chari-Turaga and Naik, 2011; Rivera et al., 2009; Soulet et al., 2005).

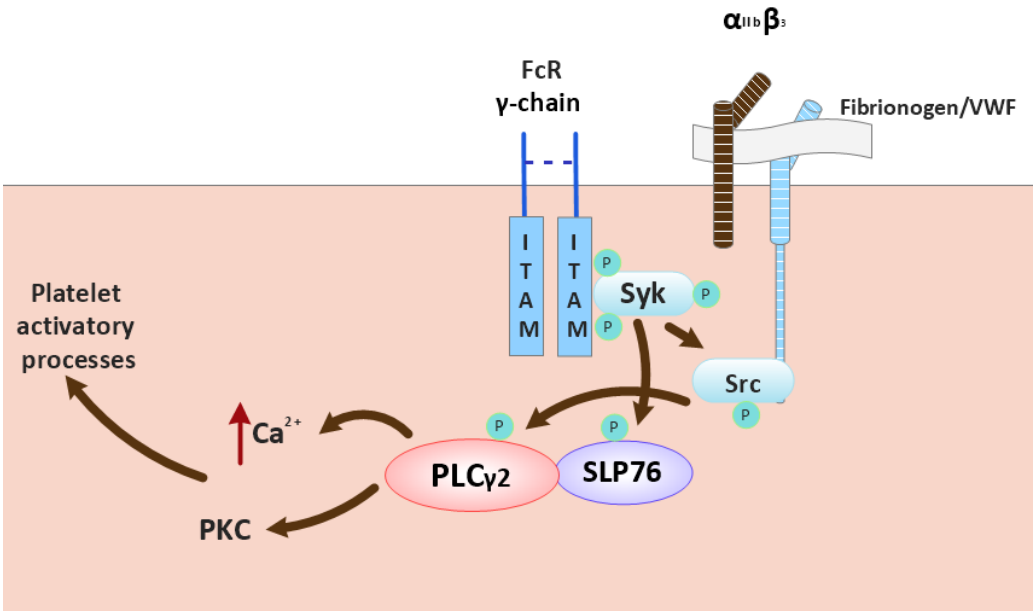

Figure 1.6. Outside-in signalling upon ligand binding to $\alpha_{IIb}\beta_3$. Ligand (fibrinogen/ VWF) binding to $\alpha_{IIb}\beta_3$, results in the phosphorylation by Src Family Kinases (SFK) and numerous enzymes and adaptor proteins. PLCγ2 mediates activatory processes in platelets by mobilising Ca^{2+} from stores and activating protein kinase C (PKC). Syk phosphorylates other proteins such as SLP76, which also mediates activation of PLCγ2. There is also the interplay of the phosphorylation of targets induced by Src and Syk, which further promotes the outside in signalling activation. Syk can also operate the position of Src on the cytoplasmic tail of the β_3 subunit.

1.2.6 Platelet shape change

Platelet activation induces cytoskeletal rearrangements that regulate shape change, which is an essential feature of platelet aggregation (Paul et al., 1999). Upon activation, platelets change from their non-active disc shape to their activated state which is spherical with protruding filopodia (Wraith et al., 2013). While this morphological state is thought to enable aggregation at a faster rate (Wraith et al., 2013), shape change is independent of, and may not be required for aggregation (Maurer-Spurej and Devine, 2001). However, shape change is an acknowledged indicator of activated platelets (Maurer-Spurej and Devine, 2001). Previous studies have observed activation-dependent morphological changes in platelets, by enabling platelets to adhere to and spread on flat surfaces such as glass, or fibrinogen-coated coverslips. Upon contact, platelets lose their discoid shape and undergo cytoskeletal contraction (Aslan et al., 2012; Li et al., 2010). This is followed by structural extensions from the platelets known as pseudopodia, which extend and contract. Following filopodia formation, structures known as lamellipodia are formed from the sides of the pseudopodia (Bearer et al., 2002). These extend utilising lipid membrane from stores within platelets (the open canalicular system), to

cover a large surface area to inhibit blood loss, and providing a substrate for coagulation (Podoplelova et al., 2016; Seifert et al., 2017; Tomaiuolo et al., 2017).

Actin is highly abundant in platelets and plays a significant role in cytoskeletal rearrangements (Bearer et al., 2002). Fully spread platelets contain stress-like fibres, lamellipodia, filopodia, and a contractile ring which are all actin structures (Maioli et al., 1985). During the morphological change of a platelet from the resting discoid state to a fully spread platelet, the contractile ring is initially formed. This process is followed by filopodia extensions, which enables lamellipodia to form, and full spread to occur (Hartwig, 1992). There are many proteins which interact with actin to regulate polymerisation and depolymerisation which occur during platelet shape change (Bearer, 1995; Bearer et al., 2002). Different Ca^{2+} dependent actin-binding proteins may play different and selective roles during the stages of platelet shape change as well as maintenance of the cytoskeleton of resting platelets; however this requires further investigation in order to elucidate the regulatory roles Ca^{2+} may have on the platelet cytoskeleton (Bearer et al., 2002; Finkenstaedt-Quinn et al., 2015). An example of a well-documented Ca^{2+} -dependent cytoskeletal protein is gelosin which has been found to be a dynamic regulator of actin filament lengths in platelets. It can be hypothesised that other cations such as Zn^{2+} may also mediate these Ca^{2+} binding proteins which regulate the platelet cytoskeleton, as these proteins may be susceptible to other cations in addition to Ca^{2+}. Cation-dependent cytoskeletal changes is a major theme of this thesis. Additionally, a major Ca^{2+} binding protein known as calmodulin can induce platelet shape change via activation of myosin light chain kinase (MLCK). Calmodulin is dependent on Ca^{2+}; however studies that focused on the structure of calmodulin have suggested that other cations such as Zn^{2+} could displace Ca^{2+} (although yet to be confirmed), thus further suggesting the potential role that cations may play in regulating the platelet cytoskeleton (Levy, 1983; Mills and Johnson, 1985).

Signalling pathways that regulate platelet shape change

Platelet shape change involves a number of proteins that regulate cytoskeletal rearrangement. Previous studies have shown that the specific signalling pathways leading to platelet shape change involve Ca^{2+}/calmodulin, myosin light chain kinase (MLCK) and the RhoA/$p160^{ROCK}$ (Rho-associated coiled-coil-containing protein kinase), (Paul et al., 1999). RhoA protein is a small GTPase which is involved in platelet cytoskeletal rearrangements, while p160ROCK is a protein kinase to which RhoA associates during cytoskeletal rearrangements during platelet shape change (Paul et al., 1999). Platelet signalling pathways that regulate shape change involve MLCK activity (Daniel et al., 1984; Retzer and Essler, 2000). Activated MLCK phosphorylates myosin light chains (MLC), resulting in

myosin-driven contraction and changes in actin dynamics which results in platelet shape change (Jalagadugula et al., 2010). The signalling pathways derived from these studies are thought to be dependent on Ca^{2+}. Upon $[Ca^{2+}]_i$ mobilisation (via the agonist-induced activation of the PLC/IP_3 pathway), Ca^{2+} interacts with the Ca^{2+}-binding protein, calmodulin which is then able to activate MLCK.

Studies have also shown the presence of a secondary Ca^{2+}-independent signalling pathway that regulates shape change. In this pathway, Rho-associated coiled-coil-containing protein kinases can phosphorylate MLCs or/and enhance MLC phosphorylation by inhibiting MLC phosphatases (MLC-P) (Paul et al., 1999; Shin et al., 2017). The exact mechanism of platelet shape change is still to be confirmed (Shin et al., 2017; Sun et al., 2007).

Vasodilator-stimulated phosphoprotein [(VASP) (which is a substrate of cAMP-dependent protein kinase A (PKA) and cGMP dependent protein kinase (PKG) in platelets (Walter et al., 1993) is involved in the regulation of actin dynamics during platelet shape change (Beck et al., 2014). While the function of phosphorylated VASP in platelets is not fully understood, recent studies have indicated that VASP may mediate actin rearrangement via nucleation, filament formation and bundling (Bachmann et al., 1999; Bearer et al., 2002; Walders-Harbeck et al., 2002). VASP also mediates the recruitment of actin-binding proteins such as profilin and therefore plays an important role in actin dynamics (Bearer et al., 2002; Hartwig, 1992; Hartwig et al., 1999; Wentworth et al., 2006). (Aburima et al., 2013; Beck et al., 2014; Wentworth et al., 2006)

1.2.7 Platelet granules and degranulation

Platelet activation results in degranulation of α and dense granules, releasing their contents into the environment of a growing thrombus. α granules are the most abundant secretory compartment in platelets (approximately 50-80 per platelet) (Sander et al., 1983; Wencel-Drake et al., 1985). α-granules contain adhesion molecules such as VWF, fibrinogen, fibronectin and vitronectin, which are vital for mediating platelet adhesion and thrombus formation. α-granules also contain a number of cytokines and coagulation factors which function in cellular repair, inflammation, angiogenesis and coagulation (Maynard et al., 2007). Furthermore, α-granules contain Zn^{2+} which may be released into the platelet cytosol upon activation. However, the role of Zn^{2+} in platelet is yet to be confirmed (Marx et al., 1993a; Milne et al., 1985; Taylor and Pugh, 2016; Watson et al., 2016). The mechanisms that induce α-granule packaging of these molecules have yet to be fully characterised and warrant further investigation. Cytoskeletal changes in platelets may regulate granule release. The

distribution of granules are dispersed in a random manner in resting platelets; however, upon activation, cytoskeletal changes centralise the granules, which results in the secretion of the granules through the open canalicular system (OCS) in platelets (Flaumenhaft, 2003). The OCS consists of a network of surface-connected channels which mediate platelet activation. The full function of the OCS is yet to be confirmed and requires further work to determine its full function and importance in platelets (Selvadurai and Hamilton, 2018). The influence of cytoskeletal changes on regulating granule secretion is also the subject of investigation due to contradictory findings, as inhibition of cytoskeletal changes does not influence granule secretion (Kirkpatrick et al., 1980; White and Rao, 1983, 1982). However, the signalling pathways that induce cytoskeletal rearrangement during platelet shape change also mediate granule secretion; for example, previous work found that Rho kinases induce cytoskeletal rearrangements and that inhibition of Rho kinase reduces granule secretion upon agonist-induced activation (Suzuki et al., 1999; Watanabe et al., 2001).

Dense granules are the second most abundant secretory compartment in platelets (approximately 3-8 per platelet) and contain many soluble agonists such as ATP, ADP, serotonin and Ca^{2+}. Upon activation-dependent degranulation, these agonists activate and recruit circulating platelets to mediate sustained platelet aggregation (Golebiewska and Poole, 2015). ADP mediates α-granule secretion and integrin activation (Andre et al., 2003). Transgenic mouse models which are deficient in dense granule secretion also have defects in other markers of platelet activation such an α-granule release and integrin activation, suggesting that ADP released from the dense granules primarily mediates activatory processes, rather than plasma-derived ADP (Golebiewska and Poole, 2015; Hashimoto et al., 1994; Woulfe et al., 2001). This highlights the importance of dense granules in platelet activation and synergy with α-granule secretion.

Granule secretion is highly important for platelet activity and thrombus formation, as defective granule secretion has been associated with bleeding tendencies, as found in patients with storage pool diseases (SPD), a result of defective granule release (Reed et al., 2000). SPD inhibits platelet responses such as aggregation and platelet signalling in response to agonist stimulation (Holmsen and Weiss, 1970; Nurden and Nurden, 2014; Smith et al., 1997).

1.2.8 Phosphatidyl-serine (PS) exposure

Activated platelets play a central role in mediating coagulation, which as described earlier in this chapter is a significant step in the haemostatic process which reinforces the stable platelet plug allowing a stable, long-lasting clot to form (Podoplelova et al., 2016). Coagulation is initiated on

activated platelets which externalise PS on their surface, as thrombin formation is promoted from several coagulation factors which assemble on the PS-rich surfaces (Gao et al., 2012; Mackman et al., 2007). Thrombin cleaves fibrin from fibrinogen, giving rise to a fibrin meshwork to enable a more stable thrombus (Knappe et al., 2013; Monroe et al., 2002; Podoplelova et al., 2016).

Previous work has shown that ATP-dependant proteins know as flippase and floppase (a family of lipid transport enzymes mediate the transportation of phospholipid molecules between the inner and outer faces of cellular membranes) as well as Ca^{2+}-dependent phospholipid scramblases (which has been identified as the lipid scramblase transmembrane protein 16F, TMEM16F in platelets) which mediates the translocation of phospholipids) mediate PS exposure (Figure 1.7, Pomorski and Menon, 2016; Suzuki et al., 2013; Yang et al., 2012). At resting states, negatively charged phospholipids such as PS are maintained at the inner face of the membrane via the floppase and flippase proteins, whereas the outer face of the membrane consists of positively charged phospholipids (Daleke, 2003; Owens and Mackman, 2011). Flippase plays a significant role in translocating phospholipids to the inner face of the membranes (floppase induces the opposing action). $[Ca^{2+}]_i$ elevation results in the inhibition of flippase and mediates scramblase to translocate phospholipids to the outer leaflet membrane, thus resulting in PS exposure (Daleke, 2003; Pomorski and Menon, 2016; Suzuki et al., 2013; Zhao et al., 2017). The exposure of increased PS on platelets serves as a marker of activated platelets and indicates that the platelets may be procoagulant (Mackman et al., 2007; Mooberry and Key, 2016; Morel et al., 2008).

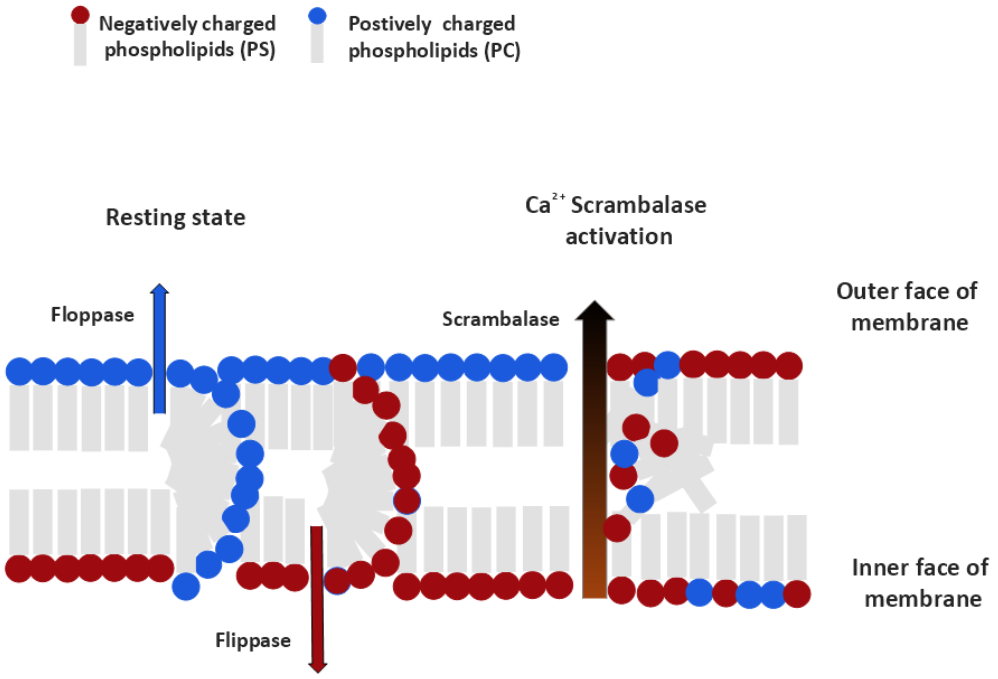

Figure 1.7. Mechanisms of Phosphatidylserine (PS) exposure in activated platelets. Negatively charged phospholipids such as phosphatidylserine (PS) are maintained at the inner face of the membrane via the floppase (translocates phospholipids to outer face of membrane) and flippase proteins (translocate phospholipids to inner face of membrane), whereas the outer face of the membrane consists of positively charges phospholipids such as phosphatidylcholine (PC). Ca^{2+} elevation inhibits flippase activity and activates the Ca^{2+} dependant scramblase which translocates the negatively charged phospholipids to the outer leaflet membrane, resulting in PS exposure.

1.2.9 Oxidative stress and redox-dependent signalling during platelet activation

Redox reactions occur in platelets during activation (Sonego et al., 2017). Modulation of the redox state in platelets and the vascular environment may result in or be the result of oxidative stress in platelets (Olas and Wachowicz, 2007). Oxidative stress occurs when there is an imbalance between antioxidants and oxidants. Modulation of the redox state may be caused by a number of different mechanisms or stimuli, which in turn could induce or inhibit the levels of reactive oxygen species (ROS) present (Pietraforte et al., 2014). Furthermore, antioxidants 'mop up' ROS and alter the redox state in platelets. The balance between redox state and oxidative stress in platelets plays a key role in regulating platelet activation (Qiao et al., 2018). Whilst epidemiological studies have given early indications that supplementation of antioxidants has a reducing effect on cardiovascular illnesses

(Pandya et al., 2013; Sinha and Dabla, 2015), other studies using vitamin antioxidant therapy have not shown any significant clinical benefits. Further work has shown a significant role for antioxidants on platelet activity, following a strong association of antioxidant supplementation and strokes (Gorog and Kovacs, 1995; Olas and Wachowicz, 2007; Sonego et al., 2017). Oxidative stress is a major mediator in cardiovascular illnesses as a result of cellular damage (Ferroni et al., 2012).

Platelet aggregation coincides with increased oxygen utilisation (Watt et al., 2012). ROS such as superoxide is produced by platelets and enhance platelet aggregation responses (Freedman, 2008). Transition metals such as Zn^{2+} may contribute to oxidative degradation of lipids (lipid peroxidation) by superoxide, resulting in the initiation of lipid radical propagation chain reactions as result of the formation of peroxyl radicals and lipid alkoxyl (Krötz et al., 2004; Schneider, 2009). Nitric Oxide (NO) can halt this radical chain reaction at the expense of losing its bioactivity, by reaction with either superoxide or the peroxyl radicals to result in the formation of peroxynitrite. NO is inactivated readily upon oxidative stress (Zhao, 2007). NO negatively regulates platelet activation. Thus inactivation of NO upon oxidative stress may evoke abnormal platelet activation and haemostasis.

The NADPH oxidase (NOX) pathway primarily serves to induce modulation of the redox signalling pathway in platelets (Begonja et al., 2006). The NOX pathway produces ROS and can also be activated by ROS (Figure 1.8), which is why the inhibition of this pathway is crucial for the maintenance of resting platelets (Begonja et al., 2006). The isoforms of the NOX complex on platelets that are currently known to be expressed on platelets are NOX-1 and NOX-2. The oxidative subunit, neutrophil cytosol factor 1 (p47phox) induces activation of the NOX complex on platelets via phosphorylation. Activation of NOX has been found to mediate efficient platelet activation, implying the importance that ROS has on platelet activity. Interestingly, differences between NOX-1 and NOX-2 regarding signalling were suggested in previous work, as NOX-1 was found to primarily mediate Thromboxane A_2 (TXA_2) production following p38 mitogen-activated protein kinase (MAPK) signalling. The PLCγ2/PKC/MAPKp38 signalling cascade is potentiated by ROS (Krötz et al., 2004). This cascade activates PLA_2 which catalyses TXA_2 synthesis, increasing platelet activation (Qiao et al., 2018). NOX-2 was found to favour signalling downstream of collagen stimulation as NOX-2 knockout studies on mouse, results in inhibition of ROS generation following collages induced activation. Thus, these findings demonstrated that the isoforms of NOX may induce activation of platelets in differing manners, further providing evidence to instigate the importance of ROS in efficient platelet activation. Furthermore, ROS scavengers such as superoxide dismutase and catalase inhibit platelet response upon stimulation thus indicating that ROS acts as a secondary messenger (Gorog and Kovacs, 1995; Sonego et al., 2017).

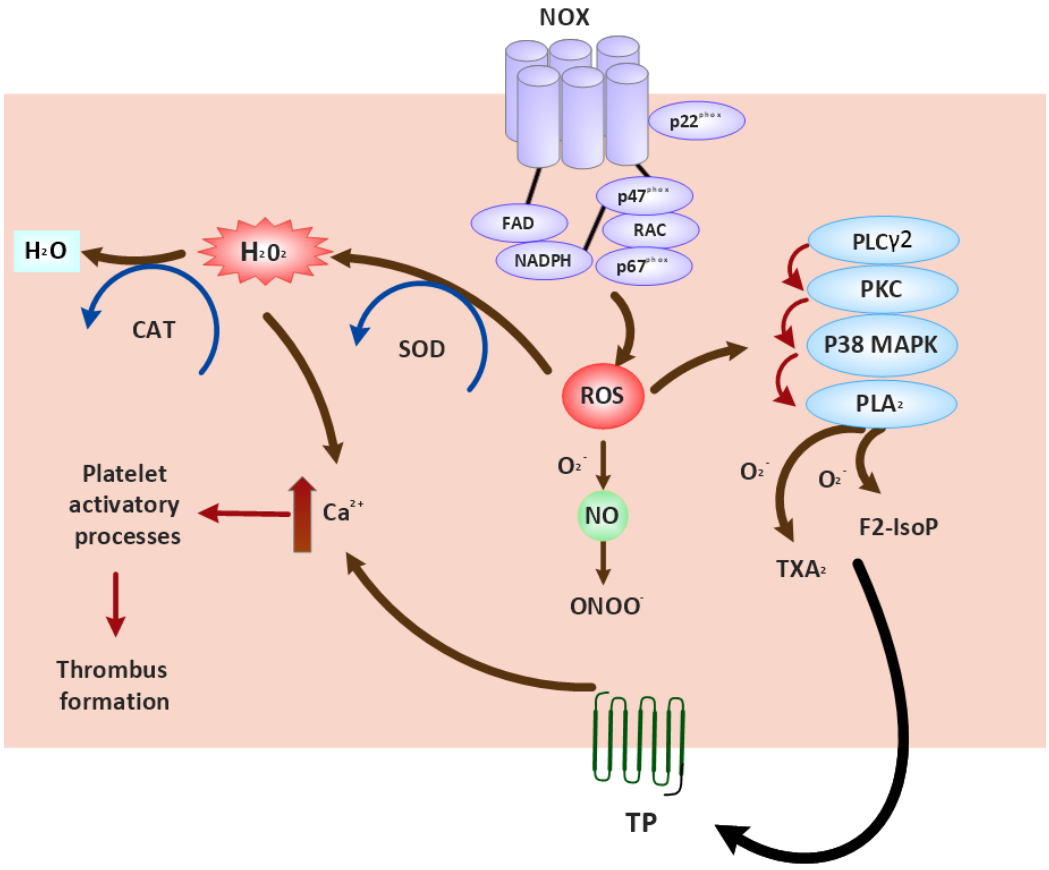

Figure 1.8. The NADPH oxidase (NOX) pathway induces thrombus formation via reactive oxygen species (ROS) formation. The NOX complex is constituted with its regulatory subunits which include $p22^{phox,}$ $p47^{phox}$, $p67^{phox}$ and the G-protein, RAC which are required for NOX assembly and activation. The subunit, $p47^{phox}$ plays the most crucial role, as it is involved in the direct activation of the NOX complex via phosphorylation. The NOX complex also consists of cytoplasmic flavin adenine dinucleotide (FAD) and NADPH binding domains, where electrons are passed down an electrochemical gradient from NADPH to FAD then through heme groups within NOX. This is followed by the transfer of electrons to oxygen, resulting in the formation of the ROS, superoxide (O_2^-). ROS elevation can mediate the PLCγ2/PKC/MAPKp38 signalling cascade resulting in PLA_2 activation. PLA_2 is then able to induce the synthesis of thromboxane A_2 (TXA_2), where F2 isoprostane (F2-IsoP) can also form as a result of oxidation by peroxides. TxA_2 and F2-IsoP can both bind to the thromboxane receptor (TP), which results in the Ca^{2+} mobilisation, which results in platelet activation and thrombus formation. Superoxide (O_2^-) may be converted (by superoxide dismutase, SOD) to hydrogen peroxide (H_2O_2) which acts as a secondary messenger, also leading to Ca^{2+} mobilisation. Therefore, elevated ROS may result in inappropriate platelet activation and thrombus formation. H_2O_2 may also be converted to dihydrogen oxide (H_2O) via catalase, CAT. Superoxide (O_2^-) can also react with nitrogen oxide (NO), which results in the formation of reactive nitrogen species such as peroxynitrite ($ONOO^-$).

1.3 Negative regulation of platelet activation

Under normal circulating conditions, platelet activation and adherence are inhibited via the action of several factors including nitric oxide and prostacyclin (PGI_2) which are released from vascular endothelial cells. Nitric oxide (NO) inhibits platelet activation by stimulating the production of cGMP,

which activates cGMP-dependent protein kinase (G-kinase) (O'Brien and Salmon, 1987). The G-kinase inhibits the activation of phospholipase C (PLC) which is crucial for the mobilisation $[Ca^{2+}]_i$ from the dense tubular system, the Ca^{2+} store in platelets (Peyvandi et al., 2011). The release of $[Ca^{2+}]_i$ is crucial for platelet activation and activity and will be discussed in much more depth in later sections. PGI_2 binds to the GPCR prostacyclin receptor (IP). This stimulates adenylyl cyclase (AC) to synthesise cyclic adenosine monophosphate (cAMP), which inhibits platelet aggregation by activating protein kinase A (PKA) (G. R. Wang et al., 1998). Thus, platelet inhibition is an active process, relying on cAMP and cGMP signalling, in contrast with activation of other cell types in which cyclic nucleotide synthesis is stimulated upon activation (Figure 1.9). Inhibition of platelets (after haemostatic processes have successfully occurred, as well as in healthy conditions) is significant to avoid the occurrence of inappropriate haemostasis, which can result in thrombosis leading to adverse cardiovascular events (Aburima et al., 2013; Beck et al., 2014; Gibbins, 2004).

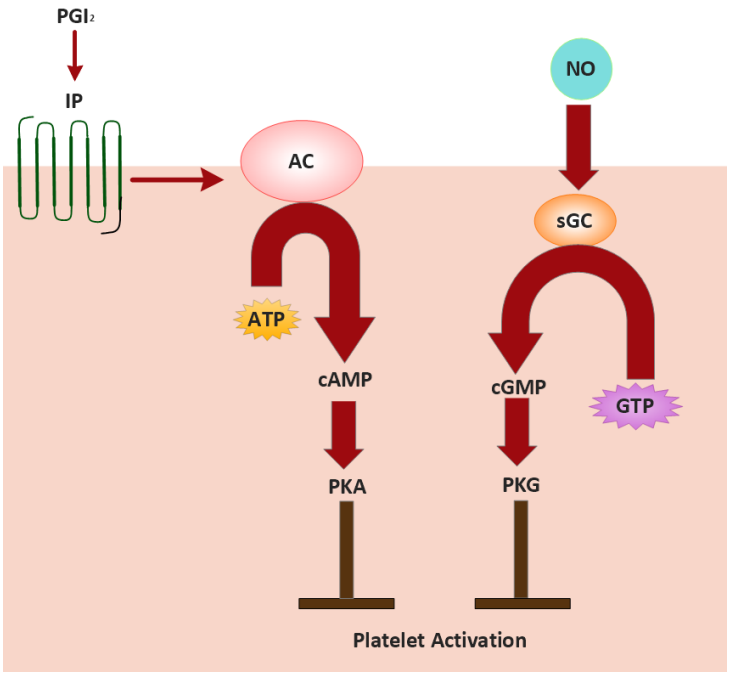

Figure 1.9. Prostacyclin and Nitric oxide signalling inhibit platelet activation. Prostacyclin (PGI_2) which is released from endothelial cells binds to the prostacyclin receptor (IP) on platelets. This then results in the activation of the transmembrane protein, adenylate cyclase (AC), which then produces cyclic adenosine monophosphate (cAMP) from adenosine triphosphate (ATP). cAMP is a secondary messenger and activates protein kinase A, which then inhibit platelet activation. Nitric oxide (NO), is also released from endothelial cells and is a gas molecule which diffuses through the platelet membrane. NO primarily targets soluble guanylate cyclase (sGC), which synthesises cyclic guanosine monophosphate (cGMP) from guanosine triphosphate (GTP). cGMP activates PKG which results in the inhibition of platelet activation.

1.4 Calcium signalling in platelets

A hallmark of platelet activation is $[Ca^{2+}]_i$ levels which is mediated by release from $[Ca^{2+}]_i$ stores and influx through cation-permeable membranes channels following agonist-dependent activation (Varga-Szabo et al., 2009). The major calcium stores in platelets are the dense tubular system (DTS). The release of Ca^{2+} from intracellular stores is mediated by phospholipase C (PLC) isoforms, of which PLCβ and PLCγ2 are present in platelets (Kamiya et al., 2014, Lever et al., 2015). Receptor-mediated platelet activation results in the activation of PLC isoforms which hydrolyse phosphoinositide-4,5-bisphosphate (PIP_2) to inositol-1,4,5-trisphosphate (IP_3) and 1,2-diacylglycerol (DAG) (Varga-Szabo et al., 2009, Lever et al., 2015). IP_3 mediates release of Ca^{2+} from the DTS into the platelet cytosol via activation of the IP_3R, a dense tubular calcium channel. The DTS, however, provides a limited source of Ca^{2+} upon agonist-induced stimulation and is thus readily depleted. This requires replenishment of the store which is carried about by a major process known as store-operated calcium entry (SOCE), in which a secondary influx of calcium via membrane ion channels such as Orai1 occurs (Figure 1.10, Guéguinou et al., 2016). The stromal interaction molecule 1 (STIM1) acts as a Ca^{2+} sensor molecule on the DTS, which binds to Ca^{2+} via its EF-hand domain. The release of Ca^{2+} from the DTS via the IP_3R results in the disruption and then dissociation of Ca^{2+} binding to STIM1, which induces the redistribution of STIM1 to the plasma membrane where it can interact with Orai1. Orai1 consists of four transmembrane domains, and structural studies have indicated that STIM1 interacts with one of these four transmembrane domains (Hou et al., 2012). Studies in Orai1- or STIM1-deficient mice have illustrated the impairment of SOCE and functional processes in platelets which confirmed the importance of STIM1 and Orai1 in the SOCE process and the importance of SOCE and sustained Ca^{2+} responses in platelet function (Hou et al., 2012; Lang et al., 2013; Steinckwich et al., 2011). In addition to SOCE, other mechanisms are in place which permits Ca^{2+} entry into the platelets. For example, transient receptor potential channels (TRPCs) are expressed in platelets and provide a further point of induced Ca^{2+} entry. The role and presence of difference TRPCs in platelet are yet to be fully confirmed. However, TRPC6 induces Ca^{2+} entry and is mediated by DAG. DAG and IP_3 are generated upon hydrolysis of PIP_2. Other channels through which Ca^{2+} can gain entry to platelets include TRPC6 (which is gated by DAG) and the ATP-gated P2X1 (Varga-Szabo et al., 2009, Gamberucci et al., 2002). The $P2X_1$ channel which is gated by ATP mediates the fastest way in which Ca^{2+} can enter cells upon agonist stimulation (Mahaut-Smith, 2012).

Alternative mechanisms regulating Ca^{2+} entry are also present in platelets. As minor elevations in $[Ca^{2+}]_i$ induce platelet activation, the maintenance of resting constant $[Ca^{2+}]_i$ (approximately 100nM) is important to enable platelets to remain in resting states and not undergo inappropriate activation (Arslan et al., 1985a; Jones et al., 2010). Sarcoplasmic/endoplasmic Ca^{2+} ATPases (SERCAs) are present on the DTS and pump Ca^{2+} back into the store (Sharov et al., 2006). Plasma membrane Ca^{2+} ATPases (PMCAs) pump Ca^{2+} out of the platelet (Jones et al., 2010). Furthermore, the Na^{2+}/Ca^{2+} exchanger (NCX) which is expressed in platelet can mediate rapid entry and exit of Ca^{2+} in platelets (Roberts et al., 2012).

Ca^{2+} plays an essential role as a secondary messenger in platelets and other cells (Varga-Szabo et al., 2009). $[Ca^{2+}]_i$ contributes to many platelet processes including aggregation, shape change, granule release, PS (Orem et al., 2017; Smith et al., 1992) Regulatory mechanism such as SOCE, TRPCs, SERCAs, PMCAs and NCX could serve to be therapeutic targets to help developing antithrombotics, due to the central role Ca^{2+} plays in platelet activation. Furthermore, these Ca^{2+} regulatory mechanisms may also be involved in the handling of other cations such as Zn^{2+}, which will be discussed below.

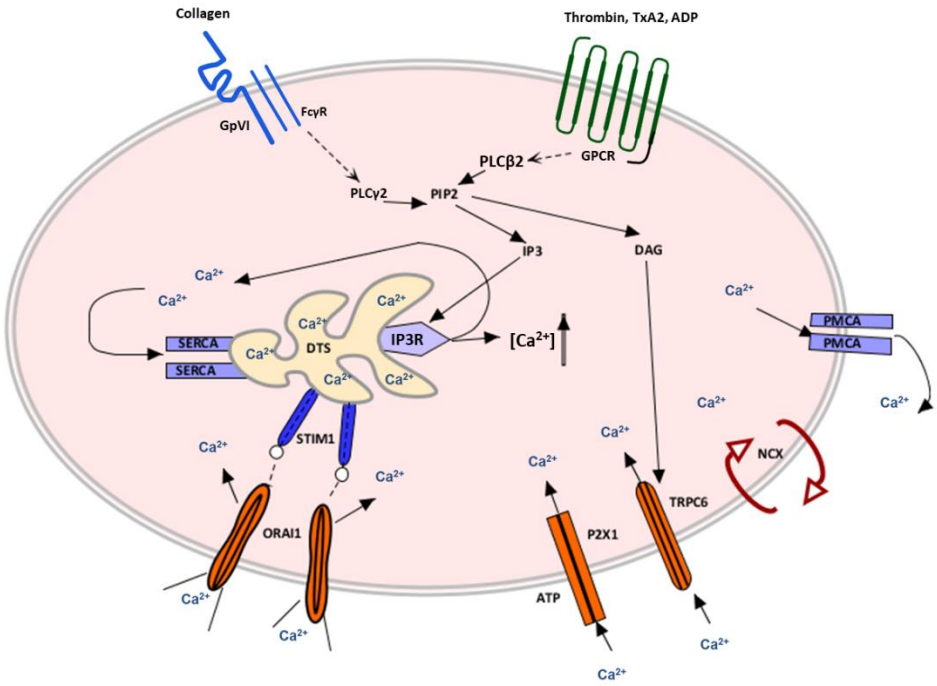

Figure 1.10. Schematic detailing Ca^{2+} mobilisation pathways in platelets. Agonist-induced stimulation results in hydrolysis of phosphatidylinositol-4,5-bisphophosphate (PIP_2) to inositol-1,4,5-trisphosphate (IP_3) and diacyl-glycerol (DAG) by different isoforms of phospholipase C (PLC) such as PLCγ and PLCβ. IP_3 mediates $[Ca^{2+}]_i$ from the DTS (calcium store) via the IP_3R, which then results in the depletion of Ca^{2+} from the DTS. A process known as store-operated calcium entry (SOCE), in which store depletion is detected by STIM1, is initiated, which signals the opening of the ORAI1 channels in the platelet plasma

membranes. DAG mediates non-SOCE via the transient receptor potential channel 6 (TRPC6). The agonist-operated calcium channel P2X1, as well as the NCX (Na^{2+}/Ca^{2+} exchanger), are also involved in elevating $[Ca^{2+}]_i$. The sarcoplasmic/endoplasmic reticulum Ca^{2+} ATPase (SERCA) pumps Ca^{2+} back into the DTS, allowing replenishment of the store. Also, the plasma membrane Ca^{2+} ATPases (PMCA) pumps Ca^{2+} back out the plasma membrane.

1.5 The role of Zn^{2+} in platelet physiology and activity

The role of Zn^{2+} as an intracellular or extracellular mediator of platelet function has received little research interest in recent years. The investigation of Zn^{2+} in platelets is to be explored in this thesis and provides a novel approach to further understanding platelet physiology. The role of Zn^{2+} in platelets may potentially be comparable to that seen by the major cation, Ca^{2+} which is a major secondary messenger in platelets.

1.5.1 The importance of Zn^{2+} in human biology

Zn^{2+} is one of the most abundant transition metals in the human body. It is found in all body tissues; 85% of total body zinc is found in bone and muscle, 11% in skin and liver, and remaining Zn^{2+} is within other tissues. (Plum et al., 2010; Stefanidou et al., 2006; Tapiero and Tew, 2003). 10-15% of the human genome encodes proteins such as enzymes, structural proteins, transcription factors and signalling proteins, which employ Zn^{2+} as a cofactor (Haase and Maret, 2003; Hyun et al., 2004a; Vu et al., 2013). In various cell types, intracellular Zn^{2+} ($[Zn^{2+}]_i$) is thought to serve as a secondary messenger for cellular activity. Furthermore, increased $[Zn^{2+}]_i$ has been shown to mediate intracellular signalling for cellular function (Andreini and Bertini, 2012; Vallee and Falchuk, 1993).

The contribution of Zn^{2+} to cellular mechanisms has received limited research interest. The role of Zn^{2+} as a bioactive molecule has been overlooked in favour of Ca^{2+} (Gordon et al., 1982; Heyns et al., 1985; Marx et al., 1991; Trybulec et al., 1993; Vallee and Falchuk, 1993; Varga-Szabo et al., 2009). This may be due to Ca^{2+}-binding fluorophores and chelators used to investigate Ca^{2+} signalling often having higher affinities for Zn^{2+} than Ca^{2+}, thus it is difficult to separate the effects of these two ions. An example of a commonly used Ca^{2+} fluorophore is Fura-2 which has a higher K_d value (i.e. lower affinity) for Ca^{2+} (0.23µM) than for Zn^{2+} (3nM) (Abbate et al., 2016). 1,2-bis(o-aminophenoxy) ethane-N, N, N', N'-tetraacetic acid (BAPTA) is a commonly used Ca^{2+} chelator which also has a higher affinity for Zn^{2+} than Ca^{2+}, with K_d values of 8 nM and 160 nM, respectively (Arslan et al., 1985a; Hyun et al., 2004a; Matias et al., 2010a). Thus, the use of BAPTA may have resulted in the underestimation of the importance of Zn^{2+} in cell function. An example of this has been demonstrated on work carried out on

neuronal damage. Previous studies confirmed Ca^{2+} as a significant mediator in the induction of neuronal damage and toxicity (Grienberger and Konnerth, 2012). However, the conclusions of this work were challenged with the observation that much of the work relied on the fluorescent indicator (Fura-2) which had a much higher affinity for Zn^{2+} than Ca^{2+}. It was suggested that the measured Ca^{2+} signal might also be attributable to Zn^{2+}. This was confirmed in other reports that showed increases in intracellular Zn^{2+} in hippocampal slices upon oxygen-glucose deprivation (OGD) (Koh et al., 1996; Sloviter, 1985; Stork and Li, 2006). Increases in $[Ca^{2+}]_i$ in hippocampal slices following OGD were found to be attributable to Zn^{2+}, as opposed to Ca^{2+}, via the employment of the highly specific Zn^{2+} chelator N,N,N',N'-Tetrakis(2-pyridylmethyl)ethylenediamine, (TPEN), implicating the role of Zn^{2+} may be more significant than Ca^{2+} in response to OGS in hippocampal slices (Koh et al., 1996; Sloviter, 1985; Stork and Li, 2006). This work provided evidence to demonstrate that effects previously attributed to Ca^{2+} may actually be a result of Zn^{2+}. It is therefore important to consider whether other cellular processes, previously thought to be mediated by Ca^{2+} alone, may also have a Zn^{2+}-dependent component.

The importance of Zn^{2+} in biology is exemplified by dietary Zn^{2+} deficiency, which results in significant consequential effects due to its multitude of biochemical functions (Hambidge, 2000). Various physiological systems, including the circulatory system, are affected by Zn^{2+} deficiency (Hambidge and Walravens, 1982), with prolonged bleeding times resulting from disruption of the circulatory integrity that is required for normal bodily function. Indeed, cancer patients who are Zn^{2+}-deficient have prolonged bleeding times which is rectified with Zn^{2+} supplementation (Stefanini, 1999), highlighting the importance of Zn^{2+} in maintaining physiological function.

The plasma concentration of Zn^{2+} ranges from 10 to 20µM and varies among individuals according to dietary intake (Roohani et al., 2013). The majority of plasma Zn^{2+} is bound to plasma proteins such as albumin and α2 microglobulin (Foote and Delves, 1984; Scott and Bradwell, 1983; Tubek et al., 2008; Vallee and Falchuk, 1993). Binding of Zn^{2+} to albumin results in exchangeable Zn^{2+} pools (exchangeable Zn^{2+} pools are the total sum of combined pools which exchange with Zn^{2+} in the plasma) and non-exchangeable Zn^{2+} pools when bound to α2 microglobulin, which in turn result in a final free plasma Zn^{2+} concentration of approximately 0.5 µM (Foote and Delves, 1984; Rükgauer et al., 1997; Taylor and Pugh, 2016; Scott and Bradwell, 1983; Krebs, 2000). Free Zn^{2+} is utilised by different cells for structural, catalytic and regulatory functions (Haeger, 1973; Halsted, 1971; International Zinc Nutrition Consultative Group (IZiNCG) et al., 2004). Cellular homeostasis of Zn^{2+} is vital to avoid the accumulation of excessive Zn^{2+} which could potentially result in cytotoxicity (Plum et al., 2010).

The regulation of Zn^{2+} homeostasis is primarily mediated by Zrt-Irt(Zinc transporter)-like proteins (ZIPs) and Zn^{2+} transporters (ZnTs) (Devergnas et al., 2004). At least 15 ZIPs and 10 ZnTs have been found in human cells (as illustrated in Figure 1.11) which enable Zn^{2+} transportation into and out of the cytosol (Sekler et al., 2007). ZIPs and ZnTs regulate $[Zn^{2+}]_i$ in the Golgi, endoplasmic reticulum and mitochondria in a variety of cell types. Vesicles which sequester high concentrations of $[Zn^{2+}]_i$ have been termed 'zincosomes', which act as Zn^{2+} stores that release Zn^{2+} upon stimulation with agonists such as growth factors (Haase and Maret, 2003; Taylor et al., 2008). Metallothioneins (MTs) are intracellular metal binding proteins play a major role in Zn^{2+} homeostasis. MTs are low molecular weight proteins (6-7 kDa) which have a high cysteine content to sequester Zn^{2+}, and can, therefore, act as Zn^{2+} stores (Romero-Isart and Vasák, 2002). *In vitro* studies show that MT cysteine residues can become oxidised. The sulphur clusters from the cysteines in MTs bind to Zn^{2+} create an environment of a shallow redox potential around Zn^{2+}. This low redox environment is susceptible to oxidation, even in mild oxidative conditions, resulting in the release of Zn^{2+} from the MT (Jiang et al., 1998). Therefore oxidative stress can induce Zn^{2+} release from MTs (Feng et al., 2006).

In neuronal cells, Zn^{2+} been reported to act as a neurotransmitter (Frederickson and Moncrieff, 1994), demonstrating a role for Zn^{2+} as a signalling molecule Zn^{2+}-containing neurons accumulate, sequester and release Zn^{2+} from their presynaptic vesicles (Frederickson et al., 2000). ZnTs which are expressed in the brain, such as ZnT-3, may facilitate Zn^{2+} uptake into these vesicles (Palmiter et al., 1996). Also, MTs, specifically MT-3, is expressed in the brain which may also contribute to Zn^{2+} trafficking in the brain, although this requires further confirmation (Aschner et al., 1997; Masters et al., 1994). The mechanisms that enable release of Zn^{2+} from the presynaptic vesicles within neurons is poorly understood, although it likely occurs via exocytosis (Pérez-Clausell and Danscher, 1986). Zn^{2+} is released from these neuron cells upon neuronal excitation as first illustrated in rats (which is indicative of a neurotransmitter), although the mechanism is yet to be elucidated. This Zn^{2+} release may contribute to toxic damage resulting in neurological disorders such as epileptic seizures (Aniksztejn et al., 1987; Assaf and Chung, 1984; Sloviter, 1985). Zn^{2+} is released from excitotoxic neurons, and upon excitotoxicity, Zn^{2+} is absent from the presynaptic neurons but is present in postsynaptic neurons and has been verified in ischaemic seizures (Frederickson, 1989; Koh et al., 1996; Sørensen et al., 1998; Suh et al., 1999; Yokoyama et al., 1986). Further studies have shown that Zn^{2+} is also present in synaptic vesicles of glutaminergic neurons, and upon neuronal activity is released into the synaptic cleft where it may go on to modulate post-synaptic receptors, ultimately relaying Zn^{2+}-mediated signals (Paoletti et al., 2009). These studies have demonstrated the importance of Zn^{2+} in

neuronal activity as a neurotransmitter and provide an exciting avenue to further explore Zn^{2+} in neurobiology (Frederickson, 1989; Frederickson et al., 2000, 1988; Suh et al., 1999).

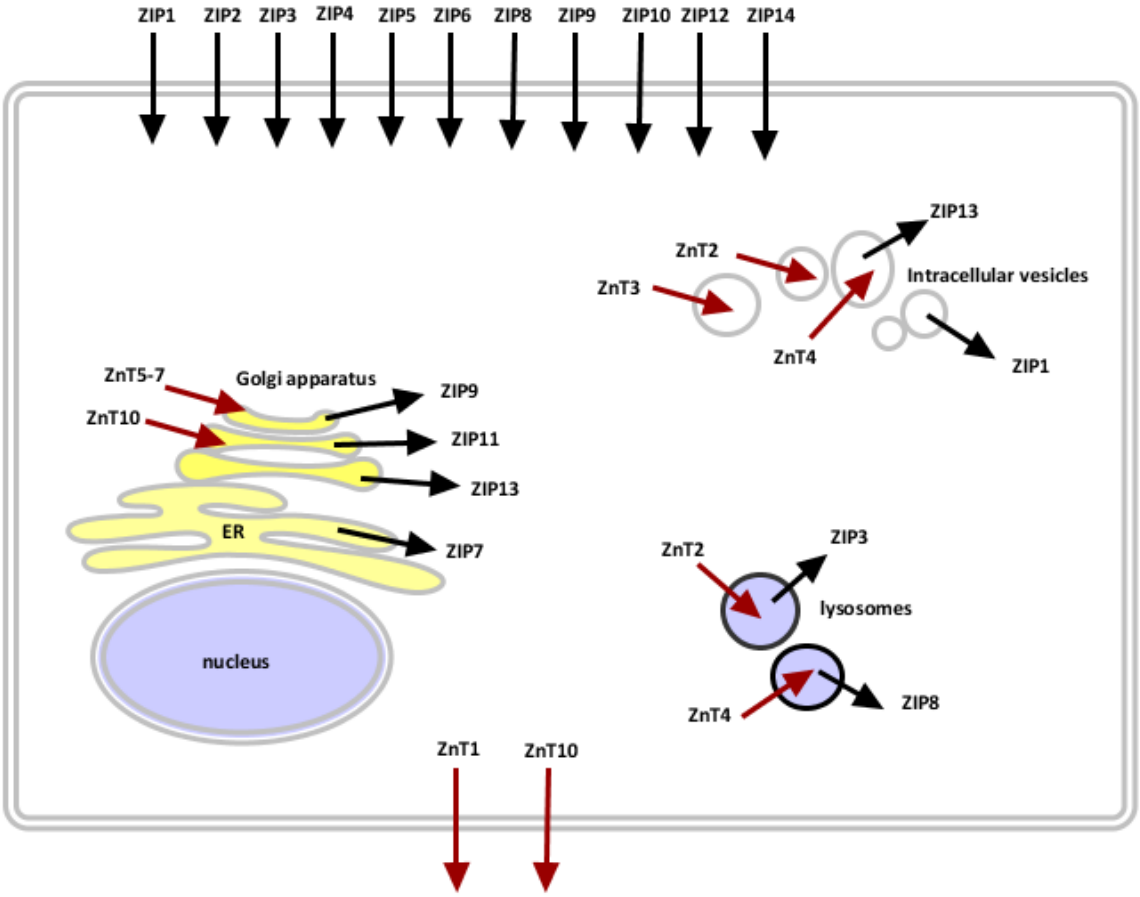

Figure 1.11. Subcellular localisation of ZIPs and ZnTs in nucleated cells. Generalised localisations of ZIPs (black arrows) and ZnTs (red arrows) are illustrated in this simple schematic in accordance with current findings. The direction of Zn^{2+} transport is illustrated by the arrows. Cytosolic Zn^{2+} is transferred in and out of different subcellular compartments such as the Golgi apparatus, lysosomes and vesicles via the ZIPs and ZnTs.

Zn^{2+} mimics actions induced by hormones, cytokines and growth factors (Beyersmann and Haase, 2001), consistent with a signalling molecule. Zn^{2+} has been found to be co-stored with insulin and plays a crucial role in mediating the processing, storage and secretion of insulin in β-cells of the pancreas (Li, 2014). Zn^{2+} can bind to insulin to form a crystalline structure in dense vesicles which are released in response to physiological signals arising from increased glucose levels (Chausmer, 1998; Jansen et al., 2009; Taylor, 2005). Due to the potential regulatory role that Zn^{2+} may have on insulin release, Zn^{2+} supplementation may play a role in the management of diabetes. However, recent studies have demonstrated that the relationship between Zn^{2+} and diabetes is complicated, as reduced

levels of Zn^{2+} in the pancreas have been associated with the development of diabetes, whereas high levels may mediate damage to pancreatic cells via increased oxidative stress (Chimienti, 2013; Li, 2014; Wijesekara et al., 2009). Recent work studied the effect of Zn^{2+} supplementation in disease progression in diabetes, which carried out randomised double-blinded placebo-controlled phase 2 clinical trial with pre-diabetic subjects (Ranasinghe et al., 2018). Subjects were supplemented daily with 20mg of Zn^{2+} or placebo over a 12-month period. A significantly higher percentage of the subjects on placebo (no Zn^{2+}) were found to develop type 2 diabetes in comparison to the treatment group (25.0% (control group) to 11.0% (treatment group), $p<0.05$). This clinical trial concluded that Zn^{2+} supplementation was able to reduce disease progression to debates by improving the β-cell function of the pancreas, as well as increasing insulin sensitivity and blood glucose. This trial, therefore, provides evidence to exploit the role that Zn^{2+} may play in preventing diabetic development, and at the correct dosage may have therapeutic potential.

1.5.2 The role of Zn^{2+} as a secondary messenger

A secondary messenger is defined as a molecule that is intracellularly modulated in response to extracellular stimuli and can then induce appropriate intracellular signalling events with regards to the extracellular stimuli, resulting in physiological changes in the cell (Lodish et al., 2000; Newton et al., 2016). Zn^{2+} regulation in cells is highly important as it contributes to the activity of proteins in signalling pathways and has a potential role as a secondary messenger (Andreini and Bertini, 2012; Taylor and Pugh, 2016; Vu et al., 2013; Yamasaki et al., 2007). Elevated $[Zn^{2+}]_i$ modulates intracellular signalling pathways in several cell types, indicative of the mechanism of a secondary messenger. Changes in Zn^{2+} concentration have been found to modulate the activity of cytosolic proteins such as protein kinase C (PKC), protein kinase A (PKA), adenylate cyclase (AC), calmodulin-dependent kinase II (CaMKII), protein tyrosine phosphatases (PTPs) and caspase 3 (Brautigan et al., 1981; Csermely et al., 1988; Daaboul et al., 2012; Hubbard et al., 1991a; Lengyel et al., 2000; Perry et al., 1997).

Zn^{2+} has been shown to act as an intracellular secondary messenger in mast cells, (Yamasaki et al., 2007). Stimulation of mast cells via the IgE receptor (Fcε receptor 1) induces increases in $[Zn^{2+}]_i$, originating from the endoplasmic reticulum (ER). The Zn^{2+} fluorophore Newport green was used in this study to determine Increases in $[Zn^{2+}]_i$. The $[Zn^{2+}]_i$ increase is described as a 'Zn^{2+} wave' and is different from exogenous signalling. In this study, the concentration of $[Zn^{2+}]_i$ was not confirmed, however, was observed by measuring increases in Newport green fluorescence which is consistent with increases in $[Zn^{2+}]_i$ (Karim and Petering, 2016). Furthermore, the $[Zn^{2+}]_i$ chelator TPEN was used in this study to confirm the increases in Newport green fluorescence was attributable to Zn^{2+}. The authors of this

study suggest that the behaviour of Zn^{2+} is consistent with the action of a secondary messenger, in that its concentration varies in response to agonist stimulation, leading to intracellular signalling changes (Yamasaki et al., 2007). Further studies on monocytes have shown that stimulation with lipopolysaccharide (LPS) induced $[Zn^{2+}]_i$ elevation and that chelation of $[Zn^{2+}]_i$ inhibits LPS induced signalling in these cells (Haase and Maret, 2005). This study employed the Zn^{2+} fluorophore Fluozin-3 [which has been said to be currently the most sensitive Zn^{2+} probe (Krezel and Maret, 2007; Muylle et al., 2006; Zhao et al., 2008)] to assess increases in $[Zn^{2+}]_i$. In the same manner, as the study described above (Yamasaki et al., 2007) TPEN was again used in this study to confirm the increases in Fluozin-3 fluorescence were attributable to Zn^{2+}. The finding from this study provide further evidence for a role for Zn^{2+} a secondary messenger (Haase et al., 2008). However further work to investigate the role of Zn^{2+} as a potential secondary messenger in other cell types has yet to be clarified (Nakashima-Kaneda et al., 2013), before it can be included with the major secondary messengers known to regulate cellular activity, including cAMP, Ca^{2+} and G-proteins (Hadfield et al., 2013; Huang et al., 2015; Kato et al., 2017; Orem et al., 2017). Such work would provide further insight into the role of Zn^{2+} in human biology and could inform on the development of therapeutics targeting Zn^{2+}-induced signalling

1.6 The importance of Zn^{2+} in haemostasis

Zn^{2+} deficiency has been found to impair the haemostatic response which is required for the cessation of bleeding. Initial studies on Zn^{2+}-deficient rodents demonstrated the importance of Zn^{2+} in platelet function (Apgar, 1968; Gordon and O'Dell, 1980), as rodents subjected to dietary Zn^{2+} deficiency have an increased bleeding tendency and prolonged tail bleeding times, consistent with impaired platelet activation (Apgar, 1968). Further studies demonstrated that removal of dietary Zn^{2+} in rats results in impaired platelet function such as aggregation and secondary activation. Platelets of Zn^{2+}-deprived rats result in impaired platelet aggregation which is the primary process in haemostasis, as platelet aggregation leads to thrombus formation (Gordon and O'Dell, 1980).

As stated earlier, as a result of Zn^{2+} binding proteins in the plasma such as albumin and α2 microglobulin which result in exchangeable and non-exchangeable Zn^{2+} pools respectively, the final free concentration of Zn^{2+} is approximately 0.5µM in the plasma (Foote and Delves, 1984; Rükgauer et al., 1997; Taylor and Pugh, 2016; Scott and Bradwell, 1983). This level may be elevated by release from the surrounding vasculature. Zn^{2+} is released from both damaged cells and activated platelets, which can give rise to elevated levels in labile free Zn^{2+} in the plasma; this suggests that free Zn^{2+} may be concentrated at sites of vascular injury, implying the biological importance of Zn^{2+} in wound healing (Barceloux, 1999; Hallmans and Lasek, 1985; Lansdown et al., 2007, 2007; Michaëlsson et al., 1980;

Savlov et al., 1962; Taylor and Pugh, 2016). Previous work has provided evidence to establish that Zn^{2+} mediates wound healing although the exact mechanisms that induce this are yet to be determined. Labile Zn^{2+} or protein bound Zn^{2+} has been found to accumulate in skin tissue, upon injury (Lansdown, 1996; Lansdown et al., 2007; Sharir et al., 2010). Furthermore, the topical application Zn^{2+} of has been widely used to mediate efficient wound healing, thus further indicating the biological importance that Zn^{2+} has for cellular repair upon injury. Haemostasis enables wound healing, where platelets are the primary determinant of this process. Since activated platelets have been found to release Zn^{2+} as stated above, platelets may serve as an additional source of Zn^{2+} that may be released into the vasculature and promote the haemostatic process upon vascular injury. In addition, this interaction of Zn^{2+} with platelets may have an essential role in platelet activation (due to the association of Zn^{2+} deprivation and loss of platelet activity, as described earlier) and thrombus growth, which is to be explored further in this thesis (Murakami and Hirano, 2008, Kren et al., 2015, Matias et al., 2010).

Zn^{2+} is involved in other haemostatic processes such as coagulation , anticoagulation and fibrinolysis (Woodier et al., 2015). Zn^{2+} plays a key role in contact-mediated activation on endothelial cells and platelets, as it can bind to a number of coagulation proteins such as FXII (Factor XII) and induce conformational changes, enabling the proteins to localise to polyanionic surfaces (Vu et al., 2013). This results in the propagation of coagulation. Previous work has indicated that Zn^{2+} is involved in other haemostatic processes such as modulating fibrin formation, as well as playing a role in the anticoagulation pathways (Vu et al., 2013). However, the exact mechanism of Zn^{2+} in these processes is ill understood. Further work is still required to determine the contribution of Zn^{2+} in haemostasis and thrombosis (Woodier et al., 2015, Andreini et al., 2006).

1.6.1 The influence of Zn^{2+} on platelet physiology

Elevation of intracellular Zn^{2+} in platelets

Exogenous Zn^{2+} has been shown in recent work to gain entry into platelets, resulting in increased intracellular Zn^{2+} ($[Zn^{2+}]_i$) in platelets (Watson et al., 2016). In this study, using fluorometry, platelets loaded with the Zn^{2+} specific probe, Fluozin-3 (FZ-3) showed concentration-dependent increases in fluorescence upon application of exogenous $ZnSO_4$ (Watson et al., 2016). In addition to this, collagen-adhered human platelets loaded with FZ-3 exhibited increases in fluorescence in a time-dependent manner. These increases in FZ-3 fluorescence are consistent with increases of $[Zn^{2+}]_i$ as a result of Zn^{2+} entry which was confirmed by the use of the specific $[Zn^{2+}]_i$ chelator TPEN (Watson et al.,

2016). However, the mechanisms involved in mediating this entry remain to be confirmed in platelets (Watson et al., 2016).

Several mechanisms including Zn^{2+} transporters, exchangers and cation channels may mediate Zn^{2+} entry into platelets. As described earlier, the ZIP family of Zn^{2+} transporters could permit $[Zn^{2+}]_i$ entry into platelets. This is the case with other cell types, where the application of exogenous Zn^{2+} has found to induce $[Zn^{2+}]_i$ elevation via members of ZIP (Eide, 2004). ZIP7 (SLC29A7) and ZIP3 (SLC39A3) are present in the platelet proteome; however, the expression and function of these are yet to be confirmed in platelets (Burkhart et al., 2012; Taylor and Pugh, 2016). Glutamate receptors, which are expressed in platelets, may provide a pathway for Zn^{2+} entry, as has previously been demonstrated in neuronal cells (Kalev-Zylinska et al., 2014) (Sensi et al., 1997; Yin and Weiss, 1995). Glutamate is present in platelet dense granules and has been shown to mediate platelet activation, suggesting that glutamate mediates a secondary effect on platelet activation (Morrell et al., 2008). The relationship between glutamate and Zn^{2+} entry has not as yet been investigated.

TRP channels may also provide a way of facilitating Zn^{2+} entry. TRP channels are non-selective cation channels, of which TRPC6 and TRPM7 are expressed in megakaryocytes. TRPC6 and TRPM7 are Zn^{2+} -permeable (Bouron and Oberwinkler, 2014; Carter et al., 2006; Monteilh-Zoller et al., 2003). TRPC6 canonically mediates DAG-dependant Ca^{2+} entry into platelets. However, work carried out on HEK293 cells shows that TRPC6 also mediates Zn^{2+} entry in a DAG-dependent manner (Chevallet et al., 2014; Gibon et al., 2011). TRMP7 is more permeable to Zn^{2+} than Ca^{2+} and regulates Zn^{2+} cytotoxicity in cortical neurones. It is also expressed on megakaryocytes, making it a candidate Zn^{2+}-entry channel (Inoue et al., 2010; Leng et al., 2015).

NCX mediates both Ca^{2+} exit and entry in platelets, by exchanging three Na^{2+} for one Ca^{2+}. NCX may also mediate Zn^{2+} exit and entry following work carried out on neuron cells, where employment of a Zn^{2+} specific probe, mag-Fura-5 was used to measure $[Zn^{2+}]_i$ in cortical neurons. In this study by Sensi et al., (1997) the neurons exposed to extracellular Zn^{2+} and K^+ show increases in mag-Fura-5 fluorescence consistent with increased $[Zn^{2+}]_i$. This increase in fluorescence is inhibited by the addition of verapamil, gadolinium, nimodipine and ш-conotoxin GVIA, all blockers of voltage-gated Ca^{2+} channels. Thus, this inhibition indicates that $[Zn^{2+}]_i$ elevation as a result of Zn^{2+} entry is consistent with entry via voltage-gated calcium channels. Furthermore, this study illustrates that increases of $[Zn^{2+}]_i$ are sensitive to benzamil-amiloride, an NCX blocker, thus demonstrating NCX involvement of Zn^{2+} entry in neuron cells (Sensi et al., 1997). In platelets, three isoforms of NCX have been reported, primarily associated with Ca^{2+}, but they may also be associated with Zn^{2+}.

Zn^{2+} modulates platelet behaviour

Upon entry, exogenous Zn^{2+} modulates platelet behaviour and influence signalling processes leading to platelet activation in a manner that is consistent with a platelet agonist (Heyns et al., 1985; Taylor and Pugh, 2016; Trybulec et al., 1993; Watson et al., 2016). Platelet aggregation which is fundamental for thrombus formation and a marker of full platelet activation occurs in response to Zn^{2+} in the millimolar ranges, whilst sub-activatory micromolar levels of Zn^{2+} potentiate platelet aggregation in response to sub activatory concentrations of collagen, ADP, U46619, thrombin and adrenaline (Heyns et al., 1985; Watson et al., 2016). In support of this observation, chelation of $[Zn^{2+}]_i$ with the highly specific $[Zn^{2+}]_i$ chelator, TPEN, prevents the potentiating effect (Trybulec et al., 1993). This work indicates a role for Zn^{2+} in platelet aggregation (Taylor and Pugh, 2016; Watson et al., 2016).

Furthermore, application of exogenous Zn^{2+} to platelet suspensions following pre-treatment with antagonists of secondary signalling pathways in platelets reveals the mechanisms by which exogenous Zn^{2+} affects platelets. Antagonism of $\alpha_{IIb}\beta_3$ (integrin that enables platelet aggregation) abrogates platelet aggregation in response to Zn^{2+}, indicating that Zn^{2+}-induced aggregation is $\alpha_{IIb}\beta_3$ dependant and not as a result of cation-mediated agglutination, and further supporting a role for Zn^{2+} in regulating platelet aggregation (Gowland et al., 1969; Watson et al., 2016; Zhang and Chen, 2012). Inhibition of TxA_2, P2X1 Pre-treatment with aspirin (inhibits TxA_2 production), NF449 and 2-MeSAMP (purinergic receptor antagonists) inhibit Zn^{2+} induced aggregation. This demonstrates that Zn^{2+}-induced aggregation is mediated by other secondary signalling pathways such as TxA_2 and purinergic signalling which occur in response to primary platelet activation to further amplify platelet activity. Furthermore, cAMP signalling may play a role in Zn^{2+} induced aggregation due to the inhibitory effect induced by PGE_1 which elevates cAMP.

Inhibition of PKC fully abrogated Zn^{2+}-induced aggregation confirming a role for PKC in Zn^{2+} -induced platelet activation (Kowalska et al., 1994; Trybulec et al., 1993; Watson et al., 2016). PKC enzymes are metal-binding enzymes, which contain cysteine-rich zinc-binding domains necessary for structural integrity (Corbalán-García and Gómez-Fernández, 2006; Hubbard et al., 1991a). PKC activity is mediated via the application of exogenous Zn^{2+}, but not other cations (Csermely et al., 1988). Furthermore, studies on Zn^{2+}-deficient rats demonstrated reduced membrane association of PKC, suggesting a role for Zn^{2+} in PKC mobility during platelet activation (O'Dell et al., 1997). PKC mediated δ-granule release occurs in a Ca^{2+}- and DAG-dependent manner, whereas Zn^{2+} induces α-granule release and not δ-granule release (Hashimoto et al., 1994; Varga-Szabo et al., 2009). This work suggests that PKC activation may potentiate platelet activation in differing pathways, possibly

mediated by Zn^{2+} (Corbalán-García and Gómez-Fernández, 2006; Harper and Poole, 2010; Hashimoto et al., 1994; Taylor and Pugh, 2016; Watson et al., 2016).

Tyrosine phosphorylation is a critical step that occurs in intracellular signalling in platelets following receptor engagement (Buitrago et al., 2013; Murugappan et al., 2005). Recent work has shown that tyrosine phosphorylation of a wide variety of proteins occurs upon exogenous Zn^{2+} treatment in a time-dependent manner. The pattern of tyrosine phosphorylation induced by Zn^{2+} was found to differ from that induced by CRP-XL or thrombin, indicating that Zn^{2+} may be inducing a novel signalling pathway (Watson et al., 2016). Furthermore, increased phosphorylation of a high molecular weight protein (approximately 95kDa) was observed upon chelation of $[Zn^{2+}]_i$, suggesting that Zn^{2+} may influence tyrosine kinase or tyrosine phosphatase activity (Watson et al., 2016).

Protein tyrosine phosphatases (PTP) positively and negatively regulate platelet activity, some of which are inhibited by Zn^{2+} (Lu and Zhu, 2014). Small fluctuations of $[Zn^{2+}]_i$ inhibit phosphatases, which would otherwise enhance tyrosine phosphorylation (Brautigan et al., 1981). The platelet phosphatase PTP1B is a positive regulator of outside-in signalling and has an IC_{50} of 17 nM for Zn^{2+} (Haase and Maret, 2003; Tautz et al., 2015). Other platelet PTPs include SHP-1 which is also a positive regulator of platelet activation via $\alpha_{IIb}\beta_3$ activation following GpVI stimulation and SHP-2 which is a negative regulator of platelet activation. The IC_{50} of SHP-1 and SHP-2 for Zn^{2+} are 93 nM and 1-2 µM respectively (Haase and Maret, 2005, 2003; Lin et al., 2004; Ma et al., 2012; Mazharian et al., 2013). Additionally, the phosphatase PTEN which is a negative regulator of collagen-induced aggregation has an IC_{50} of PTEN for Zn^{2+} of 0.59 nM (Weng et al., 2010). These phosphatases could be prone to inhibition upon $[Zn^{2+}]_i$ elevation in platelets, which could play a major role in Zn^{2+} induced platelet activation (Taylor and Pugh, 2016).

The findings demonstrate the importance that Zn^{2+} may have on regulating platelet behaviour, as Zn^{2+} deficiency impairs platelet activity and high concentrations of Zn^{2+} induce full platelet activation as described above. The high concentrations of Zn^{2+} that induce full platelet activation as shown by Watson et al., 2016 may not be reached physiologically during haemostasis. However, the release of Zn^{2+} from ruptured atherosclerotic plaques or cells of the vasculature such as endothelial cells upon vascular injury may be high enough to induce Zn^{2+} mediated platelet activation (Siegel-Axel et al., 2006; Stadler Nadina et al., 2008; Taylor and Pugh, 2016; Watson et al., 2016). Interestingly chelation of $[Zn^{2+}]_i$ reduces agonist-evoked activity as shown by Watson et al., 2016, thus indicating

that $[Zn^{2+}]_i$ may be involved in regulating platelet activation. However, fluctuations in $[Zn^{2+}]_i$ during platelet activation is yet to be studied.

Elevation of $[Zn^{2+}]_i$ may be mediated via intracellular stores in a similar manner to $[Ca^{2+}]_i$ elevation from the DTS. In this manner, Zn^{2+} may be acting as an intracellular secondary messenger, as it is known to do so in other cell types [for example mast cells, as described in section 1.5.2 (Yamasaki et al., 2007)]. The role of Zn^{2+} as a secondary messenger in platelet was the primary focus of thesis. As the principal objective, the work described in this thesis was to investigate whether Zn^{2+} concentrations in platelets changed in response to agonist stimulation, and to assess the influence $[Zn^{2+}]_i$ may have had on platelets.

1.7 Aims and objectives

The information described above indicates that exogenous Zn^{2+} can induce platelet activation at high concentrations, and potentiating platelets to activation at submaximal concentrations. Thus, Zn^{2+} can act as a platelet agonist. However, numerous questions about the role of Zn^{2+} in platelet function remain. For example, the behaviour of Zn^{2+} as a secondary messenger in nucleated cells may indicate alternative activatory methods. Whether Zn^{2+} concentrations in platelets change as a result of conventional agonist stimulation has yet to be investigated. Furthermore, the effects of increases in $[Zn^{2+}]_i$ on specific aspects of platelet activation have yet to be examined in detail. On the basis of known Zn^{2+}-binding enzyme activities, minimal alterations of Zn^{2+} concentrations (picomolar to nanomolar concentrations) could be sufficient enough to alter platelet activity significantly. However, the nature of the targets of increased $[Zn^{2+}]_i$ remain unclear. A better understanding of the role of Zn^{2+} in platelet function would provide insight into activatory processes and may provide potential targets for therapeutic application.

The experimental program described in this thesis was designed to provide a better understand the mechanisms and roles of changes in $[Zn^{2+}]_i$ on platelet function. During the course of the project, the aims changed and developed resulting in the hypothesis that Zn^{2+} is an intracellular secondary messenger in platelets. Initially, the primary aim was to investigate the influence of increased $[Zn^{2+}]_i$ on platelet activation using Zn^{2+}-specific ionophores. First findings of this project showed that application of Zn^{2+} ionophores evoked an activatory response which was shape change and sub-maximal aggregation. These early findings demonstrated that $[Zn^{2+}]_i$ elevation could be evoked in platelets and may have a role in modulating platelet behaviour in a manner consistent with a secondary messenger. Thus, the elevation and role of $[Zn^{2+}]_i$ was assessed during platelet activation

upon stimulation with platelet agonists to investigate the hypothesis that Zn^{2+} is an intracellular secondary messenger in platelets.

The work carried out in this project demonstrated the first findings that $[Zn^{2+}]_i$ is elevated upon agonist stimulation, and regulates platelet processes such as aggregation, shape change, granule release and phosphatidylserine exposure. Thus, this work provides novel evidence to illustrate that $[Zn^{2+}]_i$ plays a significant role in platelets as a secondary messenger.

The major questions addressed in this thesis are:

1) Are platelet agonists able to elevate $[Zn^{2+}]_i$ in platelets?
2) Can $[Zn^{2+}]_i$ release be modelled in a similar manner to Ca^{2+}?
3) What is the functional role of $[Zn^{2+}]_i$ in platelet activity?
4) What physiological mechanisms are employed in platelets to increase $[Zn^{2+}]_i$ and is there interplay between Ca^{2+} and Zn^{2+} in platelet activation?

Chapter 2

2.0 Materials and Methods

2.1 Reagents and Materials

Fluozin-3-AM (FZ-3, Zn^{2+} indicator) and Fluo-4-AM (FL-4, Ca^{2+} indicator) were purchased from Invitrogen (Paisley, UK). Z-VAD (Pan-caspase inhibitor) was obtained from RnD Systems (Abingdon, UK). Phospho-Vasodilator-Stimulated Phosphoprotein (VASP, Ser157) and Phospho-Myosin Light Chain 2 (Ser19) antibodies were from Cell Signalling Technology (Boston, USA) and fluorescently-conjugated PAC-1, CD62P and CD63 antibodies were from BD Biosciences (Oxford, UK). Cross-linked collagen-related peptide (CRP-XL; GpVI agonist) was from Richard Farndale, Cambridge, UK. U46619 (TPα receptor agonist) was from Tocris (Bristol, UK), thrombin (PAR agonist) was from Sigma Aldrich (Poole, UK). Cytochalasin-D (Cyt-D, actin polymerisation inhibitor) was from AbCam (Cambridge, UK). Clioquinol, (Cq, Zn^{2+} ionophore, C_9H_5ClINO, K_dZn: 10^{-7}M, KdCa: $10^{-4.9}$M), Pyrithione (Py, Zn^{2+} ionophore, $C_{10}H_8N_2O_2S_2$, KdZn: 10^{-7}M, KdCa: $10^{-4.9}$M), A23187 (Ca^{2+} ionophore, $C_{29}H_{37}N_3O_6$), N,N,N′,N′-Tetrakis(2-pyridylmethyl)ethylenediamine (TPEN, Zn^{2+} chelator, K_dZn: 2.6×10^{-16}M, K_dCa: 4.4×10^{-5}M, (Arslan et al., 1985b; Hyun et al., 2004b; Matias et al., 2010b; Qian and Colvin, 2016a), DM-BAPTA-AM ($C_{34}H_{40}N_2O_{18}$, K_dZn: 7.9×10^{-9}M, K_dCa: 110×10^{-9}M, (Arslan et al., 1985b; Hyun et al., 2004b; Matias et al., 2010b; Qian and Colvin, 2016a), and membrane permeant anti-oxidising proteins, PEG-super oxidise dismutase (SOD) and PEG-catalase (CAT) were from Sigma Aldrich. Unless stated, all other reagents were from Sigma Aldrich.

2.2 Washed platelet suspension preparation from human blood

Blood was obtained from consenting healthy donors and was extracted via venepuncture into sodium citrate anticoagulant (11 mM tri-sodium citrate) in accordance with the Declaration of Helsinki and institutional ethics requirements. The whole blood was centrifuged for 15 mins at 240g. Platelet rich plasma (PRP) was extracted and mixed with prostaglandin E1 (PGE_1, 2 µM) before being centrifuged at 640 x g for 15 min. The platelet-poor plasma (PPP) was discarded and the platelet pellet re-suspended in Calcium-Free Tyrodes (CFT) solution (10 mM N-2-hydroxyethylpiperazine-N0-2-ethanesulfonic acid (HEPES), 140 mM NaCl, 5 mM KCl, 1 mM $MgCl_2$, 5 mM glucose, 0.42 mM NaH_2PO_4,

12 mM $NaHCO_3$, pH 7.4). Platelets were counted using a coulter counter and re-suspended to $2x10^8$ /ml before being allowed to rest for at least 30 min at 37°C.

2.3 Intracellular Zn^{2+} assessment

The role of intracellular Zn^{2+} ($[Zn^{2+}]_i$) in platelets and general cellular mechanisms, as described in Chapter 1 has always been overlooked in favour of Ca^{2+}. Many (cell permanent, via the constituted acetoxymethyl (AM) ester group) modulators that have been employed to assess intracellular Ca^{2+} ($[Ca^{2+}]_i$) in platelets and various cell types include fluorescent probes (fluorophores that asses fluctuations in $[Ca^{2+}]_i$) and chelators, often have higher affinities for Zn^{2+} than Ca^{2+} as illustrated by Table 2.1. As shown by this table (Table 2.1), all the Ca^{2+} fluorophores have higher affinities for Zn^{2+} than Ca^{2+}. However, the affinity (Kd value) for the Ca^{2+} fluorophore has not been confirmed (indicated by the * in Table 2.1). However Fluo-4 has been screened to evoke a much higher fluorescent intensity compared to other cations including Zn^{2+} ("Fluo-4, AM, cell-permeant",Thermo Fisher Scientific, 2018; Li et al., 2003; Paredes et al., 2008; Smith and Parker, 2009) thus demonstrating that Fluo-4 may serve as specific Ca^{2+} probe unlike the other Ca^{2+} fluorophores (Table 2.1). Thus Fluo-4 was employed as a Ca^{2+} probe in this thesis to assess fluctuations in $[Ca^{2+}]_i$ as a comparative measure to changes in $[Zn^{2+}]_i$. The specificity and validity of FL-4 to Ca is shown in figure 2.1, in section 2.3 below. Although contradictory evidence in previous work (Sensi et al., 2009) has shown that Fluo-4 has been able to bind to Zn^{2+} which is an underlying problem with Ca^{2+} probes and is a limitation that can not be currently overcome.

In contrast to Ca^{2+} fluorophores, commonly used Zn^{2+} fluorophores have higher affinities for Zn^{2+} than Ca^{2+} (Table 2.1). Similarly to Fluo-4, the affinity (Kd) of the Zn^{2+} fluorophore Fluozin-3 (FZ-3) to Zn^{2+} is known (indicated by the * in Table 2.1) but the affinity to Ca^{2+} is not yet confirmed. However, FZ-3 is responsive to Zn^{2+} in the nanomolar range and is not significantly affected by Ca^{2+} (Zhao et al., 2008). Furthermore FZ-3 has been shown to have higher affinity to Zn^{2+} than other Zn^{2+} fluorophores, and has a higher sensitivity to Zn^{2+} (Assaf and Chung, 1984; Bailey, 2000; Gee et al., 2002), thus making this probe useful for detecting small fluctuations in $[Zn^{2+}]_i$ which is desirable due to small fluctuations in $[Zn^{2+}]_i$ expected to occur in cells and platelet (as discussed in Chapter 1). Therefore, in this thesis, FZ-3 was employed as the Zn^{2+} probe to measure fluctuations in $[Zn^{2+}]_i$

Table 2.1 Commonly used Ca^{2+} and Zn^{2+} fluorophores and chelators

Reagent	Description/application	~Kd for Ca^{2+} (*in vitro*)	~Kd for Zn^{2+} (*in vitro*)
Fura-2-AM	Ca^{2+}-fluorophore	$2.3x10^{-7}$ M	$3x10^{-9}$ M
Fluo-4-AM	Ca^{2+}-fluorophore	$3.35x10^{-7}$ M	*
BAPTA-AM	Ca^{2+}-chelator	$110x10^{-9}$ M	7.9×10^{-9} M,
Newport green	Zn^{2+}-fluorophore	$1x10^{-4}$ M	$1x10^{-6}$ M
Fluozin-3-AM	Zn^{2+}-fluorophore	*	15Nm
TPEN-AM	Zn^{2+}-chelator	4.4×10^{-5} M	2.6×10^{-16} M

Chelators are a tool which provides an assessment to see if the signalling being seen is attributable to the cation in question. The widely used Ca^{2+} chelator, as described in Chapter 1 BAPTA has a higher affinity for Zn^{2+} than Ca^{2+}. Therefore the use of BAPTA to assess Ca^{2+} signalling may not provide an accurate assessment, as the signalling evoked by Ca^{2+} may also be attributable to Zn^{2+}.

In contrast to BAPTA, the affinity of the Zn^{2+} chelator, TPEN for Zn^{2+} is much higher than for Ca^{2+}. The K_d for TPEN and Zn^{2+} is $2.6x10^{-7}$ nM whereas with Ca^{2+} is $4.4x10^{-5}$ M(Matias et al., 2010b; Qian and Colvin, 2016a). Furthermore, TPEN has a much higher affinity for Zn^{2+} than other cations such as Fe^{2+}, Mn^{2+}, and Mg^{2+} where the K_ds of TPEN and these cations are $2.4x10^{-6}$ nM, $5.4x10^{-2}$ nM, and $2x10^{7}$ nM, respectively (Matias et al., 2010a; Qian and Colvin, 2016b). Thus, the employment of TPEN has become a chelator of choice for exploring Zn^{2+} signalling and was used in this thesis.

2.4 Cation mobilisation studies

Fluozin-3-AM (FZ-3) and Fluo-4-AM (FL-4) are fluorophores (section 2.3) that can be used to detect changes in intracellular Zn^{2+} concentrations $[Zn^{2+}]_i$ or calcium concentrations, $[Ca^{2+}]_i$ respectively. These dyes were reconstituted to 5 mM in DMSO, before being loaded into PRP to a final concentration of 2 µM for 30 min at 37°C. PRP was centrifuged for 15 minutes at 640 x g, and the platelet pellet was then re-suspended to the original PRP volume using CFT and rested at 37°C for 30 min prior to use. Fluorescence was monitored using a Fluoroskan Ascent fluorometer (ThermoScientific, UK) using 485/535 nm excitation and emission filters respectively. Results are expressed as an increase of background-corrected fluorescence at each time point relative to baseline: $(F_1-F_{background})/(F_0-F_{background})$.

Specificity and validation of Fluozin-3 and Fluo-4

Figure 2.1 illustrates calibration curves showing the fluorescence induced by the cations at different concentrations and the specificity of FZ-3 and FL-4 to Zn^{2+} and Ca^{2+} respectively. This calibration curve exhibits the minimal (F_{min}) and maximal (F_{max}) fluorescent values exhibited by FZ-3 and FL-4. Washed platelets suspensions were loaded with either FZ-3 or FL-4, before being treated with different concentrations of exogenous Zn^{2+} ($ZnSO_4$) or Ca^{2+} ($CaCl_2$).

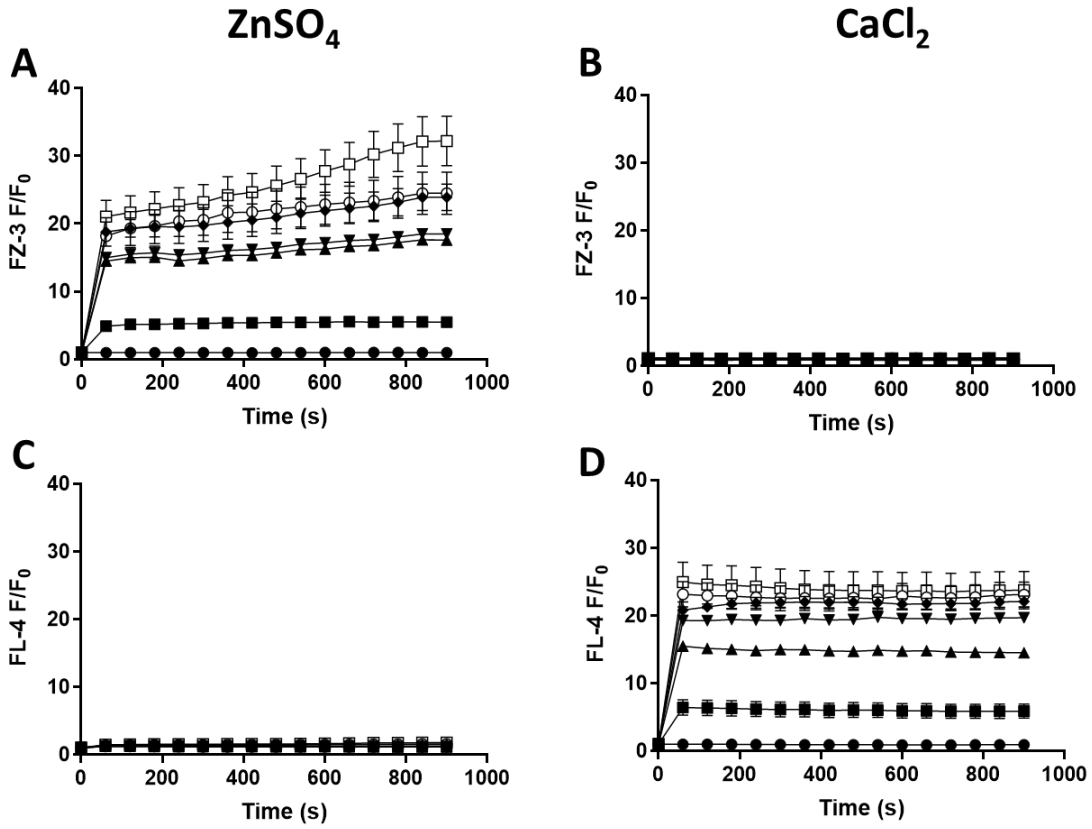

Figure 2.1 Calibration curves exhibiting the fluorescence range and specificity of FZ-3 and FL-4 to Zn^{2+} and Ca^{2+}. Washed Fluozin-3 (FZ-3) (A) and (B), or Fluo-4 (FL-4) (C) and (D) loaded platelet suspensions were treated for 15 mins with Zn^{2+} or Ca^{2+} ionophores in the presence of doses of exogenous 2 mM $CaCl_2$ or $ZnSO_4$, to determine F_{max} values. Fz-3 F_{min} was obtained from platelets pre-treated for 15 mins with 50 µM TPEN in (A), where the dose of $ZnSO_4$ is 0µM)., F_{max} was obtained following co-incubation with 5 µM Py with 2 mM $ZnSO_4$ for 15 mins as illustrated on (A). Fluo-4 F_{min} was obtained from platelets pre-treated for 15 mins with 2mM EGTA in the absence of extracellular Ca^{2+} (D). F_{max} was obtained following pre-incubation with 1 µM A23187 in the presence of 2 mM $CaCl_2$ (D). (A)and (C); ● 0µM $ZnSO_4$, ■ 1µM $ZnSO_4$, ▲3µM $ZnSO_4$, ▼ 10µM $ZnSO_4$, ♦ 30µM $ZnSO_4$,○ 100µM $ZnSO_4$, □ 2mM $ZnSO_4$. (B)and (D); ● 0µM $CaCl_2$, ■ 1µM $CaCl_2$, ▲3µM $CaCl_2$, ▼ 10µM $CaCl_2$, ♦ 30µM $CaCl_2$,○ 100µM $CaCl_2$, □ 2mM $CaCl_2$.

To measure the F_{min} value of FZ-3 platelets were pre-treated with 50 µM of TPEN and 5 µM pyrithione (Py) which enabled platelet Zn^{2+} to be equilibrated enabling more efficient chelation of Zn^{2+} by TPEN. Similarly, for measuring the F_{min} value of FL-4 to Ca^{2+}, 2 mM EGTA and 10µM BAPTA was used in conjunction with 1 µM of A23187.

To measure F_{max} values of FZ-3 and FL-4 to Zn^{2+} and Ca^{2+} respectively, 2 mM of $ZnSO_4$ or $CaCl_2$ along with 5 µM of Pyrithione for the FZ-3 loaded platelets, and 1 µM of A23187 for the FL-4 loaded platelets. For these F_{max} values, the low doses of the ionophores (Py and A23187) that were applied to equilibrate the cation (as described above) also acted as cation transporters (facilitating entry of the exogenous cation, into the platelets). This ensured that the respective cation was getting into the platelets and providing a correct fluorescent value. These values were used as a reference mark to provide indications of the levels of concentrations of the cations present (Bootman et al., 2013).

Application of $ZnSO_4$, resulted in a dose-dependent increase in FZ-3 fluorescence (Figure 2.1A), whereas application of $CaCl_2$, resulted in a dose-dependent increase in FL-4 fluorescence (Figure 2.1D). The maximum and minimum FZ-3 fluorescence (F_{max} and F_{min}) evoked by $ZnSO_4$ was 32.8 ± 3.4 and 1.0 ± 0.1, respectively (Figure 2.1A). The maximum and minimum FL-4 fluorescence (F_{max} and F_{min}) evoked by $CaCl_2$ was 24.1 ± 2.8 and 1.0 ± 0.1, respectively (Figure 2.1D).

Furthermore, the specificity of the FZ-3 and FL-4 to Zn^{2+} and Ca^{2+} respectively was also illustrated in Figure 2.5.1. There were no significant changes in FZ-3 fluctuations upon exogenous $CaCl_2$ treatment and no changes in FL-4 fluctuations upon exogenous $ZnSO_4$ treatment. Thus, providing strong evidence that FZ-3 is highly specific to Zn^{2+} and not to Ca^{2+} and that FL-4 is highly specific to Ca^{2+} and not to Zn^{2+}. Figure 2.5.1 serves a positive control for quantification of FZ-3 and FL-4 fluorescence and provide validity of these probes as indicators of fluctuations of $[Zn^{2+}]_i$ and $[Ca^{2+}]_i$, respectively.

2.5 Measurement of reactive oxygen species

Washed platelets were loaded with the reactive oxygen species (ROS) probe 2', 7'-Dichlorofluorescein diacetate (DCFH) in the same manner as FZ-3 and FL-4 in section 2.5 above. DCFH (10µM) is a widely used cell permeable ROS-specific probe (Baranwal et al., 2014; Kitajima et al., 2016; Liu et al., 2017). This probe is de-esterified intracellularly resulting in the highly fluorescent 2',7'-Dichlorofluorescein to fluoresce upon oxidation (Kitajima et al., 2016; Lopes Pires et al., 2017), enabling rapid and sensitive detection of ROS (Kitajima et al., 2016).

2.6 Light transmission platelet aggregometry

Platelet aggregation is the most widely investigated functional response that is induced by platelets (Born and Cross, 1963). This is primarily because the formation of blood clots (as a result of platelet aggregation) is of most interest to medical scientists that are studying platelet function, as aggregation served as the primary response to platelet activation and thrombus (blood clot) formation(Born, 1962). This is further reflected by antithrombotics and anti-platelet drugs being characterised as anti-aggregatory agents (Koo et al., 2010; Makris et al., 2013)

Light transmission aggregometry is a widely used technique that measures the aggregatory response of platelets(Born et al., 1978; Born and Cross, 1963). The basic principle of this technique (illustrated by Figure 2.2) is that light is passed through stirred suspensions of washed platelets (section 2.2) in cuvettes, where the light transmission at this stage represents the baseline and 0% aggregation (Born et al., 1978; Born and Hume, 1967; Michal and Born, 1971). Upon the addition of a stimulus, platelets activate and undergo shape change which results in a reduced proportion of light passing through the suspensions, thus illustrating a reduction in the percentage of light transmission upon the initial activatory stages of platelets (Michal and Born, 1971). This is followed by an increase in light transmission as the platelets aggregate and take up less volume in the cuvette (Latimer, 1983).

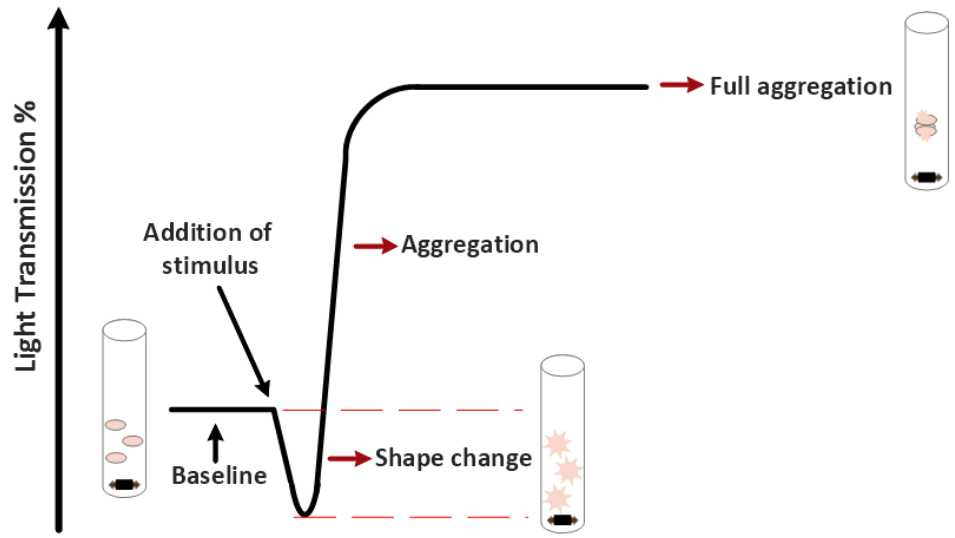

Figure 2.2. Light transmission aggregometry. Addition of a stimulus (in stirring conditions) induces a drop in the light transmission % from the baseline (0% aggregation), as a result of platelet shape change. As the platelets change shape, less light is able to pass through the cuvette. Aggregation proceeds following shape change which results in an increase in light transmission %. As the platelets aggregate, more light is able to pass through the cuvettes, eventually resulting in full platelet aggregation and maximal light transmission %.

Aggregation of washed platelet suspensions was quantified using an AggRam aggregometer (Helena Biosciences, Gateshead, UK) under stirring conditions at 37°C. Background light transmission was established using cuvettes containing CFT. Stir bars and 250 µL of rested washed platelet suspensions were added to cuvettes which were then placed in the aggregometer. 2.5 µL (a 1:100 dilution) of agonist was added to the platelets. Aggregation traces were acquired using proprietary software (Helena Biosciences) and analysed with Microsoft Excel and GraphPad Prism (Version 7.01).

2.7 Western Blotting of platelet proteins

Western blotting was used to examine the expression or changes in the phosphorylation state of specific platelet proteins in response to specific treatments. Platelets were prepared as before and stimulated with the given agonists for the given time in aggregometry cuvettes. Reducing sample buffer (0.125 M Tris HCL pH 6.8, 4% SDS, 20% glycerol, 10% 2-mercaptoethanol, 0.004% bromophenol blue) was added (5%) to the platelets, which were then heated to 95^{o}C for 10 minutes before being centrifuged at 13000 x g for 10 min to pellet insoluble materials. Samples were electrophoresed on SDS-PAGE gels at 100V for 2 hours. Electrophoresed proteins were transferred to a polyvinylidene difluoride (PVDF) membrane and preincubated with methanol for 5 mins followed by transfer buffer (1 x NuPAGE transfer buffer, ThermoFisher) for 5 mins. Sodium dodecyl sulfate-polyacrylamide gel electrophoresis (SDS-PAGE) gels were assembled with PVDF membrane and filter paper on a semi-dry protein transfer apparatus (Bio-Rad, Trans-Blot Turbo transfer system, UK). Proteins were transferred from the gel to the membrane at 15V for 30 mins. Membranes were blocked with 1 x Tris-buffered saline, TBS (20mM Tris, 150mM NaCl, pH 7.6) with 5% bovine serum albumin buffer) for 1 hour. The membranes were then incubated with primary antibody in blocking buffer (TBS; 5% bovine serum albumin; 0.05% Tween-20) and were incubated overnight at 4^{o}C under constant agitation. Membranes were washed with TBS/0.05% Tween-20 three times for 5 minutes to remove excess antibody. The membranes were then incubated for 1 hour at room temperature with horseradish peroxidase (HRP)-conjugated or the fluorescently tagged secondary antibodies. The membrane was rewashed three times as before. Antigen-antibody interactions were visualised on the membrane following incubation with Enhanced Chemiluminescent reagent (ECL). Table 2.4.1 outlines the antibodies that were used for Western blotting.

Table 2.7.1 Primary antibodies used for Western blotting

Primary Antibody	Species derived from	Dilution	Supplier	References of application on human samples
Anti-Phosphotyrosine Antibody, clone 4G10	Mouse	1:5000	Merck Millipore	(Aman et al., 2011; Bochtler et al., 2012; Lin et al., 2009; Petersen and Hagan, 2005; Roll and Reuther, 2012; Rollet-Labelle et al., 2013)
β-Actin	Mouse	1:1000	AbCam	(Du et al., 2018; Fiaturi et al., 2018; Joshi et al., 2018; Lee et al., 2018; Minashima and Kirsch, 2018)
Phospho-Myosin Light Chain 2 (Ser19)	Rabbit	1:1000	Cell Signalling Technology	(Cao et al., 2017; Miskolczi et al., 2018; Mogami et al., 2018; Ye and Sun, 2017)
Phospho- Phospho-Vasodilator-Stimulated Phosphoprotein (VASP, Ser157)	Rabbit	1:1000	Cell Signalling Technology	(Bernusso et al., 2015; Canton et al., 2016)
Anti-phospho-ZIP7 (Ser275/276)	Mouse	1:1000	Merck Millipore	(Olgar et al., 2018; Taylor et al., 2012, 2008)

Table 2.7.2 Secondary antibodies used for Western Blotting

Secondary Antibody	Species derived from	Dilution	Supplier	References of application on human samples
α – Mouse horseradish peroxidase (HRP)	Goat	1:5000	Thermo-Fisher	(Kim et al., 2016)
α – Rabbit HRP	Donkey	1:5000	Thermo-Fisher	(Zhao et al., 2015)
α – Goat HRP	Rabbit	1:5000	Thermo-Fisher	(Alsted et al., 2009; Wingelhofer et al., 2016)

2.7.1 Western blot quantification

ImageJ (v1.45, NIH, Bethesda, MD, USA) was used as a tool to quantify the expression of western blots (refer to section 30.13, Image J user guide, (Ferreira and Rasband, 2012). Levels of protein expression were quantified as a ratio of each protein band relative to the loading control of that protein bands lane. Values were expressed as arbitrary units. Quantification of western blots via Image J has been

widely used as a consistent measurement to assess levels of expression of proteins (Gassmann et al., 2009; Kumar et al., 2014; Lopes Pires et al., 2017).

2.8 Quantification of Phosphatidyl-serine (PS) exposure in platelets

Fluorescein isothiocyanate (FITC)-Annexin V binds to exposed Phosphatidyl-serine (PS) in a Ca^{2+} dependent manner (Meers and Mealy, 1993). Thus, this protein enabled assessment of PS exposure that occurs on activated platelets that may also be procoagulant (Sims et al., 1989; Thiagarajan and Tait, 1990; Zwaal et al., 1992).

Washed platelets were prepared to $2x10^8$/mL as described in section 2.2. FITC_-Annexin V antibody was diluted in Tyrode's solution (CFT buffer containing 2mM $CaCl_2$, at pH 7.4) to a 1:100 dilution (Annexin V solution). 50 µl of washed platelets were diluted into 445 µl of Tyrodes solution containing the treatment of interest at its final working concentration and allowed to incubate at the designed time. Following incubation for the designed time, 25 µl of sample (washed platelets in Tyrodes with treatment of interest) was added to 25 µl of the Annexin V solution and analysed using the BD Accuri C6 flow cytometer (Beckton Dickinson, UK) via the FL1-A laser of this instrument to detect the FITC-tagged Annexin V antibody (representation of this is shown in Figure 2.3).

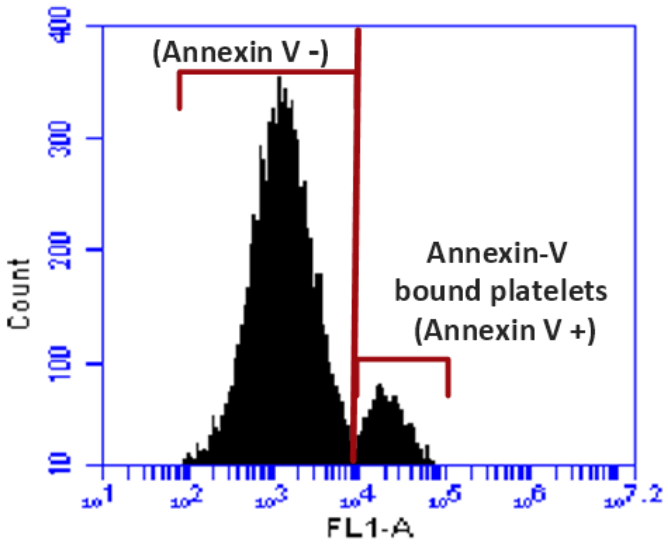

Figure 2.3. Representation of Annexin V binding via flow cytometry. Increased binding of Fluorescein isothiocyanate (FITC)-Annexin V antibody binds to exposed Phosphatidyl-serine (PS). This results in a shift of the FL1-A laser reading, which increases (shifts to the right), illustrating a population of platelet that is annexin-V bound (Annexin V +), that is distinguishable from platelets that are not bound to annexin V (Annexin V -).

2.9 Detection of platelet activation

The PAC-1 antibody is widely used to detect activation of $\alpha_{IIb}\beta_3$. PAC-1 recognises an epitope on activated $\alpha_{IIb}\beta_3$ which is very close to the binding site of fibrinogen. PAC-1 binds to of $\alpha_{IIb}\beta_3$ when it is converted into a high-affinity binding state following platelet activation (Bennett et al., 1988; Shattil et al., 1986, 1985). Activated $\alpha_{IIb}\beta_3$ binds to the arginine-glycine-aspartate (RGD) sequence found on proteins such as fibrinogen. Binding of PAC-1 to $\alpha_{IIb}\beta_3$ is inhibited by peptides which contain the arginine-glycine-aspartate sequence, thus providing further evidence to confirm the ability of PAC-1 to bind to the upregulated state (high-affinity state) of $\alpha_{IIb}\beta_3$(Gartner and Bennett, 1985; Plow et al., 1985; Taub et al., 1989).

The CD62P (a membrane glycoprotein also known as P-selectin) antibody is used to assess α-granule release in platelets which occurs upon platelet activation (Matowicka-Karna, 2016). α-granules contain CD62P which is transported rapidly and expressed on the platelet surface upon platelet activation (Fägerstam et al., 2000). The CD62P antibody specifically binds to CD62P and provides an assessment of the level of CD62P externalisation, which thus quantifies α-granule release (Frenette et al., 2000).

The CD63 antibody is widely used to assess dense granule release upon platelet activation (Vinholt et al., 2017; Wauters et al., 2015). CD63 (a membrane glycoprotein) is present in dense granules and upon platelet activation, is rapidly translocated to the surface of platelets (Heijnen and van der Sluijs, 2015; Joseph et al., 1998). Binding of the anti-CD63 antibody to CD63 quantifies dense granule release (Choudhury et al., 2007).

Washed platelet suspensions were prepared as previously described (section 2.2) and incubated with fluorescently-conjugated antibodies targeting markers of platelet activation: FITC-PAC-1 (Integrin $\alpha_{IIb}\beta_3$ activation), Phycoerythrin (PE)-CD62P (α granule release) and Alexa Fluor 647-CD63 (dense granule release). Antibody binding, following agonist or ionophore stimulation, was assessed using an Accuri C6 flow cytometer over the designed time. The total volume per sample that was analysed by the flow cytometer was 120 µL plus the volume of the antibody (1.2µL). 3 µL of washed platelets were added to 105 µl of CFT, with 1.2 µL of the fluorescently-conjugated antibodies (1:100 dilution), and 12 µl of the agonist or ionophore was added at the appropriate concentration.

2.10 Real-time analysis using flow cytometry

Washed platelets were prepared in the same manner as describes in section 2.4. The samples were analysed using the Accuri C6 flow cytometer in the same manner as described in section 2.9; however the agonist was added after 30 seconds, and changes in fluorescence of the probe were measured in real time, to assess live changes in signalling upon treatment. Real-time analysis using flow cytometry has been widely used in biological application and has been used to asses real-time mobilisation of Ca^{2+} in human platelets and depletion of Ca^{2+} stores (Park et al., 2002; Vines et al., 2010). Thus, this type of analysis was employed in this thesis to assess real-time mobilisation of cations and to assess store-operated cation entry and mobilisation. Gates were applied every 5 seconds on the plot, which gave a reading every 5 seconds for analysis.

2.11 Platelet spreading

Real-time imaging of platelet spreading was carried out using the protocol employed by Aslan et al., 2012. Glass coverslips (25mM diameter, 1.5 thickness, Fisher Scientific) were coated with 100µM of fibrinogen and were left to incubate at 4^{o}C for 24 hours. Following incubation, the coverslip was washed with PBS three times (phosphate buffered saline) and blocked with 1 % BSA (bovine serum albumin, blocking buffer), before being washed again with PBS three times, making sure the coverslips did not dry out.

Washed platelet suspensions were prepared in the same manner described in section 2.2. However, a higher concentration of $2x10^7$ was used to enable easier visualisation of platelets under the microscope. Washed platelets were stained (incubated for 1 hour at 37^{o}C, following preparation of the washes platelets) with 1µM of DIOC6 (Dihexyloxacarbocyanine Iodide) which is a green fluorescent membrane stain and was employed to enable quantification of the surface coverage of spread platelets. 10µL of platelets with their appropriate treatment was pipetted directly onto the fibrinogen-coated coverslip, and after each specified time point in the experiment, platelets were fixed with 10µL of formaldehyde (0.85% NaCl and 0.2% formaldehyde), before being washed with CFT to wash away the fixative and any unbound platelets.

Images of platelets adhering to coated fibrinogen (100µM) coverslips were acquired using an LSM510/Axiovert laser scanning confocal microscope with 60x oil NA1.45 objective (Zeiss, UK). Surface coverage of $DIOC_6$-stained platelets was quantified using ImageJ (v1.45, NIH, Bethesda, MD, USA) and the LSM reader plugin in the software. The fluorescence of the DIOC6 stain on the spread platelets

was measured to assess the surface area coverage of the platelets. The laser excitation/ emission of the confocal microscope that was used to assess DIOC6 fluorescence was 488/543nM.

2.12 Tissue culture

2.12.1 Culture of mouse embryonic fibroblast (MEF) cell lines

In addition to platelets, mouse embryonic fibroblasts (MEF) were employed to assess the influence of intracellular Zn^{2+} on cytoskeletal changes that may occur in cells that were found to be significantly influenced by Zn^{2+} in platelets in this thesis.

MEF are widely used as models to study cell spreading for a variety of reasons including; they are the primary source of extracellular matrix (ECM) proteins, which, in addition to providing a scaffold for cells, play key roles in determining cell phenotype and function (Ltd, 2011).Thus MEF are ideal cell lines to efficiently study cytoskeletal rearrangement in nucleated cells (Cai et al., 2006; Chen et al., 2016; Ltd, 2011; J. Wang et al., 2014)

MEF cells were cultured in Dulbecco's Modified Eagle's medium (DMEM) supplemented with 10% foetal bovine serum (FBS), 2 mM glutamine, 10µL/mL of the Penicillin-Streptomycin solution in an incubator at humidified conditions (37°C and 5% CO_2). Cells were passaged once they had reached approximately 80% confluence. Media was removed, and the cells were washed with Dulbecco's Phosphate Buffered Saline (DPBS) before being treated with trypsin-EDTA (5 mM for 2-3 mins in a humidified incubator) to detach the cells from the flask. Cells were then re-suspended in fresh DMEM, centrifuged 200 x g for 5 minutes, and the pellet was resuspended in fresh DMEM. The cells were diluted down to their appropriate concentrations for the designated experiment or were sub-cultured for continuous culturing.

2.12.2 Mouse embryonic fibroblast (MEF) spreading assays

MEF cells were seeded into 6 well plates prior to experimentation for the designated time periods. Following incubation, cells were rinsed with DPBS and fixed with 4% paraformaldehyde (PFA) for approximately 10 minutes at room temperature. Cells were then washed with DPBS and permeabilised with 0.2% Triton-X100 in 5% goat serum-DPBS (goat serum was added here as a blocking agent) for 15 minutes at room temperature. The cells were then washed with DPBS and actin was stained for 1 hour at room temperature with Phalloidin- iFluor 594 Conjugate (Cayman Chemical,

USA), at a 1:1000 dilution. Cells were washed with DPBS and then co-stained 4',6-Diamidino-2-Phenylindole, Dihydrochloride (DAPI). Following staining, the cells were then imaged using the ZOE fluorescent cell imager (Bio-Rad). DAPI was visualised using excitation/emission of 358/461nm, while Phalloidin-iFluor594 was visualised using excitation/emission of 590/618nm

2.13 Data Analysis

Maximum and minimum aggregation, F/F_0 values, activation marker percentages and Annexin V binding were calculated using Microsoft Excel. Western blots and platelet spreading were analysed calculated ImageJ (NIH Image) and Microsoft Excel. Data were analysed in GraphPad Prism 7.01 by either student t-test or two-way ANOVA followed by Tukey's post hoc test with Dunnett's, Tukey's or Sidak's multiple comparison tests as appropriate. Data are presented as the means±SEM and significance is denoted as **** ($P<0.0001$), *** ($P<0.001$), ** ($P<0.01$) and * ($P<0.05$).

Chapter 3

3.0 Intracellular platelet Zn^{2+} increases in response to physiological agonists and acts as a secondary messenger.

3.1 Background

The role and importance of Zn^{2+} in haemostasis and platelets has not been fully elucidated. Zn^{2+} is concentrated in atherosclerotic plaques, and also in epithelial cells, from where it is released upon damage (Sharir et al., 2010; Stadler Nadina et al., 2008). Thus Zn^{2+} present in the vasculature is likely to be present at areas of haemostasis and may be elevated in the microenvironment of a growing thrombus. Zn^{2+} has an acknowledged role in haemostasis, in particular in coagulation, where it acts as a cofactor of Factor XII (Vu et al., 2013). Exogenous Zn^{2+} enters platelets and induces platelet activation that is dependant on protein tyrosine phosphorylation, although the specific proteins that undergo tyrosine phosphorylation have not been confirmed (Watson et al., 2016). The route of Zn^{2+} entry into platelets is yet to be determined, although candidate mechanisms potential involve Zn^{2+} transporters (ZIPs), TRP channels, glutamate receptors, and the Na^{2+}/Ca^{2+} exchanger (NCX, Bouron and Oberwinkler, 2014; Carter et al., 2006; Kalev-Zylinska et al., 2014; Morel et al., 2008; Sensi et al., 1997; Yin and Weiss, 1995). Exogenous Zn^{2+} at sub activatory concentrations (30µM $ZnSO_4$) potentiates platelet aggregation in response to agonists including thrombin and CRP-Xl at low concentrations, ranging from 0.03-1U/mL for thrombin and 0.01-0.3 µg/mL for CRP-XL (Watson et al., 2016). This work provides evidence that Zn^{2+} serves as an agonist, and may play an integral part in platelet activation and signalling.

The importance of elevation of intracellular Ca^{2+} ($[Ca^{2+}]_i$) in response to agonist stimulation of platelets is well documented. Agonists such as CRP-XL, thrombin, and U46619 (a thromboxane A2 receptor agonist) induce $[Ca^{2+}]_i$ release from the DTS (dense tubular system) via the the activity of PLC isoforms (PLCβ and PLCγ, Figure 1.4.1) (Varga-Szabo et al., 2009). Increases in $[Ca^{2+}]_i$ couple to physiological responses, consistent with a role as a secondary messenger. Conversely, the physiological role of intracellular Zn^{2+} ($[Zn^{2+}]_i$) has yet to be investigated in platelets. Whilst platelets are known to release Zn^{2+} via their α-granules (Marx et al., 1993a), whether $[Zn^{2+}]_i$ increases upon activation, as well as the nature of storage sites are yet to be determined. Labile or 'free' Zn^{2+}, as well as membrane-bound and protein-bound Zn^{2+} which act as intracellular storages sites for Zn^{2+}, are found in various cell types such as neurons and immune cells. The mobilisation of Zn^{2+} from these

intracellular stores increases Zn^{2+} bioavailability which is then able to regulate downstream processes (Marger et al., 2014; Nakashima-Kaneda et al., 2013; Takeda et al., 2014).

Proteins such as metallothioneins (MT's) can sequester Zn^{2+} and act as a Zn^{2+} store. The release of Zn^{2+} from metallothionines is redox-dependent (Andrews, 2001; Hardyman et al., 2016; Marreiro et al., 2017). These proteins contain cysteines which have thiol groups that undergo redox changes (Bell and Vallee, 2009). Under reducing conditions,thiols are able to bind Zn^{2+}. However, upon oxidation (for example by reactive oxygen species, ROS), crosslinking the thiols results in liberation of Zn^{2+} (Hardyman et al., 2016; Kimura and Kambe, 2016). Thus elevation of $[Zn^{2+}]_i$ in nucleated cells is dependant on ROS concentration and signaling (Faller et al., 2014; Tang et al., 2014). ROS levels and antioxidant levels are tightly maintained to avoid oxidative stress which is evoked upon an imbalance between levels of ROS and antioxidants (such as superoxide dismutase (SOD) and catalase (CAT). The role of Zn^{2+} in the regulation of oxidative stress nucleated cells has been widely investigated (Marreiro et al., 2017). SOD utilises metal ions such as copper (Cu^{2+}) and Zn^{2+} as co-factors to convert ROS species such as O_2^- (superoxide radicals) to less harmful ROS species such as H_2O_2 (hydrogen peroxide) (Noleto Magalhães et al., 2011; Paz Matias et al., 2014; Tainer et al., 1983). Therefore Zn^{2+} is important for preventing oxidative stress, and may have evolved as a defense mechanism against oxidative stress (Foster and Samman, 2010). Tight regulation of $[Zn^{2+}]_i$ is therefore critical for the regulation of oxidative stress, as excessive Zn^{2+} can induce oxidative stress and pro-inflammation and cytotoxicity as illustrated in studies on neurons (described in Chapter 1) (Bush and Tanzi, 2008; Frederickson, 1989; Inoue et al., 2010). In support of this observation, it has been shown that Zn^{2+} deficiency evoke oxidative stress, for example in endothelial cells, where Zn^{2+} deficiency results in increased activity of inflammatory molecules as a result of oxidative stress (Abdelhalim et al., 2010; Bao et al., 2010; Biagiotti et al., 2016)

Increases in $[Zn^{2+}]_i$ induces expression of MTs in various nucleated cell types such as neurons (McCord and Aizenman, 2014). This was initially observed in rodents, where dietary Zn^{2+} supplementation resulted in increased expression of the transcription factor known as Metal Transcription Factor-1 (MTF-1) (Andrews, 2001; Hardyman et al., 2016). This Zn^{2+}-dependant transcription factor is responsible for the expression of MTs and ZnTs. MTF-1 plays a key role in the regulation of Zn^{2+} concentrations in cells, by regulating expression of both MTs (which sequester Zn^{2+}),and ZnTs (which enable the efflux of Zn^{2+} from the cytoplasm of cells, illustrated in Figure 1.11) when Zn^{2+} levels are excessive within cells (Marreiro et al., 2017). Other transcription factors such as nuclear factor (erythroid-derived 2)-like 2 (Nrf2) are also able to mediate the expression of MTs as

well as genes which encode antioxidants and contribute to the regulation of Zn^{2+} and oxidative stress in cells (Ha et al., 2006; Li et al., 2014).

The implications of elevations of $[Zn^{2+}]_i$ and the subsequent effect on the regulation of oxidative stress via ROS scavenging is yet to be studied thoroughly in platelets. The mechanism of $[Zn^{2+}]_i$ elevation in response to oxidative stress (which results in ROS level increases) may also be applicable in platelets, where it could serve as a major mechanism for $[Zn^{2+}]_i$ elevation in platelets. To summarise, nucleated cells can store Zn^{2+} via MT sequestration, which under oxidative stress releases Zn^{2+} into the cytosol (Andrews, 2001, 2001; Hardyman et al., 2016). Zn^{2+} then mediates antioxidant activity to prevent oxidative stress-induced damage (Noleto Magalhães et al., 2011; Paz Matias et al., 2014, 2014). Zn^{2+} released from the MTs may also act on other signalling proteins in cells, as Zn^{2+} interacts with various cytosolic signalling proteins.

In nucleated cells, agonist-evoked increases in $[Zn^{2+}]_i$ result in the modulation of signalling proteins such as PKC and CamKII in a similar manner to that induced by elevated $[Ca^{2+}]_i$ as described in Chapter 1 (Csermely et al., 1988; Hubbard et al., 1991a; Perry et al., 1997; Pitt and Stewart, 2015). Whilst the role of Zn^{2+} as a secondary messenger in nucleated cells has been the subject of recent research interest, the role of $[Zn^{2+}]_i$ modulation upon agonist stimulation in platelets is yet to be determined.

3.1.1 Aims and Hypothesis

The aim of the work described in this chapter was to determine whether platelet agonists are able to elevate $[Zn^{2+}]_i$ in platelets. The experiments described in this chapter focus on determining whether $[Zn^{2+}]_i$ concentrations change in response to agonist stimulation in a manner consistent with a secondary messenger. The primary hypothesis of this chapter is that $[Zn^{2+}]_i$ is elevated upon agonist stimulation. Additionally, due to the extensive work that has been previously documented with regards to oxidative stress and $[Zn^{2+}]_i$ elevation in various cell types, the role of ROS increases on $[Zn^{2+}]_i$ in platelets was also investigated. The hypothesis was that upon platelet activation, fluctuations in $[Zn^{2+}]_i$ are redox-sensitive as a result of changes in levels of ROS.

3.1.2 Methods

A review of the literature has confirmed that platelet activation occurs upon stimulation of the major collagen receptor, glycoprotein VI (GpVI), and G-protein coupled receptors (GPCR's) such as Protease-Activated Receptors (PAR) and the Thromboxane receptor (TP) (Cimmino and Golino, 2013;

Corinaldesi, 2011; Stalker et al., 2012). GpVI is activated by the collagen mimetic; cross-linked collagen-related peptide (CRP-XL), PAR is activated by thrombin, and TP is activated by the thromboxane A_2 (TxA_2) analogue, U46619 which is a more stable for experimental use than TxA_2 (Brass et al., 1993a; Dunster et al., 2015; Reséndiz et al., 2007; Smith et al., 1980; Watson et al., 2005). CRP-XL, thrombin, and U46619 mediate $[Ca^{2+}]_i$ fluctuations via the activation of either PLCβ and PLCγ, which enables mobilisation of Ca^{2+} from the DTS (dense tubular system) (Authi et al., 1993; Brüne and Ullrich, 1991; Smith et al., 1992). In a similar manner to the assessment of $[Ca^{2+}]_i$ fluctuations in previous publications, $[Zn^{2+}]_i$ fluctuations in response to the agonists stated above were measured. Agonist-dependent $[Zn^{2+}]_i$ fluctuations was recorded using fluorometry following stimulation of washed, FZ-3-loaded platelet suspension. Fluorescence fluctuations were measured over a 6min period (section 2.4, Chapter 2). $[Ca^{2+}]_i$ fluctuations (as measured by FL-4 fluorescence fluctuations) were also assessed, as a comparison to Zn^{2+}. Fluorescence responses are expressed as corrected fluorescence (F/F_0) (section 2.4, Chapter 2). Validation of the use of FZ-3 and FL-4 as probes to measure $[Zn^{2+}]_i$ and $[Ca^{2+}]_i$ respectively, is provided in Chapter 2.

Reagents used to manipulate platelet cation levels included $[Zn^{2+}]_i$ and $[Ca^{2+}]_i$ chelators, N,N,N',N'-Tetrakis (2-pyridylmethyl)ethylenediamine) (TPEN) and 2-bis(o-aminophenoxy) ethane-N, N, N', N'-tetraacetic acid (BAPTA), respectively. Previous work found that 50µM of TPEN was the most effective concentration in chelating $[Zn^{2+}]_i$ in washed human platelets, even when a high concentration of exogenous Zn^{2+} (1 mM $ZnSO_4$) was applied to the platelets (Watson et al., 2016). Thus 50µM of TPEN was used as the working concentration in this work. Several studies which investigated Ca^{2+} signalling in platelets confirmed that 10µM of BAPTA-AM is the most effective concentration to chelate $[Ca^{2+}]_i$ (Davies et al., 1989; Sargeant et al., 1994; Vostal et al., 1991). Thus 10µM of the $[Ca^{2+}]_i$ chelator was employed in this work to assess Ca^{2+} signalling.

In order to assess redox sensitivity, hydrogen peroxide (H_2O_2) was used as a ROS agonist. The antioxidants Polyethylene glycol-superoxide dismutase (PEG-SOD) and Polyethylene Glycol-catalase (PEG-CAT) were also employed at concentrations previously shown to be effective in platelets (30U/mL and 300U/mL, respectively, Lopes Pires et al., 2017). Changes in ROS concentration were measured using the ROS probe, 2', 7'-Dichlorofluorescein diacetate (DCFH) at a concentration of 10µM (Lopes Pires et al., 2017).

3.2 Results

3.2.1 Intracellular Zn^{2+} is released during platelet activation by physiological agonists

In the experiments described in this chapter, conventional platelet agonists, CRP-XL, U46619, and thrombin were employed to investigate whether $[Zn^{2+}]_i$ levels fluctuate in response to platelet activation, in a similar manner to Ca^{2+}. The hypothesis of this section was that $[Zn^{2+}]_i$ elevation occurs in response to agonist stimulation.

Treatment of FZ-3-loaded platelet suspensions with different concentrations of CRP-XL or U46619 resulted in increased FZ-3 fluorescence, consistent with increases in $[Zn^{2+}]_i$. Stimulation with thrombin did not induce a response (Figure 3.1).

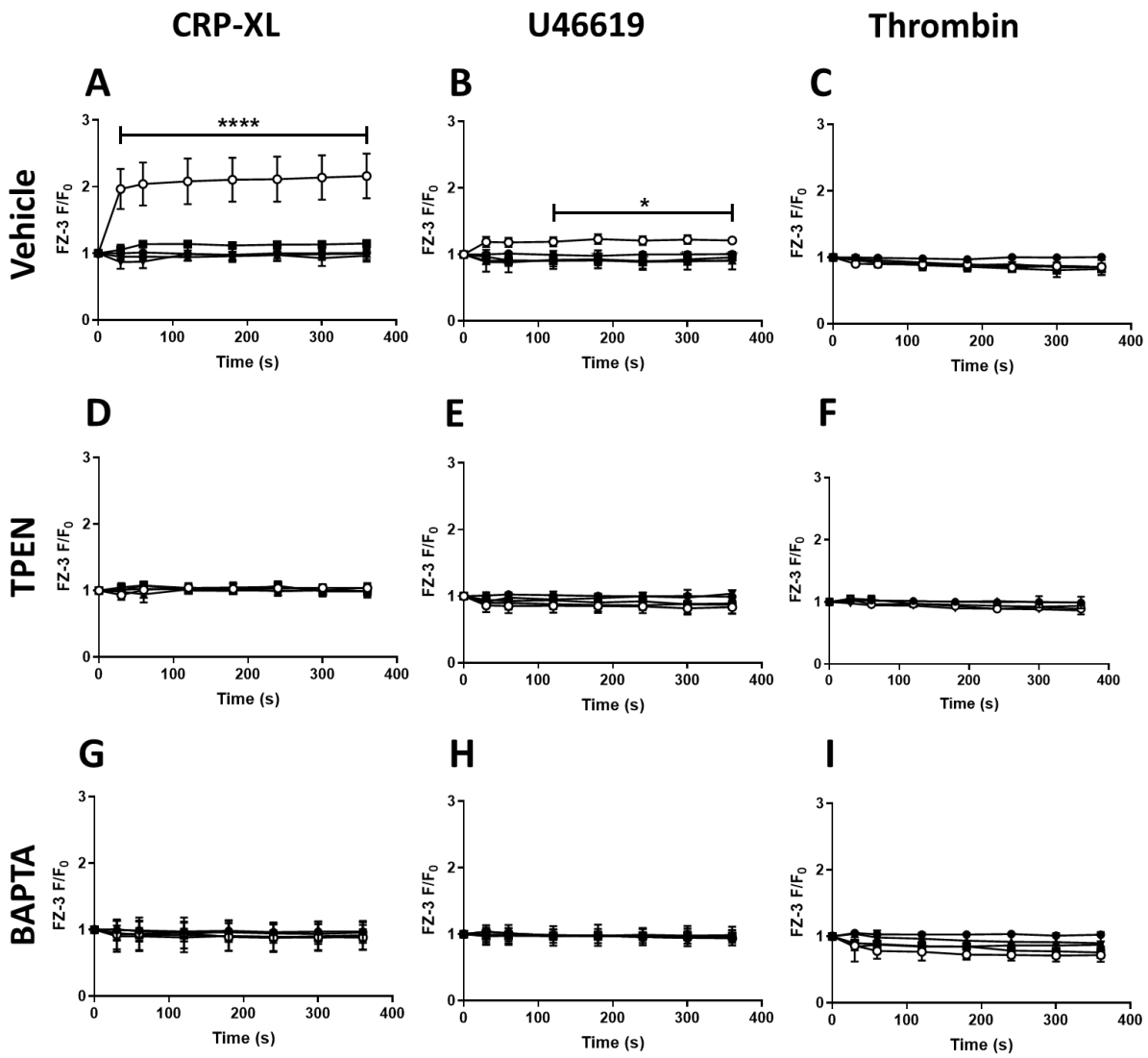

Figure 3.1. Agonist stimulation of platelets results in increases in FZ-3 fluorescence that are were abrogated by TPEN and BAPTA. Fluozin-3 (FZ-3)-labelled washed human platelets were stimulated by increasing concentrations of CRP-XL (A), U46619 (B) or thrombin (C), and FZ-3 fluctuations were recorded over 6 mins using fluorometry. FZ-3-labelled washed human platelets were also pre-treated with the Zn^{2+} chelator, N,N,N',N'-Tetrakis(2-pyridylmethyl)ethylenediamine (TPEN) (50μM), before being stimulated by increasing concentrations of CRP-XL (D), U46619 (E) or thrombin (F) over a 6 min time period using fluorometry. Similarly, FZ-3-labelled washed human platelets were pre-treated with the Ca^{2+} chelator, 2-bis(o-aminophenoxy) ethane-N, N, N', N'-tetraacetic acid (BAPTA) (10μM), before being stimulated by increasing concentrations of CRP-XL (G), U46619 (H) or thrombin (I) and FZ-3 fluorescence fluctuations were recorded over 6 mins using fluorometry. CRP-XL (1μg/mL) and U46619 (1U/mL) induced significant increases in FZ-3 fluorescence which were abrogated following TPEN (50μM) or BAPTA (10μM) pre-treatment. Thrombin did not cause any increases in FZ-3 fluorescence. A, D and G:) ○ 1 μg/mL CRP-XL, ■ 0.3 μg/mL CRP-XL, ▲ 0.1 μg/mL CRP-XL, ▼ 0.03 μg/mL and ● vehicle (dimethyl sulfoxide, DMSO). B, E, and H: ○ 10 μM U46619, ■ 3 μM U46619, ▲1 μM U46619, ▼ 0.3 μM U46619, and ● vehicle. C, F and I: ○ 1 U/mL Thrombin, ■ 0.3 U/mL Thrombin, ▲ 0.1 U/mL Thrombin, ▼ 0.03 U/mL Thrombin and ● vehicle. Data are mean±standard error of mean (SEM) from 6 independent experiments. Significance is denoted as **** (p<0.0001), *** (p<0.001), ** (p<0.01) or * (p<0.05).

Increases in FZ-3 fluorescence following stimulation with 1 μg/mL CRP-XL were evident after 30s with F/F_0 of 1.9±0.3, compared to 1.00±0.01, for the vehicle control, DMSO ($p<0.0001$, Figure 3.1A). After 30s, increases in fluorescence continued at a slower rate up until 6 mins with F/F_0 of 2.2±0.3 (Figure 3.1A). This result is consistent with a sustained increase in $[Zn^{2+}]_i$ levels following CRP-XL stimulation, suggestive of a role for $[Zn^{2+}]_i$ in mediating platelet activatory processes.

U46619 (10 μM) also induced significant increases of FZ-3 fluorescence; however, this was only significant after 3 mins of stimulation (F/F_0 increased to 1.2±0.1, compared to 1.01±0.01 for the vehicle control, $p<0.05$, Figure 3.1B). The fluorescence signal reached a plateau after 6 mins at 1.3±0.1 (Figure 3.1B). This provides further evidence in for sustained, agonist-evoked $[Zn^{2+}]_i$ elevations during platelet activation. Stimulation with lower concentrations of CRP-XL and U46619 did not induce a significant increase in fluorescence during stimulation.

Thrombin did not induce any significant Zn^{2+} fluorescence fluctuations relative to the vehicle control ($p>0.05$,ns, Figure 3.1C). This was an unexpected finding as thrombin is a potent agonist. Furthermore, thrombin mediates activation via GPCRs in a similar manner to U46619 (TxA_2 analogue), which did induce increases in FZ-3 fluorescence. This suggests that a novel signalling pathway is involved in mediating $[Zn^{2+}]_i$ elevation in platelets, that is activated and engaged upon GpVI and TP signalling, but is independent of PAR signalling.

To investigate whether the FZ-3 signal induced by CRP-XL and U46619 (Figure 3.1A-B) was specific to Zn^{2+}, platelets were pre-treated with the $[Zn^{2+}]_i$ chelator, TPEN (50μM), prior to agonist stimulation (Figure 3.1.D-F). The increase in FZ-3 F/F_0 following CRP-XL (1 μg/mL) stimulation was

abrogated in TPEN (50 µM) pre-treated platelets from 2.2±0.3 (for the vehicle) to 1.04±0.03 ($p<0.0001$, Figure 3.1.A and D). Thus these data indicate that the FZ-3 fluorescence is Zn^{2+}-specific, and not due to other cations such as Ca^{2+}. Furthermore, this data further validates the working concentration of TPEN that was selected for this work, as 50µM of TPEN effectively reduces the FZ-3 response induced by CRP-XL (Figure 3.1A, D).

A similar effect was seen with U46619 stimulation. The FZ-3 F/F_0 induced by U46619 (10 µM) was reduced from 1.3±0.1 (vehicle) to 0.8±0.1 (after 6mins) upon TPEN pre-treatment, reaching the level achieved by the vehicle control ($p<0.05$, Figure 3.1B and E).Thus confirming that agonist (CRP-XL and U46619)-evoked fluorescence fluctuations are attributable to Zn^{2+}. These findings support the hypothesis that $[Zn^{2+}]_i$ elevation is induced upon agonist stimulation in platelets. Thrombin did not induce any fluctuations in FZ-3 fluorescence and remained unaffected with TPEN treatment (Figure 3.1F).

In order to investigate the influence of Ca^{2+} signaling on changes in FZ-3 fluorescence, washed platelet suspensions were pretreated with the Ca^{2+} chelator, BAPTA, prior to agonist stimulation (Figure 3.1G-I). BAPTA pre-treatment (10µM) abolished agonist-dependent FZ-3 increases. The F/F_0 induced by CRP-XL (1 µg/mL) and U46619 (10 µM) after 6 mins was reduced from 2.2±0.3 and 1.3±0.1 (vehicle control) to 0.9±0.2 and 0.94±0.03, respectively, upon BAPTA pre-treatment ($p<0.05$, Figure 3.1A, B, G, and H). Thrombin did not induce any fluctuations in FZ-3 fluorescence and remained uninfluenced with BAPTA treatment (Figure 3.1I). These data show that chelation of $[Ca^{2+}]_i$ abrogates agonist-evoked increases in FZ-3 fluorescence. As discussed in Chapter 1, BAPTA has a higher affinity for Zn^{2+} than for Ca^{2+} and is a non-specific cation chelator. Thus the abrogation of FZ-3 fluorescence by BAPTA may be attributable to chelation of $[Zn^{2+}]_i$. Therefore, the use of BAPTA to assess in Ca^{2+} signalling in situations where Zn^{2+} fluctuations may be occurring may not be an appropriate strategy. However, due to the ability of BAPTA to chelate Zn^{2+}, application of this chelator did provide further validation of the FZ-3 probe as this chelator also abrogated the FZ-3 fluorescence induced by the agonists, indicating further that FZ-3 is a valid tool to assess $[Zn^{2+}]_i$.

The work described in this section provides evidence to address the major research question of this chapter; whether agonist stimulation evokes increases in $[Zn^{2+}]_i$ in platelets. CRP-XL and U46619, but not thrombin, induced increases in FZ-3 fluorescence, consistent with elevations of $[Zn^{2+}]$, (Figure 3.1). This implicates activation via GpVI and TP (Thromboxane receptor) but not via PARs (Protease-Activated Receptor) in mechanisms that modulate $[Zn^{2+}]_i$ elevation. Given that activation via the GPCR TP results in elevation of $[Zn^{2+}]_I$, the absence of PAR-dependent $[Zn^{2+}]_i$ elevation is an

interesting an unexpected observation that warrants further investigation. TP and PAR initiated similar signalling pathways involving $[Ca^{2+}]_i$ signalling and PLCβ activity, as illustrated in Figure 1.10. Thus TP may have mediated $[Zn^{2+}]_i$ elevation via a novel mechanism with GpVI.

3.2.2 Intracellular Ca^{2+} release differs from intracellular Zn^{2+} release during platelet activation by physiological agonists.

Agonist-mediated elevation of $[Ca^{2+}]_i$ in platelets is well documented (Authi et al., 1993; Brüne and Ullrich, 1991; Orem et al., 2017; Pozzan et al., 1988; Smith et al., 1992). Experiments discussed in section 3.2.1 determined that stimulation of platelets with CRP-XL or U46619 increased $[Zn^{2+}]_i$. However, the influence of Ca^{2+} signalling on this process was not addressed, BAPTA has a higher affinity for Zn^{2+} than Ca^{2+}. Therefore distinguishing between Zn^{2+} and Ca^{2+} signalling using this chelator is impossible. Whilst it is known that Ca^{2+} is released from intracellular stores, the existence of Zn^{2+} stores in platelets has yet to be confirmed. Experiments were carried out to assess the differences in agonist-induced $[Ca^{2+}]_i$ and $[Zn^{2+}]_i$ elevation. The hypothesis was that $[Ca^{2+}]_i$ is elevated independently to $[Zn^{2+}]_i$ upon agonist stimulation.

$[Ca^{2+}]_i$ release was assessed in platelets loaded with the Ca^{2+} fluorophore, FL-4. As previously reported, stimulation with CRP-XL, U46619 or thrombin all resulted in significant, concentration-dependent increases in FL-4 fluorescence, with 1U/mL thrombin inducing the highest response (Figure 3.2) which is consistent with previous studies (Gamberucci et al., 2002; Jones et al., 2010; Smith et al., 1992; Varga-Szabo et al., 2009).

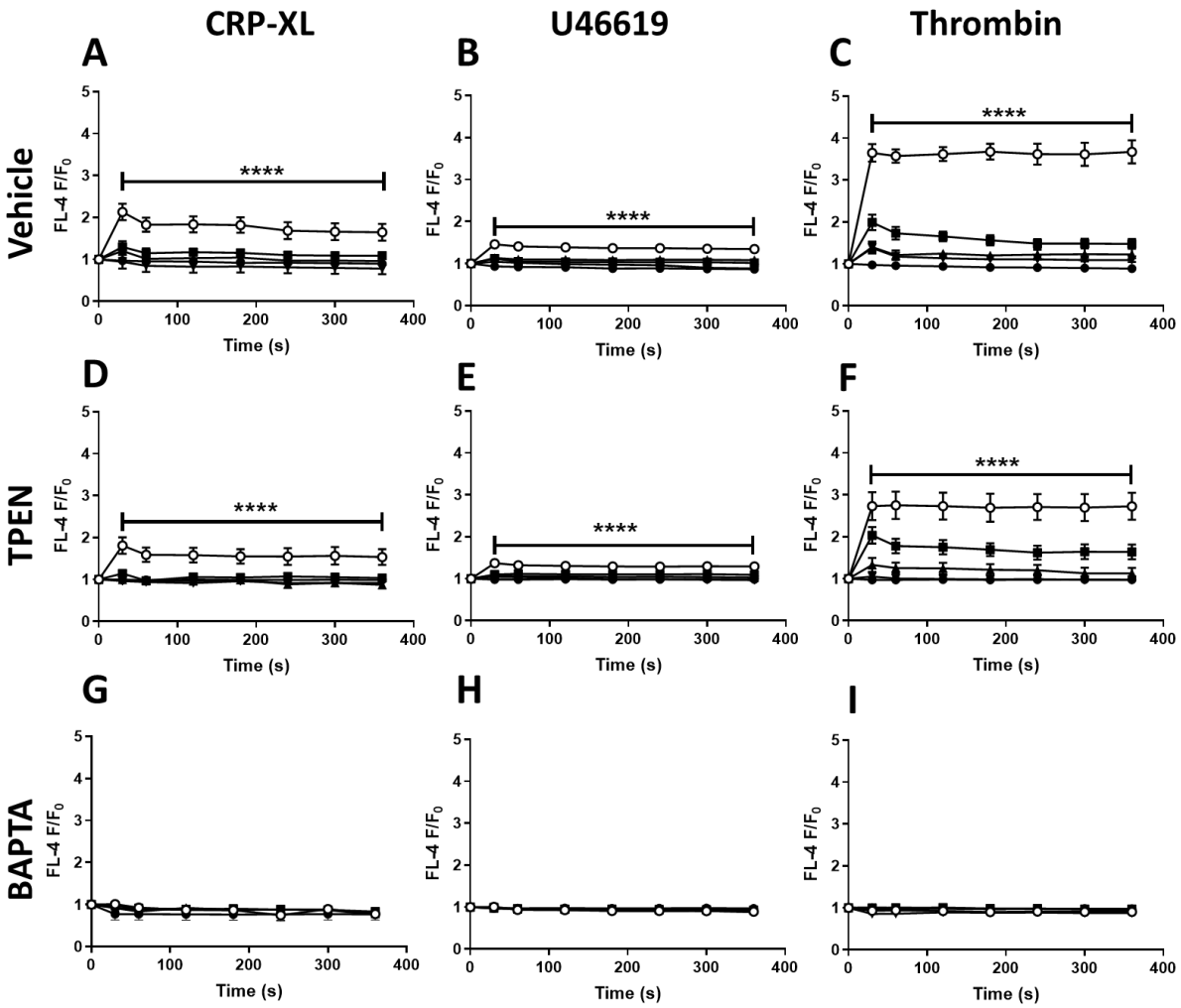

Figure 3.2. Agonist-evoked stimulation results in increases in FL-4 fluorescence that are sensitive to Ca^{2+} chelation- but not Zn^{2+}-chelation. Fluo-4 (FL-4)-labelled washed human platelets were stimulated by increasing concentrations of CRP-XL (A), U46619 (B) or thrombin (C) and FL-4 fluctuations were recorded over 6mins using fluorometry. FL-4-labelled washed human platelets were also pre-treated with TPEN (50µM), before being stimulated by increasing concentrations of CRP-XL (D), U46619 (E) or thrombin (F) over a 6 mins time period using fluorometry. FL-4-labelled washed human platelets were also pre-treated with BAPTA (10µM), before being stimulated by increasing concentrations of CRP-XL (G), U46619 (H) or thrombin (I) and again FL-4 fluctuations were recorded over 6mins using fluorometry. CRP-XL, U46619, and thrombin-induced a significant increase in FL-4 fluorescence relative to the vehicle control. TPEN treatment did not influence agonist-mediated increases in FL-4 fluorescence, whereas BAPTA treatment inhibited in agonist-evoked FL-4 fluorescence increases. A, D and G: ○ 1µg/mL CRP-XL, ■ 0.3µg/mL CRP-XL, ▲ 0.1µg/mL CRP-XL, ▼ 0.03µg/mL and ● vehicle (dimethyl sulfoxide, DMSO). B, E, and H: ○ 10µM U46619, ■ 3µM U46619, ▲1µM U46619, ▼ 0.3µM U46619, and ● vehicle. C, F and I: ○ 1U/mL Thrombin, ■ 0.3U/mL Thrombin, ▲ 0.1U/mL Thrombin, ▼ 0.03U/mL Thrombin and ● vehicle. Data are mean±standard error of mean (SEM) from 6 independent experiments. Significance is denoted as **** ($p<0.0001$), *** ($p<0.001$), ** ($p<0.01$) or * ($p<0.05$)

After 30 s of stimulation with 1 µg/mL of CRP-XL, the F/F_0 was significantly higher than the vehicle control (2.1±0.2 and 1.0±0.1 respectively, $p<0.0001$, Figure 3.2A). The FL-fluorescence signal fell during the course of the experiment, perhaps as a result of Ca^{2+} recycling through SERCA (Figure 1.10, Chapter 1) with F/F_0 falling to 1.6±0.2 after 6 mins (Figure 3.2A),

Similarly, the highest concentration of U46619 (10 µM) induced a significant increase in FL-4 fluorescence, followed by a slight reduction before reaching a plateau. The F/F_0 in response to 10 µM U46619 was 1.5±0.1 after 30 s, and 1.4±0.1 after 6 mins which were significantly higher compared to the vehicle control (where F/F_0 after 30 s and 6 mins were 1.0±0.1 and 1.0±0.1 respectively, $p<0.0001$, Figure 3.2B.).

Thrombin-induced a significant increase in FL-4 fluorescence. After 30 s of stimulation the F/F_0 in response to the highest concentrations of thrombin (1U/mL and 0.3U/mL) increased to 3.7±0.2 and 2.0±0.2 respectively (compared to the vehicle control (1.0±0.1) $p<0.0001$, Figure 3.2C). Interestingly, unlike CRP-XL and U46619, FL-4 fluorescence in response to thrombin was sustained throughout the experiment. This suggests that stronger stimulation of the PARs via higher concentrations of thrombin mediate enhances $[Ca^{2+}]_i$ mobilisation from the DTS. This data also illustrates the greater potential for thrombin to induce Ca^{2+} responses compared to CRP-XL or U46619. This was interesting given the inability of thrombin to evoke Zn^{2+} responses. There are a number of possibilities for this observation. For example, Ca^{2+} and Zn^{2+} release pathways could be distinct and unrelated. Alternatively, high levels of $[Ca^{2+}]_i$ may negatively regulate $[Zn^{2+}]_i$, suggesting an interplay between these cations in platelets. The difference in cation handling observed here warrants further investigation in understanding this potential relationship between Zn^{2+} and Ca^{2+} and it's implications on platelet activity.

TPEN was employed to examine the influence of $[Zn^{2+}]_i$ on $[Ca^{2+}]_i$ responses, and to validate the specificity of the reagents used (for example, the specificity of FL-4 in detecting Ca^{2+} and whether any of the fluorescence being detected is attributable to changes in $[Zn^{2+}]_{i)}$. Figure 3.2.D-F shows the FL-4 fluorescence responses in TPEN -treated platelets following stimulation with CRP-XL (D), U46619 (E) or thrombin (F).

Agonist-evoked FL-4 signals were not significantly affected in TPEN-treated platelets (Figure 3.2D-F). F/F_0 values after 30s or 6 mins following CRP-XL stimulation (1µg/mL) on TPEN pre-treated platelets were 2.0±0.2 and 1.5±0.2, respectively, compared to the F/F_0 induced by CRP-XL on untreated platelets which were 2.1±0.2 and 1.6±0.2, respectively ($p>0.05$, ns, Figure 3.2A, D). These data indicate that the FL-4 signal induced by CRP-XL was not attributable to changes in $[Zn^{2+}]_i$ as chelation of Zn^{2+} did not influence the FL-4 fluorescence signal.

Similar responses in FL-4 fluorescence were observed following treatment with U46619, where TPEN also had no significant influence on increases in FL-4 fluorescence. The F/F_0 induced by U46619 (10 μM) after 30s and 6mins were 1.5±0.1 and 1.4±0.1 respectively, compared to the F/F_0 induced by U46619 on TPEN pre-treated platelets of 1.4±0.1 and 1.3±0.1 respectively($p>0.05$, ns, Figure 3.2B, E).

FL-4 fluorescence increases following stimulation with thrombin were also not significantly influenced by TPEN pretreatment. TPEN pre-treatment did not inhibit thrombin-induced FL-4 fluorescence. F/F_0 in response to 1U/mL thrombin was 3.7±0.3 (vehicle control) compared to TPEN-pretreated (3.0±0.3, $p>0.05$, ns, Figure 3.2C, and F). Lower concentrations of thrombin (0.3U/mL) were also not affected by TPEN pre-treatment. FL-4 F/F_0 at 6mins in response to thrombin 0.3U/mL on TPEN pre-treated platelets was 1.7± 0.2 whereas on vehicle platelets the F/F_0 was 1.5±0.1 (ns, Figure 3.2C, and F). The data here indicate that agonist-mediated elevation of $[Ca^{2+}]_i$ is independent of $[Zn^{2+}]_i$. Further validating the FL-4 as a Ca^{2+} specific probe which is not influenced by changes in $[Zn^{2+}]_i$.

BAPTA was used to assess the validity of the FL-4 signal detected. As shown in Figure 3.2.G-I, pre-treatment with BAPTA (10μM) abolished increases of FL-4 fluorescence induced by all agonists used, providing evidence that the signal detected in these experiments is attributable to Ca^{2+}. The final FL-4 F/F_0 induced by CRP-XL (1μg/mL), U46619 (10μM) and thrombin (1U/mL) was abrogated from 1.6±0.2, 1.4±0.1 and 3.7±0.3, respectively to 1.0±0.1 ($p<0.05$, Figure 3.2A-C and G-I).

The experiments described in this section provide evidence to support the hypothesis that agonist-mediated $[Ca^{2+}]_i$ elevations are independent of $[Zn^{2+}]_i$. Initial work illustrated that all three agonists, CRP-XL, U46619 and thrombin mediate $[Ca^{2+}]_i$ increases (Figures 3.2A-C), as previously shown in the literature. Thrombin-induced the largest FL-4 response compared to the CRP-XL and U46619, leading to speculation as to whether the $[Ca^{2+}]_i$ levels attained in response to thrombin may negatively regulate $[Zn^{2+}]_i$ elevation. The interplay between these two cations in platelets could regulate platelet activity and requires further analysis.

Initial data from this section required validation to establish whether the FL-4 response being evoked by the agonist in these experiments was attributable to Ca^{2+} and to investigate whether the elevation of $[Ca^{2+}]_i$ was influenced by $[Zn^{2+}]_i$ elevation evident upon CRP-XL and U46619 stimulation. Application of TPEN (a $[Zn^{2+}]_i$ chelator) had no influence on CRP-XL or U46619-evoked FL-4 responses (Figure 3.2.D-F), indicating that FL-4 response was not attributable to changes in Zn^{2+}. Thus agonist-induced FL-4 increases were not influenced upon chelation of $[Zn^{2+}]_I$, supporting the hypothesis of this

section that agonist-induced $[Ca^{2+}]_i$ elevation is independent of $[Zn^{2+}]_i$. These data also further validate the specificity of FL-4 probe to Ca^{2+}, as chelation of $[Zn^{2+}]_i$ had no significant influence on the FL-4 fluorescence confirming that the FL-4 probe was more specific to Ca^{2+} than Zn^{2+}, thus a valid probe to measure $[Ca^{2+}]_i$.

BAPTA was employed to determine whether agonist-evoked FL-4 response were attributable to $[Ca^{2+}]_i$ elevation. Pre-treatment with BAPTA abolished all agonist-evoked FL-4 fluorescence increases (Figure 3.2G-I). This result, in conjunction with the TPEN data, indicates that the observed fluorescence was specific to Ca^{2+} and provides further evidence to validate the use of FL-4 as an appropriate $[Ca^{2+}]_i$ probe.

3.2.3 Intracellular Zn^{2+} increases in response to platelet stimulation with exogenous reaction oxygen species

Experiments described in sections 3.2.1 and 3.2.2 indicate that $[Zn^{2+}]_i$ and $[Ca^{2+}]_i$ are elevated in response to stimulation by conventional agonists. These results supported the major hypothesis of this chapter; that $[Zn^{2+}]_i$ is elevated upon agonist stimulation. The mechanism by which $[Ca^{2+}]_i$ is elevated is well documented. However, the mechanism by which these agonists induce $[Zn^{2+}]_i$ is yet to be investigated. Reactive Oxygen Species (ROS) regulate platelet activity and have been linked to the liberation of labile Zn^{2+} from Zn^{2+}-binding proteins such as metallothioneins in nucleated cells (Kimura and Kambe, 2016; Marreiro et al., 2017; Xiong et al., 1992). In order to investigate an association between cation signalling in platelets and ROS, the influence of ROS on changes in $[Ca^{2+}]_i$ and $[Zn^{2+}]_i$ were investigated in this section. Elevation of ROS induces changes in redox states in many cell types including platelets (Pietraforte et al., 2014; Zorov et al., 2014). Experiments were carried out to test the second hypothesis of this chapter; that agonist-evoked $[Zn^{2+}]_i$ fluctuations in platelets are redox sensitive, and occur as a result of changes in levels of ROS.

The commonly employed ROS, hydrogen peroxide (H_2O_2), acts as a secondary messenger at micromolar levels in various cell-signalling pathways and mediates release of intracellular $[Ca^{2+}]_i$ from stores (Freedman, 2008; Görlach et al., 2015; Krötz et al., 2004a; Sies, 2014). H_2O_2 was employed as a ROS agonist to assess fluctuations in $[Zn^{2+}]_i$ and $[Ca^{2+}]_i$ responses following agonist stimulation in the experiments described here. ROS effects on $[Zn^{2+}]_i$ were assessed by treating FZ-3-loaded platelets with different concentrations of H_2O_2 (from 0.3µM to 10µM) and changes in fluorescence were monitored using fluorometry (Figure 3.3).

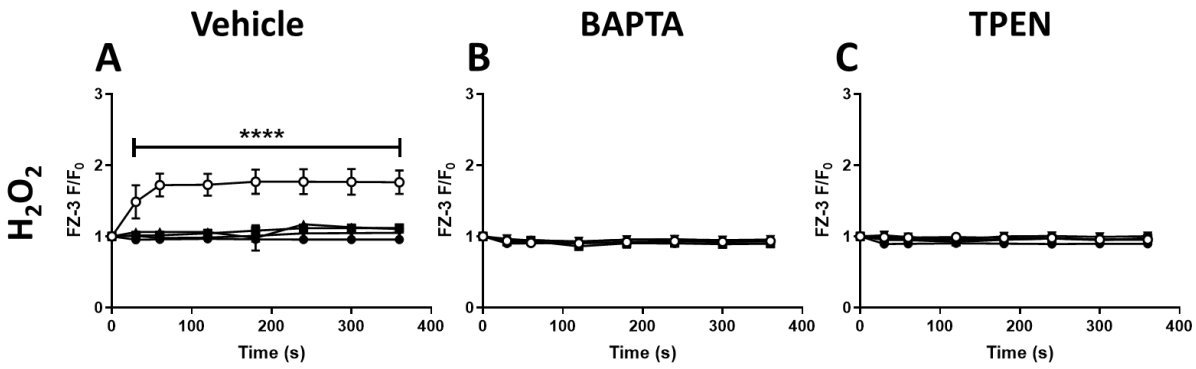

Figure 3.3. Treatment of platelets with H_2O_2 results in increases in $[Zn^{2+}]_i$. Fluozin-3 **(**FZ-3)-labelled washed human platelets were stimulated with increasing concentrations of hydrogen peroxide (H_2O_2) (A), following pre-treatment with 10μM BAPTA (B) or following pre-treatment with 50μM TPEN (C) and FZ-3 fluctuations were recorded over 6mins using fluorometry. H_2O_2 induced a significant increase in FZ-3 fluorescence, which was a loss with BAPTA and TPEN treatment. ○ H_2O_2 10μM, ■ H_2O_2 3μM, ▲ H_2O_2 1μM, ▼ H_2O_2 0.3μM and ● vehicle (dimethyl sulfoxide, DMSO). Data are mean±standard error of mean (SEM) from 6 independent experiments. Significance is denoted as **** (p<0.0001), *** (p<0.001), ** (p<0.01) or * (p<0.05).

Stimulation with the highest concentration (10 μM) of H_2O_2 resulted in a significant increase in FZ-3 fluorescence relative to the vehicle control. The FZ-3 F/F_0 increased for 1 min (to 1.7±0.2) before reaching a sustained plateau (the FZ-3 F/F_0 after 6 mins was 1.8±0.2), which were much higher than the vehicle control, DMSO (1.0±0.1, p<0.0001, Figure 3.3A). These data demonstrate that elevation of ROS within platelets evokes $[Zn^{2+}]_i$ elevations. Furthermore, the FZ-3 fluorescence response to H_2O_2 was sustained between 1-6 mins. This was similar to that seen following stimulation with CRP-XL and U46619 (Figure 3.1.A, B). Therefore, these data suggested that the elevated and sustained FZ-3 increases evoked by CRP-XL and U46619 may be dependent on ROS elevation.

The validity of the elevation of FZ-3 fluorescence increases induced by H_2O_2 was assessed using BAPTA and TPEN. The effect of BAPTA as mentioned earlier does not provide a valid assessment of Ca^{2+} signalling in Zn^{2+} signalling, due to its higher affinity for Zn^{2+} than Ca^{2+}. However, this does serve as an extra measure of validation alongside TPEN to assess whether the FZ-3 increases being induced by H_2O_2 were truly attributable to Zn^2

Pre-treatment of platelet suspensions with BAPTA (Figure 3.3B) or TPEN (Figure 3.3C) abolished any increases in FZ-3 fluorescence induced by H_2O_2, confirming a role for Zn^{2+} in this process. The final FZ-3 F/F_0 induced by H_2O_2 (10μM) was abrogated from 1.8±0.2 to 0.9±0.2 and 1.0±0.1 upon pre-treatment with BAPTA (10μM) and TPEN (50μM). (p<0.0001, Figure 3.3A-C). This data demonstrated that FZ-3 signal increases induced by H_2O_2 were in accordance with Zn^{2+}.

The effect of ROS on $[Ca^{2+}]_i$ fluctuations was also assessed by treating FL-4 loaded platelets with H_2O_2 (Figure 3.4). These experiments were carried out to assess differences between $[Ca^{2+}]_i$ and $[Zn^{2+}]_i$ evoked elevation upon ROS increases. This potential difference was assessed to help establish if the hypothesis that upon platelet activation fluctuations in $[Zn^{2+}]_i$ are redox sensitive as a result of changes in levels of ROS was also attributable to $[Ca^{2+}]_i$. In a similar manner to FZ-3 fluorescence, only the highest concentration of H_2O_2 (10µM) induced a significant increase in FL-4 fluorescence relative to the vehicle control. Increases in FL-4 fluorescence were observed in the first 30s of the experiment, following which the signal plateaued. The FL-4 F/F_0 values following stimulation with 10µM, H_2O_2 for 30s and 6mins respectively were 1.4±0.1 and 1.4±0.2 respectively compared to vehicle control (DMSO), 1.0±0.1 ($p<0.0001$, Figure 3.4A). Thus, ROS elevation evokes $[Ca^{2+}]_i$ elevation.

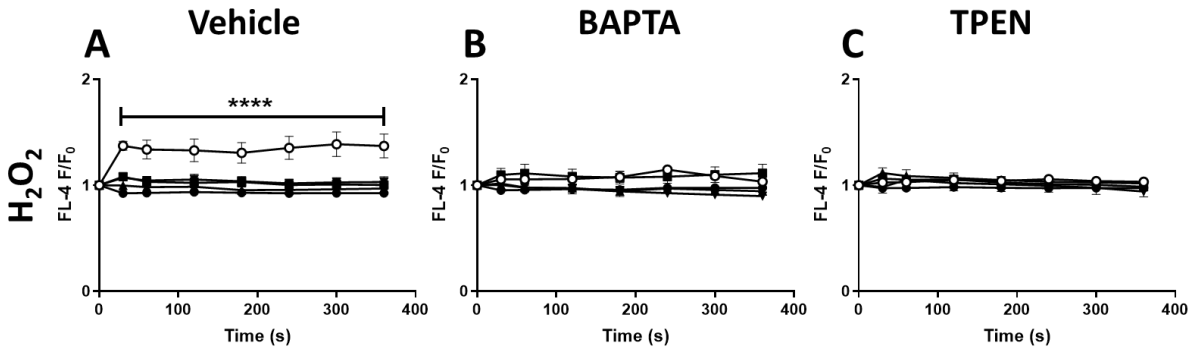

Figure 3.4. Platelet stimulation with H_20_2 results in increases in FL-4 fluorescence that are sensitive to cation chelation with BAPTA or TPEN. Fluo-4 (FL-4)-labelled washed human platelets were stimulated different concentrations of H_2O_2 (A), following 10µM BAPTA pre-treatment (B) or 50µM TPEN pre-treatment (C) and FL-4 fluctuations were recorded over 6mins using fluorometry. H_2O_2 induced a significant increase in Ca^{2+} fluorescence, which was abrogated following BAPTA or TPEN pre-treatment. ○ H_2O_2 10µM, ■ H_2O_2 3µM, ▲ H_2O_2 1µM, ▼ H_2O_2 0.3µM and ● vehicle (DMSO). Data are mean±standard error of mean (SEM) from 6 independent experiments. Significance is denoted as **** ($p<0.0001$), *** ($p<0.001$), ** ($p<0.01$) or * ($p<0.05$).

Pre-treatment with BAPTA or TPEN abolished any significant increases in FL-4 fluorescence induced by H_2O_2. The final FL-4 F/F_0 induced by H_2O_2 (10µM) was abrogated from 1.4±0.1 to 1.0±0.1 and 1.0±0.1 upon pre-treatment with BAPTA (10µM) or TPEN (50µM), respectively ($p<0.0001$, Figure 3.4A-C). These final FL-4 F/F_0 values evoked by H_2O_2 (10µM) on BAPTA and TPEN treated platelets did not significantly differ to the vehicle control as the final F/F_0 induced by the vehicle control on BAPTA and TPEN pre-treated platelets which were 0.9±0.1 and 1.0±0.1 respectively ($p>0.05$, ns, Figure 3.4A-C). These data show that ROS elevation also evokes $[Ca^{2+}]_i$ elevation. However, since the application

of the highly specific $[Zn^{2+}]_i$ chelator TPEN abrogated the FL-4 fluorescence evoked by H_2O_2, it can be surmised that the elevation of FL-4 fluorescence is attributable to Zn^{2+} and not Ca^{2+}.

The experiments described above provide evidence to confirm the hypothesis that ROS elevation mediates elevated $[Zn^{2+}]_i$. Stimulation with H_2O_2 resulted in significant increases in FZ-3 fluorescence which were inhibited by the chelators, TPEN or BAPTA (Figure 3.3A-C). As both BAPTA and TPEN were shown to act as $[Zn^{2+}]_i$ chelators (due to the higher affinity to Zn^{2+} that BAPTA has, as previously stated), these data suggested that elevation of $[Zn^{2+}]_i$ is mediated by ROS elevation.

Stimulation with H_2O_2 also resulted in significant increases in FL-4 fluorescence (Figure 3.4A) which was inhibited by BAPTA, outlining that elevation of $[Ca^{2+}]_i$ is mediated by ROS elevation (Figure 3.4B). However, this increase in FL-4 fluorescence was also inhibited by TPEN (Figure 3.4C), suggesting that the elevation in fluorescence induced by H_2O_2 was attributable to Zn^{2+} as opposed to Ca^{2+}. This suggests a potential mechanism activatory involving redox changes upon ROS stimulation. This mechanism may be independent of Ca^{2+} and may mediate elevation of $[Zn^{2+}]_i$. Changes in redox in platelets upon ROS elevation may result in the release of Zn^{2+} from redox proteins such as metallothioneins. Released Zn^{2+} may contribute to activatory responses. This proposed mechanism coincides well with the work exhibited in this section and supports the hypothesis that fluctuations in $[Zn^{2+}]_i$ are redox sensitive as a result of changes in levels of ROS in platelets.

3.2.4 Agonist-induced intracellular Zn^{2+} release is redox-sensitive in platelets

Experimental data discussed in section 3.2.3 indicates that ROS elevation mediates the elevation of $[Zn^{2+}]_i$. This section aims to investigate the validity and physiological relevance of this proposed mechanism. ROS-dependent Zn^{2+} release has been investigated in other cell types. In neurons, free Zn^{2+} is tightly coordinated by metal binding proteins such as metallothionines (MT's) and upon oxidative stress, ROS is elevated, liberating Zn^{2+} (Stork and Li, 2016). Interestingly elevated Zn^{2+} further enhanced ROS generation in neurons, producing a positive feedback effect. Whether this scheme operates in platelets is not known and may be the reason as to why the FZ-3 fluorescence in response to CRP-XL, U46619, and H_2O_2 was sustained throughout the duration of the experiments. It is possible that the positive feedback effect maintains the elevated levels of $[Zn^{2+}]_i$ (Krötz et al., 2004;

Pietraforte et al., 2014; Stork and Li, 2016). The hypothesis of this section is that elevation of $[Zn^{2+}]_i$ upon agonist stimulation is redox sensitive in platelets.

The antioxidant superoxide dismutase (SOD) was employed to assess the potential redox-mediated mechanism that may regulate agonist-dependent $[Zn^{2+}]_i$ release in platelets. SOD is a cytosolic antioxidant, which catalyzes the formation of the less reactive ROS, H_2O_2 and O_2 upon dismutation of the very reactive ROS, O_2^- (Machtay et al., 2006), as illustrated by the equation below.

$$2O_2^- + 2H^+ \xrightarrow{SOD} H_2O_2 + O_2$$

SOD has been used in various cell types to protect cells against oxidative stress by inhibiting the elevation of ROS (Pandya et al., 2013; Pietraforte et al., 2014; Sinha and Dabla, 2015). SOD has been found in platelets as a ROS scavenger (Figure 1.8, Chapter 1) and serves as an appropriate enzyme to reduce ROS levels and modulate the redox state in the platelet.

Covalent conjugation of SOD with Polyethylene Glycol (PEG) enhance the level of enzyme activity in a variety of cells (Beckman et al., 1988). PEG is widely used due to its ability to increase the solubility of the conjugate and keep toxic effects to a minimal in comparison to when there is no conjugation with PEG (Beckman et al., 1988; Kim et al., 2015). Thus PEG-SOD which is a mimetic of SOD was chosen to enable optimal SOD activity (Kim et al., 2015).

Another antioxidant, Catalase (CAT) was also employed to further investigate the potential redox-mediated mechanism that may regulate agonist-dependent $[Zn^{2+}]_i$ release in platelet. The major differences between SOD and CAT are that they target different ROS. SOD primarily inhibits superoxide anion (O_2^-) which is an unstable intermediate of H_2O_2, whilst CAT inhibits H_2O_2 as illustrated in the equation below.

$$2H_2O_2 \xrightarrow{CAT} H_2O + O_2$$

CAT catalyses the formation of H_2O and O_2 upon dismutation of H_2O_2 (Machtay et al., 2006). Thus, CAT is expected to reduce ROS elevation being induced upon exogenous H_2O_2 whereas SOD is not. However, exogenous ROS treatment induces oxidative stress in various cell types which then result in the elevation of other ROS such as O_2^- (Freedman, 2008). This suggests that SOD reduces ROS elevation of other species, which may elevate upon exogenous H_2O_2 treatment. This was evident from the work described in this section. In physiological conditions in both nucleated cells and platelets both SOD and CAT work in synergy to scavenge ROS, as SOD initially targets the more reactive ROS

species such as O_2^- which then results in the formation of H_2O_2. H_2O_2 is then catalyzed to H_2O and oxygen (Pandya et al., 2013; Sinha and Dabla, 2015). Thus, eradicating the ROS species. In this work, CAT was employed as a further antioxidant along with SOD to provide further validation of the proposed ROS-mediated $[Zn^{2+}]_i$ elevation mechanism. The mimetic of CAT, PEG- CAT was employed in a similar manner to PEG-SOD

As previously shown, stimulation of FZ-3 loaded platelets with CRP-XL, U46619 or H_2O_2 resulted in elevated FZ-3 fluorescence (Figures 3.1 and 3.3), indicating that elevation of $[Zn^{2+}]_i$ may be modulated by ROS. Platelets were pre-treated with 30U/mL of PEG-SOD (Lopes Pires et al., 2017), prior to being treated with increasing concentrations of CRP-XL (Figure 3.5D), U46619 (Figure 3.9E), or thrombin (Figure 3.5F), and changes in FZ-3 fluorescence were recorded using fluorometry as before. Pre-treatment with PEG-SOD significantly reduced CRP-XL (1µg/mL)-stimulated increases in FZ-3 fluorescence (Figure 3.5 A-F).

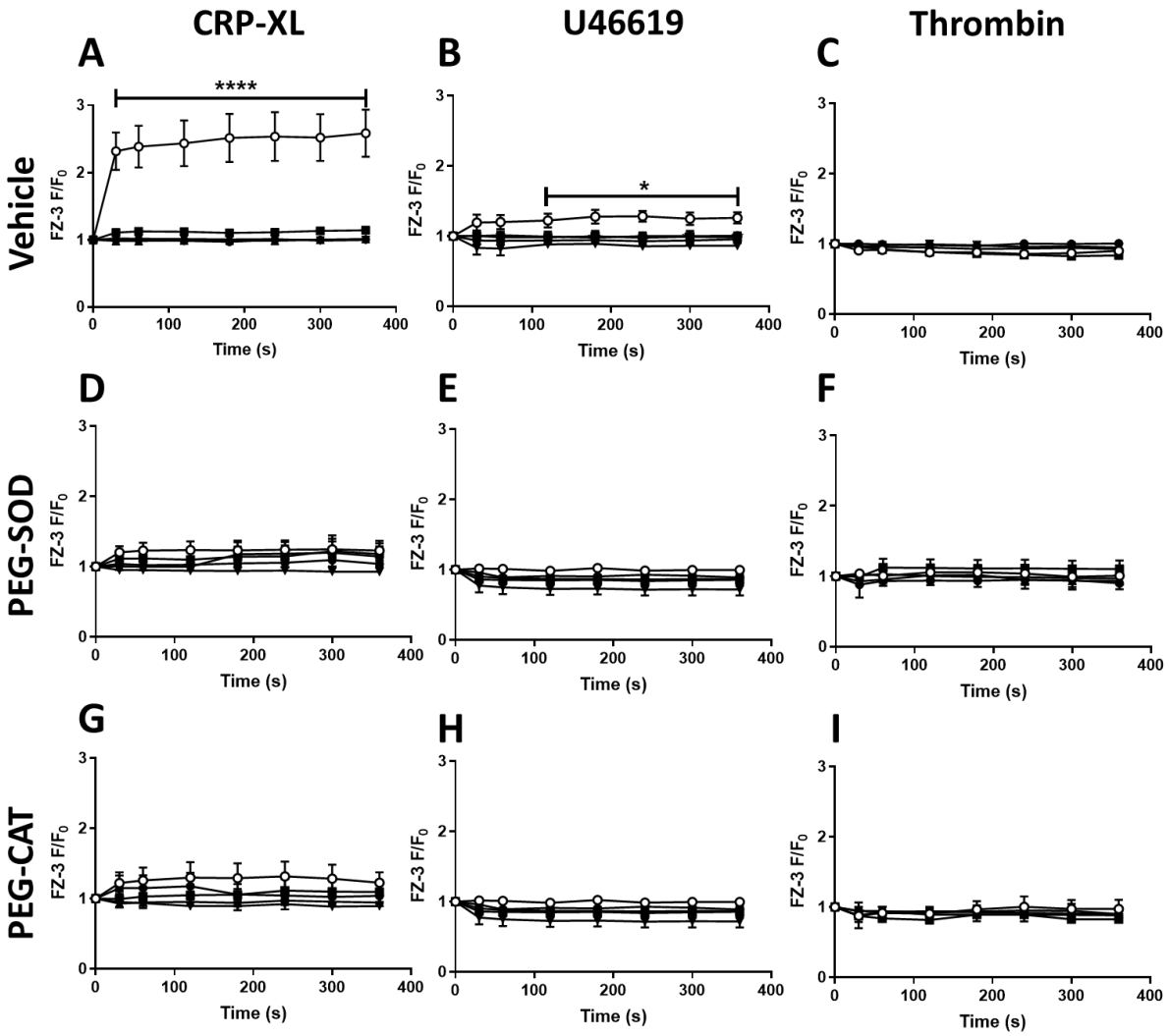

Figure 3.5. Agonist-evoked increases in intracellular Zn^{2+}_i are abrogated in PEG-SOD and PEG-CAT –treated platelets. Fluozin-3 (FZ-3)-labelled washed human platelets were stimulated by increasing concentrations of CRP-XL (A), U46619 (B) or thrombin (C), and FZ-3 fluctuations were recorded over 6mins using fluorometry. FZ-3-labelled washed human platelets were also pre-treated with the antioxidant PEG-SOD (30U/mL), before being stimulated by increasing concentrations of CRP-XL (D), U46619 (E) or thrombin (F) and FZ-3 fluctuations were recorded over six minutes using fluorometry. FZ-3 labelled washed platelets were also pre-treated with PEG-CAT (300U/mL), before being stimulated by increasing concentrations of CRP-XL (G), U46619 (H) or thrombin (I). PEG-SOD and PEG-CAT treatment inhibited the increase in FZ-3 fluorescence induced by the agonists. (A, D and G) ○ 1μg/mL CRP-XL, ■ 0.3μg/mL CRP-XL, ▲ 0.1μg/mL CRP-XL, ▼ 0.03μg/mL and ● vehicle (dimethyl sulfoxide, DMSO). (B, E, and H) ○ 10μM U46619, ■ 3μM U46619, ▲1μM U46619, ▼ 0.3μM U46619, and ● vehicle. (C, F and I) ○ 1U/mL Thrombin, ■ 0.3U/mL Thrombin, ▲ 0.1U/mL Thrombin, ▼ 0.03U/mL Thrombin and ● vehicle. Data are mean±standard error of mean (SEM) from 6 independent experiments. Significance is denoted as **** ($p<0.0001$), *** ($p<0.001$), ** ($p<0.01$) or * ($p<0.05$).

After 6mins of stimulation with CRP-XL (1μg/mL), FZ-3 F/F_0 was abrogated from 2.6±0.3 to 1.2±0.1 upon PEG-SOD pre-treatment ($p<0.0001$, Figure 3.5A and D). Furthermore, the FZ-3 signal in response to CRP-XL on PEG-SOD pre-treated platelets did not significantly differ to that induced by the vehicle control treatment (1.1±0.1, $p>0.05$, ns, Figure 3.5D). This data demonstrated that CRP-XL induced $[Zn^{2+}]_i$ elevation is dependent on ROS.

PEG-SOD treatment also reduced the FZ-3 fluorescence induced by U46619 (Figure 3.9B). F/F_0 induced by U46619 (10μM) after 6mins was abolished from 1.30 ±0.04 to 0.98±0.02 ($p<0.0001$, Figure 3.5B and E). Thus, this work further strengthened the hypothesis that agonist-induced $[Zn^{2+}]_i$ elevation is dependent on ROS, and thus sensitive to changes in redox (as fluctuations in ROS modulate redox states). No apparent fluctuations in FZ-3 signal were observed with thrombin upon PEG-SOD treatment. This was expected as thrombin stimulation did not result in increases $[Zn^{2+}]_i$.

These data support the concept that elevation of $[Zn^{2+}]_i$ upon agonist stimulation is redox sensitive in platelets, as PEG-SOD inhibited the increases in FZ-3 fluorescence induced by CRP-XL and U46619. This may be due to PEG-SOD preventing the changes in redox which would otherwise liberate Zn^{2+} from thiols on redox-sensitive metal ion-binding proteins such as metallothioneins.

Platelets were pre-treated with 300U/mL of PEG-CAT (Lopes Pires et al., 2017), prior to being treated with different concentrations of CRP-XL (Figure 3.5G), U46619 (Figure 3.5H), or thrombin (Figure 3.5I), and changes in FZ-3 fluorescence were recorded. Agonist-evoked increases in FZ-3 fluorescence was also inhibited by PEG-CAT.

In a similar manner to PEG-SOD treatment, F/F_0 induced by CRP-XL (1μg/mL after 6mins was reduced from 2.6±0.3 to 1.2±0.1 upon PEG-CAT (300U/mL) pre-treatment ($p<0.0001$, Figure 3.5A and

G). PEG-CAT treatment also reduced the FZ-3 signal by U46619, as the final F/F_0 induced by U46619 (10μM) was abrogated from 1.30±0.04 to 0.97±0.02 ($p<0.0001$, Figure 3.5B and H). Thrombin did not induce FZ-3 fluctuations thus had no effect with PEG-CAT pre-treatment as described above. Thus, PEG-CAT treatment resulted in similar effects to PEG-SOD treatment. Thus, targeting ROS via different mechanisms (i.e. SOD and CAT target different ROS) resulted in the same effect in terms of inhibition of agonist-evoked $[Zn^{2+}]_i$ elevation. The work with PEG-CAT provides further evidence in conjunction with the work carried out with PEG-SOD in this section to support the hypothesis that elevation of $[Zn^{2+}]_i$ upon agonist stimulation is redox sensitive in platelets.

Data from this section support the hypothesis that elevation of $[Zn^{2+}]_i$ upon agonist stimulation is redox-sensitive in platelets. The increases in FZ-3 fluorescence in response to CRP-XL or U46619 (Figures 3.5A-B) were significantly inhibited upon treatment with the antioxidants PEG-SOD (Figure 3.5D-E) and PEG-CAT (Figure 3.5G-H), which were employed to scavenge any ROS elevation upon stimulation. These data demonstrate that the scavenging of ROS via application of PEG-SOD and PEG-CAT may be preventing the changes in redox which enable changes in redox in platelets upon ROS elevation which result in the release of Zn^{2+} from redox-sensitive proteins such as metallothioneins. Furthermore, these data are consistent with results from section 3.2.3 which show that changes in redox in platelets upon ROS elevation results in elevation of $[Zn^{2+}]_i$. Therefore, $[Zn^{2+}]_i$ elevation is sensitive to redox changes. This may be an important mechanism by which $[Zn^{2+}]_i$ is elevated upon platelet activation.

3.2.5 Agonist-induced intracellular Ca^{2+} release is not sensitive to redox changes in platelets

Experiments described in sections 3.2.3 and 3.2.4 demonstrated that agonist-mediated $[Zn^{2+}]_i$ elevation is redox sensitive. However, the data from section 3.2.4 showed that ROS elevation that has previously been thought to be caused by increases in $[Ca^{2+}]_i$ was attributable to $[Zn^{2+}]_i$. This implies that $[Ca^{2+}]_i$ elevation is not sensitive to redox changes upon ROS elevation, indicating that $[Ca^{2+}]_i$ and $[Zn^{2+}]_i$ elevation are mediated by different mechanisms in platelets.

Whilst the mechanism through which $[Ca^{2+}]_i$ is elevated is well documented, the elevation of $[Ca^{2+}]_i$ during changes in platelet redox state upon agonist stimulation was assessed. This was carried out to investigate whether redox-sensitive $[Zn^{2+}]_i$ elevation was also independent to Ca^{2+}. The

hypothesis of this section is that agonist-evoked $[Ca^{2+}]_i$ increases are not sensitive to changes in the platelet redox state.

PEG-SOD and PEG-CAT were employed to assess the role of ROS on $[Ca^{2+}]_i$ release. Pre-treatment of washed, FL-4-loaded platelet suspensions with PEG-SOD (30U/mL) and PEG-CAT (300U/mL) had no significant influence on increases in agonist-evoked FL-4 increases in all of the experiments shown below (Figure 3.6).

The FL-4 F/F_0 following stimulation for 6 mins with CRP-XL (1.9±0.3) did not significantly differ to the F/F_0 induced by CRP-XL (1µg/mL) of PEG-SOD pre-treated platelets (2.0±0.2, $p>0.05$, ns, Figure 3.6A and D). Thus, PEG-SOD had no influence on CRP-XL evoked $[Ca^{2+}]_i$ increases. U46619 (10µM) evoked FL-4 increases were also not influenced by PEG-SOD treatment, as F/F_0 following 6 mins of stimulation with U46619 (10µM) was 1.5±0.1 compared to 1.4±0.1 in PEG-SOD pre-treated platelets($p>0.05$, ns, Figure 3.6B and E). These data confirm that PEG-SOD had no influence on CRP-XL evoked FL-4 increases.

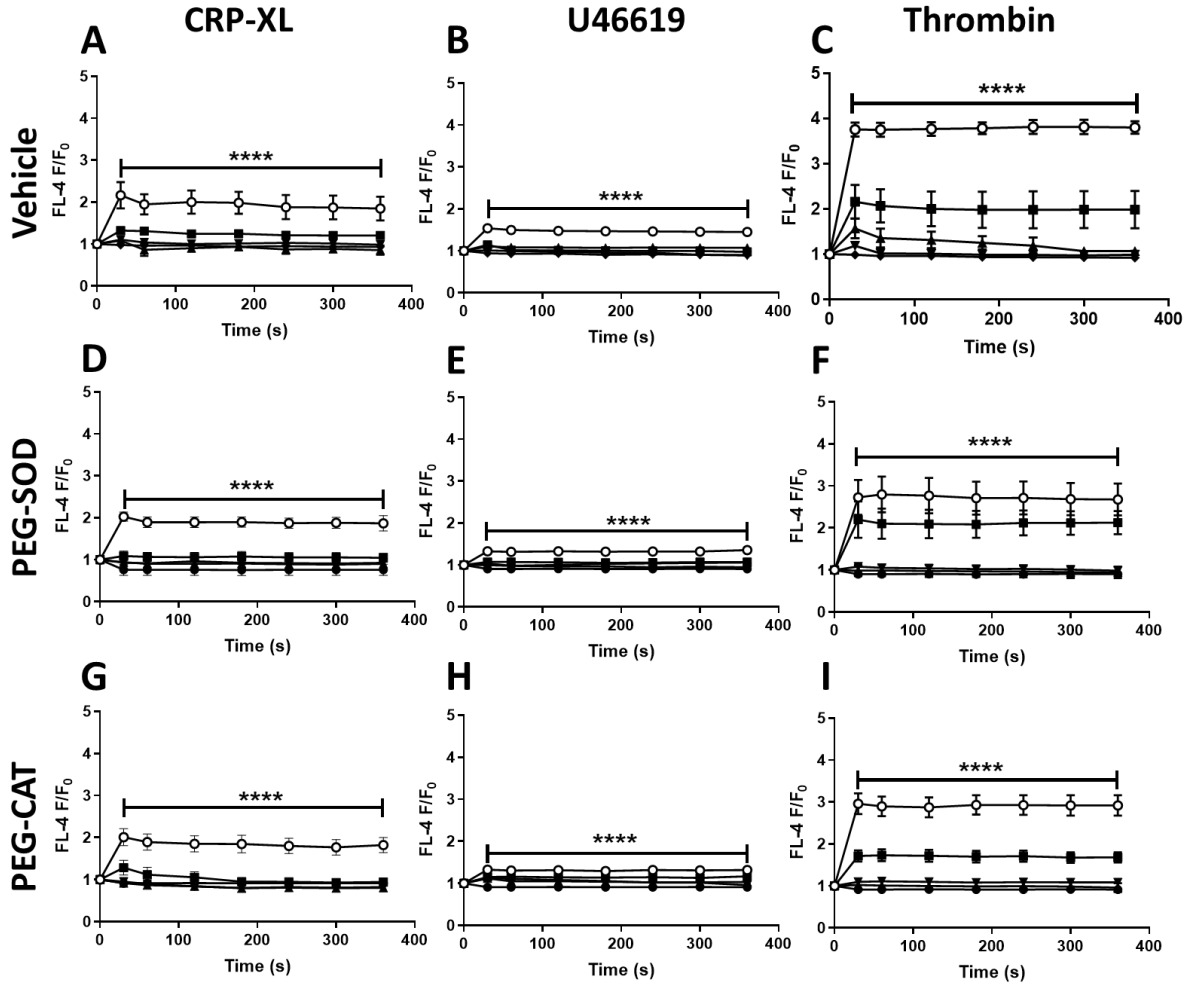

Figure 3.6. PEG-SOD and PEG-CAT treatment do not effect agonist-evoked increases in $[Ca^{2+}]_i$. Fluo-4 **(**FL-4) labelled washed human platelets were stimulated by increasing concentrations of (CRP-XL) (A), U46619 (B) or thrombin (C) and FL-4 fluctuations were recorded over 6mins using fluorometry. FL-4-labelled washed human platelets were also pre-treated with PEG-SOD (30U/mL), before being stimulated by increasing concentrations of CRP-XL(D), U46619 (E) or thrombin (F) and FL-4 fluctuations were recorded over six minutes using fluorometry. FL-4 labelled washed platelets were also pre-treated PEG-CAT (300U/mL), before being stimulated by increasing concentrations of CRP-XL(G), U46619 (H) or thrombin (I). PEG-SOD and PEG-CAT treatment had no significant influence on agonist-evoked $[Ca^{2+}]_i$ elevation. (A, D and G) ○ 1µg/mL CRP-XL, ■ 0.3µg/mL CRP-XL, ▲ 0.1µg/mL CRP-XL, ▼ 0.03µg/mL and ● vehicle (dimethyl sulfoxide, DMSO). (B, E and H) ○ 10µM U46619, ■ 3µM U46619, ▲1µM U46619, ▼ 0.3µM U46619, and ● vehicle. (C, F and I) ○ 1U/mL Thrombin, ■ 0.3U/mL Thrombin, ▲ 0.1U/mL Thrombin, ▼ 0.03U/mL Thrombin and ● vehicle. Data are mean±standard error of the mean (SEM) from 6 independent experiments. Significance is denoted as **** ($p<0.0001$), *** ($p<0.001$), ** ($p<0.01$) or * ($p<0.05$).

Thrombin treatment, which evoked significant increases in FL-4 fluorescence also was not influenced by PEG-SOD pre-treatment (Figure 3.6C, F). The final F/F_0 induced by thrombin (1U/mL and 0.3U/mL) were 3.8±0.1 and 2.0±0.4, respectively whereas on PEG-SOD pre-treated platelets were 3.0±0.1 and 2.1±0.3, respectively ($p>0.05$, ns, Figure 3.6C, and F). These data confirm that agonist-evoked $[Ca^{2+}]_i$ in not sensitive to changes in the platelet redox state

In a similar manner to PEG-SOD treatment, pre-treatment with PEG-CAT also had no effect on agonist-evoked $[Ca^{2+}]_i$ increases (Figure 3.6). The F/F_0 induced by CRP-XL (1µg/mL) after 6 mins was 1.9±0.3, compared to 2.0±0.2 with PEG-CAT pre-treated platelets ($p>0.05$, ns, Figure 3.6A and D). U46619 (10µM) evoked FL-4 increases were also not affected by PEG-CAT treatment. The F/F_0 induced by U46619 (10µM) after 6mins were 1.5±0.1 and on PEG-CAT pre-treated platelets and 1.3±0.1 on untreated platelets (ns, Figure 3.6B, and H). F/F_0 values following stimulation with 1U/ml or 0.3U/mL thrombin after 6mins on untreated platelets were 3.8±0.1 and 2.0±0.4 respectively, compared to 3.0±0.2 and 2.0±0.1, respectively for PEG-CAT pre-treated platelets ($p>0.05$, ns, Figure 3.6C and I). Thus agonist-induced $[Ca^{2+}]_i$ elevation is not sensitive to the reduction of ROS via PEG-SOD and PEG-CAT treatment.

The data from this section support the hypothesis that $[Ca^{2+}]_i$ elevation is not sensitive to redox changes upon agonist stimulation. ROS reduction (resulting in changes in redox states) via the use of PEG-SOD and PEG-CAT had no significant influence on agonist-mediated $[Ca^{2+}]_i$ (Figure 3.6). Although previous work (Görlach et al., 2015) has suggested that ROS impacts $[Ca^{2+}]_i$, Zn^{2+} was not taken into account in these studies, perhaps due to Zn^{2+} being overlooked due to the assumption that its intracellular concentration is insignificant compared to Ca^{2+}. However, the data described here demonstrate that redox-sensitive cation elevation is only applicable to Zn^{2+} and not Ca^{2+}, providing evidence $[Zn^{2+}]_i$ and $[Ca^{2+}]_i$ elevation rely on differing mechanisms.

3.2.6 Agonist-induced ROS elevation is influenced by intracellular Zn^{2+}

In nucleated cell types such as neuron cells, elevation of $[Zn^{2+}]_i$ results in increases in intracellular ROS levels, in what has suggested being a positive feedback mechanism (Stork and Li, 2016). It is possible that the same mechanism applies in platelets, whereby elevated ROS results in elevated $[Zn^{2+}]_i$ which in turn results in further ROS elevation. Whilst, activation via PAR and GpVI induce intraplatelet ROS production (Arthur et al., 2008; Qiao et al., 2018; Walsh et al., 2014), the mechanism by which ROS is elevated in platelets is yet to be fully determined. Experiments were carried out to further investigate the relationship between ROS and cation fluctuations during agonist stimulation. The hypothesis of this section is that ROS elevation is dependent on $[Zn^{2+}]_i$ elevation upon agonist stimulation.

To assess the role of ROS in platelet activity, the agonist-dependent fluctuations of ROS were measured in washed platelet suspensions following stimulation with the conventional agonists, CRP-XL, U46619, and Thrombin. The widely used cell permeable ROS-specific probe, 2', 7'-Dichlorofluorescein diacetate (DCFH), was used to detect increases in ROS (section 2.5, Chapter 2).

DCFH (10µM) -loaded platelets were stimulated with increasing concentrations of CRP-XL (A), U46619 (B) or thrombin (Figure 3.7). Stimulation with 1µg/mL CRP-XL resulted in steady increases of DCFH fluorescence throughout the 6min experiment. The final DCFH F/F_0 induced by CRP-XL (1µg/mL) was 1.8±0.1, compared to 0.9±0.3 for the vehicle control ($p<0.0001$, Figure 3.7A). Thus, GpVI stimulation results in a substantial increase in ROS elevation.

Stimulation with U46619 (10µM) or thrombin (1U/mL) also increased DCFH fluorescence, although to a lower level than that seen with CRP-XL. The final DCFH F/F_0 induced by U46619 (10µM) increased to 1.21± 0.03 compared to 1.01±0.02 for the vehicle control ($p<0.001$, Figure 3.13A). Thrombin (1U/mL) also induced a significant increase in DCFH fluorescence relative to the vehicle, as the final DCFH F/F_0 was 1.4±0.1 compared to 1.0±0.1 for the vehicle control ($p<0.0001$, Figure 3.7C). These data correlate with previous observations in the literature that agonist stimulation results in increases in platelet ROS (Arthur et al., 2008; Krötz et al., 2004; Qiao et al., 2018).

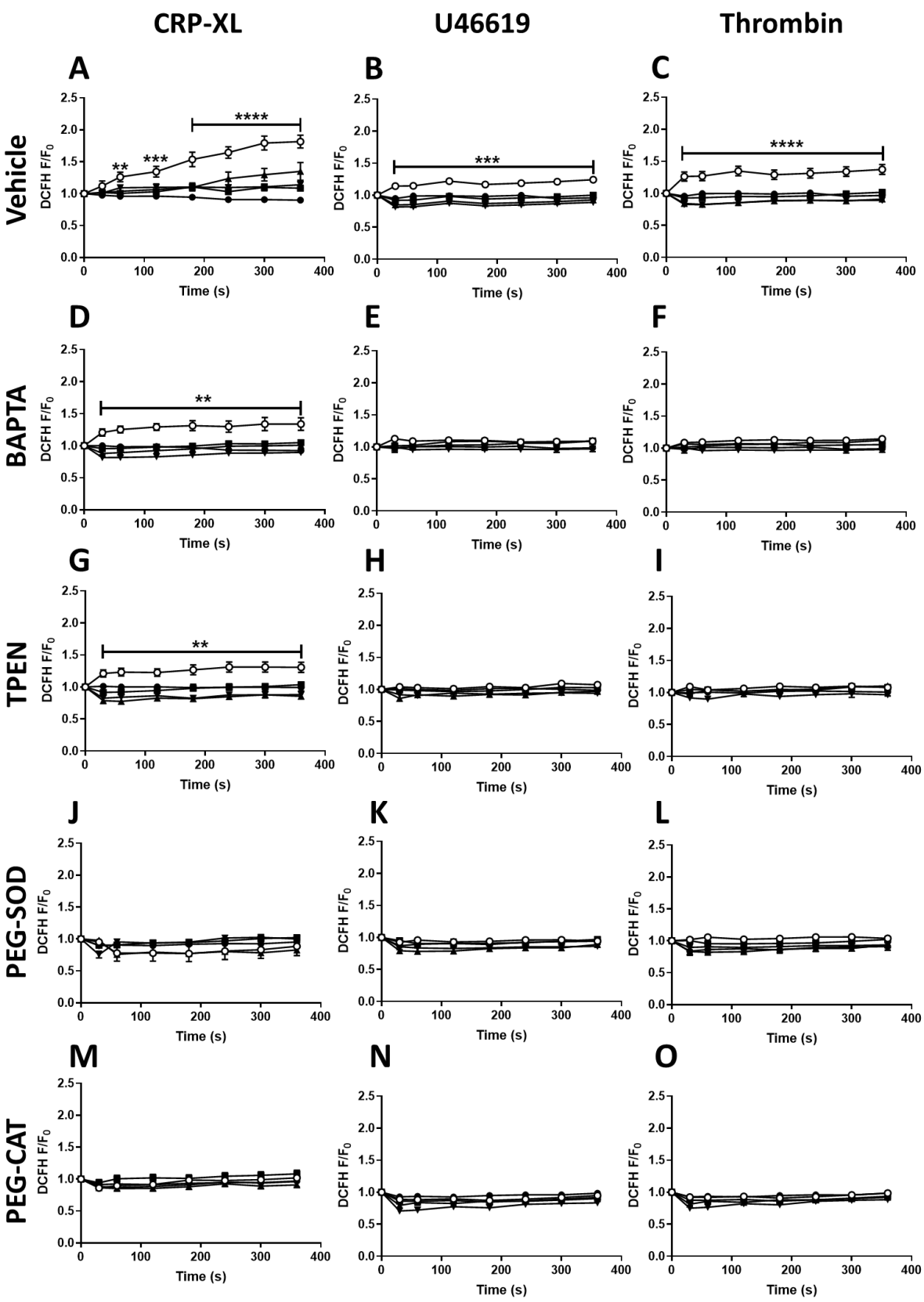
CRP-XL
U46619
Thrombin
A
B
C
D
E
F
G
H
I
J
K
L
M
N
O
Vehicle
BAPTA
TPEN
PEG-SOD
PEG-CAT
DCFH F/F0
Time (s)
**
***
****

Figure 3.7. Agonist-evoked increases in DCFH fluorescence are inhibited by TPEN and BAPTA and abrogated by PEG-SOD and PEG-CAT. DCFH-labelled washed human platelets were stimulated by increasing concentrations of CRP-XL (A), U46619(B) and thrombin (C). DCFH-labelled washed human platelets were also pre-treated with 10μM BAPTA before being stimulated by increasing concentrations of CRP-XL(D), U46619(E) and thrombin (F). DCFH-labelled washed human platelets were also pre-treated with 50μM TPEN before being stimulated by increasing concentrations of CRP-XL(G), U46619(H) and thrombin (I). DCFH-labelled washed human platelets were also pre-treated with 30U/mL PEG-SOD before being stimulated by increasing concentrations of CRP-XL (J), U46619 (K) or thrombin (L). Finally, DCFH-labelled washed human platelets were pre-treated with 300μM PEG-CAT before being stimulated by increasing concentrations of CRP-XL (M), U46619 (N) and thrombin (O). ROS fluctuations were recorded over six minutes using fluorometry. BAPTA and TPEN treatment significantly inhibited evoked CRP-XL increases and abolished U46619 and thrombin evoked increases in DCFH fluorescence. Agonist-evoked increases in DCFH fluorescence were also abolished upon PEG-SOD and PEG-CAT treatment. (A, D, G, J and M) ○ 1μg/mL CRP-XL, ■ 0.3μg/mL CRP-XL, ▲ 0.1μg/mL CRP-XL, ▼ 0.03μg/mL and ● vehicle. (B, E, H, K, and N) ○ 10μM U46619, ■ 3μM U46619, ▲1μM U46619, ▼ 0.3μM U46619, and ● vehicle. (C, F, I, L and O) ○ 1U/mL Thrombin, ■ 0.3U/mL Thrombin, ▲ 0.1U/mL Thrombin, ▼ 0.03U/mL Thrombin and ● vehicle (dimethyl sulfoxide, DMSO). Data are mean±standard error of mean (SEM) from 6 independent experiments. Significance is denoted as **** ($p<0.0001$), *** ($p<0.001$), ** ($p<0.01$) or * ($p<0.05$).

Further experiments were carried out to investigate the relationship between agonist-evoked $[Ca^{2+}]_i$ signalling and ROS generation during platelet activation. DCFH-loaded platelets were pre-treated with BAPTA (10μM) prior to agonist stimulation, and changes in DHCF fluorescence were quantified using fluorometry. CRP-XL-evoked increases in DCFH fluorescence were significantly reduced in BAPTA pre-treated platelets, as the F/F_0 after 6 mins were reduced from 1.8±0.1 down to 1.3±0.1 upon BAPTA pre-treatment ($p<0.01$, Figure 3.7A, D). Interestingly, BAPTA pre-treatment did not entirely abrogate CRP-XL-induced increases in DCFH fluorescence, as the F/F_0 after 6 mins (1.3±0.1) was higher than the vehicle control (0.9±0.02, $p<0.01$, Figure 3.7D). These data suggest that $[Ca^{2+}]_i$ may mediate ROS elevation upon CRP-XL stimulation, although another mechanism may be in place as the DCFH fluorescence was not entirely abrogated upon application of BAPTA.

In contrast, BAPTA treatment abolished any significant increases induced by U46619 and thrombin. The final DCFH F/F_0 induced by U46619 (10μM) was abrogated from 1.21±0.03 to 1.01±0.01 ($p<0.05$, Figure 3.7B and E). The final DCFH F/F_0 induced by thrombin (1U/mL) was also abolished from 1.4±0.1 to 1.01±0.01 in BAPTA pre-treated platelets ($p<0.01$, Figure 3.7C and F). Thus $[Ca^{2+}]_i$ mediates ROS elevation upon thrombin and U46619 stimulation, but not following CRP-XL stimulation. This may be due to CRP-XL inducing a greater elevation in DCFH fluorescence in comparison to that induced by thrombin and U46619, which could cause further oxidative stress and thus further increase in ROS. Such an increase may not be apparent with thrombin and U46619 stimulation, where ROS generation is reduced.

In order to investigate the role of $[Zn^{2+}]_i$ fluctuations during ROS production during platelet activation, DCFH-loaded platelets were pre-treated with the Zn^{2+} chelator TPEN (50µM) prior to being stimulated with different concentrations CRP-XL (Figure 3.7G), U46619 (Figure 3.7H) or thrombin (Figure 3.7I).

TPEN pre-treatment inhibited increases in CRP-XL-evoked DHCF fluorescence in a similar manner to BAPTA pre-treatment (Figure 3.7D-F) indicating that the reduction in DCFH seen upon BAPTA application was attributable to Zn^{2+} and not Ca^{2+}. After 6 mins, the DCFH F/F_0 was reduced from 1.8±0.1 to 1.3±0.1 in TPEN-treated platelets ($p<0.01$, Figure 3.7A, G). In a similar manner to BAPTA pre-treatment, TPEN did not fully abrogate CRP-XL-mediated (1µg/mL) increases of DHCF fluorescence. After 6 mins, the F/F_0 (1.3±0.1, in TPEN pre-treated platelets) in response to CRP-XL (1µg/mL) was still significantly higher compared to the vehicle control (0.93±0.02, $p<0.01$, Figure 3.14A). This suggests that the elevation of ROS is mediated by $[Zn^{2+}]_i$ and not $[Ca^{2+}]_i$ and that other mechanisms may be in place that enables CRP-XL induced ROS generation that is independent of cations.

Increases in DCFH fluorescence in response to U46619 or thrombin were abolished with TPEN (50µM) pre-treatment. After 6 mins, DCFH F/F_0 induced by U46619 (10µM) was abrogated from 1.2±0.03 to 1.08±0.02 in TPEN pre-treated platelets ($p<0.05$, Figure 3.7B, H). The DCFH F/F_0 induced by thrombin (1U/mL) was also abrogated from 1.4±0.1 to 1.08±0.03 upon TPEN application ($p<0.05$, Figure 3.7C, I). These data support a role for $[Zn^{2+}]_i$ and not $[Ca^{2+}]_i$ in ROS generation. As BAPTA has a higher affinity for Zn^{2+} than Ca^{2+}, the inhibition effect induced by BAPTA pre-treatment may be primarily due to the chelation of Zn^{2+} as opposed to Ca^{2+}. This is consistent with the effects seen with TPEN pre-treatment, which is highly specific to Zn^{2+}.

Further experiments were performed using PEG-SOD (30U/mL) and PEG-CAT (300U/mL) to assess the validity of the ROS being detected by the ROS probe. PEG-SOD and PEG-CAT scavenge ROS, and should, therefore, inhibit elevation of ROS mediated by the agonist (Pietraforte et al., 2014; Sinha and Dabla, 2015).

PEG-SOD and PEG-CAT pre-treatment abolished agonist-dependent increases in DCFH fluorescence (Figure 3.7J-O). The final DCFH F/F_0 induced by CRP-XL (1µg/mL) after 6mins was abrogated from 1.8±0.1 to 1.0±0.2 and 1.02±0.01 upon PEG-SOD and PEG-CAT pre-treatment, respectively ($p<0.001$, Figure 3.7A, J and M). Similarly, with U46619 (10µM) treatment, DCFH F/F_0 was also abolished from 1.2±0.03 to 0.93±0.01 and 0.95±0.01 upon PEG-SOD and PEG-CAT pre-treatment,

respectively ($p<0.05$, Figure 3.7B, K and N). Furthermore, DCFH F/F_0 induced by thrombin (1U/mL) was also abolished from 1.4±0.1 to 1.04±0.04 and 0.99±0.01 upon PEG-SOD and PEG-CAT pre-treatment, respectively ($p<0.05$, Figure 3.7C, L and O). These data confirm that the fluorescence signal generated upon agonist stimulation is attributable to ROS, thus validating the use of DCFH. The sensitivity to antioxidants described here confirm that agonist-mediated changes in fluorescence are a result of ROS elevation.

As a positive control of ROS production, platelets were treated with H_2O_2 (Figure 3.8). Treatment with the highest two concentrations of H_2O_2 (10µM and 3µM) resulted in significant increases in DCFH fluorescence relative to the vehicle control (DMSO). After 6 mins, DCFH F/F_0 induced by 10µM and 3µM H_2O_2 treatment were 4.6±0.2 and 1.9±0.2 respectively, which was significantly higher the vehicle control (0.91±0.02, $p<0.0001$, Figure 3.8A,). This data are consistent with the detection of ROS by DCFH.

Pre-treatment of platelet suspensions with BAPTA or TPEN reduced the H_2O_2-induced DCFH fluorescence signal. The final DCFH F/F_0 in response to the highest concentration (10µM) of H_2O_2 was reduced from 4.6±0.2 (vehicle) to 3.0±0.4 and 3.6±0.5 upon BAPTA and TPEN pre-treatment respectively ($p<0.0001$, Figure 3.8A-C). The reduced DCFH F/F_0 in response to H_2O_2 on BAPTA and TPEN pre-treated platelets did not significantly differ (final DCFH value on TPEN and BAPTA pre-treated platelets were 3.0±0.4 and 3.6±0.5 respectively, $p>0.05$, ns, Figure 3.8B-C). These data illustrate that TPEN or BAPTA pre-treatment had similar effects in terms of inhibition of DCFH fluorescence, suggesting that Zn^{2+}, as opposed to Ca^{2+}, can influence ROS signalling. This correlates with data from the previous sections (Figures 3.5-7), which demonstrate a role for ROS in Zn^{2+}, but not Ca^{2+} signalling. Furthermore, DCFH fluorescence following treatment with high concentrations (10µM and 3µM) of H_2O_2 in BAPTA and TPEN pre-treated platelets were still significantly higher than that observed with vehicle control. The final DCFH F/F_0 in BAPTA pre-treated platelets following stimulation with 10µM or 3µM H_2O_2 was 3.0±0.4 and 1.8±0.2, respectively, after 6mins, compared to 1.0±0.1 for vehicle control, $p<0.01$, Figure 3.18B). For TPEN pre-treated platelets, the final DCFH F/F_0 was 3.6±0.5 and 2.2±0.1, respectively for 10µM and 3µM H_2O_2, compared to 0.90±0.02 for the vehicle control ($p<0.0001$, Figure 3.8C). This finding indicates that ROS signalling is also evoked by other mechanisms (yet to be studied) that does not involve Zn^{2+} or Ca^{2+} since increases in DCFH fluorescence was still significant even with chelation of $[Zn^{2+}]_i$ and $[Ca^{2+}]_i$.

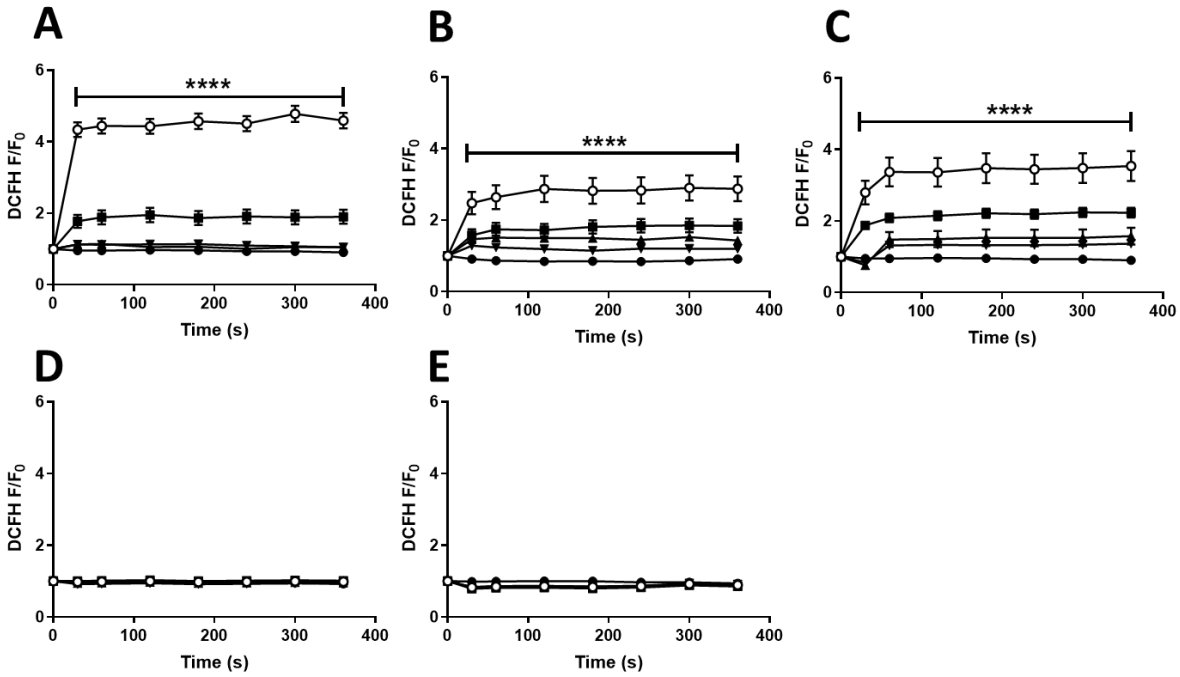

Figure 3.8. ROS-evoked increases in DCFH fluorescence are inhibited by TPEN and BAPTA and abrogated by PEG-SOD and PEG-CAT. DCFH-labelled washed human platelets were stimulated by different concentrations of H_2O_2 (A), following pretreatment with BAPTA (B), TPEN (C), PEG-SOD (D) or PEG-CAT pre (E). ROS fluctuations were recorded over six minutes using fluorometry. H_2O_2 induced a significant increase in Zn^{2+} fluorescence. This was reduced upon treatment with BAPTA, TPEN, PEG-SOD or PEG-CAT. ○ H_2O_2 10µM, ■ H_2O_2 3µM, ▲ H_2O_2 1µM, ▼ H_2O_2 10µM and ● vehicle (DMSO). Data are mean±standard error of mean (SEM) from 6 independent experiments. Significance is denoted as **** ($p<0.0001$), *** ($p<0.001$), ** ($p<0.01$) or * ($p<0.05$).

PEG-SOD and PEG-CAT were again employed to assess the validity of the ROS elevation upon H_2O_2 treatment. PEG-SOD (30U/mL) and PEG-CAT (300U/mL) pre-treatment abolished any significant increases in DCFH fluorescence in response to H_2O_2. The final DCFH F/F_0 in response to H_2O_2 (10µM, the highest concentration that resulted in the greatest elevation of DCFH fluorescence) was abrogated from 4.6±0.2 (vehicle) to 1.01±0.01 and 1.01±0.02 respectively upon PEG-SOD and PEG-CAT pre-treatment ($p<0.0001$, Figure 3.18A, D-E). These data verify that changes in DCFH are attributable to changes in ROS production.

The work described above supports the hypothesis ROS elevation occurs following the elevation of $[Zn^{2+}]_i$ upon agonist stimulation. CRP-XL stimulation resulted in a greater increase in ROS compared with thrombin or U46619 (Figure 3.7A-C). As CRP-XL treatment also resulted in the largest elevation of $[Zn^{2+}]_i$ (Figure 3.1), this indicates a causal relationship between elevation $[Zn^{2+}]_i$ and ROS

elevation. This relationship between ROS and Zn^{2+} may be independent of Ca^{2+}, as $[Zn^{2+}]_i$ chelation but not $[Ca^{2+}]_i$ chelation influenced ROS elevation upon agonist and H_2O_2 treatment (Figure 3.7D-I). These data correlate well with data from other cell types such as neuron cells, where elevated Zn^{2+} further elevates ROS levels in a positive feedback mechanism (Stork and Li, 2016). Data described here, suggests that a positive feedback mechanism may be in place in platelets, and may be independent of Ca^{2+}, and primarily dependant on Zn^{2+}. Application of the antioxidants confirmed that increases in fluorescence observed upon treatment with the agonists was in accordance with ROS elevation as PEG-SOD and PEG-CAT pre-treatment abrogated the agonist-evoked DCFH fluorescence response (Figure 3.7)

Application of PEG-SOD and PEG-CAT provided additional data to validate the ROS probe, DCFH, as the increases in DCFH fluorescence induced by H_2O_2 was abrogated upon pre-treatment with PEG-SOD and PEG-CAT (Figure 3.8D-E). Furthermore, this fluorescence was inhibited upon pre-treatment with the $[Ca^{2+}]$ chelator BAPTA (Figure 3.8B) and the $[Zn^{2+}]_I$ chelator TPEN (Figure 3.8C), further outlining the role that Zn^{2+} may have on regulating ROS fluctuations. This relationship between ROS and Zn^{2+} may serve to be the major mechanism which enables $[Zn^{2+}]_i$ elevation upon activation, as illustrated in previous sections of this Chapter.

3.3 Discussion

The experiments described in this chapter were designed to investigate whether platelet $[Zn^{2+}]_i$ fluctuates in response to agonist stimulation, and to investigate potential mechanisms for changes in $[Zn^{2+}]_i$. The data generated provides the first evidence that $[Zn^{2+}]_i$ increases upon activation with physiological agonists, in a manner that is consistent with a secondary messenger. Furthermore, the mechanisms by which $[Zn^{2+}]_i$ was elevated were found to be redox sensitive.

Stimulation of platelets with agonists that target GpVI or TP (CRP-XL or U46619) resulted in increases in FZ-3 fluorescence, consistent with a liberation of labile Zn^{2+} from stores (as yet unidentified) into the cytosol of the platelet. CRP-XL stimulation produced a much greater increase in FZ-3 fluorescence than U46619, and PAR stimulation did not result in FZ-3 fluctuations. Differential responses to agonists indicate that that fluctuations of $[Zn^{2+}]_i$ occur as a result of different signalling pathways. Signalling via GpVI differs from the signalling via TP or PAR. GpVI signalling involves tyrosine phosphorylation of platelet proteins such as Syk and LAT, resulting in the activation of PLCγ2 (Figure

1.3). Conversely, TP and PAR are G-protein coupled receptors that propagate signalling via G-proteins, resulting in activation of PLCβ2 (Li et al., 2010). It is difficult to reconcile the different responses in Zn^{2+} signalling following TP or PAR receptor stimulation, as these two receptors both couple to similar signalling pathways which involve $G\alpha_{12/13}$ and $G\alpha_q$ (Capote et al., 2015). These findings in this chapter suggest that $[Zn^{2+}]_i$ increases are regulated by proteins that are not shared by GpVI- and thrombin-dependent signalling pathways. This coincides well with the work carried out by Watson et al., (2016), which found that exogenous Zn^{2+} treatment resulted in differing patterns of tyrosine phosphorylation than from that induced by GpVI and PAR (Watson et al., 2016). Tyrosine phosphorylation is a major platelet activatory signalling event. The work carried out by Watson et al., (2016) indicates that Zn^{2+} induces activatory signalling via a novel pathway in comparison to CRP-XL and thrombin. The differential responses of $[Zn^{2+}]_i$ fluctuations to the agonists suggest that $[Zn^{2+}]_i$ elevation is mediated by a novel GpVI or TP dependent signalling pathway, although this would require further investigation. The major finding of this work is that stimulation with conventional platelet agonists results in significant increases in $[Zn^{2+}]_i$ indicating that Zn^{2+} may play a major role in platelet activity in physiological conditions.

Differences in fluorescence values for FZ-3 and FL-4, measuring Zn^{2+} and Ca^{2+} respectively, were observed following agonist stimulation. Pre-treatment of platelets with BAPTA abolished any increases in FZ-3 or FL-4 fluorescence, indicating that FZ-3 does not respond to changes in $[Ca^{2+}]_i$. This was expected, due to the strong chelating effect by BAPTA of Zn^{2+} and Ca^{2+} (discussed in Chapter 1). Although BAPTA is a strong $[Ca^{2+}]_i$ chelator, BAPTA has a higher affinity for Zn^{2+}, thus it is likely to chelate $[Zn^{2+}]_i$ in addition to $[Ca^{2+}]_i$ (Radford and Lippard, 2013) (Matias et al., 2010a). As seen in Figure 3.1, the significant increases in $[Zn^{2+}]_i$ that occurred in response to stimulation by CRP-XL or U46619 were abolished in TPEN or BAPTA treated platelets. These data provide evidence that $[Zn^{2+}]_i$ is elevated upon CRP-XL and U46619 stimulation in a similar manner to $[Ca^{2+}]_i$. Differences in agonist-dependent fluctuations in FZ-3 and FL-4 fluorescence were observed (Figure 3.1-2). As expected, pre-treatment with BAPTA abolished any significant increases in FL-4 fluorescence (Figure 3.2), as BAPTA is able to chelate Ca^{2+}. Interestingly, pre-treatment with TPEN did not significantly influence the agonist-evoked FL-4 increases (Figure 3.2), indicating that changes in $[Zn^{2+}]_i$ do not play a significant role of $[Ca^{2+}]_i$ handling. These data also provide strong evidence for the specificity of the fluorophores, FZ-3 and FL-4 for Zn^{2+} and Ca^{2+} respectively since the fluorescence being detected by FL-4 was independent of Zn^{2+} as the application of TPEN did not significantly affect the fluorescence that was exhibited using FL-4. These data validate our approach to these experiments.

The initial findings of this chapter provide the first indications that $[Zn^{2+}]_i$ may be a secondary messenger in platelets and may mediate platelet activation in conjunction with $[Ca^{2+}]_i$. Agonist-dependent elevation of $[Ca^{2+}]_i$ is well documented (Smith et al., 1992, 1992; Varga-Szabo et al., 2009). $[Ca^{2+}]_i$ elevation is a hallmark of platelet activation and is a secondary messenger in platelets (Authi et al., 1993; Li et al., 2010; Orem et al., 2017; Smith et al., 1992; Varga-Szabo et al., 2009). $[Zn^{2+}]_i$ may act in a similar manner to Ca^{2+} in platelets , due to the elevation of $[Zn^{2+}]_i$ also occurring upon platelet activation as demonstrated in this chapter. Thus $[Zn^{2+}]_i$ elevation may also occur in conjunction with $[Ca^{2+}]_i$ elevation where Zn^{2+} may also mediate platelet activatory processes similarly to Ca^{2+} therefore acting as a secondary messenger in platelets (Authi et al., 1993; Smith et al., 1992).

The mechanisms that regulate agonist-evoked $[Zn^{2+}]_i$ increases was investigated using pharmacological inhibitors. Previous work in nucleated cells has shown that alterations to the in redox state results in the release of Zn^{2+} from thiol groups on intracellular cation storage proteins such as metallothionines into the labile pool (Krężel and Maret, 2017a). Furthermore, collagen treatment of platelets stimulates ROS-dependent platelet activation (Carrim et al., 2014; Krötz et al., 2004; Sinha and Dabla, 2015). Studies have found that an adaptor receptor known as TNF (tumour necrosis factor) adaptor receptor 4 (TRAF4) mediates downstream signalling from the ligated GpVI/FcRγ complex, which in turn results in amplified ROS production via the NOX pathway (illustrated in Figure 1.8, (Cangemi et al., 2014; Violi et al., 2015)). The $p47^{phox}$ subunit of NOX is a major contributor to mediating the downstream signalling from upon GpVI stimulation. TRAF4 interacts with other proteins that are involved in the GpVI downstream signalling pathway, including Lyn and Syk (Arthur et al., 2011). Other work has indicated that there may be specific phases in which ROS is elevated during the platelet activation pathways. These studies illustrate the importance of ROS in GpVI signaling (Cangemi et al., 2014; Carrim et al., 2014; Krężel and Maret, 2017a). Due to the strong link between Zn^{2+} and redox changes and ROS in many cell types, it was hypothesized that GpVI-induced $[Zn^{2+}]_i$ elevation may be redox dependant, and thus regulated by ROS concentrations in platelets. To explore this hypothesis, the effect of ROS on elevating $[Zn^{2+}]_i$ was explored via the modeling of ROS elevation. In previous work, ROS elevation was modeled via direct administration of H_2O_2, which is a stable ROS that readily diffuses across membranes (Krötz et al., 2004). Due to its stability compared with other ROS , H_2O_2 has become the primary ROS used in the study of ROS biology in cells. Early research found that high concentrations of H_2O_2 mediate ROS-induced activities such as cellular damage, which confirmed its activity as an active ROS species in cells. Such work also indicated that application of exogenous H_2O_2 can mediate intracellular signaling (via the NOX pathways) leading onto further elevated intracellular ROS (Gough and Cotter, 2011). H_2O_2 was also employed to model ROS elevation

in platelets and was found to induce apoptotic events (Beckman et al., 1988; Gough and Cotter, 2011, ; Lopez et al., 2007). This study indicated that the application of H_2O_2 resulted in further ROS relocation endogenously (Beckman et al., 1988; Lopez et al., 2007; Wee and Jackson, 2006). Application of H_2O_2 can also induce oxidative stress which can mediate further ROS production via mechanisms such as the NOX pathway (Figure 1.8) (Cangemi et al., 2014; Krötz et al., 2004; Pietraforte et al., 2014; Violi et al., 2015).

In the work described in this chapter, H_2O_2 treatment resulted in significant increases in $[Zn^{2+}]_i$, which was sensitive to BAPTA or TPEN pretreatment (Figure 3.3), providing evidence that ROS acts to elevate $[Zn^{2+}]_i$ in platelets. Sensitivity to ROS implicates redox-sensitive Zn^{2+}-storage proteins, such as metallothioneins, as a mechanism by which Zn^{2+} is increased. Metallothioneins are cysteine-rich proteins which transiently bind heavy metals such as Zn^{2+}, and are present at a concentration of 30 µg/10^{10} in platelets (Krężel and Maret, 2017a). Metallothionein has been found to have a higher affinity for Zn^{2+} than most other Zn^{2+} binding proteins (Bell and Vallee, 2009; Krężel and Maret, 2017a). Zn^{2+} binds to cysteines, producing a sulphur and Zn^{2+} network (Sugiura and Nakamura, 1994) (Rahman and De Ley, 2008). The proposed mechanism of Zn^{2+} binding and release from and to the metallothionines is redox dependent. Sulphur and Zn^{2+} complex can undergo oxidation and reduction to release and bind Zn^{2+} (Bell and Vallee, 2009), (Maret, 2000). This mechanism enables Zn^{2+} to be released, elevating the $[Zn^{2+}]_i$ concentration. Although the role of metallothioneins in Zn^{2+}-handling in platelets is yet to be determined, previous work has suggested that metallothioneins may play inhibitory roles in platelet aggregation and thrombus formation (Sheu et al., 2003). These conclusions were reached by incubating platelets with metallothioneins, which inhibited agonist-induced aggregation. The authors of this study suggested that metallothioneins play an inhibitory role in $[Ca^{2+}]_i$ mobilization (Sheu et al., 2003). Whilst further work is required to fully elucidate the role of metallothioneins in platelets, the possibility remains that metallathionines may play a significant role in regulating the concentration of labile $[Zn^{2+}]_i$ in platelets. Since H_2O_2 provided evidence that elevation of ROS induces elevated $[Zn^{2+}]_i$ (Figure 3.7) possibly in a redox-dependent manner involving metallothionines, the specificity of this potential mechanism was explored by measuring Ca^{2+} fluorescence in response to H_2O_2 stimulation. Although Ca^{2+} mobilization upon ROS elevation has been previously documented (Görlach et al., 2015; Krötz et al., 2004) these experiments act as a positive control to measure ROS elevation on inducing intracellular cation elevation. Data show in Figure 3.4 demonstrates that increases in ROS induce intracellular Ca^{2+} mobilization, although was chelated by TPEN, indicating that this ROS elevation is attributable to Zn^{2+} and not Ca^{2+}.

The mechanism by which agonist stimulation results in $[Zn^{2+}]_i$ elevation (Figure 3.1) was investigated using the antioxidants PEG-SOD and PEG-CAT. PEG-SOD and PEG-CAT, are enzymes, that under physiological conditions, act as a defense mechanism against ROS and free radical accumulation by breaking these down into less harmful oxygen and water. Accumulation of ROS can cause extreme damage to the cells (Pandya et al., 2013; Sinha and Dabla, 2015). PEG-SOD and PEG-CAT, have been widely used to regulate ROS in various cells. In recent work, PEG-SOD and PEG-CAT were found to offer a greater level of resistance upon high levels of oxidative stress in endothelial cells, thus regulated ROS elevation (Beckman et al., 1988). Another example of the use of PEG-SOD and PEG-CAT was in research that was investigating the implications of oxidative injury upon radiation-induced tissue damage to lungs, in particular, pulmonary fibrosis in mice (Machtay et al., 2006). This work indicated that application of PEG-SOD and PEG-CAT inhibited radiation-induced pulmonary fibrosis in mice, by protecting the cells from oxidative stress. PEG-SOD and PEG-provided regulation of ROS levels in the cells, by scavenging high levels of ROS (Machtay et al., 2006). PEG-SOD and PEG-CAT were also employed in work that investigated LPS (Lipopolysaccharide) induced platelet aggregation, which has been suggested to be mediated by ROS elevation (Lopes Pires et al., 2017). In this study, the antioxidants were found to inhibit LPS induced aggregation, demonstrating the potential of these reagents to regulate ROS levels in platelets (Lopes Pires et al., 2017).

As shown in Figure 3.5 pre-treatment with PEG-SOD and PEG-CAT, inhibited agonist-dependent increases in FZ-3 fluorescence, providing evidence that the agonist-induced Zn^{2+} increases in platelets are ROS dependent. Interestingly, PEG-SOD and PEG-CAT did not inhibit agonist-evoked Ca^{2+} fluorescence increases (Figure 3.6). Thus $[Ca^{2+}]_i$ elevation is not ROS dependent. Whilst the mechanism of agonist-dependent $[Ca^{2+}]_i$ elevation are well documented and are not reliant on ROS, previous work has found that there is the interplay between Ca^{2+} signalling and ROS signalling. Studies have indicated that ROS may play a role in the regulation of Ca^{2+} signalling and that Ca^{2+} signalling is crucial for ROS production (Görlach et al., 2015). In this work, the authors stated that elevated Ca^{2+} is able to induce the formation of free radicals by activating ROS producing enzymes (Görlach et al., 2015; Zorov et al., 2014). ROS production in platelets occurs via mechanisms such as the NOX pathway (Figure 1.8, Chapter 1). The NOX pathway is regulated by cytosolic subunits such as $p47^{phox}$, which are activated by Ca^{2+} mediated PKC induced phosphorylation, thus Ca^{2+} plays a key role in ROS formation. Furthermore, in addition to ROS formation being mediated by Ca^{2+}, ROS elevation and redox modulation have been suggested to regulate Ca^{2+} channels, pumps, and exchangers. TRP channels such as TRPM2 and TRPC6 are redox sensitive (Gamberucci et al., 2002; Görlach et al., 2015; Kitajima et al., 2016; Zorov et al., 2014). Exposure to ROS induces conformational changes to these channels,

thereby regulating activation (Görlach et al., 2015; Kitajima et al., 2016). These studies indicate that ROS may play a major role in Ca^{2+} homeostasis in platelets. STIM1 and Orai1 (which are involved in SOCE, Figure 1.10) have also been suggested to be redox sensitive (Görlach et al., 2015). STIM1 and Orai1 assist in ROS formation as well as being activated by ROS (Gandhirajan et al., 2013; Steinckwich et al., 2011). IP_3R has also been suggested to be redox sensitive. Work carried out on various cell types such as endothelial cells, targeted the multiple thiol groups found in IP_3R. Application of exogenous ROS has been suggested to induce the sensitivity of IP_3R to IP_3 via modulation of thiol groups. The exact mechanism of this ROS mediated IP_3R activation is yet to be elucidated, however, may be an interesting target due to the importance of IP_3R in calcium signalling (Bánsághi et al., 2014; Lock et al., 2012). Further studies have suggested that ROS may play an inhibitory role in the Ca^{2+} pumping activity induced by SERCA , by inducing uncoupling of ATP hydrolysis from the Ca^{2+} pumping activity (Gamberucci et al., 2002; Sharov et al., 2006; Smith et al., 1992). Whilst these studies provide further support for a role for ROS and redox in Ca^{2+} signalling, the data presented in this chapter indicate that ROS is not a key determinant in agonist-dependent elevated $[Ca^{2+}]_i$ whereas it is for $[Zn^{2+}]_i$ elevation. Whilst previous studies indicate that there is the potential interplay between ROS and Ca^{2+}, all previous work has not taken Zn^{2+} into account (Görlach et al., 2015). The work carried out in this chapter, Is suggestive to a relationship between Zn^{2+} and ROS in platelets. This is a novel finding that warrants further investigation. The data described here indicates that $[Zn^{2+}]_i$ elevation in platelet is dependant on ROS and that redox changes induced by the agonists may be the major mechanism elucidating $[Zn^{2+}]_i$ elevation, which may be independent of Ca^{2+}.

Further experiments were carried out to measure ROS upon agonist stimulation. As demonstrated in Figure 3.7, agonist stimulation resulted in significant increases in ROS. CRP-XL induced the highest increase in ROS fluorescence in comparison to U46619, or thrombin. This correlates with previous work which showed that CRP-XL stimulation resulted in higher levels of ROS release than other agonists (Arthur et al., 2008; Begonja et al., 2006; Freedman, 2008; Krötz et al., 2004; Qiao et al., 2018; Walsh et al., 2014). Pre-treatment of platelets with BAPTA significantly reduced the CRP-XL-induced ROS and abolished increases that were induced by U46619 and thrombin. This was also the case when the platelets were pre-treated with TPEN, providing further evidence for interaction between ROS and Zn^{2+}. As chelation of Ca^{2+} and Zn^{2+} (using BAPTA) did not produce a ROS response that was significantly different to $[Zn^{2+}]_i$ chelation (following TPEN treatment), these data indicate that $[Zn^{2+}]_i$ elevation is redox-sensitive and independent of Ca^{2+}, providing further evidence to suggest a novel mechanism by which $[Zn^{2+}]_i$ is elevated in platelets may be in place.

Further experiments were performed to determine the biological validity of the ROS fluorescence that is being induced by the agonists. The antioxidants PEG-SOD and PEG-CAT which scavenge ROS were employed to determine whether the fluorescence increases were attributable to ROS production. As shown in Figure 3.7, the ROS fluorescence induced by the agonists was completely abolished by antioxidant treatment, confirming that changes in fluorescence are due to ROS. H_2O_2 was used again to test the biological validity of the DCFH in detecting ROS in platelets. As illustrated in Figure 3.8, H_2O_2 induced a significant increase in ROS fluorescence, which was slightly reduced with BAPTA or TPEN treatment, outlining further evidence of the relationship between cations and ROS in platelets. As expected the antioxidants, PEG-SOD and PEG-CAT, inhibited any ROS fluorescence increases induced by H_2O_2. Thereby confirming the biological validity of the ROS probe DCFH in platelets.

3.3.1. Conclusion

The data described here is the first to show fluctuations of $[Zn^{2+}]_i$ in response to agonist stimulation of platelets. This finding suggests a novel mechanism of $[Zn^{2+}]_i$ elevation upon agonist stimulation with agonists in a redox-sensitive manner in platelets. CRP-XL and U46619, but not thrombin, induced significant elevations in $[Zn^{2+}]_i$. Although thrombin treatment did not result in fluctuations in FZ-3 fluorescence, thrombin-induced the greatest increase in $[Ca^{2+}]_i$, which in contrast to CRP-XL or U46619, was sustained throughout the experiment. The reason why thrombin-induced activation does not result in Zn^{2+} fluctuations is not clear. It is possible that differential receptor engagement results in heterogeneous Zn^{2+} responses, with PAR receptors (unlike GpVI or TP), not coupling to $[Zn^{2+}]_i$ release. Conversely, since thrombin results in the largest and most sustained $[Ca^{2+}]_i$ elevation, thrombin-induced $[Ca^{2+}]_i$ elevation could be negatively regulating $[Zn^{2+}]_i$ elevation, possibly as a result of competition between the cations. Further investigation is required to determine as to why thrombin does not induce $[Zn^{2+}]_i$ elevation, however differences in ROS increases evoked by these agonists (Figure 3.7) may also provide an explanation as to why PAR stimulation by thrombin did not evoke $[Zn^{2+}]_i$ fluctuations. Collagen, thromboxane A2 and thrombin stimulation all result in increases in ROS levels, with GpVI signalling inducing the greatest rise in ROS levels as shown in previous studies (Arthur et al., 2008; Krötz et al., 2004; Qiao et al., 2018; Walsh et al., 2014). These findings correlate well with the data presented in this chapter. Stimulation via GpVI induced the greatest increase in ROS fluorescence in comparison to U46619 and thrombin. The greater increase in ROS in response to GpVI stimulation relative to thrombin indicates that perhaps the differences in $[Zn^{2+}]_i$ fluctuations are

attributable to differences in ROS signalling evoked upon GpVI and PAR stimulation. Interestingly thrombin evoked increases in ROS was found to be mediated by $[Zn^{2+}]_i$ (Figure 3.7), which is difficult to reconcile as thrombin does not mediate $[Zn^{2+}]_i$ fluctuations. Thus Zn^{2+} may serve as a mechanism for mediating ROS signalling which is most apparent upon GpVI stimulation, however, serves as a complex mechanism that requires further investigation. Overall this work provides the first reports demonstrating that agonist-dependent changes in platelet redox state result in a rapid and sustained $[Zn^{2+}]_i$ elevation. Although this is not the case with thrombin which suggests alternative mechanisms that are yet to be confirmed may be in place.

This work also shows that changes to the redox state of platelets result in an increase in FZ-3 fluorescence, consistent with the liberation of Zn^{2+} from stores. Whilst the nature of Zn^{2+} stores is not known, redox sensitivity is compatible with storage by metal ion binding proteins such as metallothioneins. $[Ca^{2+}]_i$ mobilization was not influenced by changes in redox state and was independent of such mechanisms that affected $[Zn^{2+}]_i$ mobilisation; thus cation release is differentially regulated. As Ca^{2+} is predominantly mobilized from the dense tubular system, these data correlate with a different release mechanism for Zn^{2+}. Release from Zn^{2+} binding proteins is consistent with this idea.

This work has addressed the aims of this chapter, as the data generated provides the first finding of agonist-induced $[Zn^{2+}]_i$ mobilization which is redox sensitive. $[Zn^{2+}]_i$ is elevated upon platelet stimulation and may be regulated in a redox-sensitive manner.This is consistent with a role for Zn^{2+} as a secondary messenger. However, for such a conclusion to be drawn, it is necessary for increased $[Zn^{2+}]_i$ to have a causal relationship with aspects of platelet activation. In order to test this, further experiments were designed to investigate how increases in platelet $[Zn^{2+}]_i$ affected functional responses. These experiments are described in the following chapters.

Chapter 4

4.0 Modelling intracellular Zn^{2+} release in platelets using ionophores

4.1 Background

The data described in Chapter 3 demonstrated that $[Zn^{2+}]_i$ was elevated in platelets stimulated by conventional agonists, including CRP-XL and U46619. Zn^{2+} fluctuations were redox-sensitive, suggesting that Zn^{2+}-binding proteins which are sensitive to redox changes (such as metallothioneins) may release Zn^{2+} upon changes in redox state. Whilst Zn^{2+} release is redox-dependent, the nature of the Zn^{2+} store has yet to be confirmed.

Agonist-evoked changes in $[Zn^{2+}]_i$ are consistent with a role for Zn^{2+} as a secondary messenger. However, to conclude a secondary messenging role, changes in Zn^{2+} need to be linked to functional responses. Whilst this has been done in several nucleated cell types, functional responses to increased $[Zn^{2+}]_i$ in platelets has yet to be demonstrated.

In this chapter, a number of experiments are described in which the cytosolic concentration of Zn^{2+} is artificially increased via pharmacological means, and resulting effects on platelet function are assessed. The pharmacological modulators used here are ionophores, of which a number have been described in the literature as being specific for Zn^{2+}, and not affected by other physiological cations such as Ca^{2+}.

4.1.1. Modelling cation release using ionophores

Ionophores are lipid-soluble reagents that facilitate metal ion transport across cell membranes and have been widely used to study the effects of ions in cellular activity (Ding and Lind, 2009). Ionophores tend to have moderate to low affinity to their selective metal ion. When utilised in cell research, ionophores bind to the ions in a highly concentrated area (for example in an ion store in a cell) and then diffuse to areas where the ion concentration is low (for example the cytosol of a cell). Thus ionophores can be used to equilibrate ions in a given cellular environment (Ding and Lind, 2009; Fasolato and Pozzan, 1989; Pressman, 1976). Ionophores are sensitive to protonation, due to the mechanism of cation transport which have been modelled by previous studies, where cations are exchanged for protons (H^+) in an electron neutral process (Fasolato and Pozzan, 1989; Pfeiffer et al., 1978; Shastri et al., 1987). Thus, the binding of ions to ionophores may be pH-dependent. If the pH of

the milieu surrounding the ionophore is higher than the pKa of the ionophore, then the metal ion will bind to the ionophore. However, if the pH of the surrounding space is lower than the pKa of the ionophore, then the metal ion will be released (Ding and Lind, 2009, Andreini et al., 2006). Ionophores therefore essentially transport ions from one region to another across the membrane. However, an alternate mechanism has been proposed, whereby the ionophore can form a hydrophilic pore on the cell membrane, allowing the ions to pass through the pore, in essence forming a channel for the ions (Ding and Lind, 2009; Pressman, 1976). Ionophores have been used to equilibrate ion concentrations as well to incorporate ions into cellular environments. However, most notably, ionophores have been widely used to enable increases in intracellular ion concentration in order to study the effects of ions on the specific cellular activity (Shastri et al., 1987; Verma et al., 2011; Xue et al., 2014).

On account of the magnitude of importance of Ca^{2+} in many cell processes, a widely used ionophore in cell research is the calcium ionophore, A23187(Pfeiffer et al., 1978; Shastri et al., 1987, p. 23187; Verma et al., 2011). The increase of cytosolic Ca^{2+} levels by A23187 mimics the effects of signal pathway engagement and $[Ca^{2+}]_i$ release (Pfeiffer et al., 1978). A23187 is widely accepted to have specificity for Ca^{2+} over other cations (E. Wang et al., 1998), and it is often used to increase cytosolic Ca^{2+} concentrations by liberating Ca^{2+} from intracellular stores, thus aiding in the understanding of the roles calcium plays in many cellular processes such as apoptosis and proliferation (Fasolato and Pozzan, 1989). However, A23187 may also coordinate other cations such as Zn^{2+}. A23187 has been suggested to potentially have different transport mechanisms for different cations, although this is yet to be studied. The transport of Ca^{2+} via A23187 occurs in a 2 (ionophore): 1 (cation) state, whereas if the complex were in a 1:1 state then Ca^{2+} transport does not occur (Erdahl et al., 1995, 1994; E. Wang et al., 1998). The destabilisation of the 2:1 complex state can result in the loss of an ionophore and form the 1:1 state complex, although this change in stoichiometry (2:1- 1:1) requires further investigation to confirm the validity of this proposed mechanism. These studies provide evidence to suggest that A23187 may not be as Ca^{2+} specific and could also enable Zn^{2+} transport (Erdahl et al., 1996, 1995, 1994). Work carried out in rat thymocytes found that increases in Ca^{2+} fluorescence induced by A23187 were not influenced by TPEN application; however, increases in Zn^{2+} fluorescence that was induced by A23187 was abrogated upon TPEN application (Sakanashi et al., 2009). Thus showing that A23187 was also able to evoke $[Zn^{2+}]_i$ increases in addition to $[Ca^{2+}]_i$ increases. In human platelet research, application of A23187 results in a full aggregation response, as a result of Ca^{2+} mobilisation from the Ca^{2+} store (Verma et al., 2011). A23187 has been widely used in platelet research to investigate Ca^{2+} signalling, however, due to the ability of A23817 being able to

coordinate Zn^{2+}, the behaviours in platelets induced by A23187 may also be attributable to Zn^{2+}. Therefore, further demonstrating how Zn^{2+} may have been overlooked in favour of Ca^{2+}.

Zn^{2+} ionophores have been used as a tool to model and extensively study the role of intracellular Zn^{2+}, in a similar manner to Ca^{2+} (Woodier et al., 2015), (Smith et al., 1992). Two widely used Zn^{2+} specific-ionophores are pyrithione (Py, Zn^{2+} ionophore, $C_{10}H_8N_2O_2S_2$, K_ds: 10^{-7}M, K_dCa: $10^{-4.9}$M) and clioquinol (Cq, Zn^{2+} ionophore, C_9H_5ClINO, K_dZn: 10^{-7}M, K_dCa: $10^{-4.9}$M) (Arslan et al., 1985a; Hyun et al., 2004a; Matias et al., 2010a; Qian and Colvin, 2016b). Py is an antimicrobial agent and is used as an antidandruff compound in shampoos. Similarly, Cq is used as an antifungal and is also applied as a bacteriostatic drug. However, the full mechanism of action of both of these Zn^{2+} ionophores is yet to be determined (Krenn et al., 2009).

Py has been widely used as a means of increasing $[Zn^{2+}]_i$ in various cell types to study cellular effects (Kim et al., 1999). Py induces apoptosis of cancer cells *in vitro* and is being investigated as a potential anti-cancer agent (Truong-Tran et al., 2000). Py activates a member of the transient receptor potential channel family (TRP channels) known as TRPA1, which are ion channels expressed on the membranes of various cell types. TRPA1 is expressed in dorsal root ganglia in mice. Treatment with Py induces activation of TRPA1 by elevating $[Zn^{2+}]_i$. This study provides a characterisation of the properties of Py as a Zn^{2+} ionophore (Ding and Lind, 2009; Krenn et al., 2009).

Cq is another Zn^{2+} specific ionophore which elevates $[Zn^{2+}]_i$ in various cell types (Park et al., 2011; Schimmer et al., 2012; Seo et al., 2015). Cq belongs to a class of compounds known as hydroxyquinolines and consists of two electron donor sites, one at its phenol oxygen atom and the other at its quinolone ring nitrogen atom which enables Cq to bind Zn^{2+}. Cq also contains the halogens, iodine and chlorine (Ding and Lind, 2009). Halogen groups increase lipophilicity, which may enable increased absorption at its intracellular target sites (Ding and Lind, 2009). The properties of Cq to characterise its role as an ionophore has been confirmed in studies showing Cq-induced increases in $[Zn^{2+}]_i$ in cancer cells(Yu et al., 2009). Other studies have found that Cq induces apoptosis and may potentially be used as an anti-cancer therapy via Zn^{2+} modulation (Ding et al., 2005; Ding and Lind, 2009; Rodríguez-Santiago et al., 2015; Yu et al., 2009).

4.1.2. Aims and Hypothesis

The aim of the work described in this chapter was to investigate whether ionophore-mediated increases in $[Zn^{2+}]_i$ couple to functional responses. Previous work in the literature has modelled $[Ca^{2+}]_i$

elevation using ionophores, which enabled the role of Ca^{2+} in platelets to be extensively studied (Davies et al., 1989; Erdahl et al., 1994; Sargeant et al., 1994; Verma et al., 2011). Ionophores enable a higher intracellular elevation of the cation (due to reasons discussed above) in comparison to that when stimulated with agonists. Thus the full role of the cation in platelet activity can be studied upon modelling release via ionophores, which may not be possible with agonist stimulation. The specific signalling pathways induced by the agonists result in varied responses and mobilisation of cations as illustrated in the previous chapter and the literature. The hypothesis of this chapter is that increases in $[Zn^{2+}]_i$ regulate platelet functional responses.

4.1.3. Methods

The release of $[Zn^{2+}]_i$ and $[Ca^{2+}]_i$ was measured in washed platelet suspensions in the same manner as Chapter 3, using fluorometry following staining with the $[Zn^{2+}]_i$ and $[Ca^{2+}]_i$ probes, Fluozin-3 (Fz-3) and FL-4 (FL-4), respectively (section 2.5).

The Zn^{2+} ionophores, Cq and Py, were investigated for use in platelets.The Ca^{2+} ionophore, A23187, was employed as a comparative measure to Zn^{2+} signalling as well as acting as a positive control to assess the action of ionophores in terms of modelling cation release.

In the same manner as Chapter 3, BAPTA and TPEN were employed to assess $[Zn^{2+}]_i$ and $[Ca^{2+}]_I$ fluctuations. Furthermore, the antioxidants PEG-SOD and PEG-CAT were employed in this chapter, to asses redox sensitivity in the context of cation release modelling, and changes in ROS were monitored with (DCFH) as before.

4.2 Results

4.2.1. Modelling intracellular Zn^{2+} release in platelets

Zn^{2+} specific ionophores were employed to mobilise Zn^{2+} from potential Zn^{2+} stores in platelets. This work was carried out to model $[Zn^{2+}]_i$ release using a similar scheme used to investigate $[Ca^{2+}]_i$ increases (Varga-Szabo et al., 2009).

Stimulation of FZ-3 loaded platelets with Zn^{2+} ionophores Cq or Py resulted in rapid, concentration-dependent increases in FZ-3 fluorescence, consistent with an elevation of $[Zn^{2+}]_i$ (Figure

4.1A-B). Treatment with the highest concentrations of the Cq or Py resulted in the largest increase in FZ-3 fluorescence relative to that induced by the vehicle. F/F_0 values following Cq (300µM) treatment increased throughout the stimulation time, reaching 6.2±1.1 after 6 mins. This was significantly higher than that generated by the vehicle control (0.98±0.02 after 6 mins, P<0.0001, Figure 4.1A). These results demonstrate that treatment of platelets with Zn^{2+} ionophores results in increases in $[Zn^{2+}]_i$. Treatment with the highest concentration of Py also resulted in a significant increase in FZ-3 fluorescence relative to that induced by the vehicle control, although this was lower than that in response to Cq. After 6 mins, the F/F_0 in response to 300 µM Py was 3.3±0.3, compared to 0.97±0.01 for the vehicle control (P<0.0001, Figure 4.1B). The reason why the two ionophores result in differences in Fz-3 fluorescence is unclear, as they both would be expected to elicit a similar response. It is possible that differences in ion binding affinity or differences in membrane permeability contribute to differences in ion handling.

A23187 was employed to determine whether changes in Ca^{2+} would affect FZ-3 fluorescence, and also to investigate the specificity of FZ-3 for Zn^{2+}.

Treatment with 300 µM of A23817 (the highest concentration used) resulted in a modest increase in FZ-3 fluorescence that only differed significantly from the vehicle control after 4 mins of treatment. F/F_0 values after 4 mins and 6 mins of stimulation with 300 µM A23187 were 1.6±0.3 and 1.8±0.3, respectively compared to 0.97±0.01 for the vehicle control, P<0.05, Figure 4.1C. There are different explanations for this observation. FZ-3 may be potentially detecting Ca^{2+} at high concentrations (evoked by A23817). Alternatively, A23187-dependent Ca^{2+} release may stimulate $[Zn^{2+}]_i$ release as a secondary response. However, the increase in FZ-3 fluorescence induced by A23187 (300µM) was low in comparison to that induced by the Zn^{2+} ionophores, indicating that FZ-3 is Zn^{2+} specific.

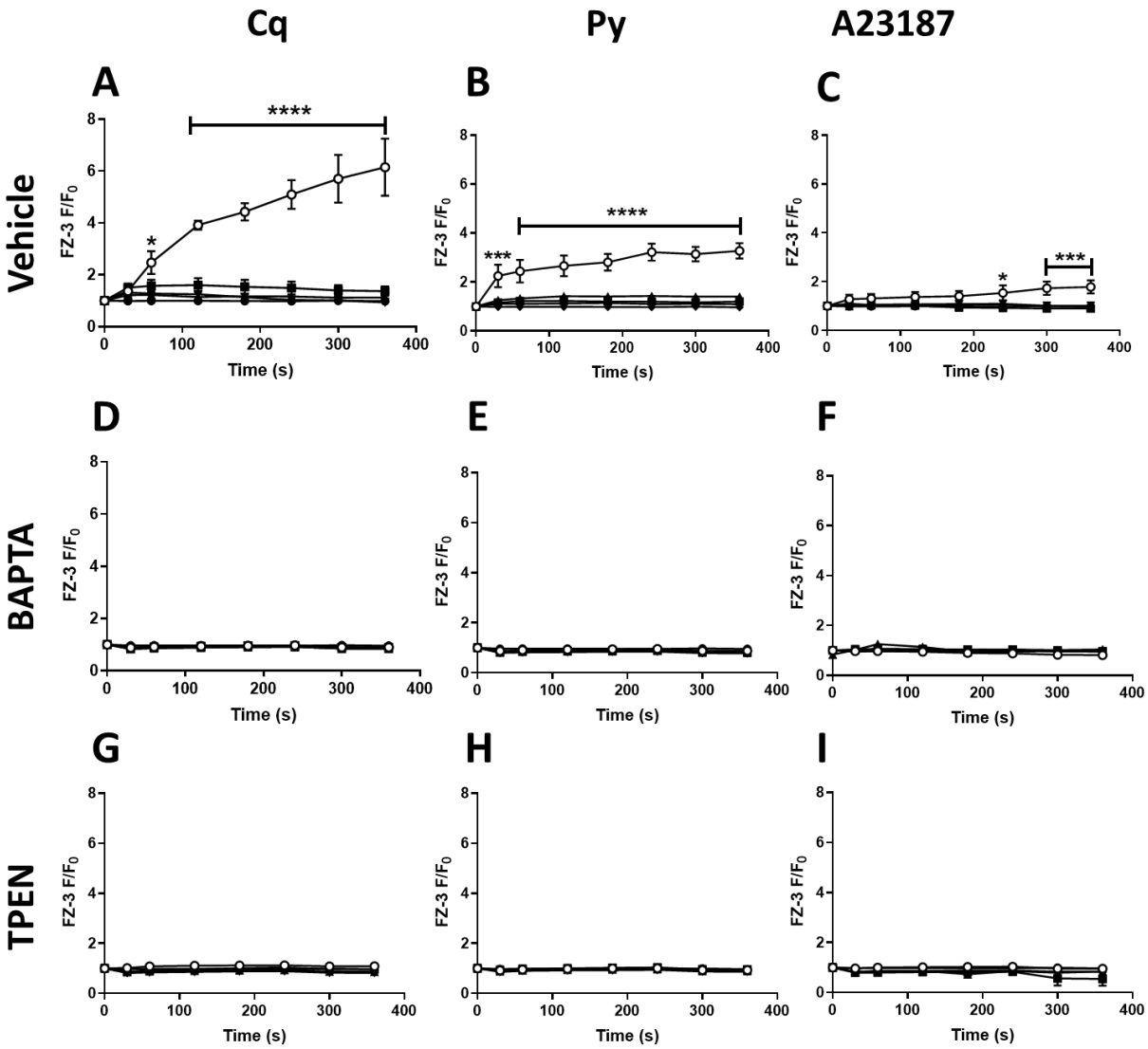

Figure 4.1. Ionophore treatment results in increases in FZ-3 fluorescence in platelets, which is abrogated by BAPTA and TPEN pre-treatment. Fluozin-3 (FZ-3)-loaded washed human platelets were stimulated by increasing concentrations of clioquinol, Cq (A), pyrithione, Py (B), or A23187 (C). FZ-3-labelled washed human platelets were pre-treated with BAPTA (10μM) before being stimulated by increasing concentrations of Cq (D), Py (E) or A23187 (F). FZ-3-labelled washed human platelets were pre-treated with TPEN (50μM) before being stimulated by increasing concentrations of Cq (G), Py (H), or A23187 (I). FZ-3 fluctuations were recorded over six minutes using fluorometry. Treatment with Zn^{2+} ionophores resulted in rapid, significant increases in FZ-3 fluorescence which was abolished upon BAPTA and TPEN pre-treatment. Treatment with the Ca^{2+} ionophore A23187 resulted in a reduced response which was also abolished upon BAPTA and TPEN pre-treatment. ○ 300μM, ■ 100μM, ▲ 30μM, ▼ 10μM and ● vehicle. Data are mean±standard error of mean (SEM) from 6 independent experiments. Significance is denoted as **** ($p<0.0001$), *** ($p<0.001$), ** ($p<0.01$) or * ($p<0.05$).

BAPTA is a potent chelator of both Ca^{2+} and Zn^{2+} and was employed to investigate the nature of the ionophore-induced fluorescent signal. BAPTA (10 μM) pre-treatment abolished any FZ-3

fluorescence increases that were induced by the ionophores (Figure 3.1D-F). After 6 mins, F/F_0 induced by Cq (300 µM) was abrogated from 6.2±1.1 (vehicle) to 0.90±0.03 on BAPTA pre-treated platelets ($p<0.0001$, Figure 3.1A, D). Similarly, F/F_0 induced by Py (300 µM) was abolished from 3.3±0.3 (vehicle) to 0.90±0.03 on BAPTA pre-treated platelets ($p<0.0001$, Figure 3.1B, E). Thus, ionophore-induced Fz-3 fluorescence is attributable to BAPTA-chelatable cations.

After 6 mins, F/F_0 in response to A23187 (300 µM) was also abrogated from 1.8±0.3 to 0.8±0.1 in BAPTA pre-treated platelets ($p<0.05$, Figure 3.1C, F). Thus these results provided validity of the FZ-3 fluorescence increases evoked by this ionophore. However, this data still did not confirm whether Zn^{2+} or Ca^{2+} were responsible for the increases in FZ-3 fluorescence. Therefore the highly specific $[Zn^{2+}]_i$ chelator TPEN (as demonstrated in chapter 3) was employed to confirm that FZ-3 fluorescence fluctuations induced by the ionophores were attributable to Zn^{2+}.

Pre-treatment of platelet suspensions with the Zn^{2+} chelator TPEN also resulted in abrogation of ionophore-induced FZ-3 fluorescence (Figure 4.1G-I). The final F/F_0 induced by Cq (300µM) was reduced from 6.2±1.1 to 1.09±0.01 on TPEN (50µM) pre-treated platelets ($p<0.0001$, Figure 4.1A, G). The final F/F_0 induced by Py (300µM) was also reduced from 3.3±0.3 to 0.94±0.02 on TPEN pre-treated platelets ($p<0.0001$, Figure 3.1B, H). As TPEN is specific to Zn^{2+} with no effect on Ca^{2+}. these data confirm that the FZ-3 fluorescence induced by Cq and Py is attributable to $[Zn^{2+}]_i$ and not $[Ca^{2+}]_i$,

Interestingly the FZ-3 fluorescence induced by A213187 was also abolished by TPEN pre-treatment in the same manner as BAPTA pre-treatment. After 6 mins, F/F_0 in response to A23187 (300µM) was reduced from 1.8±0.3 to 0.96±0.02 in TPEN pre-treated platelets ($p<0.05$, Figure 3.1C, I). This data indicates that the FZ-3 fluorescence increases evoked by A23187 are actually attributable to Zn^{2+}. This further validates FZ-3 as a specific Zn^{2+} probe, as this data confirms that the fluorescence being detected was not due to $[Ca^{2+}]_i$ elevation. Thus A23187 may not be Ca^{2+} specific and may also act on Zn^{2+} as has been the case with other commonly used cation chelators and ionophores as discussed in Chapter 2. These findings demonstrated that application with the Ca^{2+} ionophores, A23187 resulted in slight increases in FZ-3 fluorescence consistent with modest increases in $[Zn^{2+}]_i$. These data demonstrated that A23187 may not be Ca^{2+}-specific as it was able to induce increases in $[Zn^{2+}]_i$ elevation. This coincided with previous studies which show that A23187 is able to evoke increases in Zn^{2+} fluorescence as shown in rat thymocyte studies (Sakanashi et al., 2009). Thus indicating that A23187 induces $[Zn^{2+}]_i$ elevation and is not specific to Ca^{2+} as described earlier. These results indicated the increase in fluorescence induced by A23187 was attributable to Zn^{2+}. This

warrants further investigation and could further unveil the importance of Zn^{2+} in supposed Ca^{2+} specific processes.

The work conducted in this section demonstrates that Zn^{2+} ionophores increase $[Zn^{2+}]_i$ in platelets, and can therefore be used to model agonist-dependent increases in $[Zn^{2+}]_i$ to investigate potential activatory effects.Use of Zn^{2+}-specific ionophores (Cq and Py) and chelators (TPEN), and non-specific chelators (BAPTA) confirmed that Zn^{2+} is responsible for the changes in FZ-3 fluorescence.

Interestingly, these experiments were performed in the absence of extracellular Zn^{2+}. Therefore, any Zn^{2+} that is liberated by the ionophores must be present within stores in the platelets that are inaccessible to cytosolic FZ-3 under resting conditions. This would be consistent with a membrane-bound store of Zn^{2+}, similar to the DTS Ca^{2+} store. The nature of such a store is not known, although platelet a-granules contain significant quantities of Zn^{2+}. Whether this is accessible for increasing cytosolic Zn^{2+} concentrations upon agonist stimulation is not known.

4.2.2. Intracellular Ca^{2+} release is independent to intracellular Zn^{2+} release in platelets

The experiments described above demonstrate that $[Zn^{2+}]_i$ release can be modelled using Zn^{2+}-specific ionophores. However, despite having low affinities for Ca^{2+}, it is possible that the Zn^{2+} ionophores influence Ca^{2+} dynamics. To address this issue, fluctuations of $[Ca^{2+}]_i$ in response to ionophore treatment were investigated. This was primarily done as a comparison with $[Zn^{2+}]_i$ fluctuations, but also to verify the nature of the specificity of the fluorophores FZ-3 and FL-4 to Zn^{2+} and Ca^{2+} respectively.

Treatment with Cq or Py resulted in no significant fluctuations in FL-4 fluorescence. After 6 mins, the FL-4 F/F_0 following Cq (300µM) or Py (300µM) stimulation were 1.02±0.02 and 1.06±0.02, respectively compared to the vehicle control (1.01 ±0.01, $p>0.05$, ns, Figure 4.2A, B). Thus, FL-4 is specific for Ca^{2+}, and $[Zn^{2+}]_i$ has a negligible effect on FL-4 fluorescence.

Treatment with the highest four concentrations of A23187 (300µM, 100µM, 30µM and 10µM) resulted in significant increases in FL-4 fluorescence relative to the vehicle treatment. After 6 mins, FL-4 F/F_0 values were 5.8±0.9, 4.1±0.7, 2.6±0.5 and 1.9±0.2 respectively for 300µM, 100µM, 30µM and 10µM compared to 0.96±0.01 for the vehicle control ($p<0.05$, Figure 4.2C). This data illustrates the validity of A23187 as an ionophore for Ca^{2+}, as well as the validity of FL-4 as a specific $[Ca^{2+}]_i$ probe.

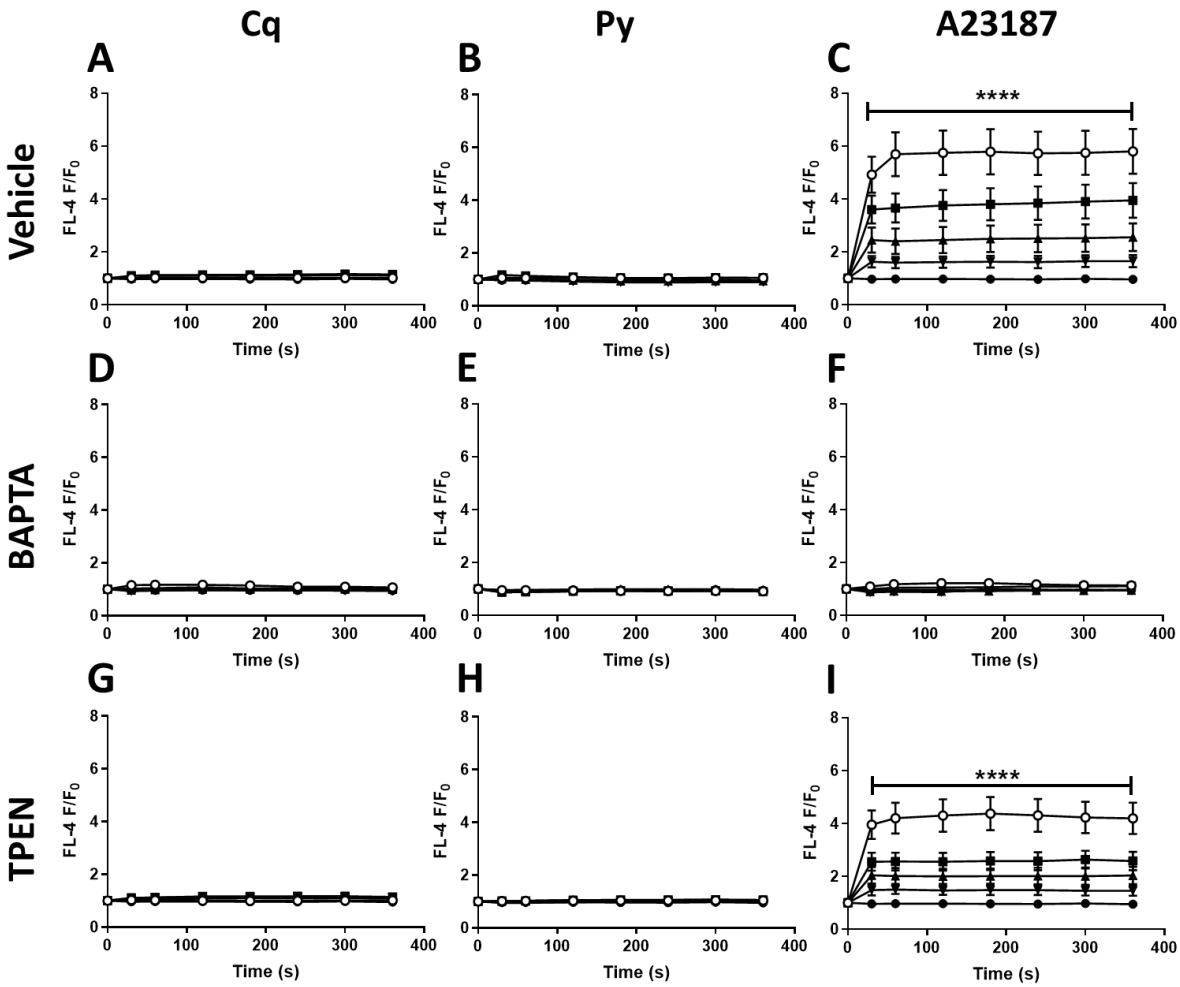

Figure 4.2. Ionophore treatment results in increases in FL-4 fluorescence, which is abrogated by BAPTA but not by TPEN pre-treatment. Fluo-4 (FL-4)-loaded washed human platelets were stimulated by increasing concentrations of Cq (A), Py (B), or A23187 (C). FL-4-labelled washed human platelets were also pre-treated with BAPTA (10μM) before being stimulated by increasing concentrations of Cq (D), Py (E) or A23187 (F). FL-4-labelled washed human platelets were also pre-treated with TPEN (50μM) before being stimulated by increasing concentrations of Cq (G), Py (H), or A23187 (I). FL-4 fluctuations were recorded over six minutes using fluorometry. Treatment with Ca^{2+} ionophore A23187, but not the Zn^{2+} ionophores resulted in rapid, significant increases in FL-4 fluorescence. BAPTA abolished increases in FL-4 fluorescence resulting from ionophore treatment. TPEN pre-treatment had no significant effect on ionophore-induced increases FL-4 fluorescence. ○ 300μM, ■ 100μM, ▲ 30μM, ▼ 10μM and ● vehicle. Data are mean±standard error of mean (SEM) from 6 independent experiments. Significance is denoted as **** ($p<0.0001$), *** ($p<0.001$), ** ($p<0.01$) or * ($p<0.05$).

BAPTA (10μM) pre-treatment inhibited FL-4 fluctuations in response to ionophore treatment, consistent with chelation of cytosolic cations. Cq and Py treatment produced no significant increase in FL-4 fluorescence; thus the effect of BAPTA pre-treatment was negligible. However, the increases in FL-4 fluorescence induced by A23187 were abolished upon BAPTA pre-treatment. The final F/F_0

induced by the highest concentration (300µM) of A23187 was reduced from 5.8±0.9 to 1.0±0.1 in BAPTA pre-treated platelets ($p<0.0001$, Figure 4.2C, F).

TPEN (50µM) pre-treatment did not significantly affect A23187 induced FL-4 fluorescence fluctuations (Figure 4.2I), confirming that ionophore-induced $[Ca^{2+}]_i$ increases were not sensitive to Zn^{2+}. Slight reductions in FL-4 fluorescence were observed following TPEN pre-treatment although this was not found to be significant. The F/F_0 induced by 300µM, 100µM and 30µM A23187 after 6 mins were slightly reduced from 5.8±0.9, 4.1±0.7 and 2.6±0.5 to 4.2±0.6, 2.6±0.3 and 2.1±0.4, respectively in TPEN pre-treated platelets ($p>0.05$, ns, Figure 4.2C, I). Again, the application of this chelator had a negligible effect on Cq or Py treatment, as no fluctuations in FL-4 fluorescence were observed with these Zn^{2+} ionophores. This data further demonstrates the specificity of FL-4 as Ca^{2+} probe, as chelation of $[Zn^{2+}]_i$ had no significant influence on the FL-4 fluctuations induced by the Ca^{2+} ionophore, A23187.

The data described above indicate that increases in $[Ca^{2+}]_i$ are not influenced by $[Zn^{2+}]_i$. Initial experiments demonstrate the specificity of FL-4 for Ca^{2+}. As $[Zn^{2+}]_i$ elevation in response to Zn^{2+} ionophores did not evoke any fluctuations in FL-4 fluorescence, and thus were also not influenced by TPEN or BAPTA (Figure 4.2A-B, D-E, G-H). Thus FL-4 does not respond to Zn^{2+}.

Application of the Ca^{2+} chelator BAPTA further demonstrated that the FL-4 fluctuations induced by A23187 were attributable to $[Ca^{2+}]_i$ elevation (Figure 4.2F). Pre-treatment with TPEN had no significant influence on the FL-4 response induced by A23187 (Figure 4.2I). Thus $[Ca^{2+}]_i$ elevation is not influenced by $[Zn^{2+}]$.

To conclude, this work justified the use of the ionophores (Cq, Py and A23187) and the fluorophores (FZ-3 and FL-4) as valid tools to model and assess Zn^{2+} and Ca^{2+} fluctuations.

4.2.3. Ionophore-induced intracellular Zn^{2+} and Ca^{2+} release is not sensitive to modulators of the redox state platelets

Experiments carried out using the ionophores demonstrated that there is $[Zn^{2+}]_I$ within platelets , possibly representing an accessible Zn^{2+} store. At present, the site from which labile Zn^{2+} is released within platelets is not known, although $[Zn^{2+}]_i$ is present in platelet granules (Marx et al., 1993a; Maynard et al., 2007; Taylor and Pugh, 2016). Experiments discussed in Chapter 3 indicate that redox-dependent metal binding proteins such as metallothioneins can store Zn^{2+} and that $[Zn^{2+}]_i$ elevation is regulated by changes to the platelet redox state. In order to further investigate the nature

of the Zn^{2+} store in platelets, experiments were performed to assess the if changes in platelet redox state influence ionophore-induced $[Zn^{2+}]_i$ fluctuations. This would help elucidate whether redox-operated mechanisms enable $[Zn^{2+}]_i$ storage and release, or if other storage mechanisms are present in platelets. To investigate whether redox changes affected ionophore-induced $[Zn^{2+}]_i$ fluctuations, platelets were pre-treated with the anti-oxidants PEG-SOD (30U/mL) and PEG-CAT (300U/mL)which have been widely employed to regulate redox changes and to investigate ROS biology in a wide variety of cells (Beckman et al., 1988; Görlach et al., 2015; Machtay et al., 2006).

Pre-treatment of washed platelet suspensions with PEG-SOD (30U/mL) or PEG-CAT (300U/mL) did not significantly influence FZ-3 fluctuations induced by Cq, Py or A23187 (Figure 4.3). FZ-3 F/F_0 values in PEG-SOD or PEG-CAT pre-treated platelets were 5.2±0.7 and 4.9±0.6, respectively following stimulation with Cq (300µM) after 6mins (Figure 4.3D, G). Whereas FZ-3 F/F_0 in response to by Cq (300µM) on untreated (vehicle) platelets was 6.5±0.4 after 6mins ($p>0.05$, ns, Figure 4.3A, D, G). This was also the case with Py treatment, as the FZ-3 F/F_0 induced by Py on PEG-SOD and PEG-CAT pre-treated platelets were 3.0±0.3 and 3.0±0.2, respectively which did not differ to the final FZ-3 F/F_0 induced by Py (300µM) on untreated (vehicle) platelets which were 3.0±0.4 after 6mins ($p>0.05$, ns, Figure 4.3B, E, H). Furthermore, the FZ-3 F/F_0 following A23187 stimulation (300µM) after 6mins, of PEG-SOD and PEG-CAT pre-treated platelets which were 1.6±0.6 and 1.7±0.2 respectively, also did not differ significantly to that induced by the vehicle-treated platelets(1.8±0.1, $p>0.05$, ns, Figure 4.3C, F, I).

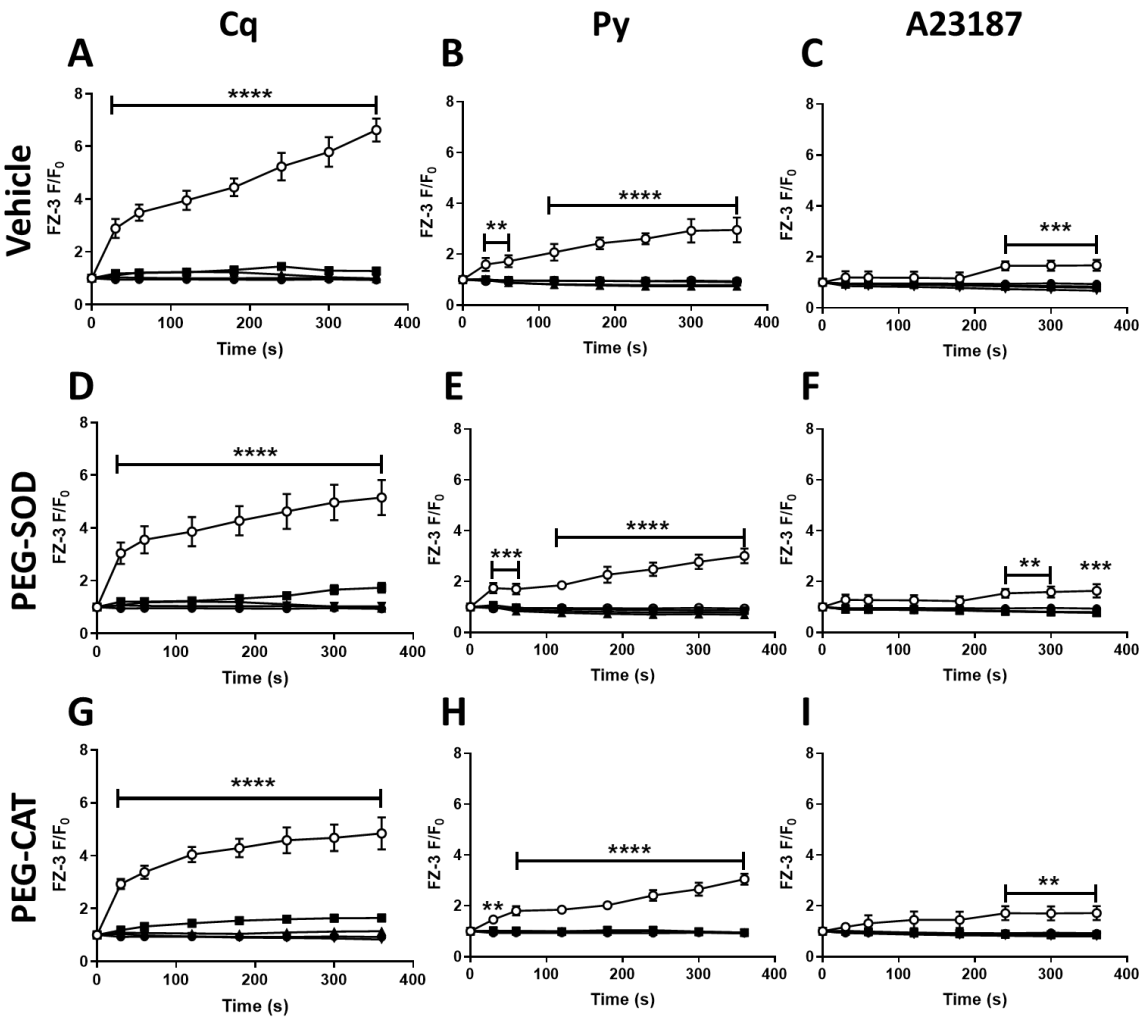

Figure 4.3. PEG-SOD and PEG-CAT do not effect ionophore-evoked increases in FZ-3 fluorescence. Fluozin-3 (FZ-3)-labelled washed human platelets were stimulated by increasing concentrations of Cq (A), Py (B) and A23187 (C) FZ-3-labelled washed human platelets were pre-treated with PEG-SOD (30U/mL) before being stimulated by increasing concentrations of Cq (D), Py (E) and A23187 (F). Finally, FZ-3-labelled washed human platelets were pre-treated with PEG-CAT (300U/mL) before being stimulated by increasing concentrations of Cq (G), Py (H) and A23187 (I). FZ-3 fluctuations were recorded over 6 minutes using fluorometry. PEG-SOD and PEG-CAT pre-treatment had no significant effect on ionophore-induced increases in FZ-3 fluorescence. ○ 300µM, ■ 100µM, ▲ 30µM, ▼ 10µM and ● vehicle. Data are mean±standard error of mean (SEM) from 6 independent experiments. Significance is denoted as **** (p<0.0001), *** (p<0.001), ** (p<0.01) or * (p<0.05).

Modulation of redox states with PEG-SOD and PEG-CAT did not significantly influence the ionophore-induced FZ-3 fluctuations, indicating that ionophore-induced $[Zn^{2+}]_i$ increases are not sensitive to the platelet redox state. These findings suggest that ionophore-induced $[Zn^{2+}]_i$ elevation do not operate through a redox-dependent mechanism, which may indicate a non- redox-sensitive store of Zn^{2+} in platelets.

Further experiments were performed to investigate whether the redox state affected ionophore-induced Ca^{2+} release. Pre-treatment of platelets with PEG-SOD or PEG-CAT did not significantly influence ionophore-induced increases in FL-4 fluorescence, (Figure 4.4).

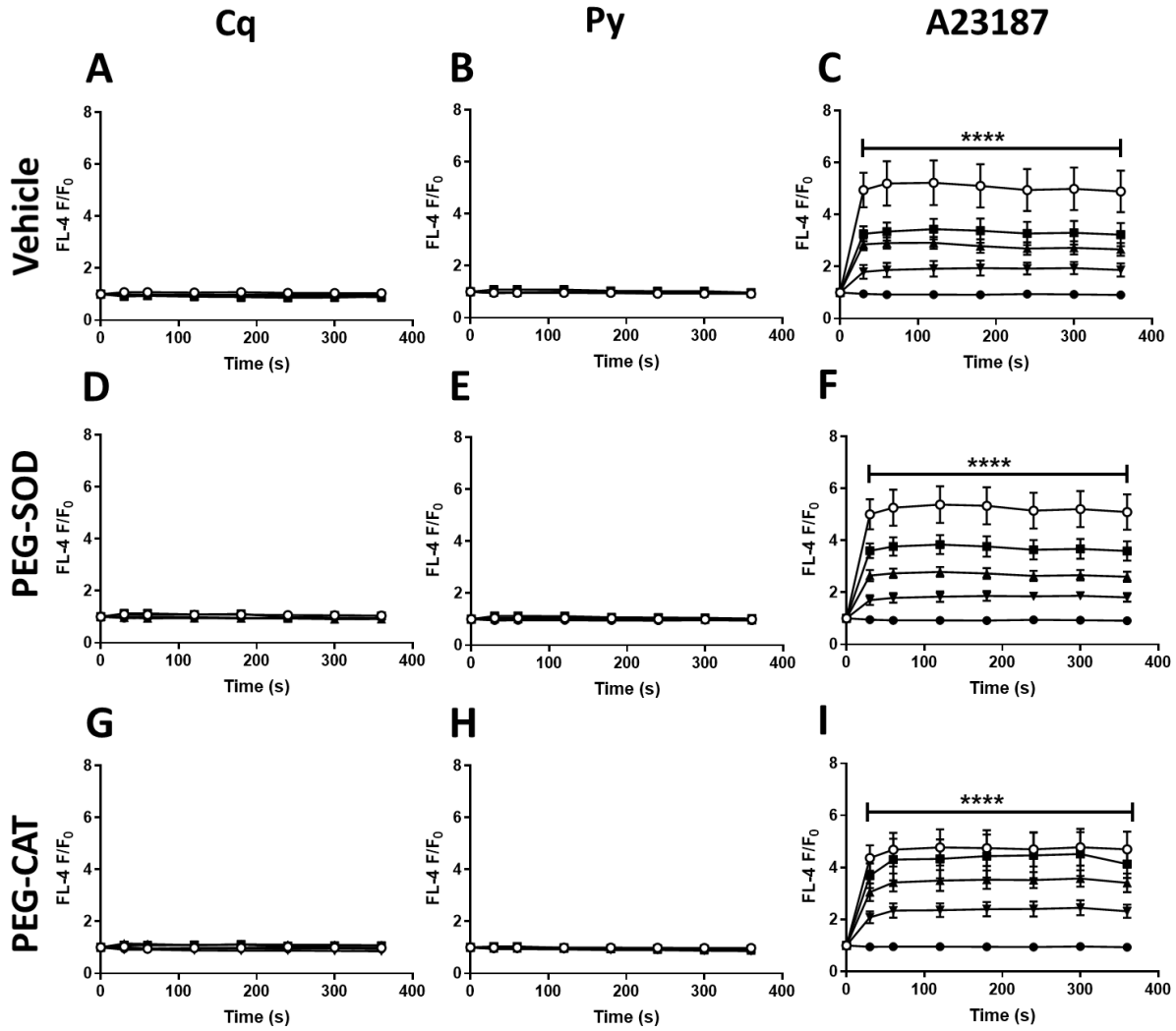

Figure 4.4. PEG-SOD or PEG-CAT do not effect ionophore-evoked increases in FL-4 fluorescence. Fluo-4 (FL-4)-labelled washed human platelets were stimulated by increasing concentrations of Cq (A), Py (B) and A23187 (C). FL-4-labelled washed human platelets were pre-treated with PEG-SOD (30U/mL) before being stimulated by increasing concentrations of Cq (D), Py (E) and A23187 (F). Finally, FL-4-labelled washed human platelets were pre-treated with PEG-CAT (300U/mL) before being stimulated by increasing concentrations of Cq (G), Py (H) and A23187 (I). FL-4 fluctuations were recorded over 6 minutes using fluorometry. PEG-SOD and PEG-CAT pre-treatment had no significant effect on ionophore-induced increases in FL-4 fluorescence. ○ 300μM, ■ 100μM, ▲ 30μM, ▼ 10μM and ● vehicle. Data are mean±standard error of the mean (SEM) from 6 independent experiments. Significance is denoted as **** ($p<0.0001$), *** ($p<0.001$), ** ($p<0.01$) or * ($p<0.05$).

As Zn^{2+} ionophores had no effect on FL-4 fluorescence, further effects of PEG-SOD and PEG-CAT were negligible (Figure 4.2A, B and 4.4A, B); nevertheless, PEG-SOD and PEG-CAT were still applied with the Zn^{2+} ionophores as a measure of control and consistency. The FL-4 F/F_0 induced by Cq (300µM) on PEG-SOD and PEG-CAT pre-treated platelets after 6mins were 1.04±0.02 and 0.99±0.03, respectively compared to 1.04±0.01 for the vehicle control ($p>0.05$, ns, Figure 4.4A, D). Stimulation with Py produced comparable results. As the FL-4 F/F_0 induced by Py (300µM) on PEG-SOD and PEG-CAT pre-treated platelet after 6mins were 0.99±0.08 and 0.94±0.03 compared to 1.03±0.03 for vehicle control ($p>0.05$, ns, Figure 4.4B, E). Although showing a negligible effect due to Cq and Py not evoking an FL-4 response, this data did provide further evidence to validate that the FL-4 probe does not detect $[Zn^{2+}]_i$ fluctuations and is Ca^{2+} specific.

A23187-induced fluctuations of $[Ca^{2+}]_i$ were not significantly affected by PEG-SOD or PEG-CAT pre-treatment. FL-4 F/F_0 in response to A23187 (300µM, 100µM, 30µM or 10µM) on PEG-SOD pre-treated platelets were 5.1±0.7, 3.6±0.4, 2.6±0.2 and 1.9±0.1 respectively, whilst on PEG-CAT pre-treated platelets these were 4.7±0.7, 4.1±0.5, 3.4±0.4 and 2.2±0.2 respectively (Figure 4.4F, I). These did not differ significantly from vehicle-treated platelets where the final FL-4 F/F_0 values were 5.4±0.8, 3.0±0.4, 2.6±0.4 and 1.9±0.1 respectively ($p>0.05$, ns, Figure 4.4C, F, I). These data provided evidence to confirm that, in a similar manner to A23187-mediated $[Zn^{2+}]_i$ elevation, $[Ca^{2+}]_i$ elevation via A23187 was not influenced by changes in redox. Thus, ionophores are able to mobilise Ca^{2+} and Zn^{2+} from stores within platelets in a redox-independent manner. However, this may be due to the artificial nature of the ionophores (releasing cations from proteins and stores which may not be physiologically accessible) overcoming any redox dependent mechanism that may be sequestering the cations. Therefore modulation of redox may have a null effect when ionophores are applied.

Initial experiments from this section illustrated that ionophore-induced FZ-3 increases were not influenced by modulation of redox upon treatment with PEG-SOD and PEG-CAT (Figure 4.3). This contrasts with data seen in Chapter 3, where PEG-SOD and PEG-CAT abolished agonist-evoked FZ-3 fluorescence increases, which provided evidence to show that redox-sensitive mechanisms evoke $[Zn^{2+}]_i$ elevation in platelets. The data from this chapter suggest the ionophores are mobilizing the Zn^{2+} from potential stores that are not sensitive to changes in redox, due to no exogenous Zn^{2+} being present in these experiments thus the increases in Zn^{2+} is evoked intracellularly in platelets from potential stores.

Further experiments were carried out to assess if $[Ca^{2+}]_i$ elevation via A23187 was also modulated by changes in redox. Modulation of the redox state upon application of PEG-SOD and PEG-

CAT had no significant influence on the FL-4 response in response to A23187. This data correlates well with the work from Chapter 3, which demonstrated that agonist induces FL-4 fluorescence increases were also not influenced by changes in redox upon PEG-SOD and PEG-CAT treatment. Therefore, mobilisation of Ca^{2+} from its store (DTS, dense tubular system) in platelets which is well documented (see Chapter 1) is not sensitive to changes in redox.

Modulation of redox (via PEG-SOD and PEG-CAT treatment) may not effect ionophore-evoked response, due to the ionophores mobilising the cations from stores that are not influenced by changes in redox or from proteins regardless of their sensitivity to changes in redox. Thus, although these experiments with ionophores illustrate that cation release can be modelled, the location from where the cations are mobilised from has not been determined. This may be the reasoning as to why changes in redox had no influence on the cation release induced by the ionophores.

To conclude the presence and mechanism of Ca^{2+} store release is well documented (Smith et al., 1992; Varga-Szabo et al., 2009; Verma et al., 2011). However, the storage capabilities of Zn^{2+} in platelets is yet to be determined. Data from chapter 3 suggest that a redox-sensitive mechanism (possibly involving metal binding proteins such as metallothionein's) act as a storage mechanism for Zn^{2+} in platelets. This work indicates the presence of another potential Zn^{2+} storage site that is accessible to ionophores in a redox-independent manner. It is not known whether this store represents a physiologically relevant, store that is accessible upon agonist stimulation.

4.2.4. ROS elevation is potentiated by increases in intracellular Zn^{2+}

The data described above show that the modulation of redox states has no significant effect on ionophore-induced $[Zn^{2+}]_i$ and $[Ca^{2+}]_i$ fluctuations. ROS has been suggested to influence $[Ca^{2+}]_i$ signalling and vice versa, although as previous work did not take Zn^{2+} into account (Görlach et al., 2015), this effect has yet to be fully studied in platelets. The data presented in this thesis thus far indicates that $[Ca^{2+}]_i$ mobilisation is not influenced by redox modulation, suggesting that ROS does not play a major role in $[Ca^{2+}]_i$ mobilisation.

$[Zn^{2+}]_i$ mobilisation via ionophores was also not influenced by changes in redox states, however this may have been due to artificial nature (as discussed above) of the ionophores potentially releasing Zn^{2+} from proteins such as redox sensitive proteins that may be sequestering Zn^{2+}. Experiments described in Chapter 3 showed that agonist-induced $[Zn^{2+}]_i$ fluctuations (but not $[Ca^{2+}]_i$ fluctuations) are redox-sensitive, indicating a key role for ROS in regulating $[Zn^{2+}]_i$ in platelets. Previous

work has shown that elevated $[Zn^{2+}]_i$ may mediate further ROS generation which in turn would elevate Zn^{2+} further (Stork and Li, 2016). This relationship between ROS and Zn^{2+} may also occur in platelets and could be a mechanism which regulates $[Zn^{2+}]_i$ concentrations in platelets. Experiments were performed to investigate this relationship further.

The effect of elevated $[Zn^{2+}]_i$ and $[Ca^{2+}]_i$ on ROS elevation in platelets was assessed. The ROS probe, DCFH was employed to assess changes in ROS upon stimulation with the Zn^{2+} and Ca^{2+} ionophores (in the same manner as the previous chapter). All ionophores induced significant concentration-dependent increases in ROS fluorescence (Figure 4.5).

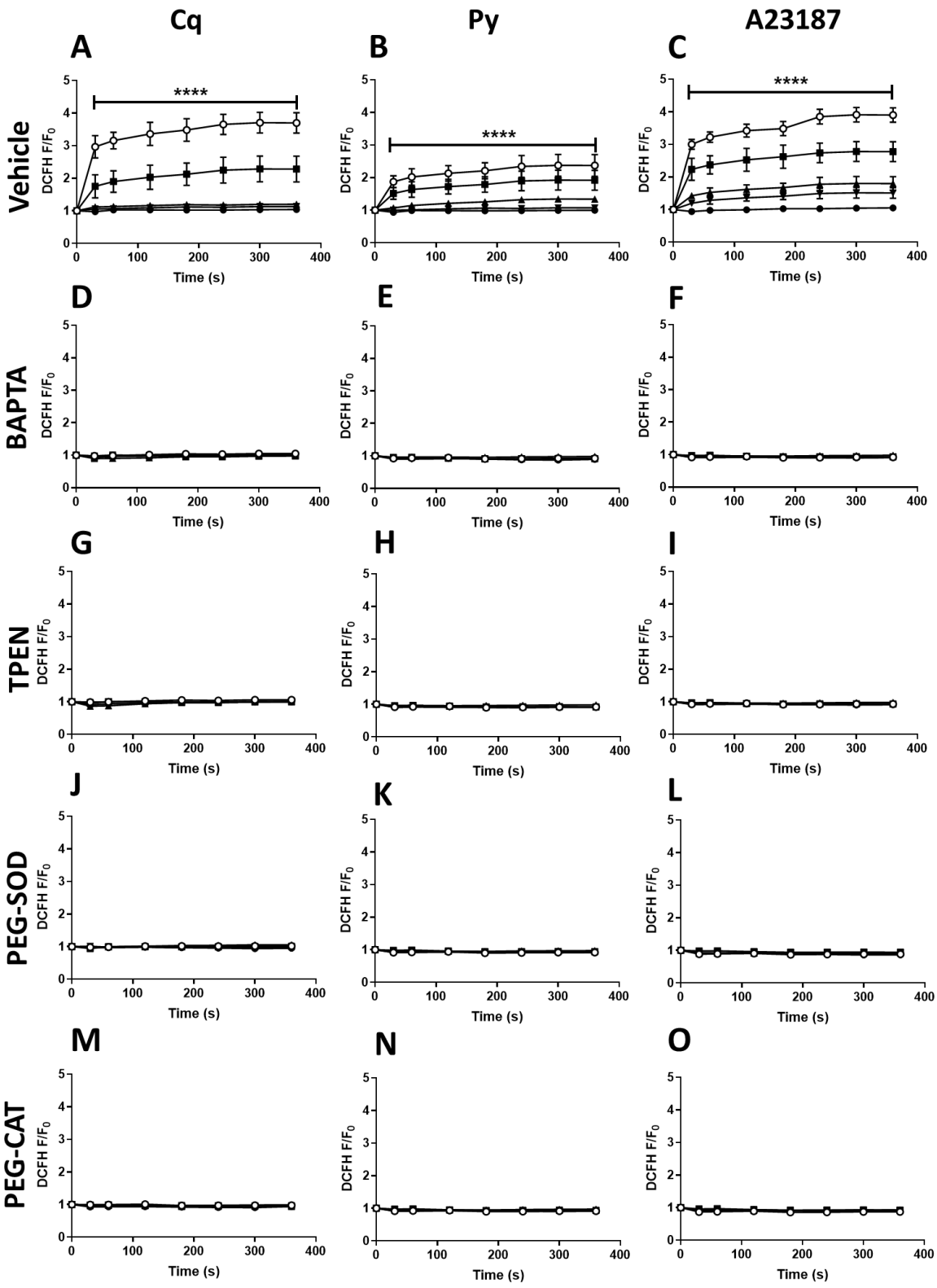

Figure 4.5. Ionophore treatment results in increases in ROS fluorescence which is abrogated by cation chelation or anti-oxidant treatment. DCFH-labelled washed human platelets were stimulated by increasing concentrations of clioquinol, Cq (A), pyrithione, Py (B) or A23187 (C). DCFH-labelled washed human platelets were also pre-treated with 10μM BAPTA before

being stimulated by increasing concentrations of Cq (D), Py (E) or A23187 (F). DCFH-labelled washed human platelets were pre-treated with 50µM TPEN before being stimulated by increasing concentrations of Cq (G), Py (H) or A23187 (I). DCFH-labelled washed human platelets were also pre-treated with 30U/mL SOD before being stimulated by increasing concentrations of Clioquinol (J), Pyrithione (K) or A23187 (L). DCFH-labelled washed human platelets were also pre-treated with 300U/mL CAT before being stimulated by increasing concentrations of Cq (M), Py (N) or A23187 (O). DCFH fluorescence fluctuations were recorded over six minutes using fluorometry. Treatment with all ionophores induced increases in ROS which was abolished upon BAPTA, TPEN, PEG-SOD and PEG-CAT pre-treatment. ○ 300µM, ■ 100µM, ▲ 30µM, ▼ 10µM and ● vehicle. Data are mean±standard error of mean (SEM) from 6 independent experiments. Significance is denoted as **** (p<0.0001), *** (p<0.001), ** (p<0.01) or * (p<0.05).

Stimulation with the highest two concentrations of Cq (300µM and 100µM) resulted in significant increases in ROS fluorescence relative to the vehicle control. DCFH F/F_0 values following stimulation by 300µM or 100µM of Cq after 6mins were 3.7±0.3 and 2.4±0.4 respectively, compared to the vehicle control of 1.04±0.03 ($P<0.05$, Figure 4.5A). A similar effect was observed with Py (Figure 4.11B). However, Py stimulation resulted in lower increases in ROS fluorescence compared to Cq which was consistent with the differences in FZ-3 increases induced by these ionophores. DCFH F/F_0 values following stimulation with 300µM or 100µM of Py after 6mins were 2.37±0.34 and 1.92±0.30 respectively, compared to 0.10±0.01 for the vehicle control ($P<0.05$, Figure 4.5B). Therefore, elevation of $[Zn^{2+}]_i$ results in increased ROS in platelets.

Ca^{2+} release, in response to A23187 also resulted in significant increases in ROS fluorescence (Figure 4.5C). Stimulation with the highest three concentrations (300µM, 100µM or 30µM) of A23187 resulted in significant increases in DCFH fluorescence relative to the vehicle control. DCFH F/F_0 values following stimulation with 300µM, 100µM or 30µM of A23187 after 6 mins were 3.9±0.2, 2.8±0.3 and 1.8±0.2 respectively, compared to the 1.05±0.07 for the vehicle control ($P<0.05$, Figure 4.5C). These data demonstrate that elevation of $[Zn^{2+}]_i$ and $[Ca^{2+}]_i$ induces ROS elevation in platelets. The $[Ca^{2+}]_i$ and $[Zn^{2+}]_i$ chelators, BAPTA(10µM) and TPEN(50µM) were employed to confirm that elevations in ROS observed were attributable to increases in $[Ca^{2+}]_i$ and $[Zn^{2+}]_i$.

Pre-treatment with BAPTA (Figure 4.5D-F) or TPEN (Figure 4.5G-I) abrogated ionophore-stimulated ROS fluctuations. DCFH F/F_0 values induced by the highest concentration (300µM) of Cq or Py after 6mins were reduced from 3.7±0.3 and 2.37±0.34, respectively to 1.05±0.07 and 0.93±0.01 on BAPTA pre-treated platelets ($p<0.05$, Figure 4.5 D-E). These F/F_0 values were comparable to that induced by Cq and Py on TPEN (50µM) pre-treated platelets, where final DCFH F/F_0 induced by Cq (300µM) and Py (300µM) was reduced from 3.7±0.3 and 2.37±0.34, respectively to 1.01±0.01 and

0.93±0.03 ($p<0.05$, Figure 4.5, G-H). These data confirm that increases in $[Zn^{2+}]_i$ mediate ROS elevation in platelets.

BAPTA pre-treatment also abolished any ROS fluctuations that were induced by A23187, indicating that ROS elevation is also mediated by $[Ca^{2+}]_i$ in platelets. However, A23187-induced ROS elevations were also abrogated by TPEN. DCFH F/F_0 values induced by the highest concentration (300µM) of A23187 after 6mins were abrogated from 3.9±0.2 to 0.92±0.01 and 0.93±0.01 on BAPTA and TPEN pre-treated platelets, respectively ($p<0.05$, Figure 4.5C, F, I). Indicating that the response being mediated by A23187 is attributable to $[Zn^{2+}]_i$ as opposed to $[Ca^{2+}]_i$. A23187 induced a slight elevation in $[Zn^{2+}]_i$, (Figure 4.1C and 4.5C), which may responsible for the ROS elevation.

This data suggests that there is a relationship between ROS and Zn^{2+} in platelets which further demonstrates that the ROS and Zn^{2+} interplay may evoke the major mechanism for inducing $[Zn^{2+}]_i$ elevation. This coincides well with the work carried out in chapter 3 which provided evidence showing that ROS elevation evoked $[Zn^{2+}]_i$ elevation and that agonist-induced $[Zn^{2+}]_i$ elevation coincides with agonist-induced ROS increases. Therefore, the work from this chapter and the previous chapter provide the first evidence to exhibit that $[Zn^{2+}]_i$ elevation is mediated by ROS increases, and thus sensitive to changes in redox (as ROS fluctuations modulate changes in redox, as described in Chapter 1 and 3).

Further experiments were performed to confirm the validity of ROS being detected upon ionophore stimulation. PEG-SOD and PEG-CAT scavenge ROS and should, therefore, inhibit elevation of ROS mediated by the agonist, and in turn, reduce in DCFH fluorescence. PEG-SOD (Figure 4.5J-L) and PEG-CAT (Figure 4.15M-O) pre-treatment abolished ionophore-induced increases in DCFH fluorescence. After 6mins, DCFH F/F_0 induced by Cq (300µM), Py (300µM) or A23187 (300µM) after was abrogated from 3.7±0.3, 2.37±0.34 and 3.9±0.2, to 1.02±0.04, 0.92±0.01 and 0.90±0.02, respectively on PEG-SOD pre-treated platelets ($p<0.05$, Figure 4.5A-C, J-L). These values were comparable to those obtained with PEG-CAT (300U/mL) pre-treatment. After 6mins, DCFH F/F_0 induced by Cq (300µM), Py (300µM) or A23187 (300µM) were also abolished from 3.7±0.3, 2.37±0.34 and 3.9±0.2, respectively to 0.98±0.03, 0.92±0.01 and 0.89±0.03, respectively on PEG-CAT pre-treated platelets ($p<0.05$, Figure 4.5A-C, M-O). These data confirm that the elevation in DCFH fluorescence induced by the ionophores was in accordance with increased ROS levels.

The data described above demonstrate that elevated $[Zn^{2+}]_i$ mediates ROS elevation. Use of Zn^{2+} and Ca^{2+} ionophores-mediated increases in DCFH fluorescence were abrogated by the BAPTA or

TPEN (Figure 4.5A-I), indicating that ROS elevation is primarily attributable to Zn^{2+} as opposed to Ca^{2+}. Pre-treatment with the antioxidants, PEG-SOD and PEG-CAT also abolished the ionophore-induced DCFH fluorescence induced by the ionophores thus validating that this increase in DCFH fluorescence is due to increased ROS levels (Figure 4.5J-O)

These data contrast with previous studies, that suggests that Ca^{2+} regulates ROS formation and that elevation of $[Ca^{2+}]_i$ may be redox sensitive (Görlach et al., 2015). This may be due to the reason that the previous work did not take Zn^{2+} account; thus the regulatory role of Ca^{2+} on ROS formation may perhaps be attributable to Zn^{2+}. This data provides further evidence to strengthen the mechanism hypothesised in chapter 3, that there may be a ROS/Zn^{2+} interplay in platelets which enables regulation of $[Zn^{2+}]_i$

4.3 Discussion

The work conducted here was designed to investigate whether increases in $[Zn^{2+}]_i$ could be modelled in platelets in a manner similar to Ca^{2+}. The Ca^{2+} ionophore, A23187, and Zn^{2+} ionophores, Cq and Py, have been widely used in nucleated cells to model changes in intracellular cation concentrations (Krenn et al., 2009; Pressman, 1976). Here, Cq and Py were employed to model $[Zn^{2+}]_i$ increases in platelets. A23187 was principally used as a positive control; however, A23187 treatment increased in $[Zn^{2+}]_i$, which may reflect a lack of cation specificity of A23187, or alternatively a functional interaction between the two cations.

Data described above support the existence of a redox-insensitive Zn^{2+} store in platelets which is accessible to Zn^{2+} ionophores. Evidence for a Zn^{2+} store in platelets is provided by experiments which show that Zn^{2+} ionophores induce significant increases in FZ-3 fluorescence (consistent with increases in $[Zn^{2+}]_i$), which is abrogated with Ca^{2+} and Zn^{2+} chelation. These experiments were carried out in a Zn^{2+} free environment, thus any elevations of FZ-3 fluorescence were from Zn^{2+} present within platelets. Interestingly, modest TPEN-sensitive increases of FZ-3 fluorescence were observed in response to A23187 treatment. This correlates with previous work on rat thymocytes which found that A23187 induced increases in Zn^{2+} fluorescence were abolished with TPEN treatment (Sakanashi et al., 2009; E. Wang et al., 1998), indicating that A23187 is able to mediate Zn^{2+} transport. This is consistent with work that has shown that A23187 also induces Zn^{2+} permeability (Pfeiffer et al., 1978). The affinity of A23187 for Ca^{2+} has been claimed to be very specific relative to other ions. The k_d value of A23187 with Ca^{2+} has been approximately found to be 10^{-6}M (E. Wang et al., 1998). However the

exact binding affinity of A23187 and Zn^{2+} is yet to be confirmed (Fujikawa et al., 2015; Xiong et al., 1992). Although as stated above A23187 was able to act on Zn^{2+} indicating A23187 may not be Ca^{2+} specific and may bind to Zn^{2+} in a similar manner to other Ca^{2+} reagents such as BAPTA and Fura-2 (see chapter 1). In contrast to this, the Zn^{2} ionophores have a high specificity to Zn^{2+} relative to Ca^{2+}, as the k_d values of Cq and Py with Zn^{2+} and Ca^{2+} are approximately 10^{-7}M, K $10^{-4.9}$M, respectively (Arslan et al., 1985a; Hyun et al., 2004a; Matias et al., 2010a; Qian and Colvin, 2016b).

To conclude, the initial data from this chapter demonstrates the $[Zn^{2+}]_i$ release could be modelled in platelets which indicated that Zn^{2+} stores were present in platelets.

The work described above also provides an assessment of the specificity of the Zn^{2+} and Ca^{2+} probes, Fz-3 and FL-4 respectively. The data illustrates opposing effect induced by the ionophores on increases in FL-4 fluorescence (consistent with increases in $[Ca^{2+}]_i$) in comparison to the increases in FZ-3 fluorescence (consistent with increases in $[Zn^{2+}]_i$). The Zn^{2+} ionophores had no effect in FL-4 fluorescence, whereas the Ca^{2+} ionophore-induced a much greater increase in FL-4 fluorescence. Also pre-treatment with the Zn^{2+} specific chelator, TPEN did not significantly influence the fluctuations in FL-4 fluorescence induced by the ionophores, indicating that the increases in FL-4 fluorescence were attributable to Ca^{2+} rather than Zn^{2+}. Experiments performed provided evidence to confirm that increases in FL-4 fluorescence were attributable to Ca^{2+}, and thus verify the specificity of the FL-4 to Ca^{2+}. To summarise, this work demonstrates the specificity of FZ-3 and FL-4 for Zn^{2+} and Ca^{2+} respectively. Also, these sections provided further evidence to indicate that Zn^{2+} is present in platelets, as extracellular Zn^{2+} were not present in these experiments, thus the increases in FZ-3 fluorescence (consistent with $[Zn^{2+}]_i$ increases) were from within the platelets.

Zn^{2+} ionophores induce a much greater increase in FZ-3 fluorescence than CRP-XL and U46619 (shown in chapter 3), indicating that ionophore-induced Zn^{2+} release may not be the principal way in which Zn^{2+} is mobilised as the location from which Zn^{2+} is mobilised via the ionophores is not known. It is likely that Zn^{2+} is mobilised from granules or another storage mechanism with the platelets by the ionophores. A good candidate here would be alpha granules, which have been shown to contain Zn^{2+}.

Agonist-induced $[Zn^{2+}]_i$ elevations was redox-sensitive, implicating metal binding proteins such as metallothioneins in $[Zn^{2+}]_i$ storage and release. In order to investigate if changes in redox were the primary mediator of evoking increases in $[Zn^{2+}]_i$, experiments were performed to determine whether ionophore-induced $[Zn^{2+}]_i$ fluctuations were redox-sensitive. Ionophore-induced FZ-3 fluorescence increases were not influenced by changes to the redox state. This is suggestive of the

presence of Zn^{2+} stores in platelets that are not mobilised by redox modulation, however ionophores may be releasing Zn^{2+} from redox-sensitive proteins thus bypassing any changes in redox.

To conclude the experiments described here show that ionophores are able to increase $[Zn^{2+}]_i$ in a manner that does not depend on the platelet redox state. This suggests that there is a Zn^{2+} store in platelets which is distinct from the cytosol. Whether this Zn^{2+} store is accessible physiologically is not known. It is possible that the Zn^{2+} stores are platelet alpha granules, which are known to contain Zn^{2+}. Whether the Zn^{2+} is accessible from the granules to the cytosol during activation, but prior to granule release is not yet known.

Further experiments were conducted to investigate if changes in redox influenced $[Ca^{2+}]_i$ fluctuations induced by the ionophores. Experiments described in chapter 3 show that agonist-induced $[Ca^{2+}]_i$ elevation are not redox-sensitive; thus ionophores induced $[Ca^{2+}]_i$ elevation was also expected not to be influenced by redox modulation, which was the case in this chapter. However, this may be due to the ionophore as stated above being able to bypass any changes in redox.

Further work was carried out to investigate the effect of ionophore treatment on ROS elevation in platelets. This was carried out to investigate further the mechanisms that relate ROS generation to Zn^{2+}, that may mediate secondary responses during platelet activation. Ionophore treatment resulted in increases in ROS that were abrogated by cation chelation. Inhibition of ROS generation by TPEN indicates that Zn^{2+} is important in ROS elevation. This correlates well with the data from Chapter 3, which showed agonist-induced ROS elevation was shown to be inhibited by chelating $[Zn^{2+}]_i$. Thus, this work provides further evidence to demonstrate that $[Zn^{2+}]_i$ and ROS interplay may mediate platelet responses. Furthermore, these findings correlate with previous work showing that elevated Zn^{2+} mediates further ROS generation, which in turn would elevate Zn^{2+} further (Stork and Li, 2016). This feedforward loop may be a major mechanism in platelets for mediating $[Zn^{2+}]_i$ as illustrated by the schematic (Figure 4.6) below.

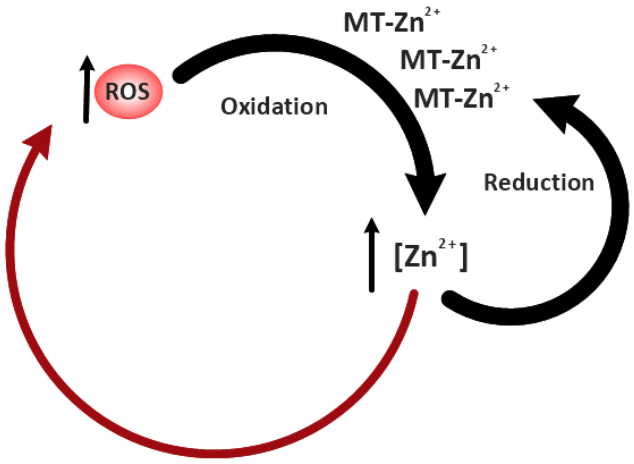

Figure 4.6. Schematic illustrating the feedforward loop mechanism evoking ROS and $[Zn^{2+}]_i$ elevation. Elevation of ROS results in the oxidation of redox sensitive (Zn^{2+} sequestering) proteins such metallothionines (MTs) which then liberate Zn^{2+} from its thiols. Therefore, resulting in increased intracellular Zn^{2+} ($[Zn^{2+}]$) concentrations. In a reducing environment, Zn^{2+} is sequestered by the MTs via reduction, thus reducing the $[Zn^{2+}]_i$ concentration. Elevation of ROS further evoked ROS elevation which in turn results in elevation of $[Zn^{2+}]_i$.

4.3.1. Conclusion

The data presented in this chapter provides evidence that Zn^{2+} stores are present in platelets and can be mobilised upon ionophore treatment. Whether Zn^{2+} release occurs from these stores during agonist-dependent activation is not known. However, unlike agonist-dependent Zn^{2+} release, the ionophore-induced Zn^{2+} release was not sensitive to modulation of the platelet redox state, suggesting that conventional store release (as per Ca^{2+} release) is not the principal mechanism by which ionophore-induced $[Zn^{2+}]_i$ increases in the cytosol.

These experiments (in conjunction with experiments described in chapter 3) indicate that ROS and $[Zn^{2+}]_i$ levels in platelets are mechanistically linked. As agonist stimulation may induce ROS elevation, resulting in changes in redox states leading on to Zn^{2+} bound to (for example) metallothioneins to be released and elevating $[Zn^{2+}]_i$. Platelet stimulation may also induce the release of Zn^{2+} from other intracellular stores (yet to be confirmed), which may contribute to elevating ROS, and thus enabling further sustained Zn^{2+} elevation. Thus, redox-sensitive proteins may synchronise with Zn^{2+} stores in platelets to induce elevated and sustained $[Zn^{2+}]_i$ release. Chapter 3 and 4 have provided evidence that $[Zn^{2+}]_i$ elevation occurs in platelets. The effect of Zn^{2+} on platelets and its potential role as a secondary messenger in platelets was assessed, and the results are discussed in Chapter 5.

Chapter 5

5.0 Investigation of the role of intracellular Zn^{2+} as a secondary messenger during platelet activation

5.1 Background

The role of Zn^{2+} in modulating platelet behaviour is not yet fully understood. Recent work by Watson et al., (2016) demonstrated that exogenous Zn^{2+} gains access to the platelet cytosol and acts as an agonist, inducing platelet activation. Furthermore, at sub-activatory concentrations, exogenous Zn^{2+} potentiates platelet activation by conventional agonists (Watson et al., 2016). This outlines the importance of Zn^{2+} in platelet activity and indicates its potential as a mediator of thrombus formation (Taylor and Pugh, 2016; Watson et al., 2016). The role of $[Zn^{2+}]_i$ as an intracellular signalling molecule has yet to be studied in platelets. In many other cell types $[Zn^{2+}]_i$ acts as a signalling molecule, for example, in mast cells where it acts as a secondary messenger (Beyersmann and Haase, 2001; Brautigan et al., 1981; Csermely et al., 1988; Daaboul et al., 2012; Hubbard et al., 1991a; Lengyel et al., 2000; Perry et al., 1997; Yamasaki et al., 2007). Whether Zn^{2+} has similar signalling roles as an intracellular secondary messenger in platelets has yet to be examined experimentally and is the primary focus of this chapter.

The work carried out in Chapters 3, and 4 demonstrated that elevation of $[Zn^{2+}]_i$ occurs upon agonist stimulation. In Chapter 3 it was shown that CRP-XL and U46619 induced significant increases in $[Zn^{2+}]_i$ in a redox-dependent manner. In Chapter 4 elevation of $[Zn^{2+}]_i$ was modelled using ionophores. The ionophores induced greater levels of $[Zn^{2+}]_i$ elevation in comparison to that induced by CRP-XL and U46619, which indicated that Zn^{2+} stores may not be fully mobilised upon agonist stimulation. Furthermore, the ionophore-induced rise of $[Zn^{2+}]_i$ was not redox-sensitive, which suggests different mechanisms may be in place in platelets which enable $[Zn^{2+}]_i$ elevation. Data provided in these Chapters show that $[Zn^{2+}]_i$ is elevated upon platelet stimulation, suggestive of a role as a secondary messenger. Although as defined in Chapter 1, a secondary messenger upon stimulation must not only be elevated in concentration but also modulate the cell activity.

Zn^{2+} may modulate platelet activity in a similar manner to Ca^{2+}, which plays a central role as a secondary messenger in platelets by mediating many platelet processes, including aggregation, shape change, degranulation and phosphatidyl-Serine (PS) exposure (Chapter 1).

5.1.2. Aims

This chapter addresses the functional effects of elevated $[Zn^{2+}]_i$ in platelets. These studies characterised the influence of increases in $[Zn^{2+}]_i$ on various aspects of platelet behaviour such as aggregation, shape change, degranulation and PS exposure providing information on the potential role of Zn^{2+} as a platelet secondary messenger.

5.1.3. Methods

A range of methodologies were employed to assess platelet functionality in response to fluctuations in $[Zn^{2+}]_i$. The major functional responses that were measured in this chapter were platelet aggregation, tyrosine phosphorylation, shape change, degranulation and PS exposure.

Light transmission aggregometry (section 2.6, Chapter 2) was carried out to assess platelet aggregation and shape change. Western blotting was carried out to assess changes in tyrosine phosphorylation of platelet proteins, via the Anti-Phosphotyrosine Antibody, clone 4G10 antibody (section 2.7, Chapter 2).Western blotting was also employed to assess shape change signalling pathways of platelets by assessing the expression of the major cytoskeletal regulator's myosin light chains via phospho-myosin light chain 2 (Ser19) antibody, and Vasodilator-stimulated phosphoprotein (VASP) via the phospho-VASP (Ser157) antibody (section 2.7, Chapter 2).

Confocal microscopy was used to assess platelet shape change, by quantifying the level of platelet spreading on fibrinogen-coated coverslips (section 2.11, Chapter 2). The role of Zn^{2+} was determined in mouse embryonic fibroblasts (MEF) to assess the wider implications of Zn^{2+} signalling on cytoskeletal rearrangements in nucleated cells in a comparable manner to that seen in platelets. The changes in morphology were observed via the fluorescence microscopy using a ZOE fluorescent cell imager (section 2.12, Chapter 2).

Flow cytometry was used to assess degranulation by detecting the expression of the conventional activation markers, CD62P and CD63 which are expressed upon α-granule release and dense granule release, respectively (section 2.9, Chapter 2). The expression of another conventional activation marker, PAC-1 was also assesed to measure the activity of the major integrin $\alpha_{IIb}\beta_3$ which mediates platelet aggregation, (Chapter 2). PS exposure was assessed via Annexin V bindings using flow cytometer (section 2.8, Chapter 2).

A wide range of reagents including ionophores, inhibitors, agonist, antagonists were employed in this work to assess the functional response of $[Zn^{2+}]_i$ in platelets. The specific reagants that were employed are discussed in each of the specific sections below.

5.2 Results

5.2.1 Increasing intra- platelet Zn^{2+} using Zn^{2+}-specific ionophores results in increases in platelet activity

The ability of platelets to aggregate, leading to thrombus formation is of fundamental importance to thrombus formation. Experiments described in this section were performed to investigate the effect that elevated $[Zn^{2+}]_i$ would have on platelet aggregation. The Zn^{2+}-specific ionophores clioquinol (Cq) and pyrithione (Py) were employed to model the release of $[Zn^{2+}]_i$ from platelet stores and to enable $[Zn^{2+}]_i$ elevation. The validity of these Zn^{2+} ionophores was demonstrated in the previous chapter, where the application of these ionophores resulted in substantial increases in FZ-3 (which is consistent with elevated $[Zn^{2+}]_i$.

Washed platelet suspensions were treated with ionophore concentrations ranging from 300µM to 0.3µM and platelet aggregation was assessed. Aggregation profiles, shown below produced by ionophore treatment (Figure 5.1A-C) were analysed to yield values of maximum aggregation (highest positive peak on the trace, Figure 5.1D) and the minimum aggregation (highest negative peak on the trace, Figure 5.1E).

A23187 was employed as a positive control to assess the validity of ionophore treatment, as this ionophore induces full platelet aggregation following the elevation of $[Ca^{2+}]_i$ (Gamberucci et al., 2002; Smith et al., 1992; Varga-Szabo et al., 2009; Verma et al., 2011). A23187 treatment resulted in a concentration-dependent effect on platelet aggregation (Figure 5.1C-E). Treatment resulted in an initial downward deflection in light transmission (consistent with a platelet shape change and quantified as minimum aggregation), followed by an increase in light transmission consistent with rapid and complete platelet aggregation (Born, 1962; Born and Cross, 1963; Gibbins and Mahaut-Smith, 2004). A23187 concentrations of 10µM or higher induced full aggregation, as platelet aggregates were observed following visual inspection of tests cuvettes at the end of each experiment (not shown). The maximum aggregation induced by 300µM, 100µM, 30µM or 10µM of A23187 were 70.19±8.64% 58.0±2.1%, 58.1±15.1% and 59.1±16.6%, respectively, which did not significantly differ

against each other ($p>0.05$, ns, Figure 5.1C-E). Maximal aggregation were also found to be significantly higher than that induced by the vehicle control (DMSO) which was 2.1±1.5% (not shown, $p<0.05$). These data confirm the validity of A23187 in these experiment as a positive control to assess platelet activity, as this ionophore evoked near maximal platelet aggregation.

The minimum aggregation in response to A23187-dependent increases of $[Ca^{2+}]_i$ was a rapid process , as illustrated in Figure 5.1C and E. The minimum aggregation induced by the highest concentration (300µM) of A23187 was -12.0±1.9%, which was significantly higher than the vehicle control (-1.2±1.1, not shown, $p<0.05$). The minimum aggregation induced by lower concentrations (100-10µM) did not significantly differ to that induced by 300µM A23187 ($p>0.05$, ns, Figure 5.1C, E). However, as illustrated in Chapter 4, the top four concentrations of A23187 all induced significant increases in $[Ca^{2+}]_i$ which may be the reason why these concentrations of A23187 displayed a similar response in terms of shape change and aggregation. Therefore, use of A23187 demonstrates that the platelet suspensions undergo shape change and aggregate in response to the elevation of platelet $[Ca^{2+}]_i$.

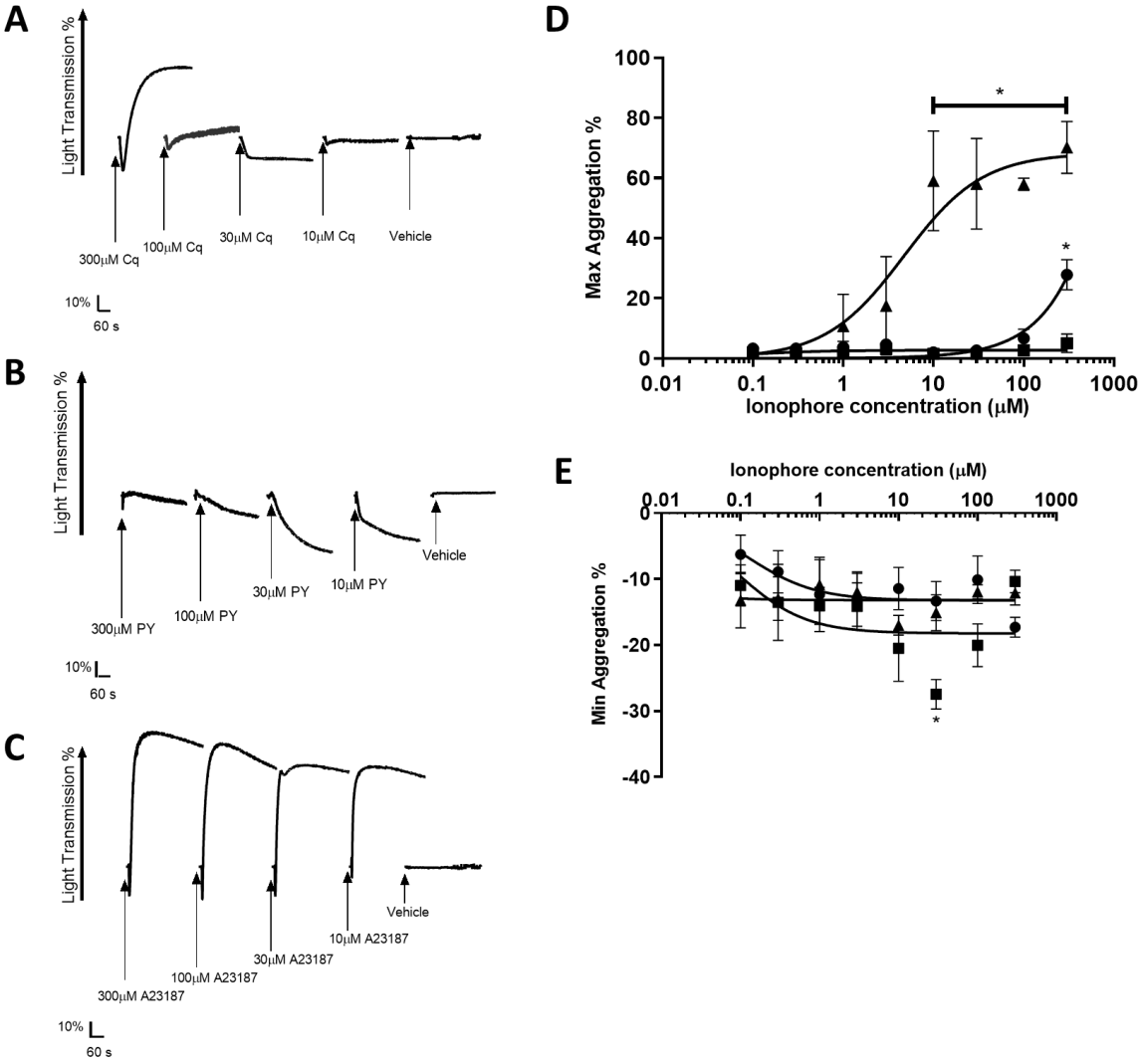

Figure 5.1. Ca^{2+} and Zn^{2+} ionophores induce platelet shape change. Representative aggregation traces were obtained following treatment of washed platelet suspensions with Zn^{2+} ionophores Clioquinol, Cq (A), Pyrithione, Py (B) or the Ca^{2+} ionophore A23187 (C). Aggregation traces were analysed to yield the maximum aggregation (D) and minimum aggregation (E), which quantifies the degree of shape change. Treatment with A23187 resulted in full aggregation, whereas Cq treatment resulted in sub-maximal aggregation at high concentrations. Py treatment did not induce aggregation. The minimum aggregation induced by ionophores did not significantly differ, with the exception of 30μM of Py inducing a significantly higher level of minimum aggregation than Cq or A23187. ▲ A23187, ● Clioquinol, ■ Pyrithione. Data are mean±standard error of mean (SEM) from 5 independent experiments. Significance is denoted as * ($p<0.05$).

Responses of platelets to the Zn^{2+} ionophores were heterogeneous. Platelet aggregation only occurred following stimulation with the highest concentration (300μM) of Cq (maximum aggregation was 27.8±5.1%. Figure 5.1D). Platelet aggregation in response to 300μM Py (5.0±2.9%) did not significantly differ from the vehicle control (2.1±1.5%,$p>0.05$, ns), and was significantly lower than that

induced by 300µM Cq (27.8±5.1%, $p<0.05$, Figure 5.1 D). This difference in aggregation responses may reflect different affinities of the ionophores for Zn^{2+} (although is approximately the same, Chapter 2), or differences in the mechanism by which the reagents penetrate the platelet cytosol. Experiments described in Chapter 4 showed a much greater increase in $[Zn^{2+}]_i$ following Cq treatment than Py, which suggest that Py is not able to induce aggregation due to its inability to induce a great enough elevation of $[Zn^{2+}]_i$.

In contrast to platelet aggregation, both Cq and Py induced initial downward deflections in light transmission, quantified by minimum aggregation levels. These downward deflections are consistent with changes in platelet morphology indicative of platelet shape change (Born et al., 1978; Caen and Michel, 1972; Frontroth, 2013; Hvas and Favaloro, 2017). The greatest minimum aggregation was observed following treatment with 300µM Cq (-17.3±1.5%). Interestingly the greatest minimum aggregation was apparent following treatment with a lower concentration of Py (30µM) which was -27.5±2.2. This was significantly greater than that induced by Cq, A23187, or every other concentration of the ionophore used ($p<0.05$, Figure 5.1E). These data reflect a biphasic response to Py, as an intermediate concentration (30µM) induced the most significant levels of shape change.

These data demonstrate that treatment of platelet suspensions with Zn^{2+} ionophores results in changes in light transmission that are consistent with shape change. At high concentrations, Cq treatment elicits a partial aggregatory response. The extent to which platelet aggregation is altered by Zn^{2+} ionophores is lower than that for the Ca^{2+} ionophore A23187. This suggests that Ca^{2+} plays a more significant role in mediating platelet activity. A23187 can mediate both $[Ca^{2+}]$ and $[Zn^{2+}]_i$ elevations (Chapter 3), whereas the Zn^{2+} ionophores are specific to Zn^{2+}. Given the effects of Zn^{2+} ionophores, it is possible that platelet aggregation and shape change (as demonstrated by A23187) is not fully attributable to Ca^{2+} but could also be influenced or mediated by Zn^{2+}. The interplay of Ca^{2+} and Zn^{2+} in platelet activity requires further investigation and would help further elucidate the mechanisms of platelet activation.

Data shown in Figure 5.1 suggests that $[Zn^{2+}]_i$ elevation induces platelet shape change and aggregation. Further experiments were performed with TPEN pre-treatment to confirm the role of Zn^{2+} in these processes. The top four concentrations (300µM-10µM) of the ionophores evoked a significant (relative to the vehicle control, DMSO) effect in terms of shape change and aggregation; thus these concentrations were selected for further studies. Washed platelet suspensions were pre-treated with 50µM TPEN prior to stimulation by Cq, Py or A23187 (Figure 5.2).

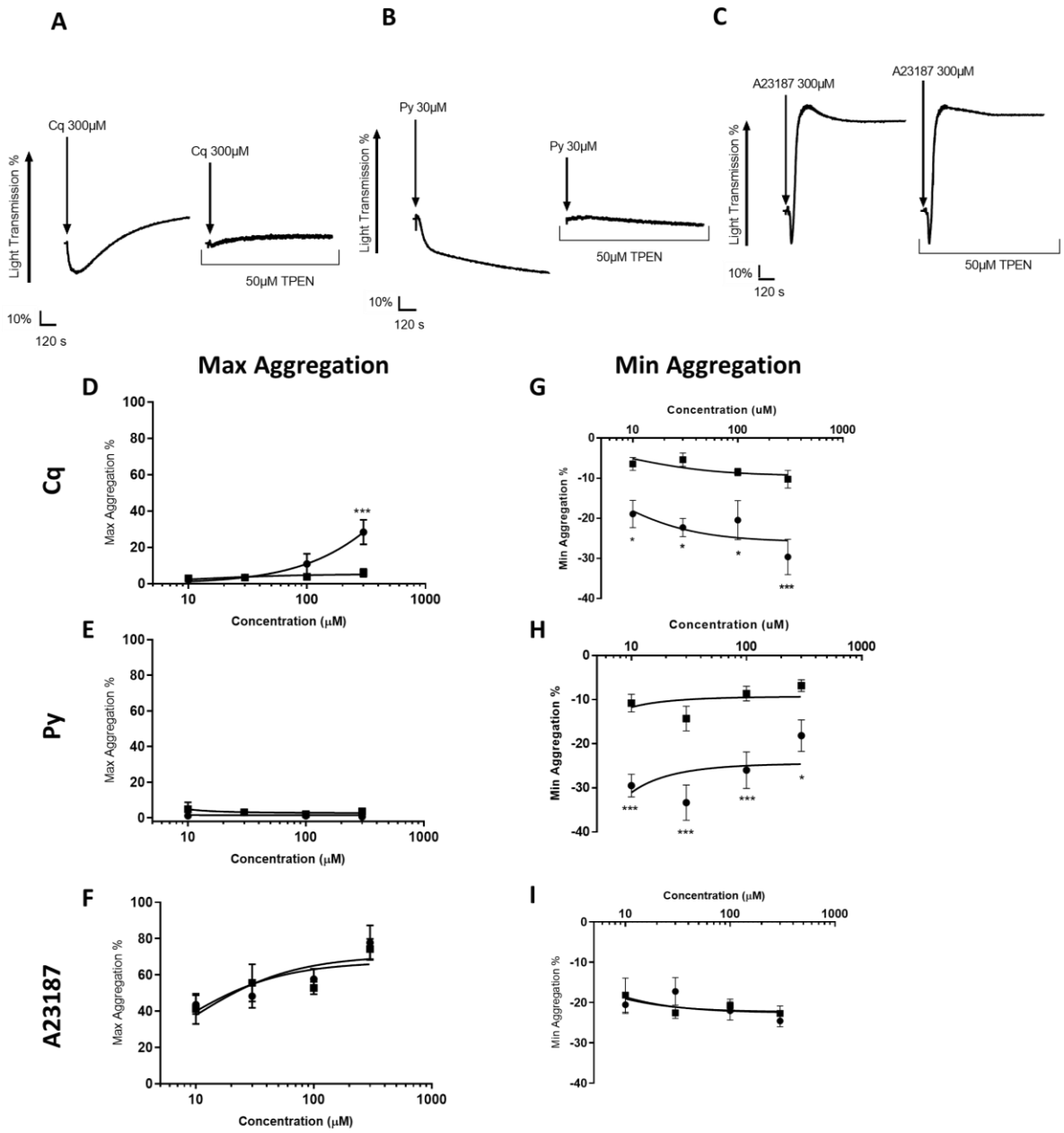

Figure 5.2. Chelation of intracellular Zn^{2+} with TPEN inhibits Zn^{2+}-ionophore-induced aggregation and shape change. In order to confirm a role for $[Zn^{2+}]_i$ in Zn^{2+}-ionophore-induced effects, platelets were pre-treated with the Zn^{2+} chelator, TPEN (50µM) prior to treatment with the given ionophores. Representative traces of the most effective concentration of Clioquinol, Cq (A, 300µM), Pyrithione, Py (B, 30µM) or A23187, (C, 300µM). Aggregation traces were quantified to yield values for maximum aggregation in response to Cq (D) Py E) or A23187 (F). Further quantification yielded values for minimum aggregation in response to Cq (G), Py (H), or A23187, (I). TPEN pre-treatment inhibited Zn^{2+} ionophore-induced aggregation and shape change but had no influence on A23187 induced shape change and aggregation. ● Vehicle control, ■ 50µM TPEN. Data are mean±standard error of mean (SEM) from 5 independent experiments. Significance is denoted as *** ($p<0.001$), ** ($p<0.01$) or * ($p<0.05$).

Maximum aggregation in response to 300µM of Cq was reduced in TPEN pre-treated platelets (50µM) from 26.4±6.8% to 5.9±2.2% ($p<0.001$, Figure 5.2A, D). Cq-mediated shape change (minimum aggregation) was also significantly reduced. Minimum aggregation in response to 300µM, 100µM, 30µM or 10µM of Cq were reduced from -29.6±4.4%, -20.5±4.9%, -21.7±2.8% and -18.1±3.6% respectively to -10.2±2.2%, -8.5±0.9%, 5.4±1.7% and 6.4±1.6% respectively ($p<0.05$, Figure 5.2G). These data confirm that the Cq induced aggregation and shape change was attributable to $[Zn^{2+}]_i$. Interestingly the lower concentrations of Cq (100µM-10µM), which did not induce an aggregation response, did induce shape change , which was inhibited upon chelation of $[Zn^{2+}]_i$ upon TPEN application. This indicates that lower concentrations of $[Zn^{2+}]_i$ evoke shape change without proceeding to aggregation. However, these lower concentrations of Cq were not shown to result in significant increases in $[Zn^{2+}]_i$ (Chapter 4). This may indicate that very low levels of $[Zn^{2+}]_i$ are enough to evoke an shape change response.

As Py treatment did not result in aggregation, no changes in Py-induced aggregation were apparent in TPEN pre-treated platelets (Figure 5.2E). However, the degree of shape change in response to Py was significantly inhibited by TPEN pre-treatment. Minimum aggregation in response to 300µM, 10µM, 30µM or 10µM Py was reduced from -18.1±3.6% to -6.8±1.3%, -25.9±4.1% to -8.6±1.7%, -33.3±4.0% to -14.3±2.8 and -29.5±2.6 to -10.8±2.0 respectively with TPEN pre-treatment, ($p<0.05$, Figure 5.2H). These data confirm that the Py induced shape change occurs in response to $[Zn^{2+}]_i$ elevation. However, as with Cq, lower concentrations of Py which induced the greatest level of shape change also induced insignificant increases in $[Zn^{2+}]_i$ (Chapter 4). This provides further evidence to suggest that small-scale rises in $[Zn^{2+}]_i$ may mediate shape change, warranting further investigation into the underlying mechanism.

A23187-induced maximum aggregation and shape change was not significantly influenced by TPEN pre-treatment (Figure 5.3C, F, I). The maximum aggregation in response to 300µM A23187 (the highest concentration used) was 77.8±9.5, whereas with TPEN pre-treatment this was 74.3±5.7 ($p>0.05$, ns, Figure 5.3C and F). No significant changes were observed in response to lower concentrations of A23187 (100µM-10µM) upon TPEN pre-treatment. The maximum aggregation induced by 100µM, 30µM or 10µM was 57.7±5.7%, 48.3±6.4% and 43.6±5.1%, respectively, whereas with TPEN pre-treatment these were 52.8±3.5%, 55.6±10.3% and 41.3±8.3%, respectively ($p>0.05$, ns, Figure 5.3F). This was also the case for the level of shape change induced by A23187, as the minimum shape change induced by A23187 was not significantly affected by TPEN pre-treatment. The highest level of minimum aggregation induced by 300µM, 100µM, 30µM or 10µM of A23187 was -24.5±1.4%,

-22.0±2.3%, -17.2±3.4% and -20.6±2.2%, respectively. These did not significantly differ from TPEN pre-treatment platelets (minimum aggregation levels were -22.7±1.9%, -20.7±1.6%, -22.6±1.4% and -18.2±4.2%, respectively ($p>0.05$, ns, Figure 5.3I).

The data shown in Figure 5.2 provide evidence that the effect induced by the Zn^{2+} specific ionophores on platelet shape change and aggregation is biologically valid, as the specific Zn^{2+} chelator TPEN reduced the effects that occurred upon Zn^{2+} mobilisation by the Zn^{2+} ionophores. This supports the hypothesis that chelation of $[Zn^{2+}]_i$ inhibit ionophore-dependant processes. Data presented in this section also provided further evidence of the specificity of TPEN to Zn^{2+}, as the application of TPEN did not significantly affect the aggregatory and shape changing effect induced by Ca^{2+} mobilisation (via A23187). This also indicates that Zn^{2+} plays a role in platelet shape change and aggregation independently of Ca^{2+} signalling, as the chelation of $[Zn^{2+}]_i$ had no significant effect on A23187 induced platelet aggregation and shape change.

Tyrosine phosphorylation is a major platelet signalling event that is induced by numerous agonists, including thrombin, CRP-XL and exogenous Zn^{2+} (Watson et al., 2016). In order to examine the mechanism of action of Zn^{2+} ionophores, immunoblotting using phosphotyrosine sensitive antibodies was carried out using suspensions of ionophore-treated washed platelets (section 2.7, chapter 2). Py (30µM) or Cq (300µM) treatment for 15 mins resulted in tyrosine phosphorylation of platelet proteins, with both high and low molecular weight protein phosphorylation observed (Figure 5.3).

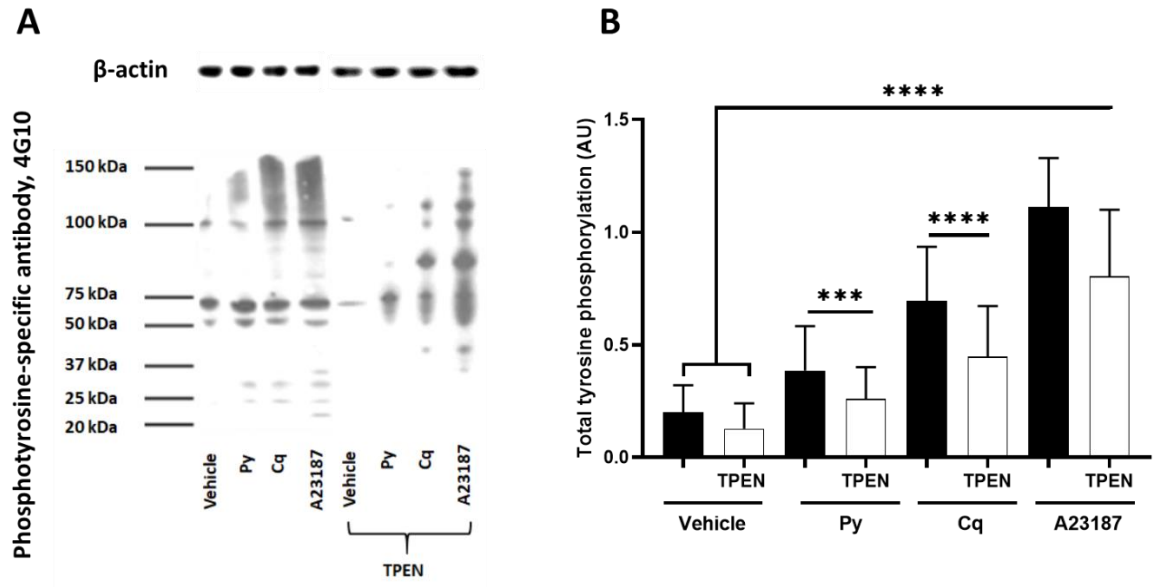

Figure 5.3. Elevation of platelet intracellular Zn^{2+} using ionophores results in increases in tyrosine phosphorylation of platelet proteins. Platelets were treated with the vehicle control (DMSO), 30µM Pyrithione (Py) 300µM Clioquinol (Cq) or 300µM A23187 for 15 minutes before being subjected to SDS-PAGE and Western blotting using the phosphotyrosine-specific antibody, 4G10. Platelets were also pre-treated with TPEN (50µM), prior to stimulation with pre-treatment. Similar patterns of tyrosine phosphorylation were observed following ionophore treatment. TPEN treatment reduced Cq or Py—induced phosphorylation, whilst not fully abrogating A23187-mediated phosphorylation. TPEN pre-treatment resulted in the phosphorylation of a different panel of proteins. (A) illustrates a representative blot of 4 independent experiments, (B) illustrates the total level of phosphorylation (average) evoked by each treatment. Data are mean±standard error of mean (SEM) from 4 independent experiments. Significance is denoted as **** ($p<0.0001$), *** ($p<0.001$), ** ($p<0.01$) or * ($p<0.05$).

The pattern of phosphorylated proteins induced by Py and Cq were similar, although Cq induced greater phosphorylation of higher molecular weight proteins, suggesting involvement by kinases or phosphatases may be influenced by elevated $[Zn^{2+}]_i$. This was further illustrated by the total (average of each band) level of tyrosine phosphorylation (section 2.7.1, Chapter 2) as the level of phosphorylation evoked by Cq (0.7±0.2) was significantly higher than induced by Py (0.4±0.2, $p<0.001$, Figure 5.3B), furthermore these levels of phosphorylation were induced by Cq and Py were both higher than the vehicle control (0.2±0.1, $p<0.0001$, Figure 5.3B).

A23187 also evoked phosphorylation of proteins of similar molecular weight as observed with the Zn^{2+} ionophores. The similarity of a pattern of phosphorylated proteins induced by the Zn^{2+} and Ca^{2+} ionophores suggests that the cations are inducing similar signalling processes. The nature of the cation responsible for A23187-mediated phosphorylation could be either Zn^{2+} or Ca^{2+}, as A23817 results in the release of both cations, although the increase in FZ-3 fluorescence (consistent with

increased $[Zn^{2+}]_i$) was moderate (Figure 4.1). However, the phosphorylation of additional proteins upon A23187 treatment suggest differences between $[Ca^{2+}]_i$ and $[Zn^{2+}]_i$ signalling, this was also evident with the increased level of total tyrosine phosphorylation evoked by A23187 (1.1±0.2) compared to that evoked by Cq (0.7±0.2, $p<0.0001$, Figure 5.3B). These data are the first to demonstrate a correlation between elevated $[Zn^{2+}]_i$ and phosphotyrosine signalling responses in platelets.

Chelation of $[Zn^{2+}]_i$ by TPEN resulted in decreased protein phosphorylation following Cq or Py treatment. The total level of phosphorylation evoked by Cq and Py decreased from 0.7±0.2 and 0.4±0.2 to 0.4±0.2 and 0.3±0.1, $p<0.001$, Figure 5.3B). This was most evident in high molecular weight proteins (ranging from approximately 100-150 kDa). Interestingly, ionophore stimulation of TPEN-treated platelets resulted in the increased phosphorylation of an unidentified protein of a molecular weight of 80-90 kDa. These data indicate that modulation of $[Zn^{2+}]_i$ may mediate the behaviour of kinases or phosphatases which regulate platelet activity. These are novel findings and provide a further area of research that warrants further investigation.

Pre-treatment with TPEN produced a pattern of phosphorylated proteins that differed from A23187 treatment. Although the total level of phosphorylation was not influenced upon TPEN treatment (as the total level of phosphorylation evoked by A2317 was 1.1±0.2 and with TPEN treatment was 0.9±0.3, $p>0.05$, ns, Figure 5.3B). However, A23187-mediated phosphorylation of low molecular weight proteins was reduced upon TPEN treatment, and the phosphorylation of the high molecular weight proteins also differed. This was interesting due to TPEN having no effect on aggregatory and shape change response induced by A23187, as illustrated above (Figure 5.2C, F, I). This suggests that A23187-induced aggregation and shape change is independent of Zn^{2+}. Furthermore, this finding indicates the potential influence of $[Zn^{2+}]_i$ on kinase and phosphatase activity that has hitherto been associated with $[Ca^{2+}]_i$ elevation. If this were the case, then A23187-induced signalling may in part be attributable to Zn^{2+}. It is possible that there is the interplay between the two cations during platelet activation. This work above demonstrates that changes in $[Zn^{2+}]_i$ assessed by Zn^{2+} ionophore and TPEN treatment results in a biologically relevant signalling event in platelets.

In conclusion, combined with the observation that $[Zn^{2+}]_i$ causes platelet shape change and platelet aggregation (Figure 5.1-2), changes in tyrosine phosphorylation of platelet proteins (Figure 5.3) implicates Zn^{2+} in a biologically important platelet processes. Whilst previous work demonstrated agonist-dependent elevations of $[Zn^{2+}]_i$, the data presented here demonstrate that increased $[Zn^{2+}]_i$ is biologically active. This supports the hypothesis that Zn^{2+} is acting as a secondary messenger in platelets.

5.2.2 Zn^{2+} ionophore-induced platelet aggregation is $\alpha_{IIb}\beta_3$ dependent

The data described above shows that aggregatory responses are induced upon $[Zn^{2+}]_i$ mobilization using Cq, but not Py. This may be attributable to the higher levels of $[Zn^{2+}]_i$ elevation induced by Cq than Py (section 4.2.1, Chapter 4). The validity of this observation was assessed by inhibition of integrin $\alpha_{IIb}\beta_3$ using the antagonist GR144053 (GR). GR144053 is effective as a $\alpha_{IIb}\beta_3$ antagonist at concentrations of 2μM which abolishes platelet aggregation (Watson et al., 2016). Here GR144053 was employed to assess whether ionophore-induced aggregation is mediated by $\alpha_{IIb}\beta_3$ (Figure 5.4).

Pre-treatment of platelets with GR144053 abolished Cq induced aggregation (Figure 5.4. A, D), demonstrating that aggregation induced by Cq is dependent on $\alpha_{IIb}\beta_3$. The maximum aggregation induced by the highest concentration (300μM) of Cq was significantly reduced from 31.5±2.8% to 6.9±2.8% upon GR144053 (2μM) treatment ($p<0.0001$, Figure 5.4D). As expected, GR144053 treatment had no effect on Py as this ionophore did not induce aggregation. The validity of these experiments was tested using A23187, as Ca^{2+} mobilization is known to induce platelet aggregation via $\alpha_{IIb}\beta_3$ (discussed in Chapter 1). A23187-induced aggregation was significantly reduced upon GR144053 treatment. The maximum aggregation in response to 300μM, 100μM, 30μM or 10μM of A23187 was reduced from 88.4± 5.8% to 22.3 ± 2.1%, 82.9 ± 2.3% to 17.6±2.3%, 74.0±3.9% to 16.7±4.6% and 60.8±2.6% to 5.6±1.0% respectively upon GR144053 treatment, ($p<0.0001$, Figure 5.4F). Thus, these data with A23187 treatment confirmed that GR144053 was a valid inhibitor of platelet aggregation in these experiments.

Pre-treatment with GR144053 had no significant effect on minimum aggregation, indicating that inhibition of platelet aggregation did not significantly influence ionophore-mediated shape change. The minimum aggregation induced by 300μM of Cq was -20.3±0.6% and with GR144053 pre-treatment was -13.1±2.9%, ($p>0.05$, ns, Figure 5.4G). This was also the case with Py, the minimum aggregation induced by 30μM (the concentration of Py which resulted in the greatest level of minimum aggregation) was -30.4±1.9% compared to 21.3±3.1% following GR144053 treatment ($p>0.05$, ns, Figure 5.4F). GR144053 pre-treatment also did not affect A23187-induced shape change. The minimum aggregation induced by 300μM A23187 was -14.6±1.4% and with GR144053 pre-treatment was -20.3±5.0% ($p>0.05$, ns, Figure 5.4I). These data provided evidence to show that ionophore-induced aggregation is independent of platelet shape change. Indicating that the inhibition of $\alpha_{IIb}\beta_3$ has no influence on the shape change process.

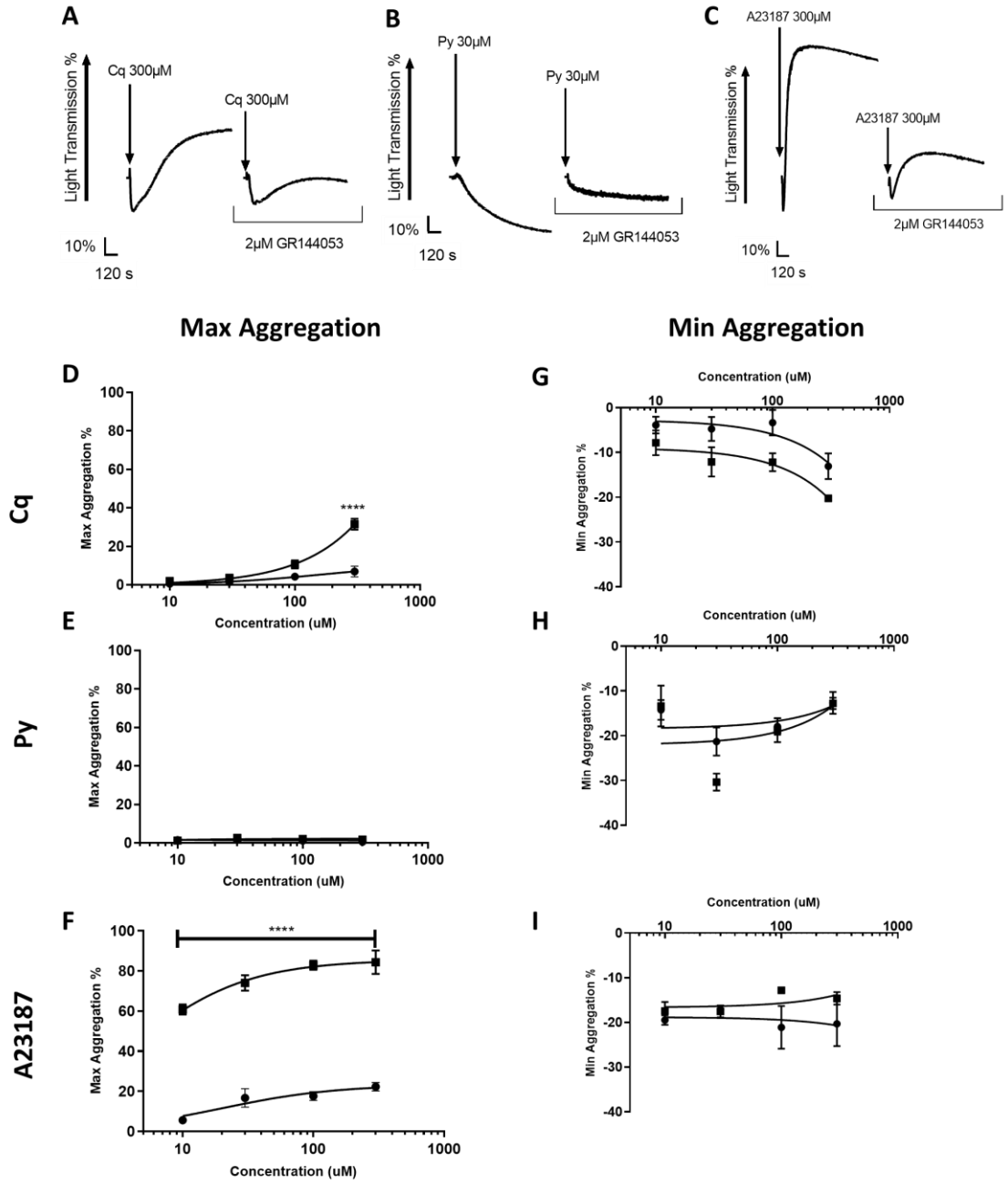

Figure 5.4. Antagonism of $\alpha_{IIb}\beta_3$ abrogates ionophore-induced platelet aggregation. In order to test the biological validity of ionophore-induced platelet aggregation, platelets were pre-treated with the $\alpha_{IIb}\beta_3$ antagonist GR144053 (2µM) prior to treatment with the given ionophores. Representative traces following treatment with the most significant concentration of Clioquinol, Cq, (A, 300µM), Pyrithione. Py (B, 30µM) or A23187, (C, 300µM) are shown. Aggregation traces were quantified to yield maximum aggregation values in response to different concentrations of Cq (D), Py (E) or A23187 (F). Minimum aggregations which were calculated following treatment with different concentrations of Cq (G), Py (H) or A23187 (I). Ionophore induced aggregation, but not shape change were inhibited with GR144053 pre-treatment. ■ Vehicle control, ● 2µM GR144053. Data are mean±standard error of mean (SEM) from 5 independent experiments. Significance is denoted as **** ($p<0.0001$), *** ($p<0.001$), ** ($p<0.01$) or * ($p<0.05$).

5.2.3 Increases in intracellular Zn^{2+} mediate platelet shape change

Figures 5.1-2 and 5.4 showed that Zn^{2+} ionophores influence light transmission of platelet suspensions in a manner that is consistent with activation-dependent shape change. 300µM Cq induced significant aggregation and the greatest degree of shape change. Treatment with lower concentrations of Cq resulted in shape change with no progression to aggregation. A similar effect was seen following treatment with all concentrations of Py. Lower concentrations (30µM or 10µM) of Py induced the highest level of shape change, consistent with a biphasic concentration response. The conclusions from these experiments were that Zn^{2+} ionophore-induced activatory-dependant shape change in a manner independent of aggregation. Thus, the role of Zn^{2+} in platelet shape change was further investigated.

5.2.3.1 Cytochalasin D inhibits Zn^{2+} ionophore mediated platelet shape change

In order to confirm a role Zn^{2+} on is effect on the platelet cytoskeleton, platelets were pre-treated with the actin cytoskeleton polymerisation inhibitor, Cytochalasin D (Cyt D), which has been widely used in studies which investigated the platelet cytoskeletal changes (Casella et al., 1981; Torti et al., 2000). As 10µM of Cyt D has previously been shown to be effective at inhibiting actin polymerisation in washed platelet suspension (Cerecedo et al., 2002; Finkenstaedt-Quinn et al., 2015; Ge et al., 2012), this concentration was used in the experiments described here.

Pre-treatment of washed platelet suspensions with Cyt D (10µM) significantly reduced the level of shape change induced by the ionophores employed (Figure 5.5). The minimum aggregation induced by 300µM, 100µM, 30µM or 10µM Cq treatment was significantly reduced from -29.3±2.6% to 4.0±1.6%, -24.2±5.1 to -8.6±1.6, -24.2±6.7% to 7.1±4.6% and -18.2±2.2% to 3.0±1.1%, respectively upon Cyt D treatment ($p<0.05$, Figure 5.5G). The minimum aggregation induced by 300µM, 100µM, 30µM or 10µM of Py was significantly reduced from -13.7±0.8% to -3.7±0.9%, -18.8±2.7% to -8.6±1.3%, -30.4±1.9% to -11.3±2.7 and -16.7±4.3% to -4.6±1.9%, respectively upon Cyt D treatment ($p<0.05$, Figure 5.5H). The minimum aggregation induced by 300µM, 100µM,30µM or 10µM of A23187 was significantly reduced from -24.8±2.0% to -14.0±1.2%, -16.8±1.3% to -6.7±1.6%, -13.3±1.3% to -4.4±1.7 and -8.9±1.6% to -1.9±0.6%, respectively upon Cyt D treatment ($p<0.05$, Figure 5.5I). This work demonstrates that ionophore-mediated shape change is sensitive to Cyt D treatment as the data

described above confirms that downward deflections in light transmission induced by Zn^{2+} ionophores are a biological response, rather than a chemical phenomenon.

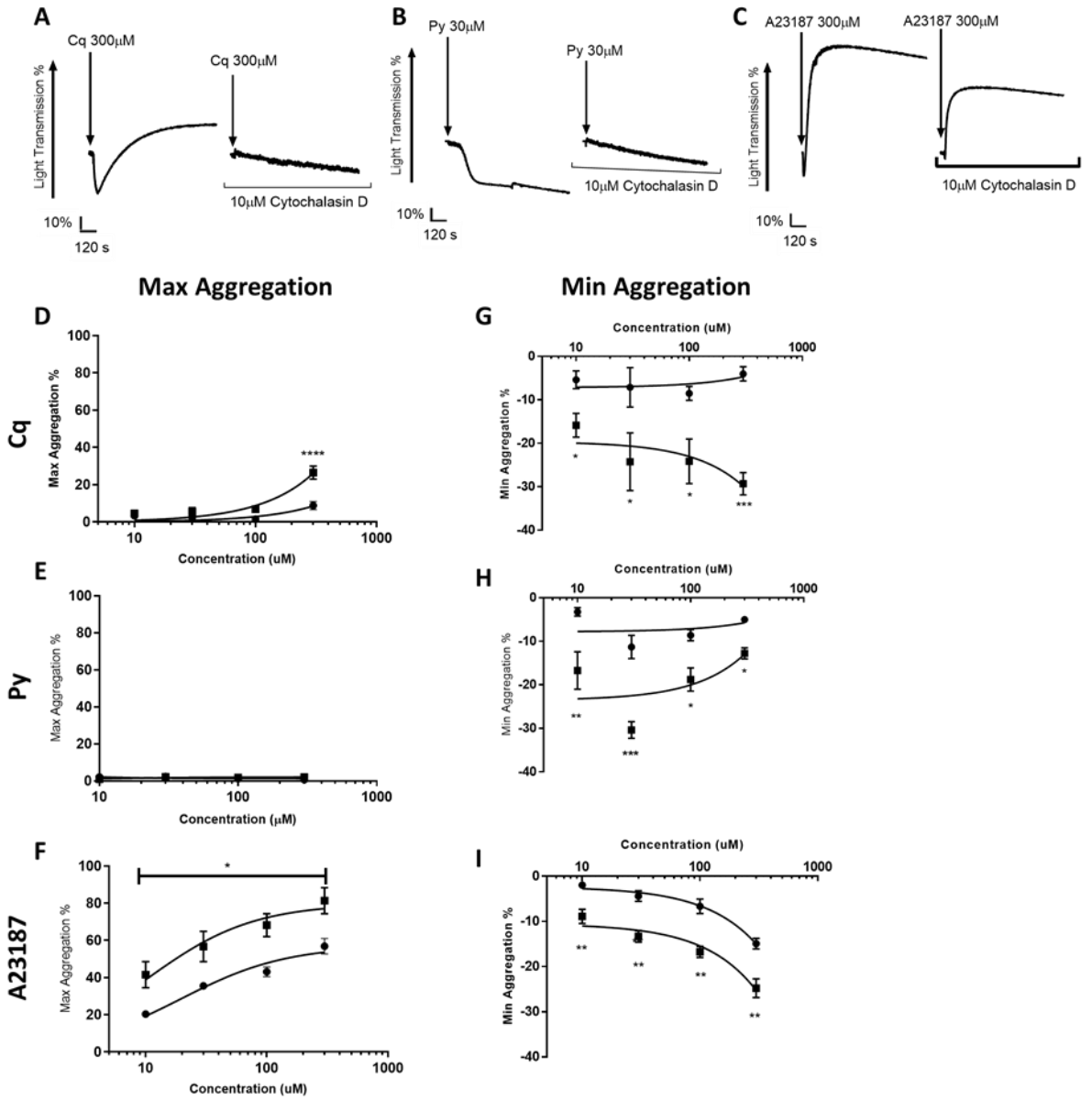

Figure 5.5. Cytochalasin D (Cyt-D) abrogates ionophore-induced platelet shape change. Washed platelet suspensions were pre-treated with 10μM Cyt-D before being stimulated with ionophores. Representative aggregation traces are shown for treatment with Clioquinol, Cq (A), Pyrithione, Py (B) or A23187 (C). Maximum aggregation in Cyt D treated and untreated platelets was quantified following stimulation with Cq (D) Py (E), or A23187 (F).) Similarly, minimum aggregation in Cyt D treated and untreated platelets was quantified following stimulation with Cq (G), Py (H) or A23817 (I). Cyt D pre-treatment significantly inhibited the ionophore-induced shape change and aggregation. ■ Vehicle control, ● 10μM Cyt D. Data are mean±standard error of mean (SEM) from 5 independent experiments. Significance is denoted as **** ($p<0.0001$), *** ($p<0.001$), ** ($p<0.01$) or * ($p<0.05$).

Cyt D treatment also significantly reduced the maximum aggregation level induced by the ionophores, indicating that cation induced aggregation may be dependent on the activatory shape change process for optimal aggregation. The maximum aggregation response to 300µM Cq was reduced significantly from 29.50±3.60% to 8.79±2.15% upon Cyt D treatment ($p<0.0001$, Figure 5.5D). Py treatment did not result in significant levels of aggregation; thus Cyt D had no effect on the maximum aggregation in response to this ionophore. The maximum aggregation induced by 300µM, 100µM, 30µM or 10µM of A23187 was significantly reduced from 81.40±7.05% to 56.84±4.21%, 68.17±6.22% to 43.10±2.63%, 56.69±8.20% to 35.53±1.90% and 41.55±7.02% to 20.35±1.69%, respectively upon Cyt D treatment ($p<0.05$, Figure 5.5F).

The observation that Zn^{2+} ionophore treatment resulted in significant shape change without progression to aggregation indicates that shape change may be independent of aggregation. Published work has provided conflicting evidence for the requirement of shape change for full aggregation, with some studies suggesting that aggregation is independent of shape change, (Maurer-Spurej and Devine, 2001; Ohlmann et al., 2000), whilst others indicate that shape change is a prerequisite for platelet aggregation (Shin et al., 2017) as evident from the reduced aggregatory response evoked by A23187 (and 300µM Cq) in the presence of Cyt D.

5.2.3.2 Zn^{2+} mediated signalling induces platelet shape change

Data described in Figure 5.5 supports the conclusion that ionophore treatment results in shape change that is dependent on cytoskeletal rearrangements and is thus biologically valid and not an artefact of ionophore treatment. Prior to the experiments described here, the role of Zn^{2+} in signalling pathways that regulate platelet shape change was unstudied. The data described above are therefore the first to indicate the potential importance of Zn^{2+} in platelet shape change. This suggests that increased $[Zn^{2+}]_i$ could act upon specific proteins in signalling cascades leading to shape change in a manner that is consistent with a secondary messenger. Further experiments were performed to investigate the role of $[Zn^{2+}]_i$ in signalling pathways that are known to mediate platelet shape change. As calmodulin, ROCK (Rho-associated coiled-coil-containing protein kinase) and MLCK are involved in mediating platelet shape change, their contributions to Zn^{2+} -dependent shape change were assessed.

The selective MLCK inhibitor, ML7 hydrochloride (ML7), the Calmodulin antagonist, W-7 hydrochloride (W-7) and the selective p160 ROCK inhibitor, Y-27632 dihydrochloride (Y-27632) were employed to assess the potential involvement of $[Zn^{2+}]_i$ in the shape changing signalling pathways.

ML7 is a widely used potent inhibitor of MLCK with working concentrations commonly being 1-10µM (Feghhi et al., 2016; Qiu et al., 2014). Similarly, Y-27632 (10µM) has been used to investigate the importance of p160 ROCK in platelet shape change (Paul et al., 1999; Wee and Jackson, 2006). W-7 is a potent calmodulin antagonist, with working concentrations for washed platelet suspensions reported in the 40-60µM range (Gardiner et al., 2004; Levy, 1983). Similar concentrations of antagonist were employed in the experiments described here.

Cq induced shape change in response to ML7, W-7 and Y-27632 application

Pre-treatment of washed platelet suspensions with ML7 (10µM) significantly reduced the level of shape change induced by Cq (Figure 5.6 A, E). The minimum aggregation induced by 300µM, 100µM, 30µM or 10µM of Cq was significantly reduced from -15.5±2.4% to -5.3±1.3%, -14.3±1.6% to -6.2±1.6, -15.7±2.2% to -3.4±1.7% and 11.1±2.6% to 3.0±0.7%, respectively upon ML7 treatment ($p<0.05$, Figure 5.6E).

Treatment with W-7 (60µM) did not affect Cq-mediated shape change, as the minimum aggregation of W-7-pretreated platelets in response to 300µM Cq was -19.5±3.1% compared to -23.6±1.2% for untreated platelets ($p>0.05$, ns, Figure 5.6F). These data are the first to show that Cq induced shape change is independent of calmodulin. This is in contrast to previous studies which have shown that Ca^{2+}-dependent calmodulin activity induces MLCK activation, and thus shape change in a Ca^{2+} dependent manner (Paul et al., 1999).

In contrast to W-7 treatment, pre-treatment with Y-27632 (10µM) significantly inhibited the level of shape change induced by Cq. The minimum aggregation induced by 300µM, 100µM, 30µM or 10µM of Cq was significantly reduced from -21.3±1.9% to -7.3±0.8%, -12.1±2.60% to -3.9±1.4, -12.7±3.7% to -3.7±1.1% and -11.9±1.9%, respectively, upon Y-27632 treatment ($p<0.05$, Figure 5.6G). This demonstrates that Cq induced shape change is mediated by p160 ROCK. These data along with data shown in Figure 5.6F confirms that p160 ROCK-mediated shape change is a Ca^{2+}-independent process (Paul et al., 1999), and may be a Zn^{2+} dependent process.

The maximum aggregation in response to Cq (300µM) was reduced upon pre-treatment of these inhibitors and antagonists (Figure 5.6B-D). Maximum aggregation was reduced from 34.4±3.4% to 22.1±2.4% upon ML7 (10µM) pre-treatment ($p<0.001$, Figure 5.6B), from 29.8±2.7% to 11.2±3.2% upon W-7 (60µM) pre-treatment ($p<0.0001$, Figure 6.6C), and from 31.4±5.6% to 12.2±4.2% upon Y-27632 (10µM) pre-treatment ($p<0.001$, Figure 6.6D). These data indicate that Cq induced aggregation

is mediated by signalling pathways that evoke platelet shape change, coinciding with earlier findings which found that Cyt D application also inhibited Cq induced aggregation. Thus, Cq-induced aggregation is dependant on shape change. Furthermore, inhibition of calmodulin did not inhibit shape change, but still significantly reduced the maximum aggregation induced by 300μM Cq. This suggests that calmodulin may not be involved in Cq induced shape change but may influence the aggregatory response of Cq; thus aggregation induced upon $[Zn^{2+}]_i$ may occur in a Ca^{2+} dependent manner.

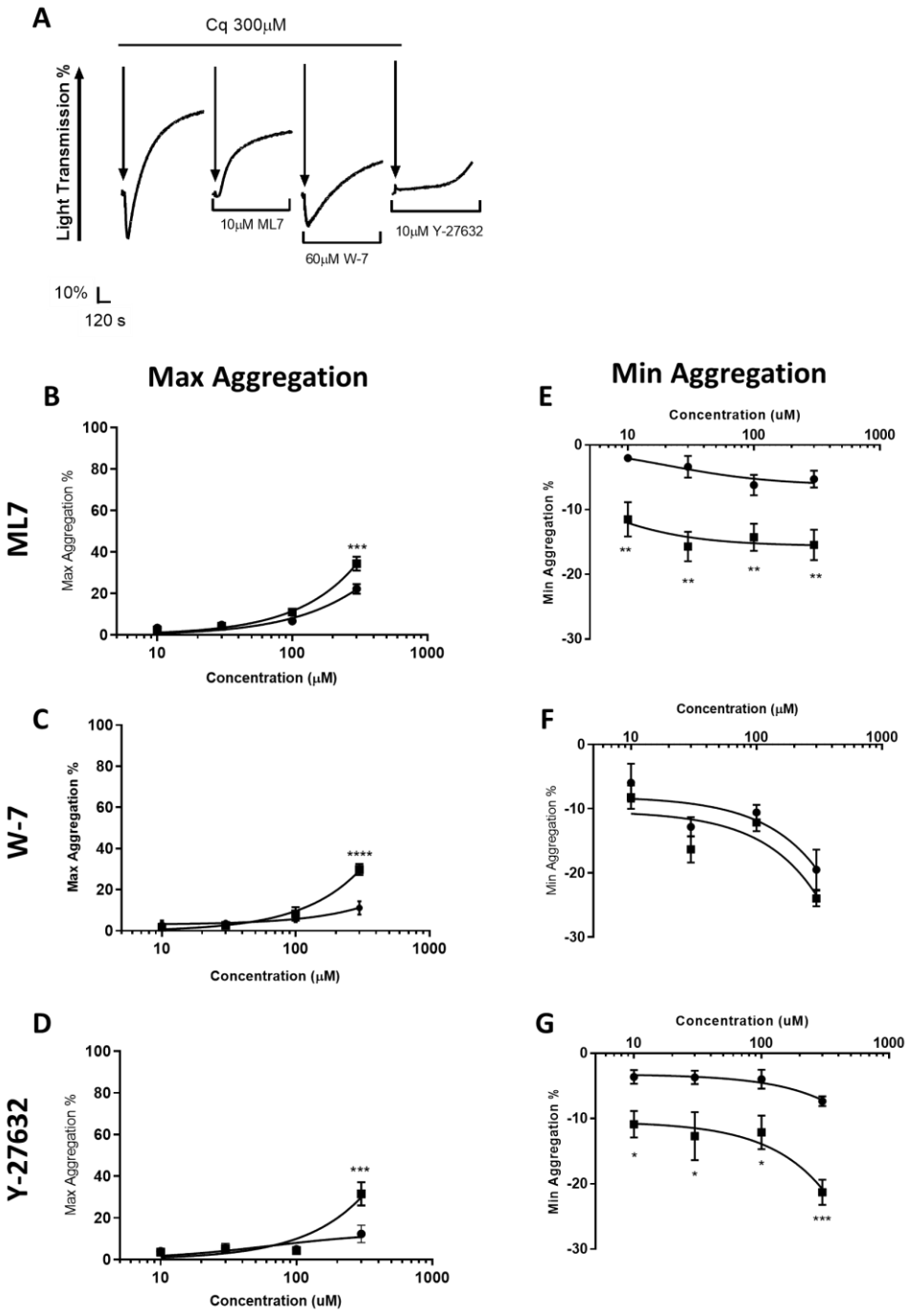

Figure 5.6. Clioquinol-induced aggregation and shape change are sensitive to inhibition of signalling proteins involved in cytoskeletal rearrangements. Washed platelets were pre-treated with 10μM ML7, 60μM W-7 or 10μM Y-27632 before being stimulated with clioquinol, Cq (300μM, A). Aggregation traces were analysed to yield values for maximum aggregation induced by the different concentrations of Cq in the absence and presence of ML7 (B), W-7 (C), or Y-27632 (D). Similarly, minimum aggregation were quantified following treatment with different concentrations of Cq in the absence and presence of ML7 (E), W-7 (F), or Y-27632 (G). ML7 and Y-27632 but not W-7 treatment inhibited Cq induced shape change. ■ Vehicle

control, ● 10µM ML7 (B and E), ● 60µM W-7 (C and F) and ● 10µM Y-27632 (D and G). Data are mean±standard error of mean (SEM) from 5 independent experiments. Significance is denoted as **** ($p<0.0001$), *** ($p<0.001$), ** ($p<0.01$) or * ($p<0.05$).

Py induced shape change in response to ML7, W-7 and Y-27632 application

Pre-treatment of platelet suspensions with 10µM of ML7 significantly reduced the level of shape change induced by Py (Figure 5.7 A and E). The minimum aggregation in response to 300µM, 100µM,30µM or 10µM of Py went down from -15.8±1.0% to -4.1±1.3%, -15.1±2.7% to -3.0±1.0%, -25.9±3.6% to -4.50±1.8 and -21.6±3.5% to -5.9±2.5%, respectively upon ML7 treatment ($p<0.05$, Figure 5.7E). Pre-treatment with 60µM of W-7 did not result in significant changes in the level of shape change induced by Py (Figure 5.7 A, F). The minimum aggregation induced by 30µM of Py following W-7 pre-treatment was -25.16±1.94% compared to -24.65±2.23% for untreated platelets ($p>0.05$, ns, Figure 5.7F). Pre-treatment with Y-27632 however significantly inhibited the level of shape change induced by Py. The minimum aggregation induced by 300µM, 100µM, 30µM or 10µM of Py was significantly reduced from -12.8±1.3% to -6.3±1.1%, -13.7±1.2% to -5.9±0.5%, -21.8±2.3% to -10.1±2.4% and -14.6±1.73% to -7.1±1.04%, respectively, upon Y-27632 pre-treatment ($p<0.05$, Figure 5.7G). Thus, Py resulted in a similar effect to these inhibitors as Cq (Figure 5.6), further demonstrating that Zn^{2+} mediated shape change occurs in a Ca^{2+} independent manner.

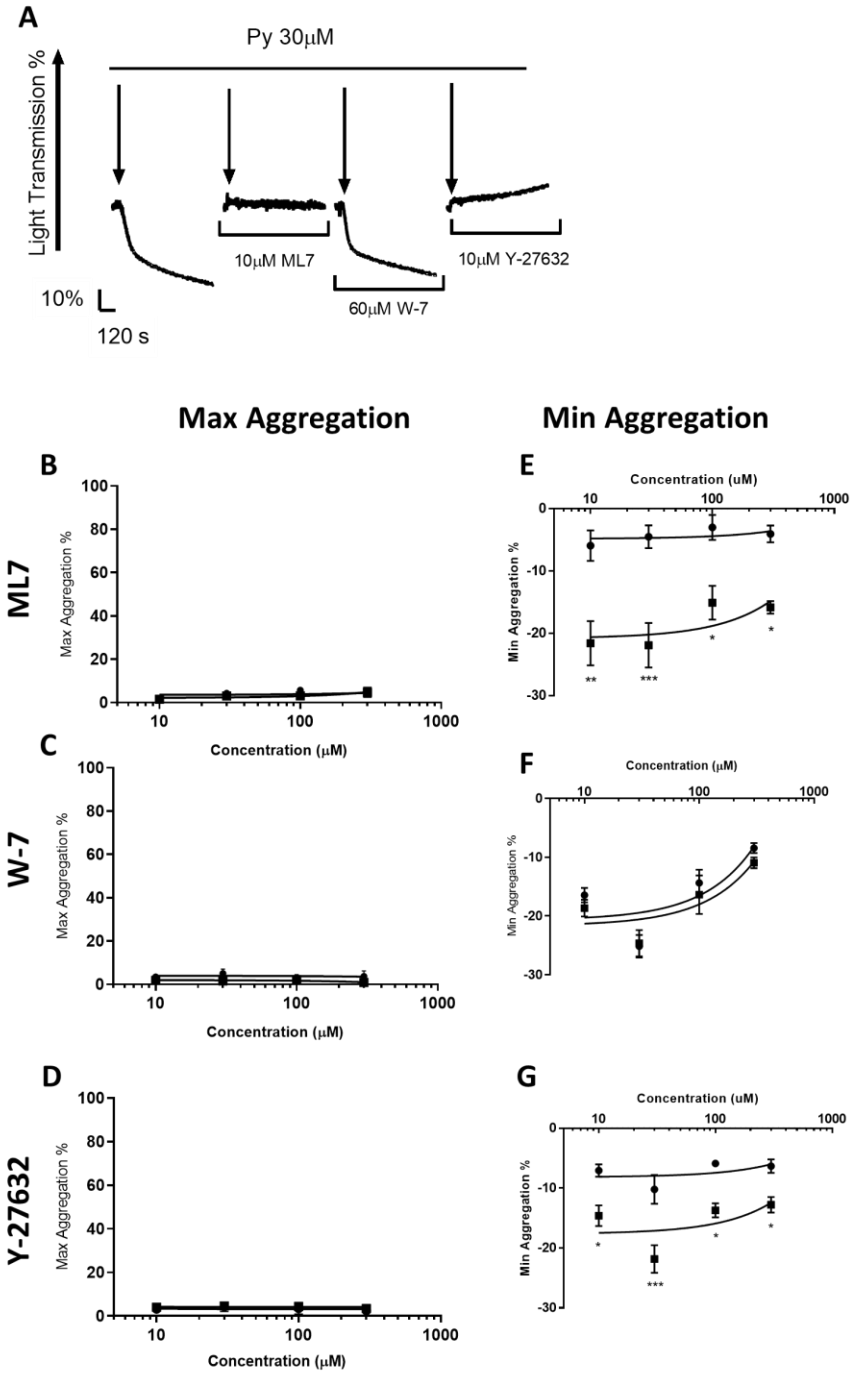

Figure 5.7. Pyrithione-induced aggregation and shape change are sensitive to inhibition of signalling proteins involved in cytoskeletal rearrangements. Washed platelets were either pre-treated with 10μM ML7, W-7 or Y-27632 before being challenged with pyrithione, Py (A) Representative aggregation traces showing the most effective concentration of Py in the platelets pre-treated with the inhibitors, ML7, W-7 and Y-27632. Aggregation traces were analysed to yield maximum aggregation values following pre-treatment with ML7 (B), W-7 (C), or Y-27632 (D). The minimum aggregation induced by the different concentrations of Py were also yielded in the absence and presence of ML7 (E), W-7 (F), or Y-27632 (G). ML7 and

Y-27632 but not W-7 treatment inhibited Py induced shape change. ■ Vehicle control, ● 10μM ML7 (B and E), ● 60μM W-7 (C and F) and ● 10μM Y-27632 (D and G). Data are mean±standard error of mean (SEM) from 5 independent experiments. Significance is denoted as *** ($p<0.001$), ** ($p<0.01$) or * ($p<0.05$).

A23187 induced shape change in response to ML7, W-7 and Y-27632 application

Further experiments were carried out using A23187 and the shape changes inhibitors (ML7, W-7 and Y-27632, Figure 5.8) as a positive control and to enable comparisons to be made with the shape induced mechanisms mediated by $[Zn^{2+}]_i$.

Pre-treatment with ML7 (10μM) significantly reduced the level of shape change induced by A23187 (Figure 5.8 A, E). The minimum aggregation induced by 300μM, 100μM, 30μM or 10μM of A23187 was significantly reduced from -14.5±2.3% to -6.8±1.0%, -11.3±0.9% to -3.9±0.8%, -13.2±2.3% to -6.3±0.8% and -12.9±0.2% to -5.8±2.0%, respectively upon ML7 treatment ($p<0.05$, Figure 5.8E). Application of W-7 (60μM) also significantly reduced the level of shape change induced by A23187 (Figure 5.8 A, F). The minimum aggregation induced by 300μM, 100μM, 30μM or 10μM of A23187 was significantly reduced from -16.0±0.8% to -7.3±0.9%, -16.2±1.35% to -7.0±1.3%, -16.6±1.8% to -7.5±1.5% and -15.5±3.2% to -5.4±2.0%, respectively upon W-7 treatment ($p<0.05$, Figure 5.8 F). However, pre-treatment with Y-27632 (10μM) did not influence the level of shape change induced by A23187 (Figure 5.8 A, G). The minimum aggregation induced by the highest concentration (300μM) of A23187 was -17.9±1.4% and with Y-27632 (10μM) pre-treatment was -18.1±1.9% ($p>0.05$, ns, Figure 5.8G). These data confirm previous studies that indicate Ca^{2+} mediated shape change is independent of p160 ROCK (Kureishi et al., 1997; Paul et al., 1999).

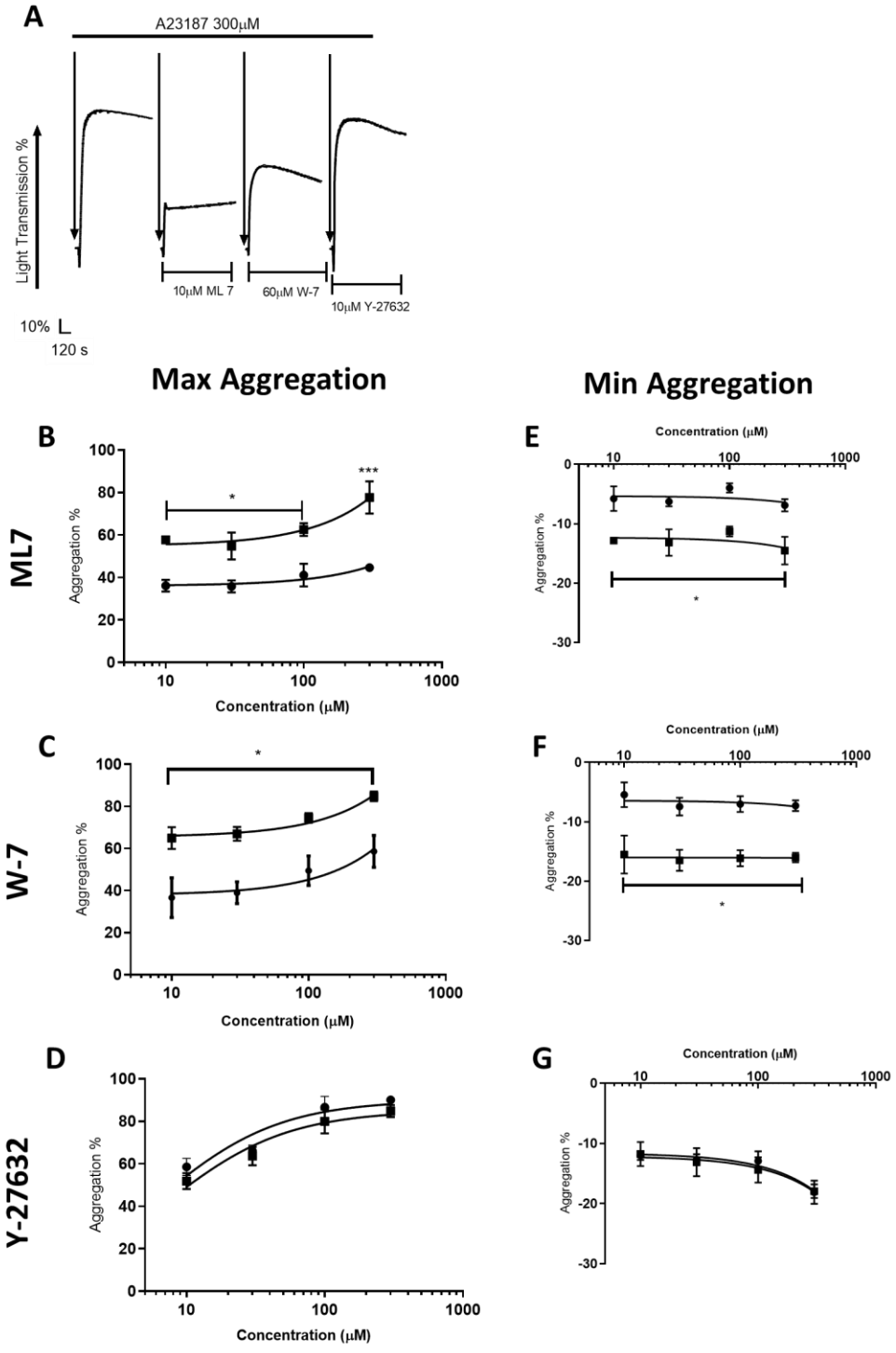

Figure 5.8. A23187-induced aggregation and shape change are sensitive to inhibition of signalling proteins involved in cytoskeletal rearrangements. Washed platelets were either pre-treated with ML7, W-7 or Y-27632 before being challenged with A23187. A) Representative aggregation traces showing the effect of A23187 treatment (300μM) on platelets pre-treated with ML7, W-7 Y-27632. Traces were analysed to yield maximum aggregation values in platelets pre-treated with ML7 (B), W-7 (C), or Y-27632 (D). As well as minimum aggregation induced by the different concentrations of A23187 in the absence and presence of ML7 (E), W-7 (F), or Y-27632 (G). ML7 and W-7 but not Y-27632 treatment inhibited A23187 induced shape

change and aggregation. ■ Vehicle control, ● 10µM ML7 (B and E), ● 60µM W-7 (C and F) and ● 10µM Y-27632 (D and G). Data are mean±standard error of mean (SEM) from 5 independent experiments. Significance is denoted as *** ($p<0.001$), ** ($p<0.01$) or * ($p<0.05$).

Maximum aggregation in response to A23187 was significantly reduced upon pre-treatment with ML7 or W-7, but not Y-267632 (Figure 5.8A, B). Maximum aggregation induced by 300µM, 100µM, 30µM or 10µM of A23187 was reduced from 77.6±7.6% to 44.7±1.7%, 62.5±3.0% to 41.1±5.3%, 54.8±6.3% to 35.8±2.8% and 57.7±0.50% to 36.1±2.8%, respectively upon ML7 treatment ($p<0.05$, Figure 5.8B). Maximum aggregation induced by 300µM, 100µM, 30µM or 10µM was significantly reduced from 84.7±2.30% to 58.7±7.6%, 74.5±2.3% to 49.4±7.0%, 66.9±3.3% to 39.0±5.2% and 64.9±5.2% to 36.6±9.4%, respectively upon W-7 (60µM) treatment ($p<0.05$, Figure 5.8C). The maximum aggregation induced by 300µM of A23187 was 84.8±3.0% and with Y-27632 (10µM) pre-treatment was 90.0±1.9% ($p>0.05$, ns, Figure 5.8D). This confirms that A23187 induced aggregation is mediated by cytoskeletal signalling involving MLCK and calmodulin but not Rho kinases. This is yet to be fully explored and correlates well with the data showing that Cq mediated aggregation is also inhibited by these inhibitors and antagonists. This suggests that full platelet aggregation is mediated by pathways that evoke shape change.

Ionophore induced myosin light chain (MLC) phosphorylation

The influence of Zn^{2+} on signalling pathways that are involved with shape change was further assessed by examination of ionophore-mediated changes in the phosphorylation state of MLC (at position ser157) in platelets pre-treated with shape change inhibitors (employed above). Phosphorylation of MLC is an important step in the shape changing signalling pathway, as phospho-MLCs mediate actin rearrangement. Ser157 of MLC is phosphorylated by both MLCKs and RhoA ROCK. Therefore measurement of the level of phosphorylation of this MLC provides a means to assess the influence of Zn^{2+} signalling on platelet shape change.

Thrombin was employed as a positive control, to see the levels of MLC phosphorylation induced by a physiological agonist. Thrombin is known to induce platelet shape change in a calcium-dependant manner by inducing elevated intracellular Ca^{2+} elevation which in turn activates the Ca^{2+}/Calmodulin-dependent MLCK, which increases in phosphorylation of MLC (Bodie et al., 2001; Hathaway and Adelstein, 1979; Shin et al., 2017b). Thrombin treatment induces shape change in a Ca^{2+} independent manner, by activating ROCK (Rho-associated coiled-coil-containing protein kinase)

which inhibits MLC-P, enabling enhanced MLC phosphorylation which in turns leads to cytoskeletal rearrangement for platelet shape change.

Significant increases in MLC phosphorylation were evident upon stimulation with 1U/ml of thrombin, 300µM of A23187, 300µM of Cq and 30µM of Py in comparison to that induced by the vehicle (DMSO, Figure 5.9A). The levels of phosphorylation induced by 1U/ml of thrombin, 300µM of A23187, 300µM of Cq and 30µM of Py were 0.52±0.13 AU, 0.74±0.06 AU, 0.54±0.06 AU and 0.55±0.03, respectively which were all significantly higher than that induced by the vehicle, which was 0.158±0.04 AU ($p<0.05$, Figure 5.9A). These findings provide further evidence to show that Zn^{2+} ionophores induce shape change via increased MLC activity. In order to confirm the role of Zn^{2+} in ionophore-induced MLC phosphorylation, platelets were pre-treated with 50µM of TPEN prior to stimulation. TPEN did not influence changes in phosphorylation in response to thrombin or A23187, but significantly reduced the level of phosphorylation induced by Cq or Py (Figure 5.9B). The levels of MLC phosphorylation in the presence of TPEN in response to 1U/ml of thrombin, 300µM of A23187, 300µM of Cq, or 30µM of Py were 0.5±0.1 AU, 0.6±0.1 AU, 0.14±0.03 AU and 0.14±0.03 AU. There were no significant differences in MLC phosphorylation in the presence of TPEN, induced by Cq, Py stimulation and the vehicle control (0.10±0.04 AU, $p>0.05$, Figure 5.9B). Thrombin and A23187 treatment resulted in significantly higher levels of phosphorylation than the vehicle, Cq or Py in the presence of 50µM TPEN ($p<0.05$, Figure 5.9B). These data confirm that Zn^{2+} ionophore-induced MLC phosphorylation is attributable to Zn^{2+}.

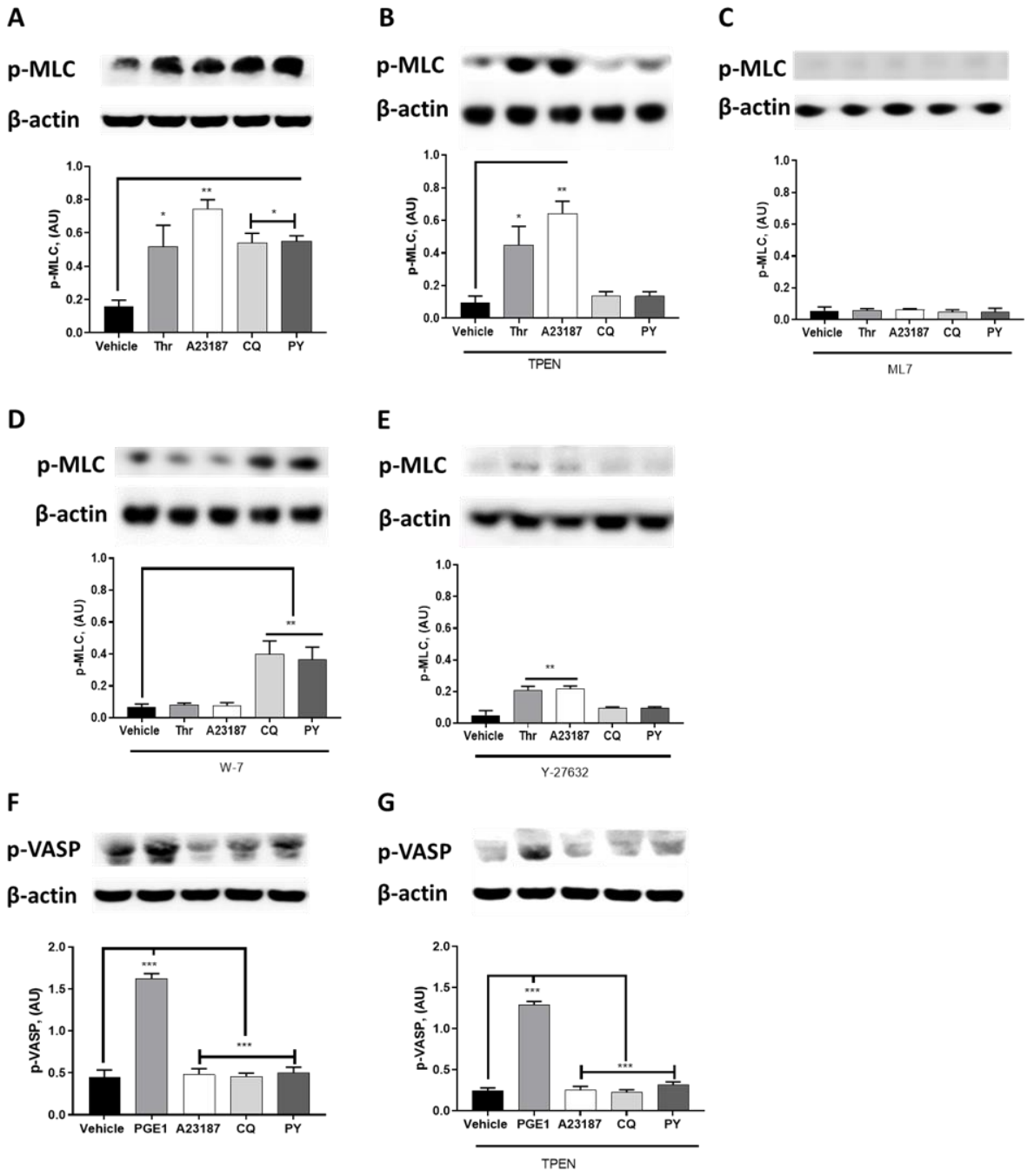

Figure 5.9. Ionophore-mediated increases in intracellular Zn^{2+}regulate platelet shape change and phosphorylation of cytoskeletal regulators. A) Representative Western blots showing changes in MLC phosphorylation following stimulation of washed platelet suspensions for 15 mins with vehicle (DMSO), thrombin (1U/mL), A23187 (300µM),clioquinol, Cq (300µM), or pyrithione, Py (30µM). Western blots of platelets pre-treated with (B), TPEN (50µM), (C) ML7 (10µM), (D) W-7 (60µM), (E) Y-27632 (10µM). Representative Western blot showing changes in VASP phosphorylation following pre-treatment of platelets for 15 mins with vehicle (DMSO), PGE_1 (1U/mL), A23187 (300µM), Cq (300µM), Py (30µM), (F) or 50µM TPEN (G). Blots and quantification (means±SEM) are representative of 4 experiments. Significance is denoted as *** ($p<0.001$), ** ($p<0.01$) or * ($p<0.05$).

Phosphorylation of MLC in response to thrombin or the ionophores was significantly reduced upon ML7 treatment. The levels of MLC phosphorylation in the presence of ML7 in response to 1U/ml of thrombin, 300µM of A23187, 300µM of Cq or 30µM of Py were 0.06±0.01 AU, 0.06±0.01 AU, 0.05±0.01 and 0.05±0.02, respectively (Figure 5.9C). MLC phosphorylation in ML7 pre-treated platelets in response to the vehicle was 0.06±0.02. Therefore, there were no significant differences in MLC phosphorylation between the vehicle, thrombin and ionophore treatments ($p>0.05$, ns, Figure 5.9C). These data correlate with the data described in Figure 5.6-8 (A, E), which showed that shape change induced by the inhibitors was significantly reduced with ML7 statement. This further supports the biological validity of the ionophore-induced shape change, as this data indicates that ionophore-dependent shape is dependent on MLC phosphorylation.

Data described in Figures 5.6 to 5.8 (A, F) showed that the shape change induced by A23187, but not the Zn^{2+} ionophores, was inhibited by W-7, indicating that Zn^{2+}-mediated shape change is independent of calmodulin. W-7 pre-treatment inhibited MLC phosphorylation induced by thrombin or A23187 but did not inhibit phosphorylation induced by Cq and Py relative to the vehicle ($p<0.05$, Figure 5.9D). MLC phosphorylation in W-7 pre-treated platelets in response to 1U/ml of thrombin, 300µM of A23187, 300µM of Cq, or 30µM of Py were 0.06±0.02 AU, 0.08±0.01 AU, 0.40±0.08 and 0.37±0.08, respectively, whereas the level of phosphorylation induced by the vehicle was 0.07±0.02 (Figure 5.9D). No significant differences were found between the level of phosphorylation between the vehicle and thrombin and A23187 in the presence of W-7, but Cq and Py induced significantly higher levels of MLC phosphorylation than the vehicle ($p<0.05$, Figure 5.9D). These findings correlate with the aggregation data (Figures 5.6-5.8) and provide further evidence to suggest that Zn^{2+} mediated signalling can induce platelet shape change in a manner independent of Ca^{2+}/Calmodulin.

Y-27632 pre-treatment reduced MLC phosphorylation in response to the ionophores. MLC phosphorylation in Y-27632 pre-treated platelets, in response to 1U/ml of thrombin, A23187 (300µM), Cq (300µM), or of Py (30µM) were 0.21±0.03 AU, 0.22±0.02 AU, 0.10±0.01 and 0.10±0.01, respectively, whereas the level of phosphorylation induced by the vehicle was 0.10±0.03 (Figure 5.9E). Thrombin and A23187 ($p<0.01$) but not Cq or Py–mediated phosphorylation differed from the vehicle ($p<0.05$, ns, Figure 5.9E). Thrombin or A23187 treatment also resulted in lower levels of MLC phosphorylation in Y-27632-treated platelets compared to untreated platelets (MLC phosphorylation induced by thrombin or A23187 on untreated platelets was 0.52±0.13 AU and 0.74±0.06 AU, respectively, $p<0.05$,

Figure 5.9A, E). This suggests that p160 ROCK enables higher levels of Ca^{2+} induced MLC phosphorylation, possibly indicating synergy between Ca^{2+} dependent and independent pathways.

Phosphorylation of VASP in response to ionophores was investigated to determine whether elevated $[Zn^{2+}]_i$ has a role in PKA or PKG signalling, as VASP is a substrate of these kinases. Furthermore, VASP plays a key role in cytoskeletal rearrangement in platelets, although its role yet to be fully elucidated (section 1.2.6, Chapter 1). This was of considerable interest as recent work has demonstrated an inhibitory role for cAMP signalling in ROCK activity, which in turn would lead to continued MLC-P (myosin light chain phosphatase) activity and inhibition of MLC phosphorylation (Aburima et al., 2017, 2013). This would inhibit platelet shape change.

Stimulation with the ionophores had no effect on phosphorylation levels of VASP compared to the vehicle control (Figure 5.9F). PGE_1 was employed as a positive mediator of VASP phosphorylation. PGE_1 activates the cAMP signalling pathway, which enables PKA to phosphorylate VASP (Beck et al., 2014). PGE_1 induced a significant increase in VASP phosphorylation relative to the ionophores and the vehicle (Figure 5.9F). The level of VASP phosphorylation induced by PGE_1 (1U/mL), A23187 (300µM), Cq (300µM) or Py (30µM) was 1.6±0.1 AU, 0.4±0.1 AU, 0.5±0.4 AU and 0.5±0.1 AU, whereas the level of VASP phosphorylation induced by the vehicle was 0.5±0.1 AU (Figure 5.9F). Only PGE_1 induced a significantly higher level of VASP phosphorylation compared to the vehicle treatment ($p<0.05$, Figure 5.9F). TPEN was used to correlate phosphorylation events with Zn^{2+} increases further. TPEN pre-treatment did not affect the levels of phosphorylation induced by PGE1 or the ionophores (relative to the vehicle treatment,), as the level of VASP phosphorylation in TPEN-treated platelets in response to PGE_1 (1U/mL), A23187 (300µM), Cq (300µM), Py (30µM) or the vehicle control were 1.3±0.1, 0.26±0.04, 0.22±0.03, 0.32±0.04 and 0.25±0.03, respectively ($p>0.05$, ns, Figure 5.9. F-G) These data indicate that $[Zn^{2+}]_i$ plays no significant role in mediating cAMP signalling (Aburima et al., 2013).

5.2.3.3 Chelation of intracellular Zn^{2+} abrogates platelet shape change and spreading

The data described above demonstrate that increases in $[Zn^{2+}]_i$ result in platelet shape change independently of Ca^{2+}/Calmodulin suggesting a potential mechanism by which Ca^{2+} -independent signalling can result in MLC phosphorylation. Further experiments were performed to explore the importance of $[Zn^{2+}]_i$ on platelet shape change. Previous work has demonstrated that morphological changes in platelets can be observed microscopically during adhesion to onto fibrinogen-coated

coverslips (Aslan et al., 2012; Li et al., 2010). A similar approach (Section 2.11, Chapter 2) was used here to investigate the influence of Zn^{2+} on platelet shape change.

Platelets rapidly adhered and spread on fibrinogen-coated coverslips (100µM, Figure 5.10) which evoke outside-in signalling (Figure 1.2.5, Chapter 1). The influence of $[Zn^{2+}]_i$ on cytoskeletal changes was investigated by pre-treating platelets with TPEN (50µM). TPEN -treated platelets were able to adhere to fibrinogen, but did not spread, as evidenced by an absence of visible lamellipodia or filopodia (Figure 5.10A). Mean platelet surface coverage for TPEN treated platelets after 2, 5 and 10mins were significantly lower than for untreated platelets. After 2, 5 and 10mins the mean surface area coverage for untreated platelets was reduced from 13.4±0.9µm^2 to 9.8±0.6µm^2, 18.9±1.9µm^2 to 10.1±0.6µm^2 and 22.7±1.6µm^2 to 12.8±1.5µm^2 upon TPEN (50µM) pre-treatment respectively ($p<0.001$, Figure 5.10B). This further demonstrates that $[Zn^{2+}]_i$ is required for cytoskeletal rearrangements in platelets.

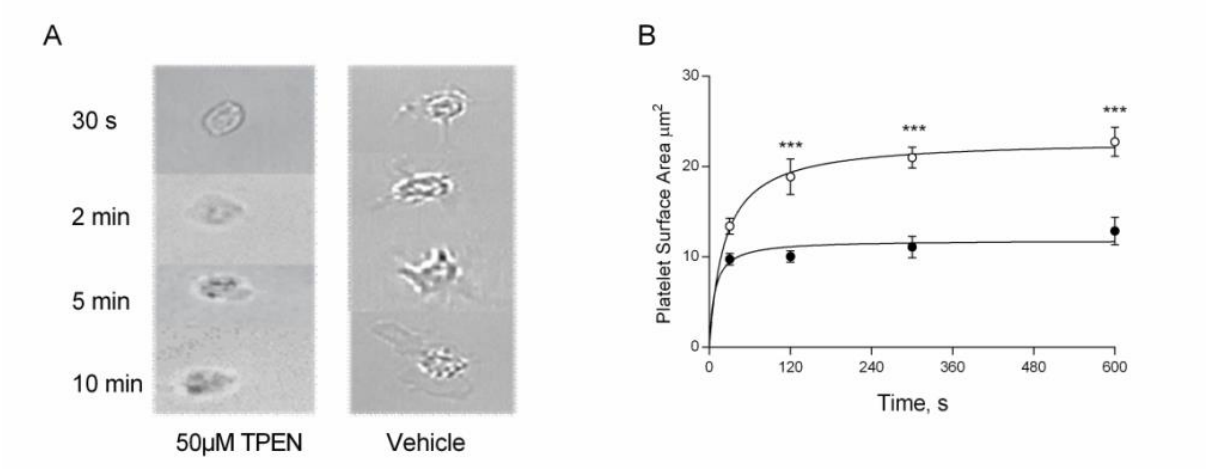

Figure 5.10. Intracellular Zn^{2+} is required for platelet spreading on fibrinogen. Washed platelet suspensions were incubated on fibrinogen-coated coverslips following pre-treatment with 50µM TPEN or vehicle control (DMSO). A) Representative images of platelet spreading. B) Quantification of the surface coverage by adherent platelets. Pre-treatment with 50µM of TPEN significantly inhibited platelet spreading. ○ Vehicle, ● 50µM TPEN. Data are mean±standard error of mean (SEM) from 4 independent experiments. Significance is denoted as *** ($p<0.001$), ** ($p<0.01$) or * ($p<0.05$).

5.2.3.4 Intracellular Zn^{2+} is required for cytoskeletal changes in nucleated cells

The data discussed above outlines the importance of $[Zn^{2+}]_i$ in platelet shape change. The data in this section explores the wider application of $[Zn^{2+}]_i$ by investigating whether its role in cytoskeletal rearrangement is platelet-specific or is also viable in other cells types. Experiments were conducted using a model cell line, Mouse Embryonic Fibroblasts (MEF) (Chen et al., 2016; J. Wang et al., 2014). These were selected because they readily undergo spreading, making them a suitable candidate for investigating the role of intracellular Zn^{2+} on cytoskeletal rearrangement (section 2.12, Chapter 2).

Attachment and spreading of MEF cells on glass coverslips following pre-treatment with TPEN was imaged using a fluorescent cell imager (section 2.12, Chapter 2). After 2 hours attachment of untreated MEFs to the glass substrate, subsequent cytoskeletal changes were apparent (subjective observations, Figure 5.11). Cells appeared firmly adhered and were beginning to increase in surface area. After 6 hours of incubation, the cells had spread more extensively. Upon treatment with the vehicle (DMSO) after 2 hours cellular attachment and spreading was apparent. Slight increases in cell spreading were observed after 6 hours of DMSO treatment. TPEN pre-treatment resulted in minimal cell attachment after 2 hours, with no indication of cell spreading. No further changes were seen after 6 hours.

The data described here correlates a role for Zn^{2+} in both platelets spreading, and in nucleated cell spreading. This may be indicative of a wider role for Zn^{2+} in cytoskeletal behaviour.

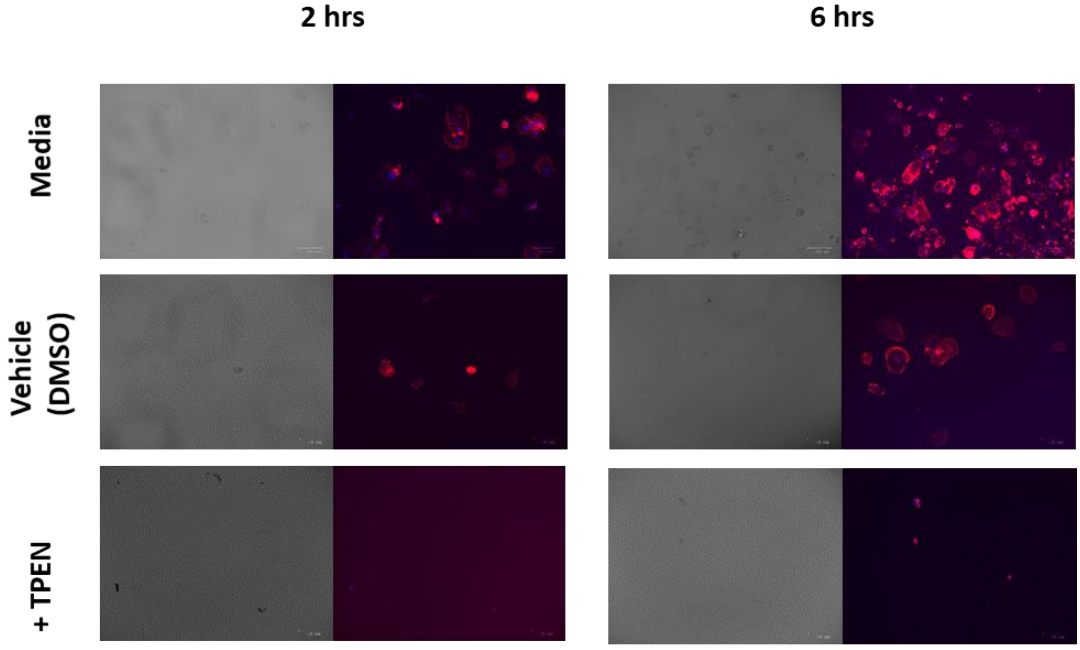

Figure 5.11. Intracellular Zn^{2+} mediates adhesion and cytoskeletal changes in mouse embryonic fibroblast (MEF) cells. MEF cells were pre-treated with 50µM TPEN, vehicle control (DMSO), or no pre-treatment prior to incubation on glass coverslips for 6 hours. Cells were stained with Phalloidin-iFluor 594 and DAPI and were imaged by Zoe imager. Representative images (n=3) of Phalloidin- iFlour 594 Conjugate and DAPI stained MEF cells undergoing adhesion and spreading are shown.

5.2.4 Intracellular Zn^{2+} mediates platelet activation

The data presented thus far in this chapter demonstrates that elevating $[Zn^{2+}]_i$ induces platelet activatory processes such as aggregation and shape change in a manner which may be independent of Ca^{2+}-signalling mechanisms. To better understand the extent to which changes in $[Zn^{2+}]_i$ regulate platelet activation, the influence of ionophore treatment on conventional markers of platelet activation (including granule release and integrin activation) was investigated.

In order to correlate Zn^{2+} increases with platelet activation, and also to verify data obtained from light transmission aggregometry, experiments were performed to assess the influence of increasing $[Zn^{2+}]_i$ on PAC-1 binding to platelets using flow cytometry. Thrombin was employed as a comparison to see the levels of PAC-1 binding upon physiological stimulation. Zn^{2+} ionophore-induced elevation of $[Zn^{2+}]_i$ increased PAC-1 binding (Figure 5.12A), supportive of a role for Zn^{2+} in mediating $\alpha_{IIb}\beta_3$ activity. The level of PAC-1 binding after 60mins of stimulation with Cq (300µM), Py (300µM,), A23187 (300µM) or thrombin (1U/mL) were 47.4±4.2%, 28.6±5.4%, 64.5±5.8%, 69.4±5.8%, respectively. These were significantly higher than that induced by the vehicle control (3.9±1.5%, $p<0.0001$, 5.12A). Interestingly, Py evoked increased levels of PAC-1 binding but not full aggregation (Figure 5.1-5.2 and 5.4). This is difficult to reconcile as increased PAC-1 bindings is associated with aggregation. It is possible that the level of Py mediated-$\alpha_{IIb}\beta_3$ activation is not sufficient to fully activate $\alpha_{IIb}\beta_3$ mediated aggregation as a result of low increases in $[Zn^{2+}]_i$ This would be consistent with data showing lower increases in $[Zn^{2+}]_i$ compared to Cq (Chapter 4). Furthermore, PAC-1 binding experiments were quantified after 60mins of stimulation as A233187 and thrombin (positive controls in these experiments) evoked optimal PAC-1 binding after 60mins. Thus this was the chosen time for analysis in this work. This was also the case with the other activation makers CD62P and CD63 as discussed below.

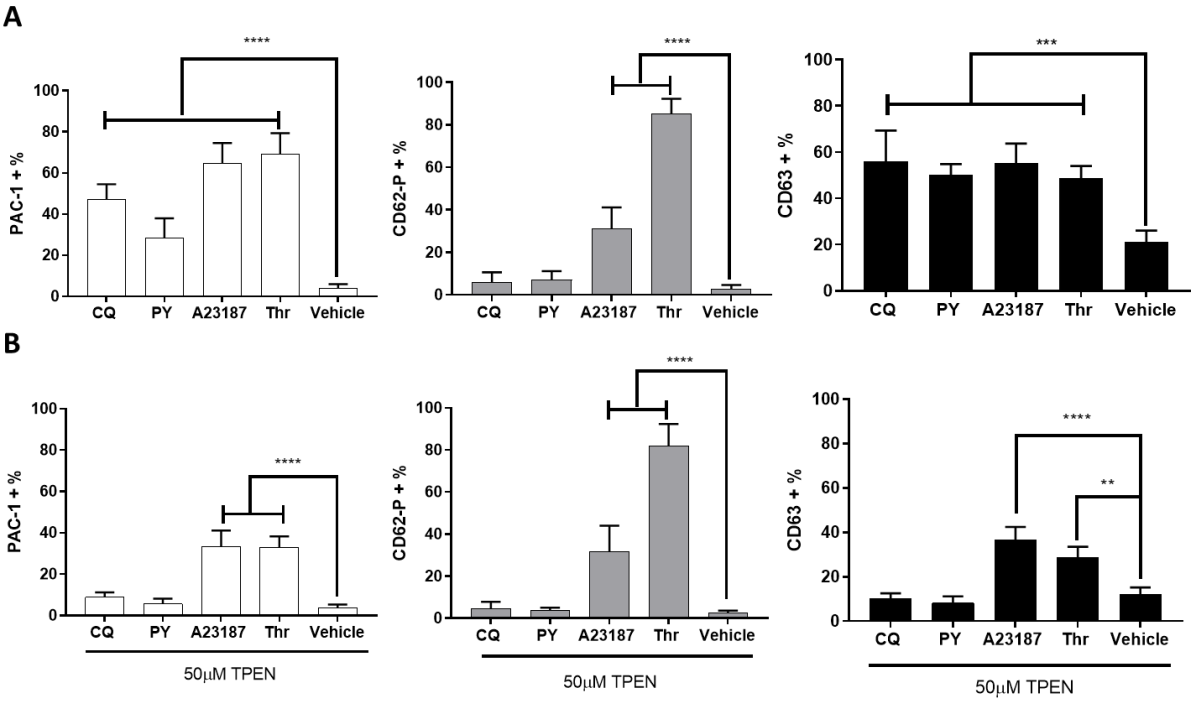

Figure 5.12. Elevated intra-platelet Zn^{2+} increases platelet activation markers. (A) Washed platelet suspensions were stimulated by thrombin (Thr, 1U/mL), Clioquinol (Cq, 300μM), Pyrithione (Py, 300μM) or A23187 (300μM) and changes of PAC-1 (white), CD62P (grey), and CD63 (black) binding were recorded after 60 mins. **(B)** Washed platelet suspensions were pre-treated with TPEN (50μM) prior to stimulation with thrombin (Thr, 1U/mL), Clioquinol (Cq, 300μM), Pyrithione (Py, 300μM) or A23187 (300μM) and changes of PAC-1 (□), CD62P (■), and CD63 (■) binding were obtained after 60 mins. Data are means±SEM, of at least 5 independent experiments. Significance is denoted as **** (p<0.0001), *** (p<0.001), ** (p<0.01) or * (p<0.05).

The $[Zn^{2+}]_i$ chelator TPEN was employed to assess the validity of the Zn^{2+} induced PAC-1 binding. Pre-treatment of platelet suspensions with TPEN reduced the levels of ionophore- or thrombin-induced PAC-1 binding (Figure 5.12B). The percentage of PAC-1 binding of platelets following stimulation with Cq (300μM), Py (300μM,), A23187 (300μM) and thrombin (1U/mL) were significantly reduced from 47.4±4.2% to 8.9±1.3%, 28.6±5.4% to 5.6±1.50%, , 64.5±5.8% to 33.3±4.5% and 69.4±5.8% to 33.0 ±3.10%, respectively in TPEN pre-treated platelets (50μM, p<0.05, Figure 5.12A-B). Cq- or Py- induced PAC-1 binding in TPEN pre-treated platelets (8.9±1.3% and 5.6 ±1.5%, respectively) was not significantly different to the vehicle control (3.80±0.90%, p>0.05, Figure 5.13B). These data further support a role for $[Zn^{2+}]_i$ in the regulation of the activation of $\alpha_{IIb}\beta_3$.

Conversely, A23187 or thrombin-induced PAC-1 binding in TPEN pre-treated platelets (33.3±4.5% and 33.0±3.1, respectively) were still significantly higher the vehicle control (3.80±0.90%) after 60 mins (p<0.001, Figure 5.12B). This indicates that A23187 or thrombin-induced PAC-1 binding is only partially influenced by $[Zn^{2+}]_i$. This was interesting, as TPEN did not influence A23187 induced

aggregation, as shown earlier (Figure 5.2C, F). However, A23187 has shown to be non-specific and is also able to coordinate Zn^{2+} (Chapter 4). Therefore A23187-mediated activity may also be attributable to Zn^{2+}. This finding correlates with Py induced PAC-1 binding, which did not display aggregation but did evoke significant increases in PAC-1 binding. Thus Zn^{2+} may play a potentiating role in inducing aggregation by mediating the upregulation of $\alpha_{IIb}\beta_3$ at low concentrations.

Investigation of the influence of increased intracellular Zn^{2+} on granule release

Experiments were performed to assess the role of $[Zn^{2+}]_i$ in other activatory processes. Granule secretion releases bioactive molecules into the vicinity of a growing thrombus, mediating activation in a para-and autocrine manner (Corinaldesi, 2011; Joseph et al., 1998; Stalker et al., 2012; Wauters et al., 2015; Yacoub et al., 2006). Assessment of the level of CD62P and CD63 on the platelet surfaces quantifies the degree to which α and dense granule release respectively are released.

Treatment of washed platelet suspensions with Cq or Py did not evoke CD62P externalisation as measured using flow cytometry (Figure 5.12A). The percentage of CD62P positive platelets after 60 minutes of stimulation with Cq (300µM) or Py(300µM) was 5.5 ±2.8% and 7.1±2.3%, respectively, compared to that induced by the vehicle control (2.9±1.3%, $p>0.05$, ns, Figure 5.12A)

Treatment with A23187 or thrombin both resulted in significant increases in CD62P and CD63 externalisation. The percentage of CD62P positive platelets after 60 minutes following A23187 (300µM) or thrombin (1U/mL) treatment was 31.20±5.72%, 85.11±4.20%, respectively, (both significantly higher than the vehicle control, 2.90±1.03%, $p<0.0001$, Figure 5.12A).

TPEN was used to further assess the influence of Zn^{2+} on granule secretion. Pre-treatment with TPEN had no significant influence on the CD62P externalisation in response to the ionophores or thrombin (Figure 5.12B). The percentage of CD62P positive TPEN-pre-treated platelets followed by 60 minutes of stimulation with Cq (300µM), Py (300µM), A23187 (300µM), thrombin (1U/mL) or vehicle were 4.7±1.8%, 3.7±0.8%, 31.9 ±7.0%, 81.9±6.1% and 2.8±0.5%, respectively($p>0.05$, ns, Figure 5.12). This data indicate that increases in $[Zn^{2+}]_i$ have no influence on α granule release.

Conversely, elevation of $[Zn^{2+}]_i$ significantly increased CD63 externalisation. All ionophores and thrombin-induced significant increases in CD63 externalisation in comparison to that induced by the vehicle (Figure 5.12A). The percentage of CD63 positive platelets after 60 minutes of stimulation with Cq (300µM), Py (300µM,), A23187 (300µM) or thrombin (1U/mL) were 56.0±7.8%, 50.2±2.7%, 55.0±5.0% and 48.9±3.1%, respectively. These were significantly higher than that induced by the vehicle control 21.0±2.9%, $p<0.001$, Figure 5.12A).

TPEN was then employed to confirm the role of Zn^{2+} in this process. Pre-treatment with TPEN reduced the percentage of CD63 externalisation induced by the ionophores and thrombin. The background (vehicle) CD63 expression was also reduced in following vehicle treatment although this was not found to be significant ($p>0.05$, Figure 5.12B). The percentage of CD63 positive platelets after 60 mins of stimulation with Cq (300µM), Py (300µM), A23187 (300µM) or thrombin (1U/mL) were significantly reduced from 56.0±7.8% to 10.1±1.4%, 50.2±2.7% to 8.2±1.7%, 55.0±5.0% to 36.9±7.0% and 48.90±3.1% to, 28.2±6.1%, respectively upon 50µM TPEN pre-treatment ($p<0.05$, Figure 5.12A-B). However, A23187 and thrombin-induced CD63 externalisation in TPEN pre-treated platelets (33.3±4.5% and 33.0±3.1, respectively) were still significantly higher than CD63 externalisation induced by the vehicle control after 60 mins which were 12.1±1.8% ($p<0.01$, Figure 5.12B). This indicates that whilst A23187 and thrombin-induced CD63 externalisation is not fully dependent on $[Zn^{2+}]_i$, Zn^{2+} is a requirement for optimal dense granule secretion. Whereas Cq or Py induced CD63 externalisation in TPEN pre-treated platelets, (10.12±1.42% and 8.20±1.74%, respectively) was not significantly different from the vehicle control (12.1±1.8%, $p>0.05$, Figure 5.12B). This data suggest that $[Zn^{2+}]_i$ regulates the activity of dense granule release and supports a role for $[Zn^{2+}]_i$ in activation-dependent platelet behaviour.

5.2.5 Agonist-induced platelet activation is mediated by intracellular Zn^{2+}

The data discussed in the previous section demonstrate that increased $[Zn^{2+}]_i$ results in dense granule release, supporting the role of Zn^{2+} as a secondary messenger. Additionally, thrombin-induced PAC-1 binding and dense granule release are inhibited upon chelation of $[Zn^{2+}]_i$ via further indicating the importance Zn^{2+} in agonist-induced platelet activation. As thrombin-mediated platelet activation is shown to be influenced by Zn^{2+}, further experiments were designed to test whether activation by other conventional agonists was also sensitive to Zn^{2+} levels. Agonists targeting GpVI or TP (CRP-XL, U46619) were selected to further assess a physiological role for Zn^{2+} in platelet activation (Figure 5.13), as these agonists were found to evoke $[Zn^{2+}]_i$ elevation (Chapter 3).

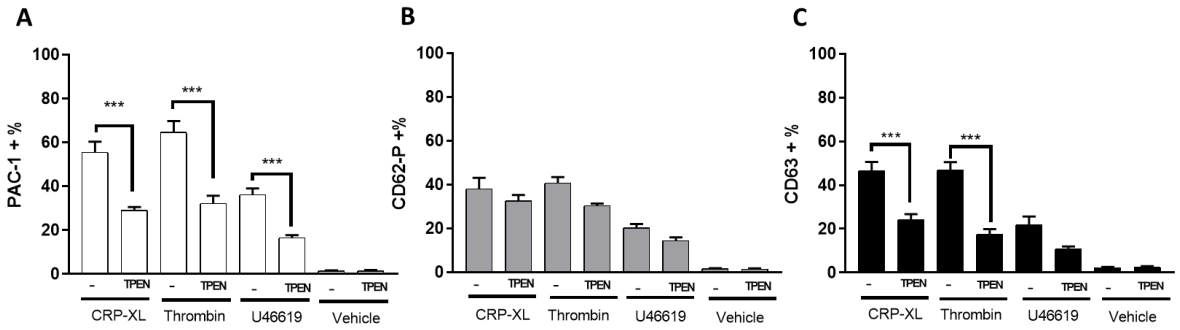

Figure 5.13. Agonist-induced platelet activation is mediated by intracellular Zn^{2+}. Washed platelet suspensions were stimulated by CRP-XL (1µg/ml), Thrombin (1U/mL) or U46619 (10µM) with or without TPEN (50µM) pre-treatment. Changes of PAC-1 (A), CD62P (B), and CD63 (C) binding were obtained after 60 mins. Data are mean±standard error of mean (SEM) from 5 independent experiments. Significance is denoted as *** (p<0.001), ** (p<0.01) or * (p<0.05).

Pre-treatment with TPEN (50µM) significantly reduced the percentage of PAC-1 binding induced by all agonists tested. Upon TPEN treatment, the percentage of PAC-1 binding platelets induced by CRP-XL (1µg/ml), thrombin (1U/ml) or U46619 (10µM) was reduced from 55.4±5.0% to 29.0±1.5%, 64.6±5.2% to 32.1±3.4% and 36.3±2.8% to 16.5±1.20%, respectively (p<0.001, Figure 5.13). This indicates that $[Zn^{2+}]_i$ levels are important during activation initiated by heterogeneous signalling pathways. These data correlate with the previous experiments (Figure 5.12), which illustrated that $[Zn^{2+}]_i$ evokes PAC-1 binding.

Pre-treatment with TPEN did not significantly affect agonist-evoked CD62P externalisation (Figure 5.13). In TPEN pre-treated platelets, the percentage of CD62P externalising platelets following CRP-XL (1µg/ml), thrombin (1U/ml) or U46619 (10µM) treatment did not differ significantly from untreated platelets. Untreated and treated platelets had CD62P levels respectively of 38.0±5.1% and 32.54±2.80% for CRP-XL, 40.70±2.73% and 30.40±1.02% for U46619, and 20.43±1.84% and 14.43±1.52%, for thrombin (p>0.05, ns, Figure 5.13). These data support previous results showing that alpha granule release was not mediated by Zn^{2+} (Figure 5.12)

Pre-treatment with TPEN significantly reduced CD63 externalisation induced by CRP-XL or thrombin (Figure 5.13). Upon TPEN treatment, CD63 externalisation induced by CRP-XL (1µg/ml) or thrombin (1U/ml) was reduced from 46.6±4.0% to 24.2±2.6%, 40.8±3.8% to 17.6±2.3%, respectively, (p<0.001, Figure 5.13), further supporting a role for $[Zn^{2+}]_i$ as a mediator of dense granule release.

A significant reduction in CD63 binding was not observed following U46619 stimulation of TPEN-pre-treated platelets, suggesting TxA_2-mediated dense granule release may not be influenced by $[Zn^{2+}]_i$. This requires further investigation to determine as to why $[Zn^{2+}]_i$ had no significant influence on TxA_2 induced platelet dense granule release. U46119 induces $[Zn^{2+}]_i$ elevation (chapter 3) suggesting that $[Zn^{2+}]_i$ may play a role in TxA_2 signalling. However, the increase in $[Zn^{2+}]_i$ evoked by U46619 was much lower to that induced by CRP-XL. Thus, the greater elevation of $[Zn^{2+}]_i$ induced by CRP-XL may be responsible for mediating the higher level of CD63 externalisation. Therefore, it can be suggested that U46619 does not evoke a high enough increase in $[Zn^{2+}]_i$ to mediate a CD63 externalisation response that is influenced by $[Zn^{2+}]_i$. This may explain why the chelation of $[Zn^{2+}]_i$ had no influence on U46619-induced CD63 externalisation.

The data from this section is supportive of a role for $[Zn^{2+}]_i$ in agonist-induced activation. Upregulation of $\alpha_{IIb}\beta_3$ activity and dense granule release upon agonist stimulation were reduced upon chelation of $[Zn^{2+}]_I$, indicating a role for $[Zn^{2+}]_i$ in these processes (Figure 5.13) This data provides novel findings outlining the importance of $[Zn^{2+}]_i$ in physiological platelet activation, which further provides evidence to confirm Zn^{2+} as a secondary messenger in platelets.

5.2.6 Intracellular Zn^{2+} mediates phosphatidylserine exposure in platelets

Further experiments were performed to investigate the influence of $[Zn^{2+}]_i$ on phosphatidylserine (PS) externalisation in platelets. Both extracellular Zn^{2+} and agonist-induced changes in $[Zn^{2+}]_i$ have been linked to apoptosis and related responses in nucleated cells (Eron et al., 2018; Hamatake et al., 2000; Iitaka et al., 2001; Treves et al., 1994). PS exposure serves as an activation marker in platelets, being induced upon $[Ca^{2+}]_i$ elevation (Suzuki et al., 2013; Zhao et al., 2017). However, the role of Zn^{2+} in PS exposure during platelet activation has yet to be studied. To investigate the influence of $[Zn^{2+}]_i$ on PS exposure, platelets were treated with ionophores, and annexin-V binding was quantified in real time using flow cytometry (section 2.8, Chapter 2).

Elevation of $[Zn^{2+}]_i$ via Cq (300µM) or Py (300µM) stimulation, or elevation of $[Ca^{2+}]_i$ using A23187 resulted in significant increases in annexin-V binding. After 30mins of stimulation, Annexin-V binding was modestly (although significantly) increased upon Zn^{2+} ionophore treatment, whilst A23187 treatment resulted in a large increase in Annexin-V binding. The percentage of Annexin-V binding after 30 minutes of stimulation with Cq (300µM), Py (300µM) or A23187 (300µM) were 13.6±0.9%, 24.1±2.9%, 77.6±3.40% respectively. Binding was significantly higher than that induced by

the vehicle (3.7±0.7%, p<0.05, Figure 5.14). After more extended time periods of stimulation annexin-V binding following treatment with Zn^{2+} and Ca^{2+} ionophores reached similar plateau levels. The percentage of Annexin-V binding after 3 hours of stimulation with Cq (300µM), Py (300µM) or A23187 (300µM) and the vehicle were 90.9±0.9%, 88.7±2.4% and 88.6±2.7%, respectively. These were significantly higher than the vehicle control (7.3±2.0%, p<0.05, Figure 5.14).

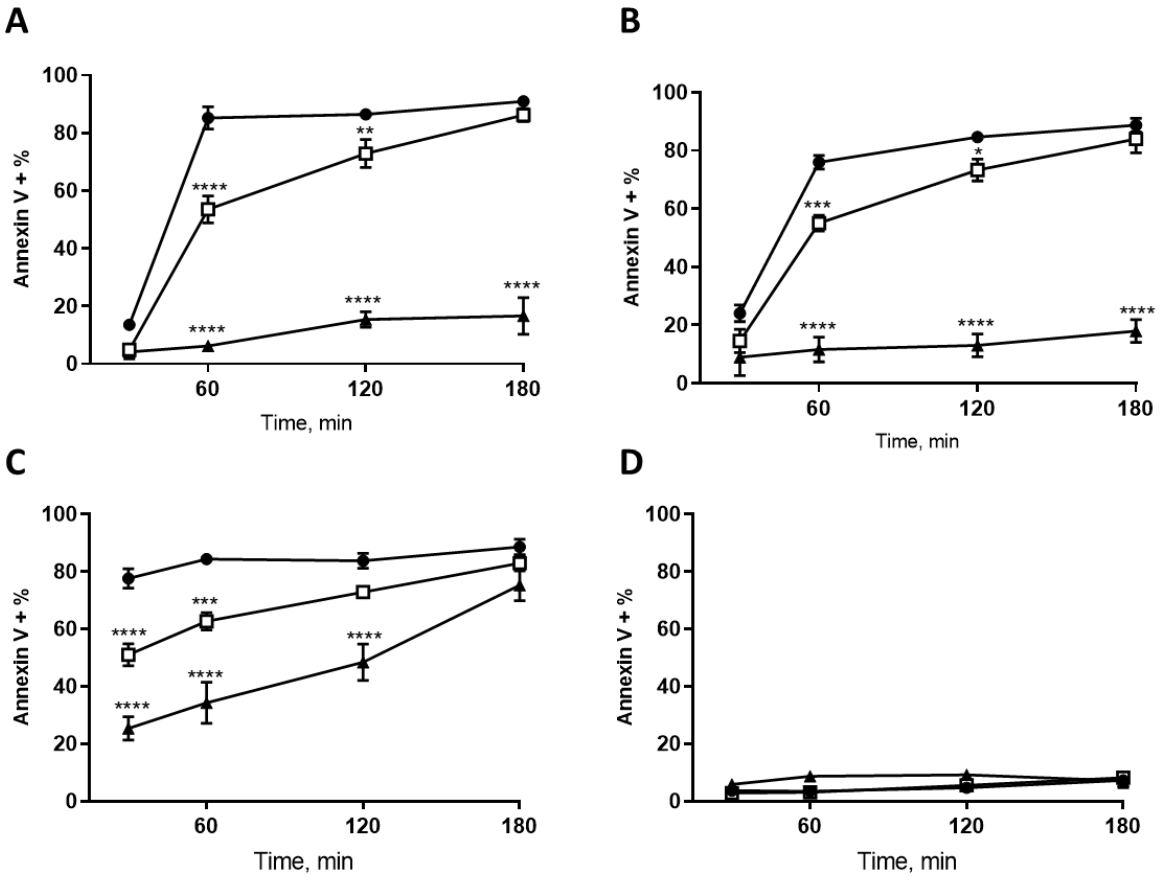

Figure 5.14. Elevation of intracellular Zn^{2+} in platelets using Zn^{2+} ionophores increases PS externalisation. Washed platelet suspensions were treated with Ca^{2+} or Zn^{2+} ionophores prior to analysis of annexin-V binding by flow cytometry. Changes in the percentage of platelets binding to annexin-V were recorded over a 3-hour time period. Platelets were stimulated by Clioquinol (A, 300µM), Pyrithione (B, 300µM), A23187 (C, 300µM), Vehicle (D, DMSO), either without pre-treatment (●), following pre-treatment with the caspase inhibitor Z-VAD (20µM) (□), or following pre-treatment with the Zn^{2+} chelator, TPEN (50 µM) (▲). Data are means±SEM, of at 5 independent experiments. Significance is denoted as **** (p<0.0001), *** (p<0.001), ** (p<0.01) or * (p<0.05).

Pre-treatment of platelet suspensions with TPEN was carried out to confirm the role of Zn^{2+} ionophore-induced PS exposure. TPEN significantly reduced annexin-V binding following Zn^{2+} ionophore treatment throughout the experiment. Annexin-V binding following by Cq (300µM) or Py (300µM) treatment was reduced from 90.93±0.86% and 88.72±2.40% to 16.61±6.35% and 17.94±3.94%, respectively upon TPEN (50µM) pre-treatment after 3 hours ($p<0.0001$, Figure 5.14A-B). These data confirm a role for Zn^{2+} in regulating PS exposure. TPEN treatment also significantly reduced annexin-V binding induced by A23187 throughout the whole experiment. After 30 mins, 1 hour, 2 hours and 3 hours of stimulation A23187 treatment was reduced from 77.6±3.4% to 25.4±4.0%, 84.4±1.7% to 35.3±7.2%, 83.8±2.6% to 48.4±6.4% and 88.6±2.6% to 75.2±5.5%, respectively following TPEN pre-treatment ($p<0.05$, Figure 5.14C). These data confirm that Zn^{2+} is important in cellular processes leading to PS exposure in platelets.

Caspases are involved in mediating PS exposure, usually upon apoptosis. Previous work has shown that caspases are present in platelets, and inhibition of caspases with the caspase inhibitor Z-VAD inhibits ADP and A23187 induced PS exposure (Cohen, 1999; Cohen et al., 2004a). Here Z-VAD was employed to examine the mechanisms by which ionophore treatment results in PS exposure, and also to assess the biological validity of the observed responses (Cohen et al., 2004b) (Cohen et al., 2004), Previous studies showed that 20µM of ZVAD is sufficient to inhibit caspase activity in washed platelet suspensions(Cohen, 1999; Cohen et al., 2004a).

Pre-treatment of washed platelet suspensions with Z-VAD resulted in a significant reduction in annexin-V binding after 1 to 2 hours of stimulation with Cq (300µM). The percentage of platelets binding to annexin-V was reduced from 85.2±3.8% to 53.6±4.7% and 86.4±1.8% to 72.9±4.8% respectively upon Z-VAD (20µM) pre-treatment ($p<0.01$, Figure 5.14A). Pre-treatment with 20µM of Z-VAD also resulted in significant reduction in annexin-V binding after 1 to 2hours of stimulation with Py (300µM). Here, Annexin-V positive platelets were reduced from 75.9±2.3% to 55.1±2.7% and 84.6±1.9% to 73.3±3.8% respectively upon Z-VAD (20µM) pre-treatment ($p<0.05$, Figure 5.14B). Thus, indicating that caspase inhibition does not fully inhibit but may partially inhibit Zn^{2+} ionophore-induced PS exposure. Similarly, A23187 induced annexin-V binding was reduced following Z-VAD pre-treatment, but only during the first hour. As the percentage of annexin-V–positive platelets was reduced from 77.6±3.4% to 51.0±3.9% after 30 mins and 84.4±1.7% to 62.70±3.10% after 1 hour upon Z-VAD pre-treatment ($p<0.01$, Figure 5.13C). Z-VAD did not inhibit the annexin-V binding after 1 hour,

The experiments described in this section demonstrate that [Zn^{2+}] induces PS exposure in platelets in a manner that may be partially mediated by caspases (Figure 5.14A-B). The data also

suggest that Ca^{2+}-mediated PS exposure is dependent on the presence of $[Zn^{2+}]_I$ (Figure 5.14C). These experiments represent the first example of work to investigate the signalling pathways that operate during Zn^{2+}-induced PS exposure in platelets. The data provided here are consistent with a role for Zn^{2+} as a secondary messenger in platelets

5.2.7 Agonist-induced phosphatidylserine exposure is mediated by intracellular Zn^{2+}

Further experiments were performed to examine the influence of $[Zn^{2+}]_I$ on agonist-evoked PS exposure. In these experiments, changes were observed in annexin-V binding to TPEN pre-treated platelets following stimulation with conventional platelet agonists (CRP-XL, U46619 and thrombin, Figure 5.15).

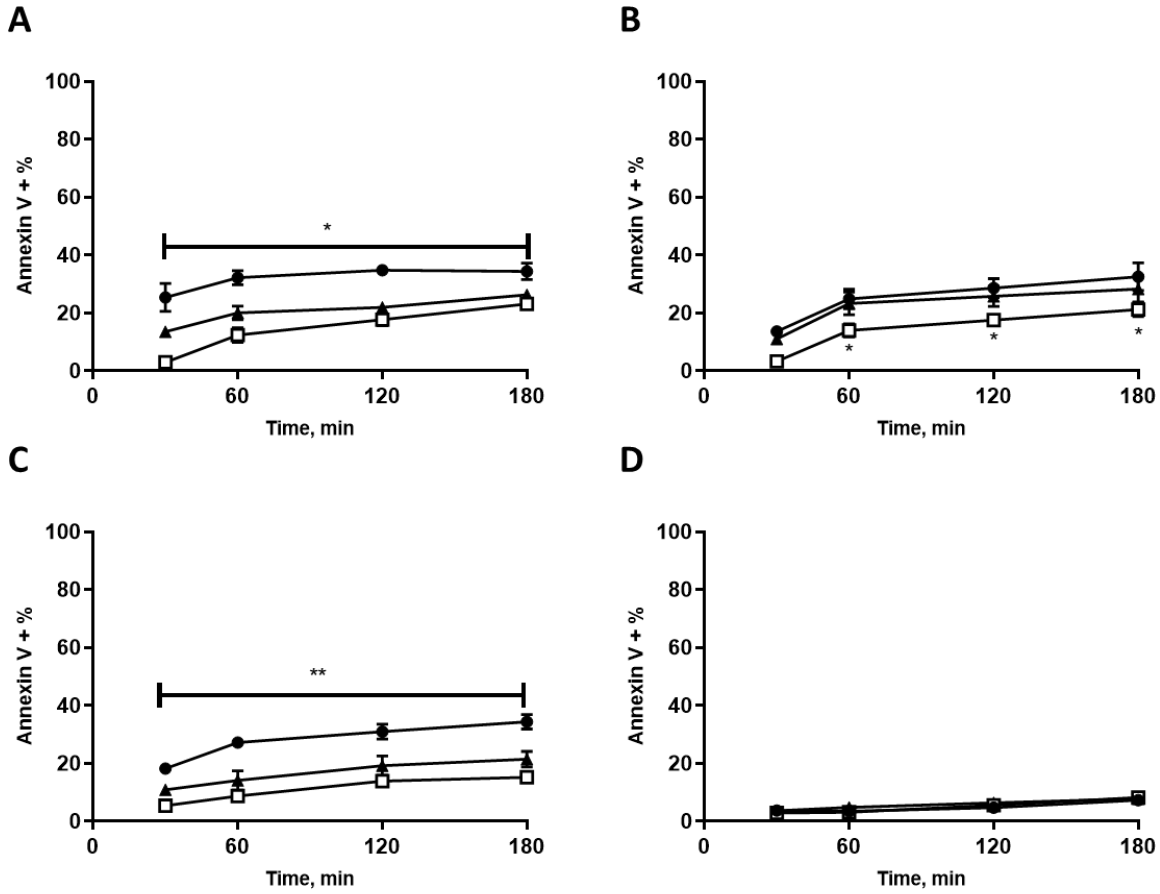

Figure 5.15. Platelet PS exposure occurs following agonist-evoked activation is sensitive to Zn^{2+} chelation. Washed platelet suspensions were treated with conventional agonists prior to analysis of annexin-V binding by flow cytometry. Changes in the percentage of platelets binding to annexin-V were recorded. Platelets were stimulated by (A) CRP-XL (1µg/ml), (B) thrombin (1U/ml), (C) U46619 (10µM), (D) vehicle (DMSO) following pre-treatment with vehicle (●), with the caspase

inhibitor Z-VAD (20μM) present (□), or with the Zn^{2+} chelator, TPEN (50 μM) (▲). Data are mean±standard error of mean (SEM) from 6 independent experiments. Significance is denoted as **** (p<0.0001), *** (p<0.001), ** (p<0.01) or * (p<0.05).

Pre-treatment of washed platelet suspensions with TPEN reduced the level of PS exposure induced by CRP-XL, and U46619, but did not influence thrombin-evoked PS exposure (Figure 5.15), Upon TPEN (50μM) pre-treatment, the percentage of annexin-V positive platelets following CRP-XL (1μg/ml) or U46619 (10μM) treatment was reduced at every time point measured. Annexin-V positive TPEN-treated platelets following treatment with CRP-XL (1μg/mL) after 30 minutes, 1 hour, 2 hours and 3 hours was reduced from 25.4±4.8% to 13.6±1.5%, 32.2±2.50% to 20.1±2.4%, 34.8±1.5% to 21.9±2.0% and 34.4±2.90% to 26.3±1.0%, respectively (p<0.05, Figure 5.15A). TPEN pre-treatment reduced U46619-mediated annexin-V binding after 1, 2 and 3 hours from 18.2±0.9% to 10.9±1.7%, 27.2±1.6% to 14.1±3.5%, 30.9±2.5% to 19.2±3.32% and 34.40±2.53% to 21.43±2.70%, respectively (p<0.05, Figure 5.15C).

The percentage of annexin-V positive platelets did not significantly differ following thrombin treatment. After 30 minutes, 1 hour, 2 hours and 3 hours in the absence and presence of TPEN (50μM) annexin-V binding was 13.60±1.53% and 11.0±1.2%, 24.9±3.7% and 23.3±3.4%, 28.7±3.3% and 25.8±3.6% and 32.5±4.8% and 28.3±4.6% respectively for untreated and TPEN-treated platelets (p>0.05, Figure 5.15B). These data indicate that $[Zn^{2+}]_i$ may play a significant role in mediating PS exposure in response to CRP-XL or U46619, but not thrombin, providing further support for a role Zn^{2+} following GpVI and TP signalling, but not via PARs.

Z-VAD was again employed to assess the biological validity of the observed response as previously demonstrated, (Cohen et al., 2004b) (Cohen et al., 2004). Z-VAD significantly reduced the Annexin-V binding in response to CRP-XL, U46619 and thrombin. Significant reductions in CRP-XL-mediated annexin-V binding with Z-VAD pre-treatment were evident at every time point tested. Annexin-V binding percentages were reduced from 25.4±4.8% to 3.0±1.7%, 32.2±2.5% to 12.4±2.5%, 34.8±1.5% to 17.7±2.1% and 34.4±2.9% to 23.1±2.0% after 30 minutes, 1 hour, 2 hours and 3 hours stimulation, respectively upon Z-VAD (20μM) pre-treatment (p<0.05, Figure 5.15A). A similar effect was seen with U46619 as where annexin-V binding in the presence of Z-VAD was reduced from 18.2±0.9% to 5.4±1.2%, 27.2±1.6% to 8.70±1.62%, 30.9±2.6% to 13.9±2.0% and 34.4±2.5% to 15.2±2.0% after 30 mins, 1 hour, 2 hours and 3 hours stimulation, respectively (p<0.05, Figure 5.15C). Thrombin-induced annexin-V–binding was reduced from 13.6±1.5% to 3.3±1.1%, 24.9±3.4% to

13.9±2.3%, 28.7±3.3% to 17.5±1.1% and 32.56±4.8% to 21.2±2.4%, respectively upon Z-VAD treatment after 30 mins, 1 hour 2 hours and 3 hours of stimulation ($p<0.05$, Figure 5.15B).

These results correlate well with the data showing that $[Zn^{2+}]_i$ elevation mediates PS exposure (Figure 5.14). The experiments described in this section provide further evidence indicating the importance of $[Zn^{2+}]_i$ in mediating agonist-induced PS exposure which is a major activatory process in platelets (discussed in chapter 1). As agonist-evoked PS exposure was inhibited upon chelation of $[Zn^{2+}]_i$. Thus, the elevation of $[Zn^{2+}]_i$ may have mediatory roles in PS exposure which further strengthens the hypothesis that Zn^{2+} is a secondary messenger in platelets.

5.3 Discussion

The work described in this chapter was designed to investigate the effect of elevated $[Zn^{2+}]_i$ on platelet activity, and the importance of $[Zn^{2+}]_i$ in agonist-dependent activation. The hypothesis being tested here is that Zn^{2+} acts as a secondary messenger in platelets. A secondary messenger is defined as a molecule that is intracellularly modulated in response to extracellular stimuli and can then induce appropriate intracellular signalling events with regards to the extracellular stimuli, resulting in physiological changes in the cell. In Chapters 3 and 4 experiments demonstrated that $[Zn^{2+}]_i$ elevation occurs in platelets in response to agonist stimulation. Here, experiments were performed to investigate whether increases in $[Zn^{2+}]_i$ influenced platelet behaviour. The data described in this chapter confirms that upon elevation, $[Zn^{2+}]_i$ mediates a variety of platelet processes. These experiments are consistent with a role for Zn^{2+} as a secondary messenger in platelets.

Increases in $[Zn^{2+}]_i$ elevation were modelled using Zn^{2+} ionophores. Initial experiments were performed to investigate the effect of ionophore treatment on platelet behaviour using light transmission aggregometry. In these experiments, Zn^{2+} ionophore treatment resulted in aggregometry traces that were consistent with platelet shape change (Figure 5.1). Platelet responses to Cq and Py were heterogeneous. Cq induced sub-maximal aggregation whereas Py did not evoke an aggregatory response. The differences in responses to the two Zn^{2+} ionophores suggests differing mechanisms. Cq induced a much greater increase in $[Zn^{2+}]_i$ than Py (Chapter 4). This could explain the differences in ionophore responses, as an increased level of $[Zn^{2+}]_i$ in response to Cq correlates with an increased aggregation response. Thus, the differing responses induced by Cq and Py could be due to the different levels of $[Zn^{2+}]_i$ elevation induced by these ionophores. However, as both ionophores have approximately the same affinity for Zn^{2+}, other factors may have an effect. These ionophores may

interact with platelets in a different manner, for example as their ability to enter platelets may differ, the way in which the ionophores enter stores in platelet may also differ. However, the nature of these differences requires further investigation.

Increases in $[Zn^{2+}]_i$ mediate platelet aggregation

Cq induced aggregation may have occurred as a result of substantial increases in $[Zn^{2+}]_i$. This correlates with recent studies which demonstrated that treatment with Zn^{2+} at a millimolar range was able to gain access to the platelet cytosol to induce full platelet aggregation and activation (Watson et al., 2016). Further work from this indicated that sub-activatory micromolar concentrations of Zn^{2+} potentiate agonist-induced activation. Here, increases in $[Zn^{2+}]_i$ in response to agonist stimulation occur independently of extracellular Zn^{2+} and therefore rely on the liberation of stores. It is likely that the release of intracellular Zn^{2+} is having a similar effect to Zn^{2+} entry observed by Watson et al., (2016). In this scheme, substantial increases in $[Zn^{2+}]_i$ in response to agonist stimulation would initiate platelet aggregation, whilst low levels of Zn^{2+} release would potentiate activatory changes in platelets.

Experiments were carried out to assess the biological validity of the ionophore-induced aggregation, to address concerns that changes in light transmission were not attributable to platelet aggregometry but could be an artefact of drug treatment. These experiments utilised the $[Zn^{2+}]_i$ chelator, TPEN and the $\alpha_{IIb}\beta_3$ antagonist, GR144053 (Figure 5.2, 5.4).

TPEN abrogated Cq induced aggregatory response (Figure 5.2A), confirming that aggregation was a result of elevated $[Zn^{2+}]_i$. Furthermore, TPEN application did not influence the aggregatory response induced by the Ca^{2+} ionophore, A23187, indicating that A23187-induced aggregatory responses are not attributable to Zn^{2+}. This is an interesting observation because A23187 has been reported to act as both Ca^{2+} and Zn^{2+} ionophore (Chapter 4), so a Zn^{2+}-dependent response might have been expected. One explanation is that there is a higher concentration of Ca^{2+} in platelets, compared to Zn^{2+} (resting concentration of Ca^{2+} in platelets is approximately 100nM, whereas Zn^{2+} is much lower, although is yet to be confirmed (Oliver et al., 1999; Taylor and Pugh, 2016; Watson et al., 2016)), so A23187 might be saturated with Ca^{2+} on application. As Py and Cq are specific to Zn^{2+}, a reciprocal saturation with Ca^{2+} is not possible.

Pre-treatment of platelets with GR144053 inhibited Cq-induced aggregation. This indicates aggregation induced upon elevation of $[Zn^{2+}]_i$ is mediated by $\alpha_{IIb}\beta_3$. These findings confirm that the aggregation trace profile is attributable to aggregation, and not non-specific agglutination. Agglutination has

been reported to occur as a result of direct binding of cations to platelet integrins activating the integrin directly as opposed to upregulation of the integrin via platelet signalling (Gowland et al., 1969; Watson et al., 2016). A23187-induced aggregation was also inhibited by GR144053 which validated the use of the antagonist. The data presented here confirm that elevated $[Zn^{2+}]_i$ (via Cq) is able to mediate platelet aggregation via $\alpha_{IIb}\beta_3$, this was also the case with exogenous Zn^{2+} treatment which induced platelet aggregation in recent work (Watson et al., 2016). Furthermore, the use of TPEN abrogated the aggregatory response evoked by Cq, thus demonstrating that the Cq induced aggregation via $\alpha_{IIb}\beta_3$ is a result of elevated $[Zn^{2+}]_i$ and not the ionophore itself having a direct effect on the $\alpha_{IIb}\beta_3$. Thus, these data (Figure 5.2, 5.4) provide evidence showing that the Cq induced aggregation is mediated by $\alpha_{IIb}\beta_3$ as a result of $[Zn^{2+}]_i$ elevation. The mechanisms by which Zn^{2+} upregulates $\alpha_{IIb}\beta_3$ requires further investigation. Such work could assist in the development of safer antithrombotics which have lower bleeding risks, which has been an issue with current antithrombotics as Abciximab impose high bleeding risks (Makris et al., 2013; Tcheng et al., 2001).

The role of $[Zn^{2+}]_i$ in platelet aggregation was further examined using flow cytometry. PAC-1 binding is a measurement of $\alpha_{IIb}\beta_3$ activation. Elevation of $[Zn^{2+}]_i$ via Cq or Py induced increases in PAC-1 binding, confirming that $[Zn^{2+}]_i$ mediates aggregation via $\alpha_{IIb}\beta_3$. Whilst treatment with either ionophore resulted in increases in PAC-1 binding; only Cq produced an increase in aggregation (Figure 5.1-5.4). PAC-1 binding in response to Cq was higher than that for Py, indicating that $\alpha_{IIb}\beta_3$ upregulation did not reach a minimal threshold required for aggregation. The level of PAC-1 binding following Cq treatment were consistent with the sub-maximal aggregation observed during aggregometry).

As expected, A23187 induced a significant increase in PAC-1 binding This is consistent with aggregation data (Figures 5.1-2, 5.4), and consistent with previous work (Authi et al., 1993; Brüne and Ullrich, 1991; Smith et al., 1992; Varga-Szabo et al., 2009; Verma et al., 2011). Interestingly TPEN reduced the level of PAC-1 binding evoked by A23187 although did not influence the level of aggregation. it is possible that the level of PAC-1 binding induced by A23187 following TPEN pre-treatment is enough to evoke the levels of platelet aggregation induced by A23187. Data presented in Chapter 4 demonstrated that A23187 treatment resulted in modest increases in $[Zn^{2+}]_i$, thus the greater level of PAC-1 binding that was induced by A23187 in the absence of TPEN may be attributable to Zn^{2+}. This suggests that although Zn^{2+} may not significantly influence A23187-induced aggregation, it may potentiate A23187 induced $\alpha_{IIb}\beta_3$ activation, implying a potential role for Zn^{2+} in Ca^{2+}-evoked activity. This interplay between these cations in platelets warrants further investigation.

Chelation of $[Zn^{2+}]_i$ via TPEN also significantly reduced the level of PAC-1 binding in response to conventional agonists (CRP-XL, U46619 or thrombin), supporting a role for Zn^{2+} in agonist-evoked platelet activation.

In summary, these findings demonstrate that elevated $[Zn^{2+}]_i$ regulates platelet aggregation, supporting a role for Zn^{2+} as a secondary messenger in platelets. The mechanisms by which Zn^{2+} upregulates $\alpha_{IIb}\beta_3$ and induced aggregation is yet to be investigated and provides a platform for future work.

Increases in $[Zn^{2+}]_i$ induce phosphorylation of platelet proteins

Elevation of $[Zn^{2+}]_i$ using ionophores resulted in increases in tyrosine phosphorylation of platelet proteins, which is an acknowledged signalling event that is induced by numerous agonists, including thrombin, CRP and exogenous Zn^{2+} (Watson et al., 2016). This observation further implicates elevations of $[Zn^{2+}]_i$ results in platelet signalling leading to functional responses. Cq and Py elicited similar patterns of tyrosine phosphorylation, although Cq induced greater levels of phosphorylation than Py. This may explain differences in the aggregation profiles of these ionophores and is consistent with the heterogeneous effects of these reagents on platelet function. A23187 treatment resulted in a similar pattern of tyrosine phosphorylation to the Zn^{2+} ionophores. This may be due to the reason that A23187 has been reported to act as both Ca^{2+} and Zn^{2+} ionophore (Chapter 4). Thus A3187 may be mediating Zn^{2+}-induced as well as Ca^{2+}-induced phosphorylation. Whilst A23187 did not induce phosphorylation of proteins which were not apparent with the Zn^{2+} ionophore treatment, chelation of $[Zn^{2+}]_i$ resulted in a different pattern of phosphorylation to A23187 stimulation. This further suggests that the A23187-induced tyrosine phosphorylation is influenced by $[Zn^{2+}]_i$. However, the difference in tyrosine phosphorylation induced by A23187 with TPEN treatment did not correlate with data (Figure 5.2C, F) showing that TPEN had no influence on A23187 induced aggregation. Thus, these findings suggest that A23187 induced aggregation is not attributable to Zn^{2+}. However, since the Zn^{2+} ionophore Cq was able to mediate aggregation, and evoked phosphorylation in a similar manner to A23187 , a similar signalling event which occurs by these ionophores, may be the reason as to why Cq is able to evoke aggregation.

Chelation of $[Zn^{2+}]_i$ reduced the level of Cq and Py dependent tyrosine phosphorylation, confirming that ionophore-dependent phosphorylation is attributable to Zn^{2+}. Interestingly, chelation of $[Zn^{2+}]_i$ increased phosphorylation of another high molecular weight protein (approximately 80-90

kDa) , possibly reflecting the activity of a phosphatase or kinase that is activated or inhibited respectively by Zn^{2+}. The identity of such a kinase or phosphatase is currently unknown.

These data correlate well with the recent work carried out by Watson et al., (2016), which demonstrated that exogenous Zn^{2+} treatment induced tyrosine phosphorylation. As the pattern of phosphorylated protein differed from that induced by conventional agonists, it was concluded that tyrosine phosphorylation occurred in a novel manner. In this work pre-treatment with TPEN resulted in increased phosphorylation of a high molecular weight protein (approximately 95kDa). As chelation of Zn^{2+} resulted in increases of phosphorylation here, it can be inferred that phosphorylation of this protein is under the control of Zn^{2+}-dependent kinases or phosphatases. Published work has shown that elevation of $[Zn^{2+}]_i$ inhibits specific phosphatases, including SHP-2 and PTEN. In platelets these proteins are negative regulator of platelet activation upon GpVI stimulation, with and have IC_{50}s of 1-2µM and 0.59nM respectively (Haase and Maret, 2005, 2003; Lin et al., 2004; Ma et al., 2012; Mazharian et al., 2013; Weng et al., 2010). Thus, elevation of $[Zn^{2+}]_i$ to these levels could inhibit these phosphatases. This could explain the increase in phosphorylation of proteins following TPEN treatment. In this scheme, chelation of Zn^{2+} would inactivate phosphatases which would then be unable to dephosphorylate given proteins. Whether the concentration of $[Zn^{2+}]_i$ is able to reach the required level to modulate these phosphatases is not yet known. Interestingly, GpVI stimulation mediates $[Zn^{2+}]_i$ elevation (Chapter 3), suggesting that $[Zn^{2+}]$ may enhance GpVI induced activation by inhibiting these phosphates. These findings warrant further investigation and could be carried out in more depth in future projects as the primary focus of the investigation. This work from this thesis has demonstrated that $[Zn^{2+}]_i$ can regulate platelet behaviour and has opened many avenues of research to solely investigate each of these behaviours regulated by $[Zn^{2+}]_i$.

Increases in $[Zn^{2+}]_i$ mediate platelet shape change

A significant finding of the experiments performed in this chapter was that platelet shape change occurred following $[Zn^{2+}]_i$ elevation with the ionophores. This was first observed as a downward deflection in aggregation traces and was subsequently investigated using platelet adhesion to fibrinogen, and by pharmacological inhibition of cytoskeletal reorganisation. Whilst shape change occurred following treatment with both the Zn^{2+} ionophores; it was more evident following Py treatment. Here, shape change did not progress to a full aggregation response. However, it did result in the upregulation of $\alpha_{IIb}\beta_3$. Previous studies have shown that a large proportion of the $\alpha_{IIb}\beta_3$ complex

resides in the plasma membrane of resting platelets in association with an intracellular cytoskeletal lattice (Fox et al., 1993; Hartwig, 1992). Platelet activation disrupts this cytoskeletal lattice as a result of platelet shape change, leading to the disruption of the association between $\alpha_{IIb}\beta_3$ and cytoskeletal, which alters the state of $\alpha_{IIb}\beta_3$ (Bennett et al., 1999). This suggests a mechanism by which Py-induced shape change mediates $\alpha_{IIb}\beta_3$ upregulation. Cq stimulation resulted in shape change at a lower concentration, with no progression to aggregation. Py-induced shape change was biphasic with lower concentrations (30µM and 10µM) of Py inducing a greater level of shape change in than high concentration. The reasons for different responses to the ionophores is not clear. Both ionophores are specific for Zn^{2+}, and in neither case is Zn^{2+} included with the reagent. Possible suggestions relate the relative penetration of the ionophores into the platelet cytosols, as mentioned earlier. Further work will be required to determine the reasons for this.

Validation and investigation of the mechanism of ionophore-induced shape change in platelets were further explored. An important role for Zn^{2+} in regulating cytoskeletal changes has also been shown in nucleated cells (Rudolf et al., 2008a). In HeLa and prostate cancer (PC)-3 cells, Zn^{2+} regulates the actin cytoskeleton, cellular migration and focal adhesion dynamics (Li et al., 2016a). The chelation of Zn^{2+} in these cells results in the loss of filopodia formation whereas application of the Zn^{2+} ionophore enabled increases in filopodia formation (Li et al., 2016a). Studies on neuronal cells show that Zn^{2+} also regulates the polymerisation for tubulin which is required the transport of transcription factors in these cells (Mackenzie and Oteiza, 2007; Perrin et al., 2017a).

In addition to these studies illustrating the role of Zn^{2+} in regulating cytoskeleton rearrangement in nucleated cells, further work carried out in this chapter showed that the chelation of $[Zn^{2+}]_i$ resulted in a loss of attachment, and cellular spread of mouse embryonic fibroblast (MEF) cells (Figure 5.11). Quantification of MEF spreading (Figure 5.11) was problematic, due to varied structures and numbers of cells that were observed. Furthermore, the staining of actin, via the stain, Phalloidin-iFluor 594 , was also not an appropriate method to accurately quantify these images, as the purpose of these experiments was to assess cellular spread (i.e. cytoskeletal changes in cells that results in this spread), as the cells spread, the brightness of the stain dispersed and was brighter on cells which had not fully spread, as illustrated by Figure 5.11). Therefore, the subjective analysis was sufficient for these experiments, as clear differences were observed upon TPEN treatment (Figure 5.12). TPEN treatment inhibited cellular attachment as the number of cells that adhered to the coverslips were very minimal relative to that seen when TPEN was absent, and cellular spread was also not apparent with TPEN treatment. This may have been due to the prevention of cells adhering thus not undergoing spreading on the coverslips. The mechanisms for this are yet to be confirmed.

However, this finding demonstrates the role that Zn^{2+} may have on regulating MEF cell surface adhesion and spreading. Integrins which are cell surface adhesion receptors mediate adhesion upon activation which results in the integrin to switch to their high-affinity state (Harburger and Calderwood, 2009). Inside out signalling in MEF cells upregulates the integrins from their low to high affinity (Calderwood, 2004)results as a result of stimulation occurring once in contact with the coverslips or adjacent cells in these experiments , which as shown in the absence of TPEN resulted in adhesion and spread (Figure 5.11). Since chelation of $[Zn^{2+}]_i$ in MEF prevented adhesion, it can be suggested that Zn^{2+} may be regulating the affinity state of integrins in these cells by influencing inside out signalling. These findings outline the importance of Zn^{2+} on regulating cytoskeletal changes in other cells types, thus indicating the likelihood of Zn^{2+} also mediating cytoskeletal changes in platelets. Therefore, warranting the further exploration of Zn^{2+} in platelet shape change.

Zn^{2+} ionophore-induced shape change was abrogated following Cyt D treatment. This validates the downward deflection on the aggregation traces induced by the Zn^{2+} ionophores as an indication of biologically relevant shape change, as opposed to a non-specific chemical response. Further experiments were carried out to assess the influence of $[Zn^{2+}]_i$ on the signalling pathways that induce platelet shape change. Previous studies have shown that the specific signalling pathways leading to platelet shape change are primarily Ca^{2+} dependent and involve Ca^{2+}/calmodulin, myosin light chain kinase (MLCK) and RhoA-p160 ROCK. Platelet shape change is also known to occur in a Ca^{2+} independent manner, where ROCK either phosphorylates MLC and/or enhances MLC phosphorylation by inhibiting MLC phosphatases (MLC-P) (Paul et al., 1999; Shin et al., 2017). In order to investigate the role of increased $[Zn^{2+}]_i$ in shape change, the influence of these proteins on ionophore-induced events was investigated. Inhibition of MLCK and p160 ROCK via the inhibitors ML7 and Y-27632 respectively resulted in similar levels of inhibition of shape change in response to both Zn^{2+} ionophores tested. Conversely, inhibition of calmodulin via W-7 did not significantly influence Zn^{2+} ionophore-induced shape change. In contrast, shape change in response to A23817 was sensitive to Y-27632, W-7 and ML7 treatment. This is consistent with a role for Zn^{2+}-induced shape change that is independent of Ca^{2+} dependent signalling pathways. Furthermore, these findings indicated that $[Zn^{2+}]_i$ induced shape change influences the signalling pathways that involve both direct and indirect phosphorylation of MLC, which is mediated by p160 ROCK and MLCK, as illustrated by the speculative signalling pathway (Figure 5.16) drawn from these findings.

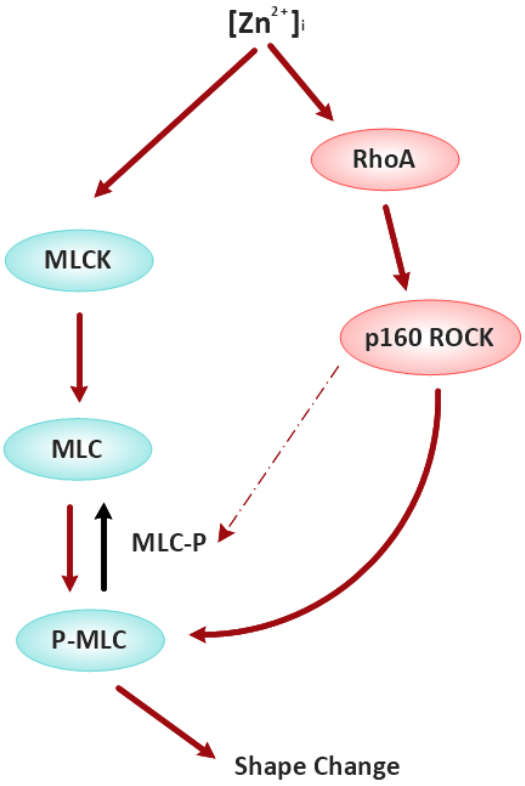

Figure 5.16. Schematic of signalling pathways involved in Zn^{2+} induced shape change in platelets. Elevation of $[Zn^{2+}]_i$ may mediate the association of RhoA and p160 ROCK, resulting in direct and indirect activation of myosin light chain (MLC), by either directly inducing phosphorylation of the MLC, or by inhibiting MLC-P. $[Zn^{2+}]_i$ may also mediate the activation of myosin light chain kinase (MLCK) which can then phosphorylate MLC to its active form phosphorylated-MLC (P-MLC). P-MLC can then evoke actin rearrangement and induce platelet shape change. The dashed arrow represent an inhibitory effect whilst the solid arrows represent a stimulatory effect.

This work provides the first reports demonstrating a role for Zn^{2+} in regulating p160 ROCK induced platelet shape change. Previous studies have shown that Rho-binding domain of p160 ROCK (which enables association with RhoA and p160 ROCK) consists of a cysteine-rich Zn^{2+} finger-like motif, although the contribution of this motif to p160ROCK activity has not been confirmed. Previous work that investigated the role for Zn^{2+} in regulating hypoxia-induced contractile events in pulmonary endothelium showed a role for Zn^{2+} in regulating hypoxia-induced MLC phosphorylation by inhibiting the MLC phosphatase MYPT1 (myosin phosphatase target subunit 1) (Bernal et al., 2011). This was shown to be dependant on ROCK such as ROCK1 (Rho-associated binding protein kinase 1), which similar to p160 ROCK consists of a cysteine-rich Zn^{2+} binding motif, however the relationship between ROCK induced cytoskeletal rearrangement and Zn^{2+} has not been investigated in this study (Bernal et al., 2011; Leung et al., 1996). These studies implicate the potential mechanism by which Zn^{2+} may evoke p160 induced platelet shape change, as Zn^{2+} may regulate p160 ROCK activity by binding to the Zn^{2+} binding motif found within this kinase. The relationship between p160 ROCK signalling and Zn^{2+} serves as a novel signalling pathway to investigate in platelets

This putative Zn^{2+}-dependent shape changing signalling pathway illustrated by Figure 5.16 was further explored by assessing levels of MLC phosphorylation in response to ionophore treatment

(Figure 5.10). Phosphorylation of ser157 of MLC, mediated by MLCK or RhoA/ROCK, is a major step in the shape changing signalling pathway. Initial experiments demonstrated that treatment with Zn^{2+} ionophores resulted in significant increases in P-MLC. This phosphorylation was significantly reduced upon $[Zn^{2+}]_i$ chelation, which confirms that the increases in P-MLC evoked by the ionophores were attributable to Zn^{2+}. Furthermore, application of the inhibitors of MLCK and p160 ROCK also significantly reduced Zn^{2+}-ionophore-mediated MLC phosphorylation whereas inhibition of calmodulin had no effect. This correlates with data from aggregometry experiments using these inhibitors. These data provide further evidence to indicate that $[Zn^{2+}]_i$ induced platelet shape change is independent of Ca^{2+}/Calmodulin and mediates shape change via the p160 ROCK pathway. This is in contrast to A23187 induced phosphorylation of MLC, which was abrogated by ML7 (MLCK inhibitor) or W-7 (calmodulin antagonist). Interestingly inhibition of P160 ROCK reduced the levels of P-MLC induced by A23187, however, this level of P-MLC was still significantly higher than the vehicle control (Figure 5.9E). This suggested that Ca^{2+} dependent and independent pathways synergise to enable efficient platelet shape change. Conversely, published work has shown that Zn^{2+} can occupy Ca^{2+} binding sites on calmodulin (Hathaway and Adelstein, 1979; Mills and Johnson, 1985). Calmodulin consists of 2 globular domains, each with EF-hand motifs. Ca^{2+} binding to the EF-hand domains of calmodulin induces significant conformational changes which result in calmodulin induced signal transduction (Warren et al., 2007a). On the basis of these models, it has been proposed that Zn^{2+} plays an intermediate role in calmodulin induces signal transductions (Warren et al., 2007a). These concepts have been tested in the experiments described in this chapter. The work carried out in this chapter does not correlate with previous work stated above that suggests Zn^{2+} could mediate calmodulin induced signalling. As inhibition of calmodulin (which is a major mediator of Ca^{2+} dependent shape change (Paul et al., 1999)) had no significant influence on the shape change response evoked by $[Zn^{2+}]_i$ elevation.

Increases in $[Zn^{2+}]_i$ did not result in phosphorylation of VASP. This indicates that $[Zn^{2+}]_i$ elevation does not influence the activity of cyclic nucleotide-dependent kinases such as PKG or PKA, which play inhibitory roles in platelet shape change (Aburima et al., 2013). Thus $[Zn^{2+}]_i$ is not a negative regulator of cytoskeletal rearrangements but acts in a positive manner to initiate shape change.

Chelation of $[Zn^{2+}]$ also abrogated platelet spreading on fibrinogen, providing further evidence of a link between Zn^{2+} and regulation of the platelet cytoskeleton. The shape change observed here was as a result of outside-in signalling, due to the platelet shape change occurring in response to binding to fibrinogen via $\alpha_{IIb}\beta_3$ (illustrated in Figure 1.7, Chapter 1). Therefore these findings demonstrate that chelation of $[Zn^{2+}]_I$ inhibit shape change occurring upon outside-in signalling,

although the exact mechanisms of how this is caused require further work. Furthermore, this finding also suggested that perhaps Zn^{2+} may be influencing the binding of $\alpha_{IIb}\beta_3$ to fibrinogen by disrupting the inside-out signalling that enables $\alpha_{IIb}\beta_3$ to switch to its high-affinity state which is essential for enabling fibrinogen to bind to $\alpha_{IIb}\beta_3$ (Figure 1.6, Chapter 1). This suggests that Zn^{2+} may play a key role in regulating the upregulation of $\alpha_{IIb}\beta_3$ via inside-out signalling, further outlining the importance that Zn^{2+} may have on platelet activatory shape change. These findings require further work and open an avenue to explore in terms of platelet shape change that occurs via outside-in signalling, which may be significantly influenced by Zn^{2+} as the data from this work suggests.

In summary, these data demonstrated that $[Zn^{2+}]_i$ may play a major role in mediating platelet shape change and provide further evidence to indicate its modulatory role as a secondary messenger in platelets.

Increases in $[Zn^{2+}]_i$ induce platelet degranulation

From these data discussed above, it can be concluded that agonist-evoked increases in $[Zn^{2+}]_i$ are able to regulate or initiate platelet shape change. As shape change is linked to aggregation and granule release, further experiments were performed to better understand the effects of increasing platelet $[Zn^{2+}]_i$ on activatory processes in addition to aggregation, tyrosine phosphorylation and shape change.

Experiments were carried out to assess the effect of $[Zn^{2+}]_i$ elevation on dense and alpha-granule release. Interestingly $[Zn^{2+}]_i$ elevation resulted in the externalisation of CD63, but not CD62P, supporting a role for Zn^{2+} in regulating dense, but not α granule release (Figure 5.12). Furthermore, chelation of $[Zn^{2+}]_i$ using TPEN inhibited agonist-induced dense granule release but not α-granule release (Figure 5.13). This provides evidence for differential regulation of release of the two granule subtypes. The signalling pathways and mechanism which contribute to the differential release of α and dense granules are poorly understood. Previous work has shown that granule secretion is regulated by cytoskeletal rearrangement, which occurs as a result of platelet activation. For example, inhibition of Rho kinases inhibits granule secretion (Suzuki et al., 1999; Watanabe et al., 2001). Thus Zn^{2+} induced shape change may play a role in regulating dense granule release upon $[Zn^{2+}]_i$ elevation. This is yet to be investigated and would be interesting to explore further as this potential relationship between Zn^{2+} induced shape change, and granule release provides a novel approach to understanding granule release regulation.

PS exposure increases in response to $[Zn^{2+}]_i$ elevation

Elevation of $[Zn^{2+}]_i$ via ionophore treatment also resulted in increases in PS exposure and the development of a pro-coagulant phenotype, which is an important process in platelet activation. Interestingly the percentage of platelets that expresses PS increased were much higher following treatment with the Zn^{2+} ionophores, in comparison to that evoked by conventional agonist (CRP-XL, thrombin or U46619, Figure 5.14-15). This correlates with previous data that show greater levels of $[Zn^{2+}]_i$ following ionophore treatment than for conventional agonists (Chapter 3-4). Given that only a subset of platelets adopts a pro-coagulant phenotype following agonist stimulation, this observation implicates $[Zn^{2+}]_i$ elevation as a potential mechanism that initiates the procoagulant pathway. Whilst, the mechanisms by which Zn^{2+} induced PS exposure is not fully understood, A23187 is thought to induce significant increases in PS exposure as a result of elevated $[Ca^{2+}]_i$. $[Ca^{2+}]_i$ influences PS exposure by mediating the translocation of PS from the inner leaflet of the membrane to the outer leaflet of the membrane via the activation of the Ca^{2+} dependent scramblase protein (Figure 1.9, Chapter 1). Interestingly $[Zn^{2+}]_i$ chelation via TPEN also inhibited A23187-induced PS exposure suggesting that $[Ca^{2+}]_i$ mediated PS exposure may depend on basal $[Zn^{2+}]_{i.,}$ PS exposure in platelets is mediated by caspase and caspase-independent mechanisms (Schoenwaelder et al., 2009; van Kruchten et al., 2013). Inhibition of caspases reduces the level of PS exposure induced by A23187 or conventional agonists (Cohen et al., 2004a; Schoenwaelder et al., 2009). In the experiments described here, inhibition of caspases with the inhibitor Z-VAD partially reduced PS exposure implicating caspases in $[Zn^{2+}]_i$-induced PS exposure. These data further outline the importance $[Zn^{2+}]_i$ may play in modulating platelet behaviour and provides further evidence to suggest that Zn^{2+} is a secondary messenger in platelets.

5.4 Conclusion

In conclusion, the work carried out in this chapter provides evidence to support the hypothesis of this thesis that Zn^{2+} is a secondary messenger in platelets. $[Zn^{2+}]_i$ elevation was found to evoke a functional role in many activatory processes including aggregation, tyrosine phosphorylation, shape change, upregulation of $\alpha_{IIb}\beta_{3,}$ dense granule release and PS exposure. Thus, $[Zn^{2+}]_i$ may have novel roles in the signalling pathways in platelets that are consistent with that of the secondary messenger. The mechanisms by which $[Zn^{2+}]_i$ mediates these activatory processes are not yet known, however, this work provides the first report outlining the importance of Zn^{2+} in platelet activity.

The work carried out in the previous chapters demonstrated that $[Zn^{2+}]_i$ elevation occurs upon agonist stimulation in a redox-sensitive manner (Chapter 3) and could also be modelled via ionophores in a non-redox sensitive manner (Chapter 4). Therefore, the work carried out in Chapter 3, 4 and this chapter provides the first reports demonstrating that $[Zn^{2+}]_i$ elevation can occur upon activation and also be modelled, which then results in the modulation of platelet activity. This is consistent with the definition of a secondary messenger which is defined as a molecule that is intracellularly modulated in response to extracellular stimuli and can then induce appropriate intracellular signalling events with regards to the extracellular stimuli, resulting in physiological changes in the cell.

Chapter 6

6.0 Investigation of the signalling pathways which mediate intracellular Zn^{2+} release

6.1 Background

The work detailed in Chapters 3 and 4 demonstrates the presence of Zn^{2+} storage mechanisms in platelets, which act to release Zn^{2+} into the platelet cytosol following stimulation with conventional platelet agonists. This results in significant elevations of $[Zn^{2+}]_i$. These elevations are redox sensitive, indicating a possible mechanism involving thiol-containing storage proteins. The work described in Chapter 4 demonstrated that increases in platelet $[Zn^{2+}]_i$ could be modelled using Zn^{2+} ionophores, in a similar manner to the Ca^{2+} ionophore, A23187 which has been widely used to explore Ca^{2+} signalling in platelets. Data from this chapter demonstrated the presence of Zn^{2+} stores which were accessible using Zn ionophores. Other potential mechanisms that could contribute to $[Zn^{2+}]_i$ increases include release from the dense tubular system via the inositol-1,4,5-trisphosphate receptor (IP_3R), in a similar manner to Ca^{2+} (Figure 1.10). The DTS may also store Zn^{2+} in addition to Ca^{2+}, although this yet to be investigated.

In nucleated cells, ZIP7 associates with Ca^{2+} store membranes such as the DTS (Hogstrand et al., 2013; Taylor et al., 2008) where it mediates Zn^{2+} release in response to signalling in a similar manner to PLC/IP_3R mediated Ca^{2+} release, and it may be performing a similar role in platelets (Taylor and Pugh, 2016). Most notably previous work illustrating ZIP7 mediated Zn^{2+} release from stores within nucleated cells is consistent with Zn^{2+} acting as a secondary messenger in platelets. Thus investigation of ZIP7 [which has been found to be expressed in platelets (Burkhart et al., 2012)] in platelets would provide further evidence to strengthen the hypothesis of this thesis that Zn^{2+} is a secondary messenger in platelets.

The observation of agonist-evoked increases of both $[Zn^{2+}]_i$ and $[Ca^{2+}]_i$ raises the possibility of functional interplay between these cations. Zn^{2+} and Ca^{2+} associate with similar proteins via the same motif. For example, calmodulin has been shown to bind to Zn^{2+} at the same EF-hand motifs to which Ca^{2+} binds(Mills and Johnson, 1985; Schumacher et al., 2004; Warren et al., 2007). Interestingly these studies indicate that Zn^{2+} may bind to calmodulin as an intermediate step (inducing structural changes) before the binding of Ca^{2+}, suggesting that signalling via calmodulin may require Zn^{2+} to play an

intermediate role (Warren et al., 2007b). Other calcium-binding proteins which contain EF-hand motifs include calcineurin B, CIB (Ca^{2+} and integrin binding protein), and S100 family members which are involved in Ca^{2+}-dependent signal transduction pathways, and are also expressed in platelets (Naik et al., 1997; Y. Wang et al., 2014). Therefore Zn^{2+} may be able to bind to the EF-hand motifs to these Ca^{2+} binding proteins, influencing Ca^{2+} transduction pathways(Lood et al., 2016). Previous studies have shown that Zn^{2+} binds to S100 proteins (Nakayama and Kretsinger, 1994; Schäfer et al., 2000). Similarly to calmodulin Zn^{2+} has also been suggested to play an intermediate role in mediating the S100 function by evoking an increase in affinity between S100 and Ca^{2+} (via structural changes)(Baudier et al., 1986). Furthermore in nucleated cells, Zn^{2+} has been shown to compete with Ca^{2+} for a range of bindings sites, for example in mitochondrial Ca^{2+} transporters and tubulin (Jemiolo and Grisham, 1982; Jeng et al., 1978). These studies provide evidence to suggest that Zn^{2+} influences Ca^{2+} signalling. This may also apply to platelets and warrants investigation, as the interplay between these two cations may be a major feature of platelet activation regulation.

6.1.1 Aims

Experiments discussed in previous chapters showed that both $[Zn^{2+}]_i$ $^+$ and Ca^{2+} are elevated upon platelet activation. As both cations bind to and regulate similar proteins, there is the potential for the actions of the two cations to synergise in platelets. The work described in this chapter was designed to investigate the interplay of Zn^{2+} and Ca^{2+}, and to investigate the potential storage mechanisms which these cations might share.

6.1.2 Methods

A range of methodologies were employed in this chapter, and the specific application of reagants are discussed in depth in the results section accordingly. Here a general overview of the methods employed in this chapter will be discussed.

The release of $[Zn^{2+}]_i$ and $[Ca^{2+}]_i$ was measured in washed platelet suspensions using fluorometry following staining with the $[Zn^{2+}]_i$ and $[Ca^{2+}]_i$ probe, Fluozin-3 (FZ-3) and Fluo-4 (FL-4), respectively (section 2.4, Chapter 2).

The IP_3R antagonist, 2-aminoethoxydiphenyl borate (2-APB) was employed to assess cation mobilisation from the dense tubular system upon agonist stimulation. The working concentration of 2-APB that was employed by previous studies to antagonise IP3R was 100µM. Thus similar

concentrations were employed in the experiments described in this chapter (Diver et al., 2001; Djillani et al., 2014).

Western blotting was used to assess changes in the phosphorylation status of ZIP7 using the anti-phospho-ZIP7 (Ser275/276) antibody (section 2.7, Chapter 2). ZIP7 activity was also assessed using CX-4955 which is an inhibitor of the protein kinase CK2, which is responsible for inducing ZIP7 activation (Taylor et al., 2012). Previous work has determined that 10μM of CX-4955 is sufficient to inhibit protein kinase CK2 activity in platelets (Ampofo et al., 2015). A similar concentration was used here.

Store-operated cation entry was measured using real-time flow cytometry (section 2.10, Chapter 2). The sarcoplasmic/endoplasmic reticulum Ca^{2+} ATPase (SERCA) inhibitor thapsigargin (TG) was used to evoke the store-operated cation entry response. 1μM of TG has been widely used in previous work thus similar concentrations were also used here (Authi et al., 1993; Tepel et al., 1994; Vostal and Shafer, 1996)

6.2 Results

6.2.1 Agonist-induced $[Zn^{2+}]_i$ elevation is mediated by Ca^{2+} store mobilisation

Experiments using the IP_3R antagonist 2-APB were performed to investigate whether agonist-evoked elevation of $[Zn^{2+}]_i$ occur as a result of release via IP3R, in a similar manner to agonist-evoked $[Ca^{2+}]_i$ release.

$[Zn^{2+}]_i$ release was assessed using fluorometry FZ-3. Data from chapter 3 demonstrated that stimulation with CRP-XL and U46619, but not thrombin, resulted in significant increases in FZ-3 fluorescence, consistent with elevated $[Zn^{2+}]_i$. Pre-treatment of washed platelets with 2-APB (100μM) significantly reduced the levels of FZ-3 fluorescence in response to CRP-XL (1μg/mL) or U46619 (10μM) throughout the duration of the experiment (Figure 6.1A). The FZ-3 F/F_0 in response to CRP-XL (1μg/ml) after 6mins was reduced from 2.2±0.2 to 1.5±0.1 upon 2-APB pre-treatment ($p<0.05$, Figure 6.1A). The FZ-3 fluorescence in response to CRP-XL in 2-APB pre-treated platelets was significantly higher than the vehicle treatment in the absence and presence of 2-APB where FZ-3 F/F_0 values were 1.01±0.5 and

1.0±0.1, respectively ($p<0.05$, Figure 6.1A). This suggests that CRP-XL-evoked increases in $[Zn^{2+}]_i$ is potentially mediated by IP_3R activity.

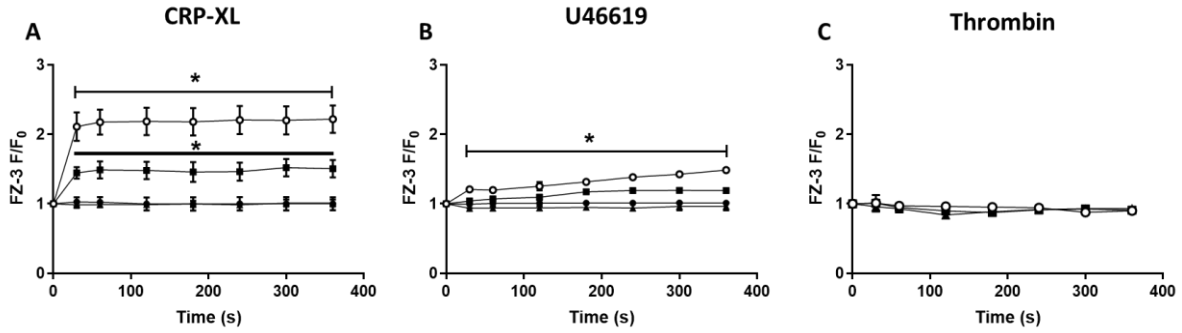

Figure 6.1. 2-APB treatment inhibits agonist-evoked increases in FZ-3 fluorescence. Fluozin-3 (FZ-3)-labelled washed human platelets were pre-treated with the IP_3R antagonist, 2-APB, before being stimulated by CRP-XL (A), U46619 (B) or Thrombin (C) and FZ-3 fluctuations were recorded over six minutes using fluorometry. A) Stimulation with CRP-XL in platelets pretreated with vehicle control (○ 1µg/ml), 2-APB (■, 100µM), or pretreated with 2-APB (100µM) in the absence of stimulation (●). Vehicle control (DMSO, ▲). B) Stimulation with U46619 (10µM) in platelets pretreated with vehicle control (○, 1µg/ml), 2-APB (■, 100µM), or pretreated with 2-APB (100µM) in the absence of stimulation (●).Vehicle control (DMSO, ▲). C) Stimulation with thrombin (1U/mL) in platelets pretreated with vehicle control (○, 1µg/ml), 2-APB (■, 100µM), or pretreated with 2-APB (100µM) in the absence of stimulation (●).Vehicle control (DMSO, ▲). Data are mean±standard error of mean (SEM) from 6 independent experiments Significance is denoted as *** ($p<0.001$), ** ($p<0.01$) or * ($p<0.05$).

Similarly, upon U46619 (10µM) stimulation, FZ-3 F/F_0 after 6mins was reduced from 1.49±0.03 to 1.19±0.01 in 2-APB pre-treated platelets ($p<0.05$, Figure 6.1B). This was significantly higher than the vehicle treatment in the presence and absence of 2-APB (0.94±0.06 and 1.01±0.04, respectively, $p<0.05$, Figure 6.1B). Therefore, TP receptor engagement leading to increases in $[Zn^{2+}]_i$ is mediated by IP_3R activity. As expected, Thrombin stimulation did not result in fluctuations of Fz-3 fluorescence.

These findings (Figure 6.1A) indicate that agonist-evoked $[Zn^{2+}]_i$ increase is mediated by a 2-APB-sensitive route, most likely involving the activation of IP_3R. This implies that Zn^{2+} is also present alongside Ca^{2+} within the DTS and may perhaps be co-released upon activation. Alternatively, Ca^{2+} release may be required to act a prerequisite for Zn^{2+} release from alternative stores. Further work would need to be carried out to explore this potential mechanism of $[Zn^{2+}]$ elevation

Fluctuations in FL-4 fluorescence following 2-APB treatment were also assessed primarily to validate the use of 2-APB as an inhibitor of IP_3R. Pre-treatment with 2-APB (100µM) abolished increases in Fluo-4 fluorescence induced by the agonists (Figure 6.2).

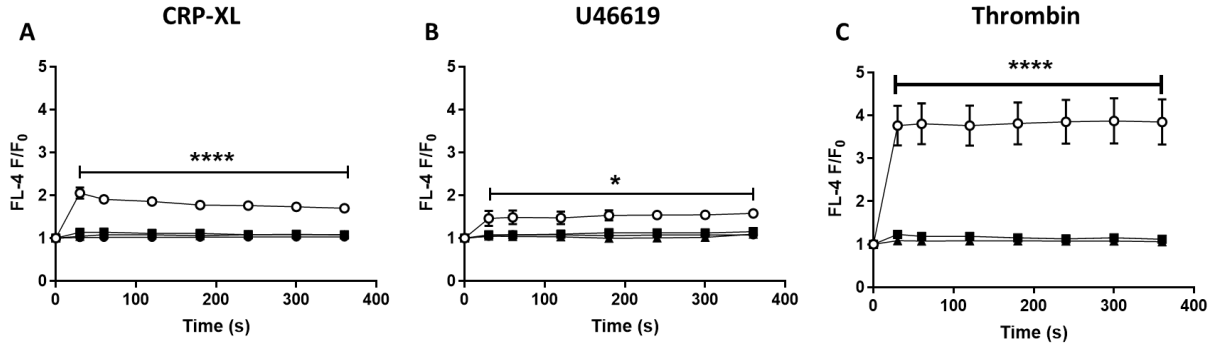

Figure 6.2. 2-APB treatment inhibits agonist-evoked increases in FL-4 fluorescence. Fluo-4 (FL-4)-labelled washed human platelets were pre-treated with the IP_3R antagonist, 2-APB, before being stimulated by CRP-XL (A), U46619 (B) or Thrombin (C) and FZ-3 fluctuations were recorded over six minutes using fluorometry. A) Stimulation with CRP-XL in platelets pretreated with vehicle control (○ 1µg/ml), 2-APB (■, 100µM), or pretreated with 2-APB (100µM) in the absence of stimulation (●).Vehicle control (DMSO, ▲). B) Stimulation with U46619 (10µM) in platelets pretreated with vehicle control (○, 1µg/ml), 2-APB (■, 100µM), or pretreated with 2-APB (100µM) in the absence of stimulation (●).Vehicle control (DMSO, ▲). C) Stimulation with thrombin (1U/mL) in platelets pretreated with vehicle control (○, 1µg/ml), 2-APB (■, 100µM), or pretreated with 2-APB (100µM) in the absence of stimulation (●).Vehicle control (DMSO, ▲). Data are mean±standard error of mean (SEM) from 6 independent experiments Significance is denoted as *** (p<0.001), ** (p<0.01) or * (p<0.05).

The FL-4 F/F_0 after 6mins in response to CRP-XL (1µg/ml) was abrogated from 1.69±0.07 to 1.07±0.04 upon pre-treatment with 2-APB ($p<0.0001$, Figure 6.2A). This did not significantly differ from vehicle treatment (DMSO) in 2-APB treated, and untreated platelets (1.08±0.04 and 1.03±0.07, respectively, $p>0.05$, ns, Figure 6.2A).

Upon U46619 stimulation (10µM), FL-4 F/F_0 after 6mins was also abrogated from 1.58±0.04 to 1.15±0.04 in 2-APB-treated platelets ($p<0.05$, Figure 6.2B). This also did not differ from the vehicle control 2-APB treated and untreated platelets (1.10±0.01, respectively $p>0.05$, ns, Figure 6.2B).

FL-4 F/F_0 following thrombin (1U/mL) stimulation for 6mins was also abrogated from 3.9±0.5 to 1.2±0.1 in 2-ABP-pretreated platelets ($p<0.0001$,Figure 6.2C) compared to 1.1±0.1 for the vehicle control ($p<0.0001$, Figure 6.2C). The final FL-4 F/F_0 induced by thrombin on 2-APB-pre-treated platelets also did not significantly differ to the vehicle control in 2-APB treated and untreated platelets (1.1±0.1 and 1.0±0.1 respectively, $p>0.05$, ns, Figure 6.2B). In demonstrating 2-APB-dependent

reductions in agonist-evoked FL-4 fluorescence, these data validate the use of 2-APB as an IP_3R antagonist

The data described above indicate that $[Zn^{2+}]_i$ may be mobilised from the dense tubular system in a similar manner to Ca^{2+}. Inhibition of IP_3R did not completely abrogate agonist-induced increases in FZ-3 fluorescence. This is consistent with a more substantial role for redox-dependent mechanisms in Zn^{2+} release. The demonstration of two potential 2-APB and redox-sensitive release routes indicates that at least two mechanisms are responsible for regulating increases in $[Zn^{2+}]_i$. It is possible that both vesicular- and protein-based Zn^{2+} stores exist and are accessible upon agonist stimulation. Accessibility may be dependent on heterogeneous signalling. To investigate this, potential Zn^{2+}-release mechanisms were investigated further.

6.2.2 CK2 induces intracellular Zn^{2+} signalling via phosphorylation of the Zn^{2+} channel ZIP7

The release of $[Zn^{2+}]_i$ from 2-APB-sensitive stores was further investigated. Whilst it is well documented that IP_3R mediates $[Ca^{2+}]_i$ release from the DTS upon activation (Figure 1.10, Chapter 1), the release of Zn^{2+} from this store is yet to be determined. A similar mechanism to IP_3R mediated $[Ca^{2+}]_i$ release in platelets may also be apparent for $[Zn^{2+}]_i$,allowing co-release of Zn^{2+} with Ca^{2+} during activation. Whether Zn^{2+} release occurs via IP_3R is unknown. Other potential candidates for mediating Zn^{2+} release from the DTS include the Zn^{2+} transporter ZIP7 which is present in the platelet proteome although its expression in platelets has yet to be confirmed (Burkhart et al., 2012).

Phosphorylation of ZIP7 as demonstrated in nucleated cells (such as breast cancer cells) is required to enable activation to drive Zn^{2+} release from intracellular stores (Taylor et al., 2008). Phosphorylation is mediated by protein kinase CK2 (CK2) which phosphorylates $Ser^{275/276}$. Platelet CK2 activity has been implicated in thrombus formation, and also in mediating platelet interactions with platelets and other vascular cells types (Ampofo et al., 2015). Thus a potential mechanism for Zn^{2+} release may involve phosphorylation of ZIP7 by CK2. Experiments were performed to investigate the expression of ZIP7, and the roles of CK2 and ZIP7 in mediating $[Zn^{2+}]_i$ release upon agonist stimulation.

The role of ZIP7 in this agonist-induced $[Zn^{2+}]_i$ elevation was initially assessed by examining changes in the phosphorylation state of ZIP7. Due to there being no specific, commercially available ZIP7 inhibitors, pharmacological investigation of ZIP7 activity is not possible. Therefore CK2 was

targetted to assess ZIP7 activity. The widely used specific inhibitor of CK2, CX-4945 was employed to assess the role of CK2 in ZIP7 phosphorylation in platelets. As previous work determined that 10µM was sufficient to inhibit CK2 activity in platelets, a similar concentration was used here (Ampofo et al., 2015).

Western blotting of platelet lysates with anti-phospho-ZIP7 antibodies revealed a protein at 48kDa, consistent in size with phosphorylated ZIP7. Upon stimulation of platelets with CRP-XL (1µg/mL), the intensity of this band increase, in a manner consistent with increased phosphorylation. CRP-XL-mediated ZIP7 phosphorylation was significantly higher than vehicle treatment (0.40±0.05 and 0.16±0.01 respectively, $p<0.01$, Figure 6.3).

This phosphorylation was significantly reduced in 2-APB treated platelets (from 0.40±0.05 to 0.18±0.02 , $p<0.01$, Figure 6.3A). Interestingly, U46619 treatment did not result in significant increases in ZIP7 phosphorylation, indicating that U46619-induced $[Zn^{2+}]_i$ elevation does not result in ZIP7 activation. The level of phosphorylation induced by the U46619 (10µM) in the presence and absence of 2-APB (10µM) was 0.15±0.03 and 0.12±0.01, respectively ($p>0.05$, ns, Figure 6.3A). This data correlates CRP-XL induced $[Zn^{2+}]_i$ increases with ZIP7 activity, and a reliance on IP_3R signalling.

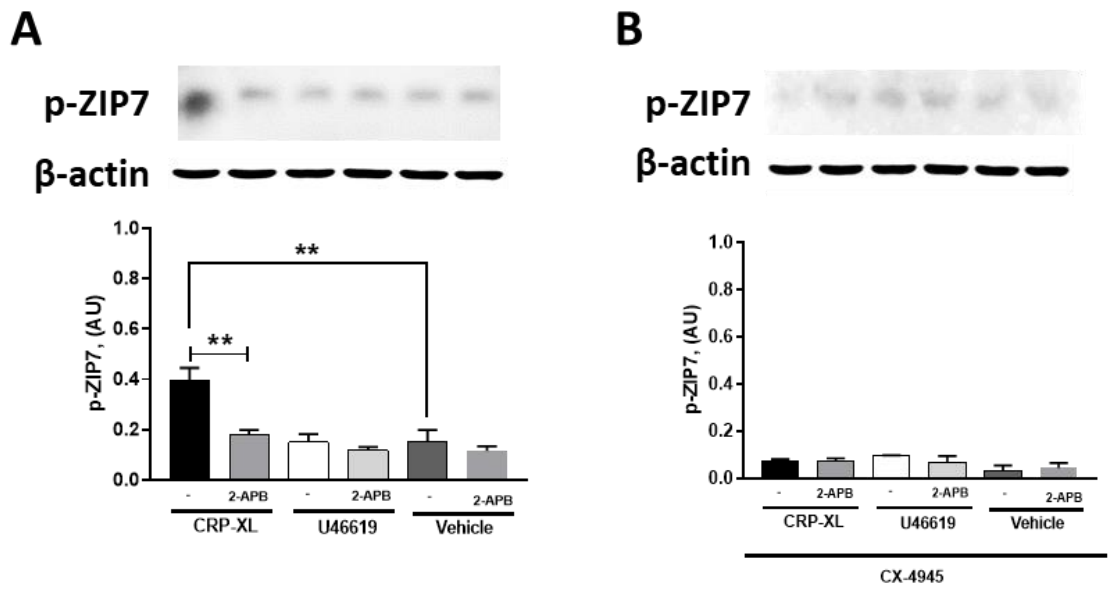

Figure 6.3. ZIP7 phosphorylation occurs in response to platelet stimulation with CRP-XL, but not U46619, which is abrogated by CX-4945. Representative Western blots and quantification showing changes in ZIP7 phosphorylation in untreated platelets (A) or in CX-4945 pre-treatment platelets (B), following stimulation for 15mins with CRP-XL (1µg/ml) (U46619 (10µM)or the vehicle (DMSO) in the absence and presence of 2-APB (30µM). CRP-XL induced significant increases in ZIP7 phosphorylation which was abrogated with CX-4945 (10µM) pre-treatment. B-actin was used as a loading control.

The level of B-actin did not vary with drug treatment (not shown). Blots and quantification are representative and means±SEM of 4 experiments. Significance is denoted as *** ($p<0.001$), ** ($p<0.01$) or * ($p<0.05$).

The level of ZIP7 phosphorylation in response to CRP-XL (1µg/ml) was abrogated from 0.40±0.05 to 0.08±0.01 in CX-4945 pre-treated platelets ($p<0.01$, Figure 6.3A-B). This did not differ to that induced by the vehicle control (0.07±0.01 ,$p>0.05$, ns, Figure 6.3B). Furthermore, no ZIP7 phosphorylation was observed in CX-4945 pre-treatment platelets relative to vehicle treatment (Figure 6.3B)

These data demonstrate that agonist-evoked activation mediates the phosphorylation of ZIP7 in platelets. CRP-XL, but not U46619 induced significant levels of phosphorylation. This correlates with the observation that CRP-XL induces significantly higher $[Zn^{2+}]_i$ elevations than U46619 (Chapter 3). Thus the greater level of $[Zn^{2+}]_i$ increase following CRP-XL activation may be attributable to ZIP7 activation and subsequent $[Zn^{2+}]_i$ release from intracellular stores.

Further experiments were performed to assess the role of ZIP7 activation on agonist-mediated $[Zn^{2+}]_i$ elevation. CX-4945 was again employed to modulate ZIP7 activity. $[Zn^{2+}]_i$ fluctuations in FZ-3-loaded platelets were measured using fluorometry. Pretreatment of washed platelet suspensions with CX-4945 (10µM) significantly reduced increases in FZ-3 fluorescence induced by CRP-XL (1µg/ml, Figure 6.4A). FZ-3 F/F_0 values after 6mins in response to stimulation by CRP-XL (1µg/ml) were reduced from 2.2±0.2 to 1.40±0.03 upon pre-treatment with CX-4945 (10µM, $p<0.0001$, Figure 6.4A). Interestingly, in a similar manner to 2-APB pre-treatmentwith CX-4945 did not completely abrogate increases in CRP-XL-induced FZ-3 fluorescence. The FZ-3 F/F_0 in response to CRP-XL was higher than the vehicle control (1.0±0.1, $p<0.01$, Figure 6.4A). No significant differences in FZ-3 fluctuations were shown in CX-4945 treated or untreated platelets following U46619 (10µM) stimulation. Respective FZ-3 fluorescence values were 1.57±0.02, and 1.51±0.06 respectively ($p>0.05$, ns, Figure 6.4B). These FZ-3 F/F_0 values were significantly higher than that induced by the vehicle controls (in the presence and absence of CX-4945) which were 1.01±0.01 and 1.0±0.01 respectively ($p<0.0001$. Figure 6.4B). Thus, TP signalling may not mediate $[Zn^{2+}]_i$ elevation via ZIP7.

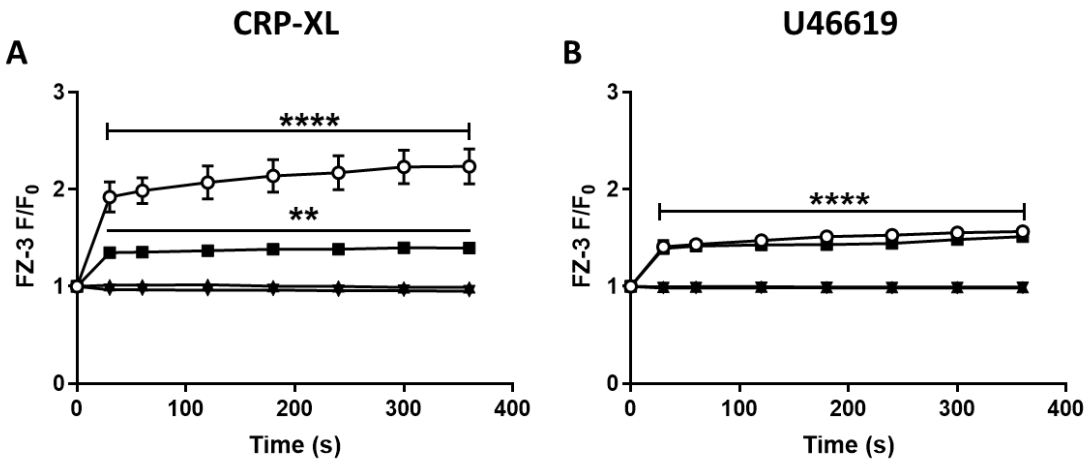

Figure 6.4. CX-4945 treatment inhibits agonist evoked increases in FZ-3 fluorescence. Fluozin-3 (FZ-3)-labelled washed human platelets were stimulated by 1µg/ml of CRP-XL (A) or 10µM U46619 1(B) following pre-treatment with vehicle (DMSO, ○, CX-4945 (10µM, ■), or without agonist stimulation (DMSO, ▲), or with CX-4945 pretreatment in the absence of agonist stimulation (▼). $[Zn^{2+}]_i$ fluctuations were recorded over 6 minutes using fluorometry. CX-4945 treatment inhibited CRP-XL evoked increases in FZ-3 fluorescence but did not influence U46619 induced increases in FZ-3 fluorescence. Results are representative and means±SEM of 6 experiments. Significance is denoted as **** ($p<0.00010$, *** ($p<0.001$), ** ($p<0.01$) or * ($p<0.05$).

These data are consistent with data described in Figure 6.3, and both correlate CK2 with CRP-XL-mediated ZIP7 phosphorylation and subsequent increases in Zn^{2+} fluorescence. U46619 treatment did not increase ZIP7 phosphorylation (Figure 6.3) and was unresponsive to CX-4945 suggesting that U46619 mediated Zn^{2+} elevations occurs via a different mechanism, and are not mediated by canonical membrane store release. Other interpretations are possible. For example,as mentioned earlier the increase in $[Zn^{2+}]_i$ (measured by FZ-3 increases) following U46619 is modest compared to CRP-XL (as shown in Chapter 3, and in Figure 6.4 above). Thus CRP-XL, but not U46619, induced $[Zn^{2+}]_i$ elevation may be attributable to ZIP7 mediated store release. This may explain the lower $[Zn^{2+}]_i$ increase in response to U46619 stimulation.

Further experiments were performed to investigate the influence of increased $[Ca^{2+}]_i$ on ZIP7 phosphorylation and CK2 activity. Pre-treatment of washed platelet suspensions with CX-4945 (10µM, CK2 inhibitor) had no influence on the agonist-induced $[Ca^{2+}]_i$ release in Fluo-4 (FL-4) loaded platelets. The FL-4 F/F_0 induced by CRP-XL (1µg/ml) after 6 mins were 1.97±0.10 and 1.91±0.05 in untreated and CX-4945-treated platelets respectively. These values did not significantly differ from each other but were significantly higher than the vehicle control (1.0±0.1, $p<0.0001$, Figure 6.5A). FL-4 F/F_0 after 6

mins in response to U46619 (10µM) was 1.34±0.02, and 1.40±0.03 respectively in untreated and CX-4945-treated platelets. Again these values did not significantly differ from each other but were significantly higher than the vehicle control (1.0±0.1, p<0.0001, Figure 6.5B).

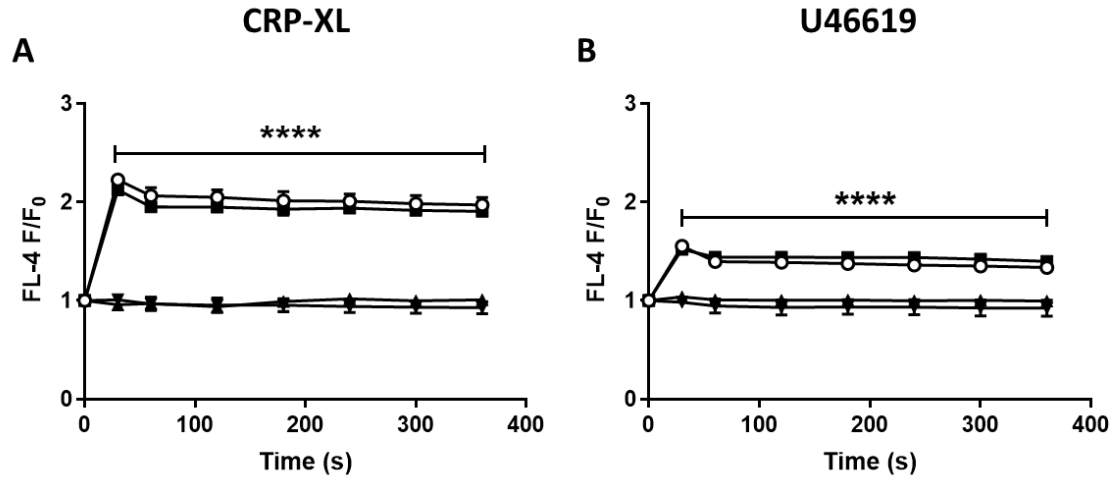

Figure 6.5. CX-4945 treatment does not effect agonist-evoked increases in FL-4 fluorescence. Fluo-4 (FL-4)-labelled washed human platelets stimulated by 1µg/ml of CRP-XL (A) or 10µM U46619 (B) following pretreatment with vehicle (DMSO, ○), CX-4945 (10µM , ■), or without agonist stimulation (DMSO, ▲), or with CX-4945 pretreatment in the absence of agonist stimulation (▼). $[Ca^{2+}]_i$ fluctuations was recorded over six minutes using fluorometry. Results are representative and means±SEM of 6 experiments. Significance is denoted as **** (p<0.0001), *** (p<0.001), ** (p<0.01) or * (p<0.05).

These data indicate that whilst ZIP7 activation by CK2 influences agonist-evoked $[Zn^{2+}]_i$ increases, it does not influence $[Ca^{2+}]_i$ elevation. This suggests a difference between the mechanisms responsible for Zn^{2+} and Ca^{2+} handling in response to agonist stimulation in platelets. Furthermore, this data from this section also suggests that ZIP7 mediated $[Zn^{2+}]_i$ elevation from the DTS may be dependent in IP_3R induced $[Ca^{2+}]_i$ elevation since inhibition of IP_3R inhibited ZIP7 activity (Figure 6.3). Therefore store mediated $[Zn^{2+}]_i$ is dependant on store mediated $[Ca^{2+}]_i$ release. However, $[Ca^{2+}]_i$ elevation via IP_3R activation may be independent of ZIP7 induced $[Zn^{2+}]_i$ elevation since inhibition of ZIP7 activity did not influence agonist-evoked $[Ca^{2+}]_i$ elevation.

The interplay between Ca^{2+} and Zn^{2+}, both of which are elevated upon agonist-evoked activation, remains a complex subject to explore.The work carried out in the following section aimed to investigate the influence of these cations on each other in terms of signalling.

6.2.3 Intracellular Zn^{2+} signalling is independent of Ca^{2+} signalling

Experiments to assess changes in $[Zn^{2+}]_i$ described herein were carried out in a Ca^{2}-free environment. It is possible that extracellular Ca^{2+} is able to influence intracellular mechanisms that regulate fluctuations in $[Zn^{2+}]_i$. For example, in a Ca^{2+}-free environment store-operated Ca^{2+} entry (SOCE) is reduced. Furthermore, storage of platelets in a Ca^{2+}-free environment may result in depletion of Ca^{2+} from intracellular stores. This would reduce Ca^{2+} signalling upon platelet activation, possibly enabling a greater potential for Zn^{2+} to act as the major mediator in the activatory signalling pathways.

To explore the influence of extracellular Ca^{2+} on agonist or ionophore avoked Zn^{2+} -mediated platelet activation, measurements of $[Zn^{2+}]_i$ fluctuations were acquired in the presence of physiological levels (2mM) of extracellular $Ca^{2+.}$ 2mM extracellular Ca^{2+} did not influence the changes in FZ-3 fluorescence following stimulation with CRP-XL or U46619 (Figure 6.6A, C). FZ-3 F/F_0 in response to CRP-XL (1µg/mL) after 6mins in the absence and presence of 2mM extracellular Ca^{2+} were 2.2±0.1 and 1.81±0.20, respectively ($p>0.05$, ns, Figure 6.6A, C). FZ-3 F/F_0 in response to U46619 (10µM) stimulation for 6mins, in the presence absence of 2mM Ca^{2+} was 1.34±0.20 and 1.30±0.03, respectively ($p>0.05$, ns, Figure 6.6A, C). As expected, extracellular Ca^{2+} also had no influence on thrombin-induced FZ-3 fluctuations, as thrombin stimulation was previously shown to not result in FZ-3 responses (Figure 6.6A, C).

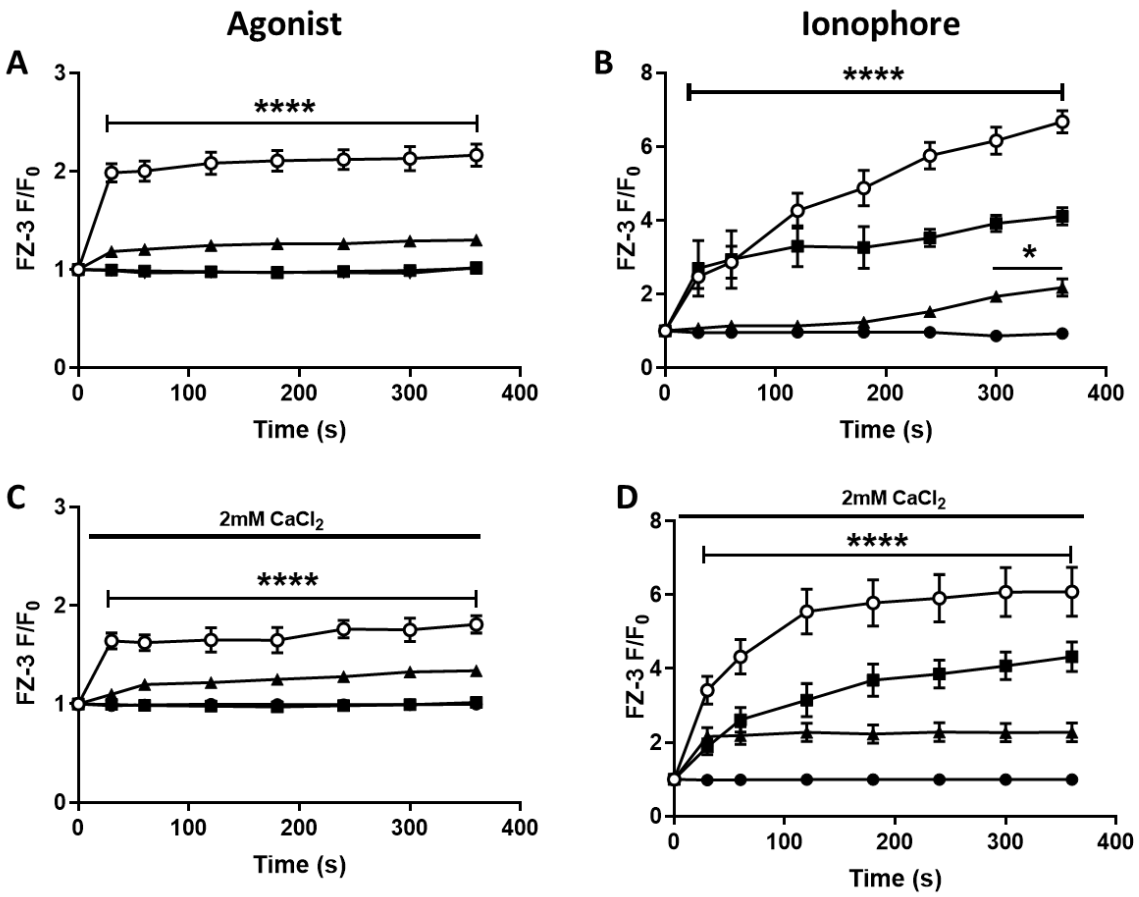

Figure 6.6. Agonist or ionophore evoked increases of FZ-3 in the presence of 2mM $CaCl_2$. Fluozin-3 (FZ-3) loaded washed platelets were stimulated with platelet agonists in the absence (A) or presence (C) of extracellular Ca^{2+} (2mM calcium chloride, $CaCl_2$). CRP-XL (1µg/mL, ○), U46619 (10µM, ▲), Thrombin (1U/mL, ■), vehicle control (DMSO) ●. Fluozin-3 (FZ-3) loaded washed platelets were stimulated with ionophores in the absence (B) or presence (D) of 2mM $CaCl_2$; Clioquinol (○, 300µM), Pyrithione, (■, 300µM), A23187 (▲, 300µM), or vehicle control (DMSO) ● . Changes in FZ-3 fluorescence were monitored. Data are mean±SEM of 5 independent experiments. Significance is denoted as **** ($p<0.0001$), *** ($p<0.001$), ** ($p<0.01$) or * ($p<0.05$).

Extracellular 2mM $CaCl_2$ also did not significantly influence ionophore-induced increases in FZ-3 fluorescence. FZ-3 F/F_0 after 6mins in response to Cq (300µM), Py (300µM) or A23187 (300µM) in $CaCl_2$-free medium were 6.7±0.3, 4.1±0.2 and 2.2±0.2, respectively (Figure 6.6B), whereas in the presence of 2mM $CaCl_2$ (Figure 6.6B) these were 6.10±0.70, 4.32±0.40 and 2.30±0.30, respectively ($p>0.05$, ns, Figure 6.6B, D). therefore, ionophore evoked Zn^{2+} signalling is not influenced by exogenous Ca^{2+}. Conversely, A23187 evoked FZ-3 increase was apparent after 30s of stimulation before reaching a plateau in the presence of 2mM $CaCl_2$, whereas in the absence of $CaCl_2$ fluctuations

in FZ-3 were only apparent towards the end of the experiment. Although the end point FZ-3 fluorescence values in response to A23187 did not differ in relation to Ca^{2+} concentration these data show that the presence of exogenous Ca^{2+} results in increases in FZ-3 at an earlier stage in response to A23187. This may be due to the coordination of Zn^{2+} by A23187.

Published work has shown that exogenous Zn^{2+} is able to mediate platelet activation (Taylor and Pugh, 2016; Watson et al., 2016). High concentrations of extracellular Zn^{2+} (300µM) directly activates platelets, whilst lower concentrations (30µM) are subactivatory. In order to investigate whether agonist stimulation potentiates Zn^{2+}-entry into platelets, experiments were performed in the presence of sub-activatory concentrations of Zn^{2+} (Watson et al., 2016). The comparison between exogenous Ca^{2+} or exogenous Zn^{2+} on $[Zn^{2+}]_i$ elevations was of interest to study the potential interplay between these cations.

Supplementation with 30µM $ZnSO_4$ elevated CRP-XL or U46619-mediated Fz-3 fluorescence above levels that were achieved in the absence of extracellular Zn^{2+}. Interestingly, stimulation with thrombin in the presence of 30µM Zn^{2+} also increased Fz-3 fluorescence, indicating that thrombin-mediated simulation results in increased penetrance of extracellular Zn^{2+} into the platelet cytosol. This activation-dependent Zn^{2+} entry mirrors Ca^{2+}-entry as a result of activation-dependent gating of TRP channels (ROCE, receptor-operated Ca^{2+} entry) on the platelet surface and store-operated Ca^{2+} entry (SOCE, Figure 1.10). F/F_0 in response to thrombin (1U/ml) after 6 mins of stimulation was significantly increased from 0.9±0.3 to 1.7±0.1 upon supplementation with 30µM $ZnSO_4$ ($p<0.0001$, Figure 6.7A, C). The F/F_0 in response to U46619 (10µM) after 6 mins of stimulation was significantly increased from 1.4±0.1 to 2.1±0.2 upon supplementation with 30µM $ZnSO_4$ ($p<0.01$, Figure 6.7B). The F/F_0 in response to CRP-XL (1µg/ml) after 6mins in the presence and absence of exogenous Zn^{2+} was 2.7±0.2 and 4.2±0.3 ($p<0.01$, Figure 6.7A, C)).

These data indicate that activation by all agonists tested results in entry of Zn^{2+} from the extracellular medium to contribute to increases in $[Zn^{2+}]_i$. This may indicate a conserved mechanism which regulates Ca^{2+} entry channels. It is possible that these include canonical Ca^{2+} channels, through which Zn^{2+} has previously been shown to be conducted (for example TRP channels). Further work would be required to confirm the mechanism.

Supplementation with 30µM of $ZnSO_4$ resulted in faster increases in FZ-3 fluorescence induced by the Zn^{2+} ionophores relatively to non-supplemented platelets. Cq-induced FZ-3 fluorescence in the first 30s of treatment, with a plateau being reached at an earlier stage compared to non-

supplemented platelets. The FZ-3 F/F_0 in response to Cq with 30µM of $ZnSO_4$ present after 30s was 7.3± 1.0 which was significantly higher than when no exogenous Zn^{2+} was present (1.4±0.3, $p<0.0001$ Figure 6.7B, D). These data support the proposed mechanism of Cq as an ionophore, as the increased availability of Zn in the media enables increased Cq mediated-Zn^{2+} entry followed by equilibration. However, the endpoint fluorescence induced by Cq in the presence and absence of extracellular Zn^{2+} did not significantly differ. After 6 mins, FZ-3 F/F_0 induced by Cq (300µM), after 6.2±0.7 whereas upon supplementation 30µM of $ZnSO_4$ was 7.9±1.0 ($p>0.05$, ns, Figure 6.7B, D). This may be due to an equilibrium state of Zn^{2+} reached within platelets; thus no further increases in FZ-3 fluorescence were observed.

Conversely, FZ-3 fluorescence induced by Py did however significantly increase upon $ZnSO_4$ (30µM) supplementation. After 6 mins, FZ-3 F/F_0 in response to Py (300µM) was significantly increased from 3.7±0.3 to 7.6±0.6 ($p<0.01$, Figure 4.1B, Figure 6.7B). These data provide further validation of the mechanism of Py as a suitable ionophore, as Py was able to mediate Zn^{2+} entry into the platelets.

Supplementation of Zn^{2+} also resulted in a significant increase in A23187 induced FZ-3 fluorescence in comparison to when no exogenous Zn^{2+} was present. This may be due to the potential for A23187 to act as a Zn^{2+} ionophore (in addition to being a Ca^{2+} ionophore), resulting in more Zn^{2+} being transported into the platelets. Conversely, increased $[Ca^{2+}]_i$ as a result of A23817 treatment may regulate cation entry channels on the platelet surface to mediate further Zn^{2+} entry. The FZ-3 F/F_0 following 6 mins of treatment with A23187 (300µM) was significantly increased from 1.7±0.2 to 2.7±0.3 ($p<0.05$, Figure 6.7B, D).

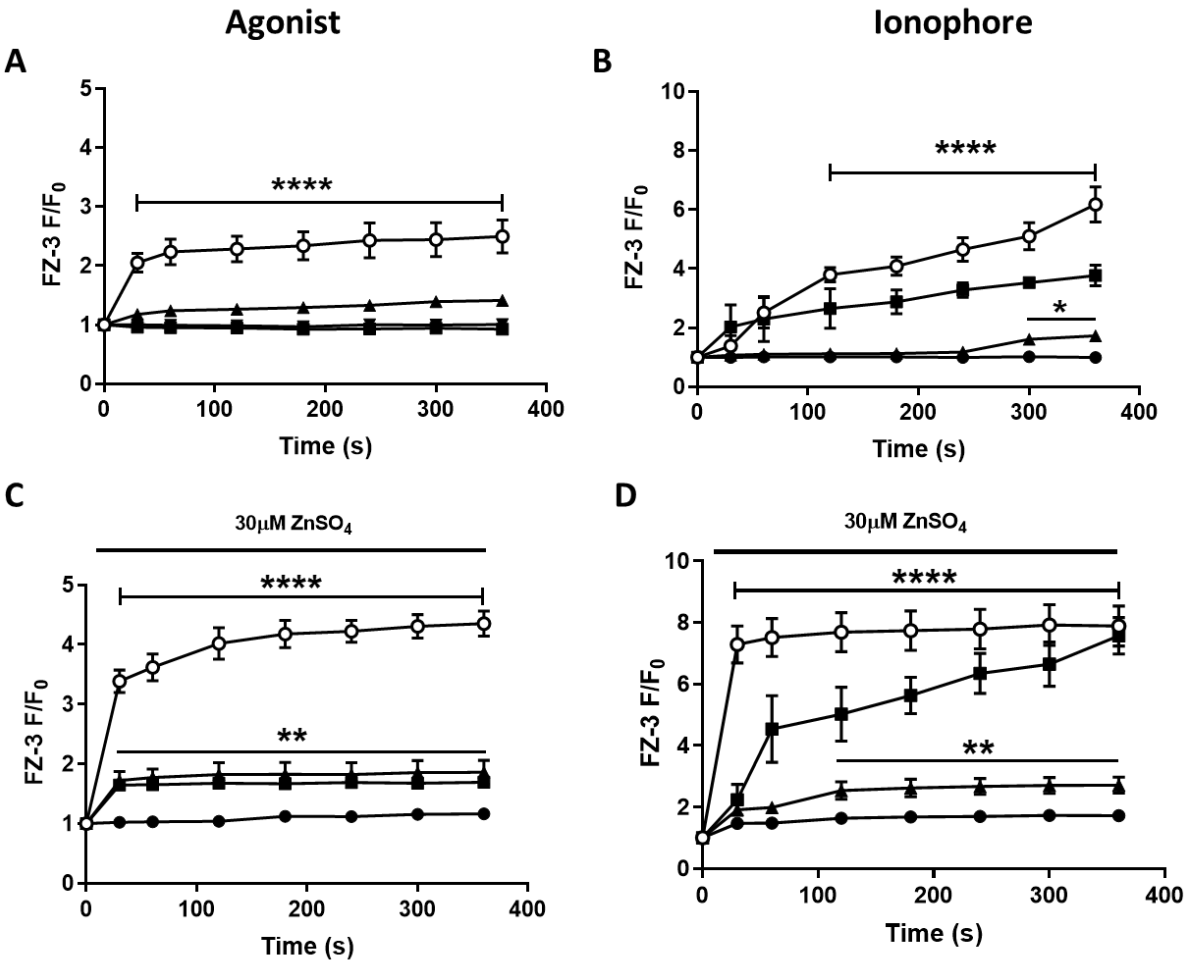

Figure 6.7. Agonist or ionophore evoked increases of FZ-3 are influenced by subactivatory levels of extracellular Zn^{2+}. Fluozin-3 (FZ-3)-loaded washed platelets suspended in CFT buffer supplemented with 30μM $ZnSO_4$ were stimulated with platelet agonists in the absence (A) or presence (C) of extracellular Zn (30μM $ZnSO_4$); CRP-XL (1μg/mL, ○), U46619 (10μM, ▲), Thrombin (1U/mL, ■),Vehicle control (DMSO) ●. FZ-3-loaded washed platelets suspended in CFT buffer supplemented with 30μM $ZnSO_4$ were stimulated with ionophores in the absence (B) or presence (D) of extracellular Zn^{2+} (30μM $ZnSO_4$) ; Clioquinol (○, 300μM), Pyrithione, (■, 300μM), A23187 (▲, 300μM), Vehicle control (DMSO) ● during which changes in Zn^{2+} fluorescence were monitored. Data are mean±SEM of 5 independent experiments. Significance is denoted as **** ($p<0.0001$), *** ($p<0.001$), ** ($p<0.01$) or * ($p<0.05$).

Further experiments were carried out to assess the influence of extracellular Ca^{2+} on $[Ca^{2+}]_i$ fluctuations evoked by the agonists and ionophores. This work served as a positive control to assess if extracellular Ca^{2+} entry is being mediated by agonist into the platelets, which has been demonstrated in the literature (Brüne and Ullrich, 1991; Lang et al., 2013; Pozzan et al., 1988; Xia et al., 2015).

As expected agonist-mediated $[Ca^{2+}]_i$ elevation was increased throughout the experiment in the presence of extracellular 2mM $CaCl_2$, as a consequence of store-operated calcium entry (SOCE) as well as activation-dependent gating of TRP channels such as TPC6 (Figure 1.10). The FL-4 F/F_0 in response to CRP-XL (1µg/ml), U46619 (10µM) or Thrombin (1U/ml) after 6mins increased from 1.7±0.3, 1.5±0.1 and 3.9±0.3, respectively to 4.42±0.57, 2.90±0.34 and 6.21±0.80, upon supplementation with 2mM $CaCl_2$ ($p<0.01$, Figure 6.8A, C).Thus these findings are consistent with SOCE as described previously in the literature, and validate the approach used to investigate Zn^{2+}-operated store entry here (Authi, 2007; Hassock et al., 2002; Lang et al., 2013; Varga-Szabo et al., 2009; Xia et al., 2015).

2mM $CaCl_2$ did not significantly influence ionophore-induced Ca^{2+} release. The FL-4 F/F_0 induced by Cq (300µM), Py (300µM) or A23187 (300µM) were 1.7±0.2, 1.47±0.10 and 6.9±0.9, respectively (Figure 6.8B). These values did not the significantly differ values upon supplementation of 2mM $CaCl_2$, where the FL-4 F/F_0 induced by Cq (300µM), Py (300µM) or A23187 (300µM) was 1.52±0.10, 1.41±0.20, 7.80±0.73, respectively ($p>0.05$, ns, Figure 6.8B, D).

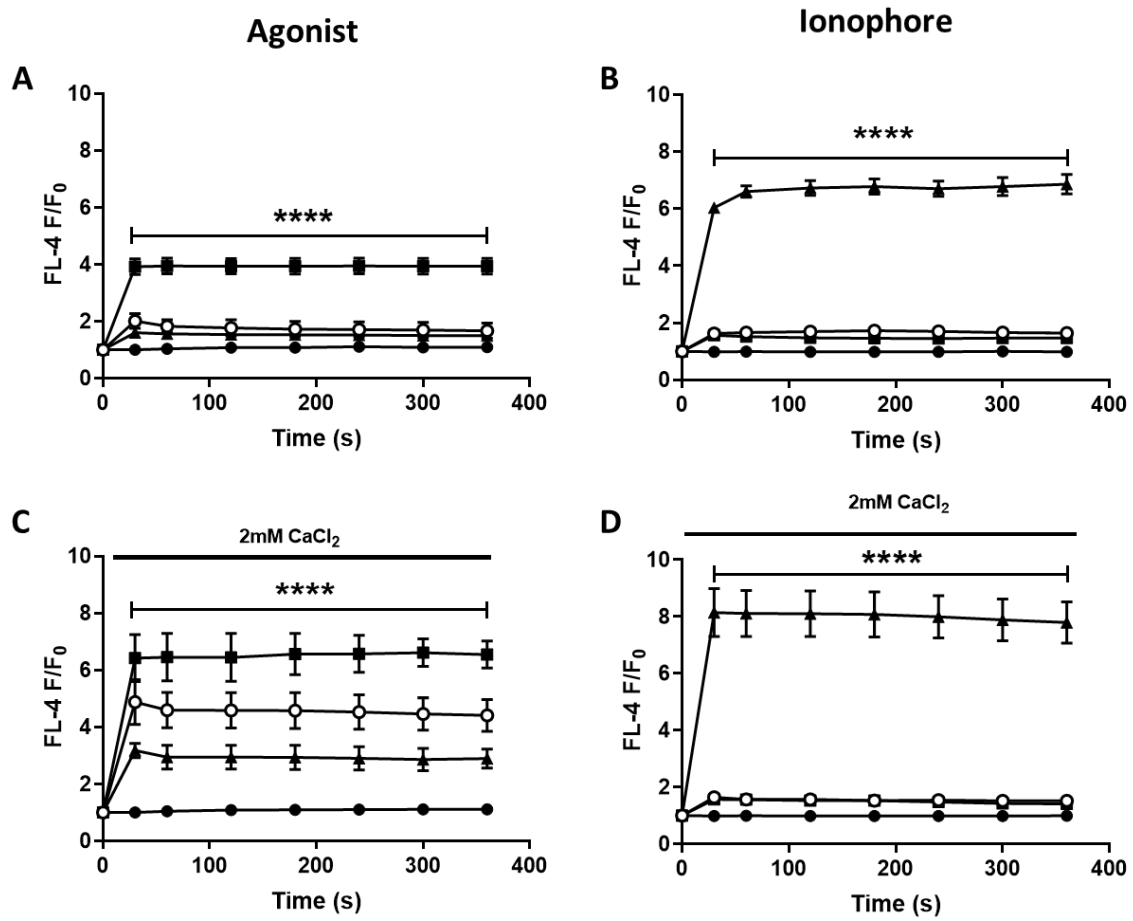

Figure 6.8. Agonist but not ionophore evoked increases of FL-4 are increased in the presence of extracellular 2mM $CaCl_2$. Fluo-4 (FL-4) loaded washed platelets were stimulated with platelet agonists in the absence (A) or presence (C) of extracellular Ca^{2+} (2mM $CaCl_2$); CRP-XL (1µg/mL, ○), U46619 (10µM, ▲), Thrombin (1U/mL, ■), or vehicle control (DMSO) ●. Fluo-4 (FL-4) loaded washed platelets were stimulated with ionophores the absence (B) or presence (D) of 2mM $CaCl_2$; Clioquinol (○, 300µM), Pyrithione, (■, 300µM), A23187 (▲, 300µM), or vehicle control (DMSO) ● during which changes in FL-4 fluorescence were monitored. Data are mean±SEM (n=5) independent experiments. Significance is denoted as **** (p<0.0001), *** (p<0.001), ** (p<0.01) or * (p<0.05).

The absence of A23187-mediated increases in FL-4 fluorescence in the presence of extracellular $CaCl_2$ could reflect saturation of the FL-4 probe with Ca^{2+}. Under such circumstances, $CaCl_2$ supplementation may have had a negligible effect on and increases in fluorescence of this probe. Interestingly exogenous Ca^{2+} did not have any significant influence on the low elevation of FL-4 fluorescence induced by the Zn^{2+} ionophores. This further indicated the specificity of the Zn^{2+} ionophores Cq and Py for Zn^{2+} as these Zn^{2+} ionophores did not act as Ca^{2+} carriers in these experiments since no increase in FL-4 fluorescence was observed with exogenous Ca^{2+} supplementation.

Fluctuations in $[Ca^{2+}]_i$ in the presence of extracellular Zn^{2+} were assessed to determine whether Zn^{2+} entry into platelets was able to regulate Ca^{2+} homeostasis.

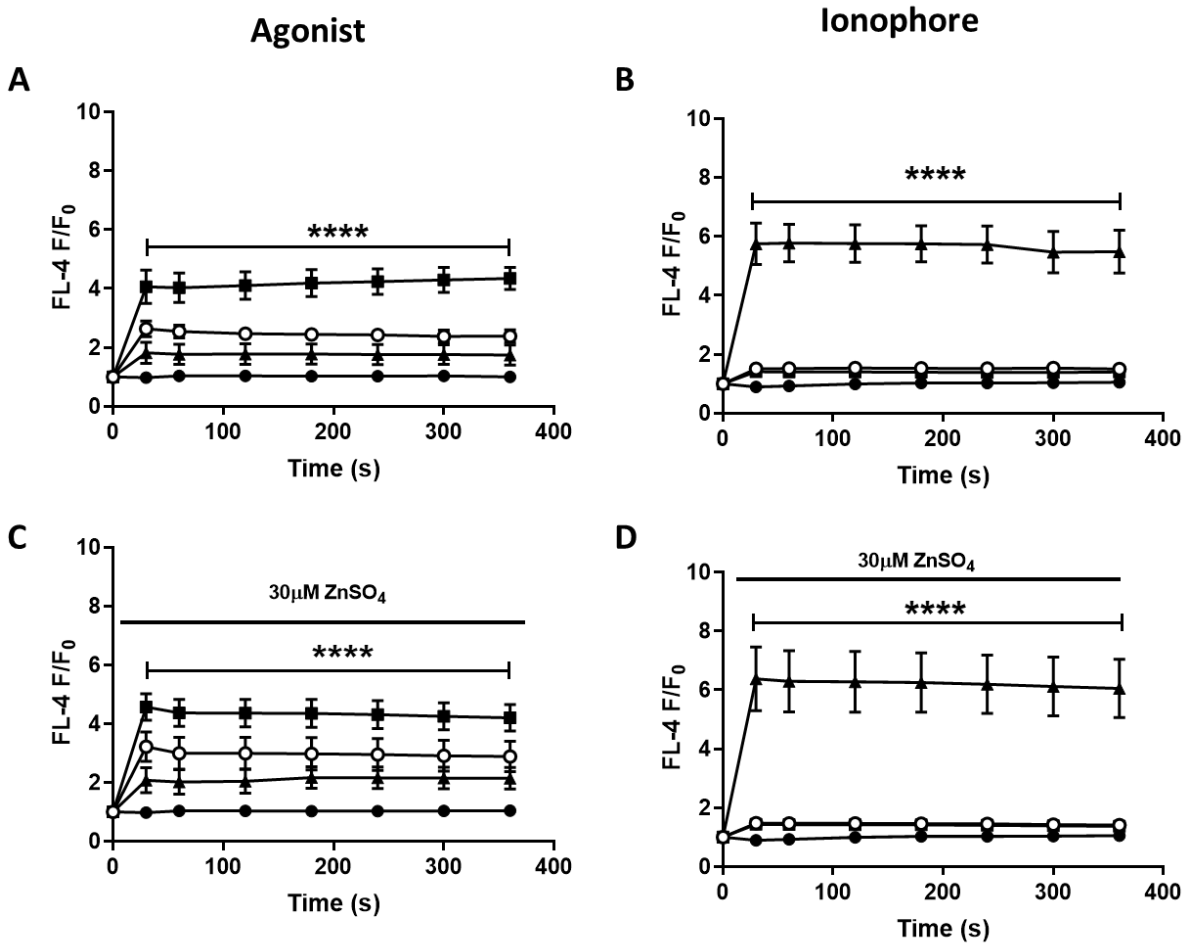

Figure 6.9. Agonist or ionophore evoked increases of FL-4 are not influenced upon supplementation with sub-activatory levels of exogenous Zn^{2+}. Fluo-4 (FL-4) loaded washed platelets were stimulated with platelet agonists in the absence (A) or presence (C) of extracellular $ZnSO_4$; CRP-XL (1μg/mL, ○), U46619 (10μM, ▲), Thrombin (1U/mL, ■), or vehicle control (DMSO) ●. Fluo-4 (FL-4) loaded washed platelets were stimulated with, ionophores the absence (B) or presence (D) of 30μM $ZnSO_4$; Clioquinol (○, 300μM), Pyrithione, (■, 300μM), A23187 (▲, 300μM), or vehicle control (DMSO) ● during which changes in FL-4 fluorescence were monitored. Data are mean ± SEM of 5 independent experiments. Significance is denoted as **** ($p<0.0001$), *** ($p<0.001$), ** ($p<0.01$) or * ($p<0.05$).

Supplementation with 30μM of $ZnSO_4$ did not significantly affect agonist-evoked FL-4 fluorescence levels. The FL-4 F/F_0 induced by CRP-XL (1μg/ml), U46619 (10μM), or thrombin (1U/ml) after 6mins in the presence of 30μM $ZnSO_4$ were 3.2±0.6, 4.2±0.5 and 2.2±0.4 respectively (Figure 6.9A). These did not significantly differ to results obtained in the absence of extracellular Zn^{2+}, where the final F/F_0 evoked by CRP-XL (1μg/ml), U46619 (10μM), or thrombin (1U/ml) were 3.1±0.6, 2.1±0.6

and 4.4±0.4 ($p>0.05$, ns, Figure 6.9A, C). This data shows that exogenous Zn^{2+} does not influence agonist-mediated elevations of $[Ca^{2+}]_i$.

Supplementation with 30µM $ZnSO_4$ did not influence ionophore-induced increases in Ca^{2+} fluorescence. The FL-4 F/F_0 after 6 mins in response to Cq (300µM), Py (300µM) or A23187 (300µM) in the presence of 30µM $ZnSO_4$ were 1.42±0.10, 1.40±0.10, 6.10±1.04 and 1.10±0.10, respectively (Figure 6.9B). This compared to 1.5±0.1, 1.4±0.1 and 5.5±0.8, respectively on unsupplemented platelets does not differ ($p>0.05$, ns, Figure 6.9B, D)

These experiments demonstrate that agonist-evoked increases in Zn^{2+} signalling occur in the presence of exogenous Ca^{2+}, as agonist evoked Zn^{2+} was not influenced upon application of exogenous Ca^{2+} at physiological. This is an important observation, as it further indicates that platelet activity in response to Zn^{2+} reagents is not an artefact of Ca^{2+}-dependent processes.

6.2.4 Store-Operated Zn^{2+} Entry (SOZE) enables Zn^{2+} entry into platelets

The mechanisms that mediate $[Ca^{2+}]_i$ elevations in platelets are well documented. SOCE is a major mechanism employed by platelets to enable entry of Ca^{2+} into the platelets and to replenish Ca^{2+} stores that are depleted upon platelet activation $[Ca^{2+}]_i$ elevation upon stimulation is crucial for platelet activity. It was hypothesised that similar mechanisms may be available to regulate $[Zn^{2+}]_i$ mobilisation from stores in platelets. In a similar manner to Ca^{2+} entry during SOCE, potential Zn^{2+} stores may also require Zn^{2+} entry into the platelets to increase $[Zn^{2+}]_i$ regulating activatory events, or alternatively replenishment of store Zn^{2+} which may be depleted following platelet activation. Recent work by Watson et al., 2016, found that Zn^{2+} gains entry into platelets from the extracellular medium. However, the mechanisms which enable Zn^{2+} entry into platelets is yet to be identified. Furthermore, the work described in section 6.2.3 showed that supplementation of exogenous Zn^{2+} resulted in increased FZ-3 upon agonist stimulation (Figure 6.8). Interestingly, thrombin treatment also resulted in increases in FZ-3 fluorescence, indicating that thrombin stimulation activates Zn^{2+} entry pathways. This novel finding is suggestive of a similar process to SOCE (Figure 1.10), in which store depletion results in Zn^{2+} entry (termed Store-Operated Zn^{2+} Entry, SOZE). Further work was carried out this section to test the hypothesis that SOZE operates as an activatory process in platelets.

Thapsigargin (TG) is widely used to investigate Ca^{2+} influx and the SOCE process in platelets. TG inhibits Ca^{2+} uptake into the Ca^{2+} stores by inhibiting the sarcoplasmic/endoplasmic reticulum Ca^{2+} ATPase (SERCA) which pumps Ca^{2+} back into the DTS (Brüne and Ullrich, 1991; Islam and Berggren, 1993). As it blocks SERCA without playing an inhibitory effect on the plasma membrane calcium

ATPase (PMCA), TG treatment effectively results in the depletion of the DTS, therefore, evoking SOCE via STIM1 and ORAI1 (Islam and Berggren, 1993; Lang et al., 2013; Pozzan et al., 1988; Xia et al., 2015).

FZ-3- or FL-4-loaded platelets were assessed in real time using flow cytometry (section 2.10, Chapter 2) over a 6 min time period in the presence of exogenous Zn^{2+} (30µM $ZnSO_4$) or Ca^{2+} (2mM $CaCl_2$). Application of TG (1µM) resulted in significant increases in FZ-3 fluorescence when exogenous Zn^{2+} was present, compared to experiments conducted in the presence of exogenous Ca^{2+} or in the absence of cations (via treatment with the potent cation chelator EGTA, (2mM) Figure 6.11). The peak F/F_0 upon addition of TG (1µM) in the presence of exogenous Zn^{2+} was 3.1±0.3 which was significantly higher than the vehicle control (EGTA treatment, 1.1±0.1) or in the presence of exogenous Ca^{2+} (1.2±0.1, $p<0.0001$, Figure 6.10B). Exogenous Ca^{2+} did not significantly effect TG-evoked fluctuations of FZ-3, providing further evidence of the specificity of FZ-3 to Zn^{2+}.

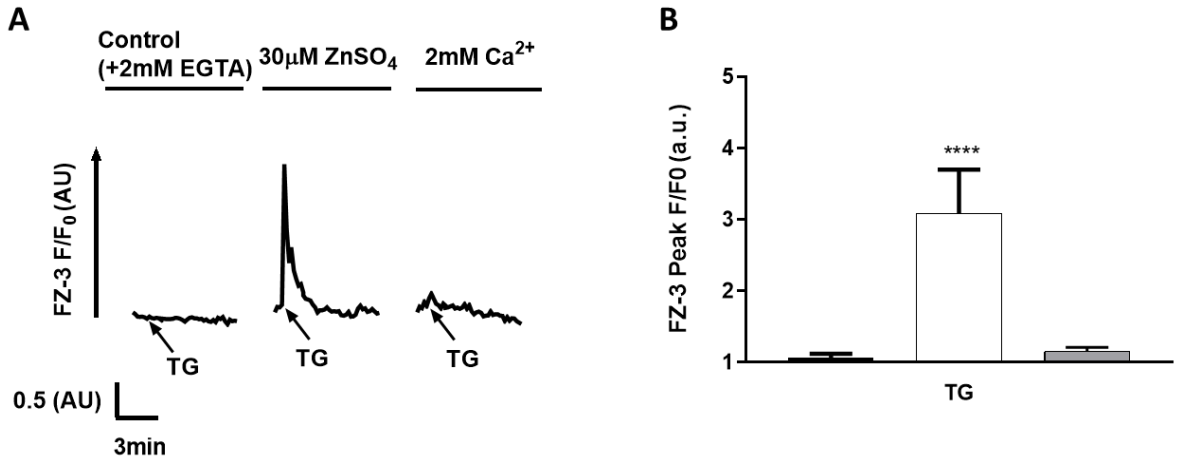

Figure 6.10. Thapsigargin treatment results in increases in FZ-3 fluorescence in the presence of extracellular Zn^{2+}. Fluorescence changes in Fluozin-3 (FZ-3) loaded washed human platelets were observed for 30s prior to treatment with thapsigargin (TG, (1µM). Experiments were performed in the absence of cations (2mM EGTA, control), in buffer containing 30µM $ZnSO_4$, or in buffer containing 2mM $CaCl_2$. Representative peak traces are shown (A), and the fluorescent peaks are quantified (B), ■, Control (2mM EGTA), □,30µM extracellular $ZnSO_4$, ■,2mM extracellular $CaCl_2$. TG treatment induced a significant increase in FZ-3 fluorescence, consistent with store-operated Zn^{2+} entry. Significance is denoted as **** ($p<0.0001$), *** ($p<0.001$), ** ($p<0.01$) or * ($p<0.05$). Data are representative of 6 independent experiments.

Similar experiments were performed to assess FL-4 fluctuations in response to TG treatment in the presence of exogenous cations. TG treatment resulted in greater FL-4 fluorescence compared to either the vehicle control or Zn^{2+} supplementation. The peak FL-4 F/F_0 induced upon the addition of

TG (1μM) in the presence of exogenous Ca^{2+} was 5.4±0.5 which was significantly higher the vehicle control (1.2±0.2), or in the presence of exogenous Zn^{2+} (1.7±0.4, p<0.0001, Figure 6.11B).

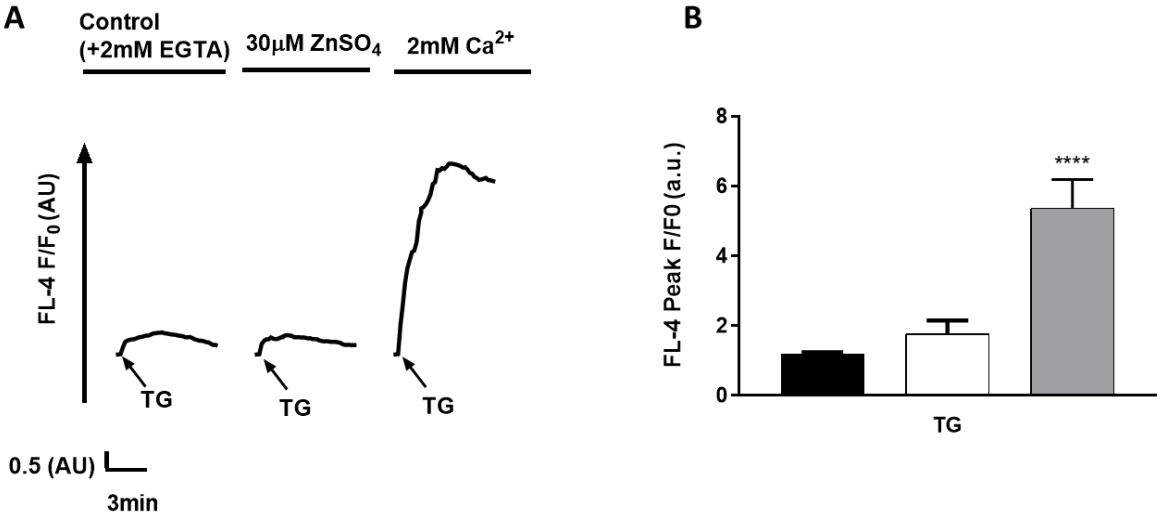

Figure 6.11. Thapsigargin treatment results in increases in FL-4 fluorescence in the presence of extracellular Ca^{2+}. Fluorescence changes in Fluo-4 (FL-4) labelled washed human platelets were observed for 30s prior to treatment TG (1μM). Experiments were performed in the absence of cations (2mM EGTA), in buffer containing 30μM $ZnSO_4$, or in buffer containing 2mM $CaCl_2$. Representative peak traces are shown (A) and Fluorescent peaks were quantified (B), ■, Control (2mM EGTA), □,30μM extracellular $ZnSO_4$, ■,2mM extracellular $CaCl_2$. TG treatment induced a significant increase in Fluo-4 fluorescence, which is consistent with SOCE. Significance is denoted as *** (p<0.001), ** (p<0.01) or * (p<0.05). Data are a representative of 6 independent experiments.

These experiments provide the first description of SOZE as a phenomenon in platelets. Whilst considerable work needs to be done to test this hypothesis further, it is possible that SOZE contributes to platelet activation at sites of vascular injury or plaque rupture, where exogenous Zn^{2+} is increased. Whilst the work described in this section has diverged from the main aims of this thesis, these data provide a platform to further investigate in future projects.

6.3 Discussion

Work described in previous chapters demonstrated that $[Zn^{2+}]_i$ is elevated upon agonist stimulation to mediate platelet processes. This is indicative of behaviour as a secondary messenger in a similar manner to Ca^{2+}. As both intracellular Zn^{2+} and Ca^{2+} are elevated upon activation, the possibility

exists that these two cations may work in synergy during platelet activation. The work in this chapter aimed to further the relationship between Zn^{2+} and Ca^{2+} in platelets.

Initial experiments demonstrated that agonist-evoked $[Zn^{2+}]_i$ increases are sensitive to inhibition of IP_3R, suggesting that Zn^{2+} is mobilised from the Ca^{2+} store (DTS) (Figure 6.1). This indicates that the DTS may contain Zn^{2+} which is co-released with Ca^{2+}, contributing to the elevation of $[Zn^{2+}]_i$. IP_3R inhibition did not completely abolish the agonist-evoked increases in $[Zn^{2+}]_i$ whereas redox modulation did. This implies that elevation of $[Zn^{2+}]$ was primarily mediated by redox modulation and that release from stores such as the DTS may be a secondary source of $[Zn^{2+}]_i$ required for large increases in $[Zn^{2+}]_i$ to regulate activatory processes.

Further experiments were performed to assess $[Ca^{2+}]_i$ fluctuations in response to IP_3R inhibition to assess the validity of the inhibitor used. As expected, agonist-evoked $[Ca^{2+}]$ elevation was abrogated upon 2-APB pre-treatment validating this inhibitor and confirming that agonist-evoked Ca^{2+} increases occur downstream of IP3R activity (including direct release from stores and SOCE). A further complication of the interpretation of these data is that 2-APB has also been shown to inhibit TRP channels in addition to IP_3R. TRP channels present on the external membrane of platelets and act to enable cation entry upon activation. As most experiments described here were performed in a cation-free buffer, the action of TRP channels is not likely to have been significant (Authi, 2007; Hassock et al., 2002).

The release of $[Zn^{2+}]_i$ from 2-APB-sensitive stores was further assessed. The Zn^{2+} transporter ZIP7 mediates Zn^{2+} release in a similar manner to PLC/IP_3R mediated Ca^{2+} and also associates with the membranes of Ca^{2+} stores (in a similar manner to IP_3R) in MCF-7 breast cancer cells (Hogstrand et al., 2013; Taylor et al., 2008). ZIP7 is present in the platelet proteome and may act as a Zn^{2+} release channel in a similar manner as IP_3R for Ca^{2+}. (Burkhart et al., 2012). CRP-XL stimulation resulted in increased phosphorylation of ZIP7, consistent with increased activity of the transporter. This correlates well with the data showing that CRP-XL stimulation results in the highest elevation of $[Zn^{2+}]_I$ compared to other agonists. Interestingly U46619 stimulation did not result in phosphorylation of ZIP7 even though U46619 induces elevation of $[Zn^{2+}]_{i.,}$ However, the increase in $[Zn^{2+}]_i$ induced by U46619 was less than that induced by CRP-XL, which could explain the reduction in phosphorylation. Alternatively, this may indicate heterogeneous response mechanisms. For example, GpVI signalling may regulate the release of Zn^{2+} from stores in conjunction with release from redox-sensitive proteins, whereas U46619 induced $[Zn^{2+}]_i$ elevation may solely be induced upon redox modulation.

Pharmacological inhibitors of ZIP7 are not currently available. However, ZIP7 activity has been shown to be regulated by CK2 (Taylor et al., 2012). Targetting CK2 was therefore performed as a strategy to investigate agonist-evoked changes to ZIP7 activity. In platelets, CK2 is involved in mediating platelet-platelet interactions leading to thrombus formation, and also in by mediating platelet interactions other cells types in the vasculature (Ampofo et al., 2015). Inhibition of CK2 results in a reduction in expression of key adhesion molecules on platelets and endothelial cells such as $\alpha_{IIb}\beta_3$, CD62P, VWF and other vascular cell adhesions molecules (Ampofo et al., 2015). Reduced CK2 activity also inhibits the conversion of fibrinogen to fibrin during the coagulation cascade (Ampofo et al., 2015; Ryu and Kim, 2013). In this chapter Inhibition of CK2 significantly reduced CRP-XL-mediated ZIP7 phosphorylation, confirming that ZIP7 phosphorylation and subsequent activity is downstream of CK2 activity. Inhibition of CK2 also resulted in the inhibition of agonist-evoked FZ-3 fluorescence further indicating a mechanistic relationship between CK2, ZIP7 leading to $[Zn^{2+}]_i$ increases. This data suggest that ZIP7 is involved in the elevation of $[Zn^{2+}]_i$ in a manner similar to that of IP_3R. These ideas are still in their infancy and require further experimental validation, but could represent a mechanism by which platelets become activated.

Further experiments showed that $[Zn^{2+}]_i$ elevation is independent of exogenous physiological levels of Ca^{2+}, as exogenous Ca^{2+} had no significant influence on agonist and ionophore evoked $[Zn^{2+}]_i$ elevation (section 6.2.3). Therefore, Ca^{2+} and Zn^{2+} can induce platelet activation independently, and Zn^{2+} signalling is not biased by an absence of extracellular Ca^{2+}.

Interestingly exogenous Zn^{2+} resulted in increases in FZ-3 fluorescence in response to agonists and in particular thrombin which does not mediate FZ-3 fluctuations (Chapter 3). Therefore these findings are suggestive of a process mirroring ROCE and SOCE (Figure 1.10) , where agonist stimulation results in entry of Zn^{2+} via TRP channels (activation-dependent gated on the platelet surface) and store-operated entry of Zn^{2+} following the depletion from the DTS. Further experiments showed that TG stimulation results in increases in $[Zn^{2+}]_i$ in the presence of extracellular Zn^{2+}, indicating that store depletion opens Zn^{2+}-channels in the platelet membrane permitting Zn^{2+} entry. TG initiates SOCE by blocking the replenishment of the DTS (via the SERCA pumps, Figure 1.10). These findings indicate that SOCE also evoked a Zn^{2+} entry response, however, the exact mechanism by which Zn^{2+} entry occurs is yet to be confirmed. Depletion of cations from the DTS may evoke entry of Zn^{2+} in a similar manner to Ca^{2+}. Thus STIM1 and ORAI1 may be involved in enabling store-operated Zn^{2+} entry.Whilst this is yet to be investigated in platelets, STIM1 which is the Ca^{2+} sensor molecule binds to Ca^{2+} via its EF-hand domain. Interestingly as described earlier in this chapter, Zn^{2+} may also bind to EF-hand domains as

illustrated in other proteins consisting of this motif (Baudier et al., 1986; Mills and Johnson, 1985; Nakayama and Kretsinger, 1994; Schäfer et al., 2000; Schumacher et al., 2004; Y. Wang et al., 2014; Warren et al., 2007b). During the SOCE process, when Ca^{2+} is released from the DTS via the IP3R, Ca^{2+} dissociates from STIM1 which results in the redistribution of STIM1 to the plasma membrane where it interacts with ORAI1 (a Ca^{2+} channel on the membrane which evokes Ca^{2+} entry upon interaction with STIM1) (Hodeify et al., 2015; Lang et al., 2013; Nonato et al., 2016; Varga-Szabo et al., 2009). In this similar manner, Zn^{2+} may also be bound to STIM1 which may dissociate from STIM1 upon DTS induced Zn^{2+} release, thus resulting in STIM1/ORAI1 interactions which may mediate Zn^{2+} entry in addition to Ca^{2+}, although this has not been studied yet and is still very speculative. A more likely explanation could be upon the SOCE process the ORAI1 channels may also be permeable to Zn^{2+}, thus enabling the entry of extracellular Zn^{2+} in addition to Ca^{2+}. However the permeability of ORAI1 for Zn^{2+} has not been shown yet.This is an area which warrants investigation and would provide evidence to elucidate this store-operates Zn^{2+} entry process. A speculative schematic (Figure 6.12) is shown below illustrating this potential mechanism termed as Store-Operated Zn^{2+} Entry (SOZE).

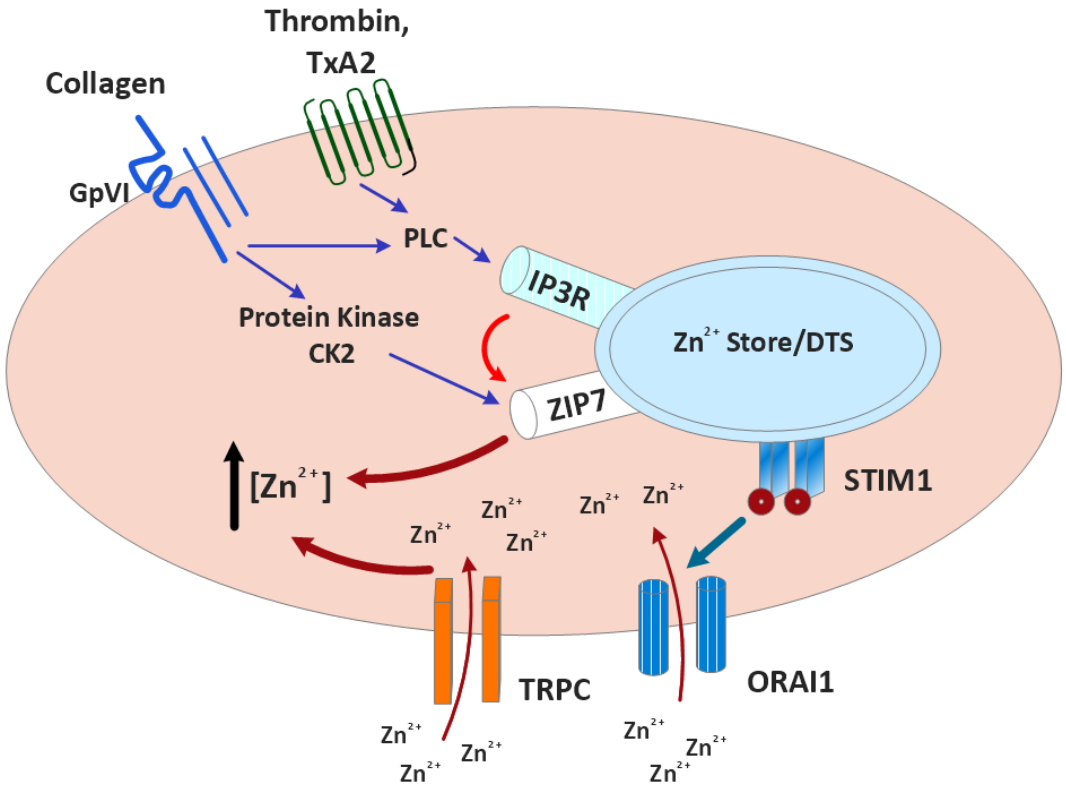

Figure 6.12. Schematic model of store-operated Zn^{2+} entry in platelets. Agonist-induced stimulation results in phospholipase C (PLC) mediated IP_3R activation on the Zn^{2+} store (hypothesised to be the dense tubular system, DTS). IP_3R may contribute to intracellular Zn^{2+} ($[Zn^{2+}]_i$ elevation which may involve ZIP7 activity. ZIP7 is activated by protein kinase CK2

via phosphorylation which is activated upon GpVI stimulation. Following depletion of the DTS , cation entry is evoked in a manner analogous to store operates Ca^{2+} entry (SOCE) termes as store-operated Zn^{2+} entry (SOZE). This would result in Zn^{2+} entry from the extracellular space via ORAI1 channels which may be permeable to Zn^{2+} (unconfirmed). TRP channel (TRPC) may also evoke Zn^{2+} in a manner analogous to receptor operatedd Ca^{2+} entry (ROCE) termed as receptor-operated Zn^{2+} entry (ROZE). SOZE and ROZE may replenish the Zn^{2+} store and also elevate the $[Zn^{2+}]_i$ concentration.

6.3.1 Conclusion

This chapter provided the first reports demonstrating a novel mechanism by which $[Zn^{2+}]_i$ may be elevated in addition to the redox-sensitive mechanism (Chapter 3). ZIP7 may be associated with IP_3R on the DTS, in a manner which is yet to be studied. The association of ZIP7 and IP_3R may evoke the co-release of both Ca^{2+} and Zn^{2+} from the DTS via the IP_3R and ZIP7 respectively. Depletion of the DTS may also evoke SOZE in a similar manner to SOCE. Furthermore, Zn^{2+} signalling was independent of Ca^{2+} which suggested that these two cations may be co-released but modulate platelet function independently of each other. The work carried out in this chapter has provided preliminary novel findings, and provides a platform for a much in-depth investigation into the findings of this chapter.

Chapter 7

7.0 Discussion and Future work

7.1 Discussion

The role of Zn^{2+} as a secondary signalling molecule has received limited research interest, possibly owing to Zn^{2+} being overlooked in favour of Ca^{2+} which is present at much higher concentrations in cells (Faure et al., 1995; Matiaa sa et al., 2010; Woodier et al., 2015). Furthermore many cation ionophores, fluorophores and chelators that have been widely used to investigate Ca^{2+} signalling (including in platelet research), have higher affinities for Zn^{2+} than Ca^{2+}. Therefore, any conclusions drawn from the use of these reagents may be attributable to Zn^{2+}. Thus, the importance of Zn^{2+} has likely been underestimated in platelets. The work described in this thesis provides initial evidence to indicate that Zn^{2+} plays an important role in platelet physiology. Experiments described herein are the first to show agonist-evoked increases of $[Zn^{2+}]_i$ in platelets, resulting in activation-related responses, in a manner consistent with a secondary messenger. The primary aim of this thesis was to investigate the influence of increased Zn^{2+} on platelet activation using Zn^{2+}-specific ionophores. During the course of this work, further aims were developed to investigate agonist-evoked increases in $[Zn^{2+}]_i$, and to investigate the mechanisms of release.

Receptor-specific signalling leads to Zn^{2+} responses

In Chapter 3, it was shown that $[Zn^{2+}]_i$ elevation occurred in response to agonist stimulation. These were the first reports illustrating that there are mobilizable Zn^{2+} stores in platelets that are accessible upon agonist stimulation. These findings implicate Zn^{2+} as a modulator of in platelet activity, consistent with observations from previous studies using exogenous Zn^{2+} as an agonist (Watson et al., 2016). Elevations of $[Zn^{2+}]_i$ in platelets occurred following stimulation of GpVI and TP, but not PAR stimulation (Figure 3.1), indicating that $[Zn^{2+}]_i$ elevation is regulated via differing signalling pathways.

Differences in Zn^{2+} handling as a result of GpVI or PAR stimulation

Signalling downstream of GpVI results in a tyrosine phosphorylation signalling cascade of platelet proteins involving Syk and LAT, which leads to the activation of PLCγ2 and intracellular Ca^{2+} mobilisation (Dunster et al., 2015; Gibbins et al., 1998; Judd et al., 2002; Nieswandt and Watson, 2003). This process was observed in experiments described in Chapter 3, which illustrated $[Ca^{2+}]_i$

increases following GpVI stimulation. Increases in Zn^{2+} as a result of GpVI stimulation may indicate conserved cation release pathways that mediate both $[Zn^{2+}]_i$ and $[Ca^{2+}]_i$ release.

Whilst PAR stimulation resulted in $[Ca^{2+}]_i$ increase, it did not have an effect on $[Zn^{2+}]_i$. Engagement of PARs, therefore, initiates a different signalling cascade than that induced by GpVI. Current understanding is that PAR induced signalling culminates in the activation of PLCβ, leading to Ca^{2-} mobilisation from the DTS. These findings suggested that, unlike Ca^{2+}, the elevation of $[Zn^{2+}]_i$ is independent of PAR and may therefore be attributable to a different signalling pathway. PAR stimulation via thrombin induced a larger $[Ca^{2+}]_i$ elevation than GpVI (Figure 3.2). It is possible that large $[Ca^{2+}]_i$ increases induced upon thrombin treatment negatively regulate $[Zn^{2+}]_i$ elevation. This may occur due to both Ca^{2+} and Zn^{2+} competing for similar signalling pathways, for example as both of these cations able to bind to similar motifs (such as the EF-hand domain) in signalling proteins such as calmodulin (Mills and Johnson, 1985; Schumacher et al., 2004; Warren et al., 2007b). Thus, greater elevation of $[Ca^{2+}]_i$ induced by thrombin (PAR stimulation) relative to that induced by CRP-XL (GpVI stimulation) may be evoking Ca^{2+} to outcompete Zn^{2+} and perhaps negatively regulate Zn^{2+} signalling. These findings also suggest that GpVI signalling could be linked to a specific Zn^{2+} response which does not involve Ca^{2+} which is yet to be identified.

TP but not PAR evoked increases in $[Zn^{2+}]_i$. This observation is difficult to reconcile, as both receptors engage similar signalling pathways which couple to $G_\alpha12/13$ and $G_\alpha q$. In the same manner, as PAR induced signalling, TP evoked signalling also results in the activation of PLCβ, leading to Ca^{2-} mobilisation from the DTS. This scheme was confirmed in experiments described in Chapter 3, which showed Ca^{2+} release in response to U46619 and thrombin and validates the observation of heterogeneous Zn^{2+} responses to different agonists. Due to the similar signalling pathways evoked by TP and PAR stimulation, it is difficult to currently provide speculation as to why the Zn^{2+} response evoked upon stimulation of these GPCR's differ. However, the work from this thesis suggests that there are likely to be differential mechanisms that are differentially regulated by Zn^{2+} upon TP and PAR stimulation, suggestive of a specific Zn^{2+} response independent of PAR signalling.

These findings provided the first reports suggesting a novel GpVI or TP dependant signalling pathway which mediates $[Zn^{2+}]_i$ elevation. This potential novel signalling pathway warrants further investigation and provides a new platform to assess the platelet physiology, which in turn would contribute to the development of antiplatelet therapies.

The mechanism of agonist-evoked intracellular Zn^{2+} release

Modulation of the platelet redox state regulated $[Zn^{2+}]_i$ fluctuations in a similar manner to that seen in nucleated cells (Krezel et al., 2007; Li et al., 2016b). Whilst ROS is commonly associated with oxidative stress and cellular damage, by modulating protein thiols via oxidation such as catalytic cysteines in protein tyrosine phosphatases, it has also been shown to act as a secondary messenger (Chen et al., 2009; Wu et al., 2005). ROS evoked $[Zn^{2+}]_i$ elevation is known to occur in neurons, where it is tightly regulated via redox-sensitive proteins such as metallothionines (MTs) (Hardyman et al., 2016). MTs play a major role in the hemostasis of Zn^{2+}, and under reducing conditions readily sequester Zn^{2+} (Stork and Li, 2016). Thus, the elevation of ROS may have major implications for Zn^{2+} activity in cells, for example in neurons where excessive free Zn^{2+} as a result of increases in ROS can evoke neurotoxicity. The role of ROS in modulating $[Zn^{2+}]_i$ is likely to be translated into platelets, as redox-sensitive proteins such as MTs, which have found to be present in platelets, may be responsive to changes in redox and regulate $[Zn^{2+}]_i$ in platelets.

Changes in redox states occur in response to fluctuations in ROS, where increases in ROS result in oxidative stress (Ferroni et al., 2012; Freedman, 2008; Sies, 2014). Antioxidants such as superoxide dismutase (SOD) and catalase (CAT) were used to regulate ROS levels and maintain reducing conditions (Beckman et al., 1988; Machtay et al., 2006; Pandya et al., 2013; Tainer et al., 1983). GpVI- or TP- dependent stimulation resulted in increases of $[Zn^{2+}]_i$ that were sensitive to the platelet redox state. Agonist-induced $[Zn^{2+}]_i$ elevations were abrogated upon antioxidant treatment and were increased upon H_2O_2 application. Published data show that binding of Zn^{2+} to thiols on proteins such as MTs is redox-sensitive, and Zn^{2+} liberation is mediated from the thiol containing proteins upon redox modulation resulting in the elevation of free Zn^{2+} (Andrews, 2001; Hardyman et al., 2016; Krężel and Maret, 2017b). Therefore, redox-sensitive Zn^{2+} binding proteins may act as a storage mechanism for Zn^{2+} in platelets. In contrast, agonist-induced increases in $[Ca^{2+}]_i$ were not influenced by changes in redox states, indicating that Zn^{2+} and Ca^{2+} liberation may be regulated differently in platelets. As the DTS is the primary Ca^{2+} store which is mobilised upon activation and is the primary mechanism for $[Ca^{2+}]_i$ elevation, these data indicate that the DTS is not utilised as a Zn^{2+} store.

Interestingly GpVI induced the greatest ROS increase in comparison to that evoked by thrombin and U46619. This is consistent with GpVI being more able to induce increases in $[Zn^{2+}]_i$, indicating that the two processes may be mechanistically linked. The generation of ROS via GpVI induced activation may evoke the liberation of Zn^{2+} from redox-sensitive proteins. As of yet, the role of Zn^{2+} in GpVI induced ROS generation is yet to be studied, however $[Zn^{2+}]_i$ elevation upon GpVI stimulation may occur in response to ROS elevation.

GpVI-induced activation results in the generation of different ROS such as superoxide anions and hydrogen peroxides which contribute to evoking the full activatory response upon stimulation of GpVI (Krötz et al., 2002; Pignatelli et al., 1998). Generation of ROS upon GpVI activation occurs via the NADPH oxidase (NOX) pathway (Figure 1.8) which is mediated by the adaptor receptor TNF (tumour necrosis factor) adaptor receptor 4 (TRAF4) (Cangemi et al., 2014; Violi et al., 2015). TRAF4 is a binding partner of GpVI in human platelets (Arthur et al., 2011). TRAF4 associated proteins including Hic-5 and the NOX subunit $p47^{phox}$ interact with GpVI (Arthur et al., 2012, 2011). The NOX subunit $p47^{phox}$ generates ROS via the NOX Pathway (Figure 1.8), as $p47^{phox}$ activates the NOX pathway via phosphorylation. Thus the bridging between GpVI and the TRAF4/$p47^{phox}$ complex evokes GpVI-induced ROS generation. Hic-5 which is part of the TRAF4/$p47^{phox}$ complex associates with the Src family tyrosine kinase Lyn, where it is constitutively bound to Lyn via the SH3 domain of Lyn. Lyn plays a key role in propagating GpVI signalling upon activation (Figure 1.3), suggesting a role for this ROS mediating complex in propagating GpVI signalling. In addition to this, previous work has shown that NOX mediated ROS formation initiates Syk activation (Syk activation occurs upon coming into close proximity with ITAM, which occurs following phosphorylation of ITAM by the Src family tyrosine kinases, Figure 1.3). Therefore, it can be suggested that ROS formation during bridging of the TRAF4/$p47^{phox}$/Hic-5 complex mediates the activation of Src family tyrosine kinases, which then results in the activation of Syk. Therefore ROS may play a key regulatory role during GpVI signalling via a TRAF4 mediated pathway involving $p47^{phox}$ and Hic-5. Interestingly TRAF4 consists of Zn^{2+} finger domains which are involved in mediating interactions with other receptors although the full mechanisms and understanding of TRAF4 have still to be confirmed, particularly in platelets (Arthur et al., 2012; Glauner et al., 2002; Rousseau et al., 2011). Although the role of Zn^{2+} has yet to be confirmed in GpVI induced ROS activity, it can be suggested that Zn^{2+} may bind to the Zn^{2+} domains found in TRAF4 and potentially regulate this protein. A potential positive feedback mechanism involving Zn^{2+} and ROS may be in place as initially suggested in Chapter 4. This may involve GpVI evoking ROS formation which would then oxidise redox-sensitive proteins such as metallothioneins (MTs) that sequester Zn^{2+}, resulting in the liberation of Zn^{2+} from MTs (Figure 7.1). Labile Zn^{2+} may then bind to Zn^{2+} domain in TRAF4 which could then further induce GpVI evoked ROS formation. This mechanism is speculative and would require substantial work for confirmation. Furthermore, studies have shown that ROS can target and regulate the phosphatase SHP-2 which is a negative regulator of collagen-induced activation. Production of ROS via GpVI induced TRAF4 mediated pathway is able to induce oxidative inactivation of SHP-2, which enhances phosphorylation of Syk and other proteins in the LAT signalosome (Figure 1.3). Thus ROS elevation can also result in enhanced GpVI mediated

platelets activity (Jang et al., 2014). Interestingly Zn^{2+} has an IC_{50} of 1-2 µM for SHP-2, thus $[Zn^{2+}]_i$ elevation upon agonist-evoked stimulation may regulate SHP-2 to also enhance GpVI induced activation (Dunster et al., 2015; Mazharian et al., 2013). Therefore, ROS and Zn^{2+} upon elevation can both mediate GpVI upregulation of tyrosine phosphorylation induced signal transduction via the inhibition of SHP-2. This proposed mechanism warrants further investigation and serves SHP-2 as a target to assess the role that Zn^{2+} along with ROS is having on this phosphatase during platelet activation.

The NOX pathway also generates TxA_2, following GpVI activation via the p38 MAPK signalling pathway (Figure 1.8), thus mediating further platelet activation via the TP receptor. Interestingly as described above TP stimulation also results in increases in ROS. Although this increase was modest, it is consistent with the modest increases in $[Zn^{2+}]_i$ upon stimulation of this TxA_2 receptor. The mechanism linking TP stimulation to ROS elevation is unclear, although previous studies have also shown that TP stimulation results in ROS elevation in platelets. This has been suggested to occur via the NOX pathway, as inhibition of NOX inhibited ROS elevation upon TP stimulation by U46619 (Begonja et al., 2006, 2005; Tang et al., 2011; Violi and Pignatelli, 2014). The generation of ROS upon TP stimulation requires further work and may be a process which is mediated by Zn^{2+} as work in this thesis showed that chelation of $[Zn^{2+}]_i$ via TPEN abolished U46619 evoked ROS increase.

These findings suggested an interplay between Zn^{2+} and ROS, where increased Zn^{2+} evokes ROS increases and vice versa. This would demonstrate a mechanistic link between these two secondary messengers in platelets. The understanding of ROS activity in platelets is still however limited, thus requires further investigation to elucidate the ROS induced mechanism that is involved in platelet activation which may be primarily dependant on Zn^{2+} as the data suggests from this thesis. Figure 7.1 below presents a schematic of the ROS mediated mechanism that evoked $[Zn^{2+}]_i$ upon agonist stimulation.

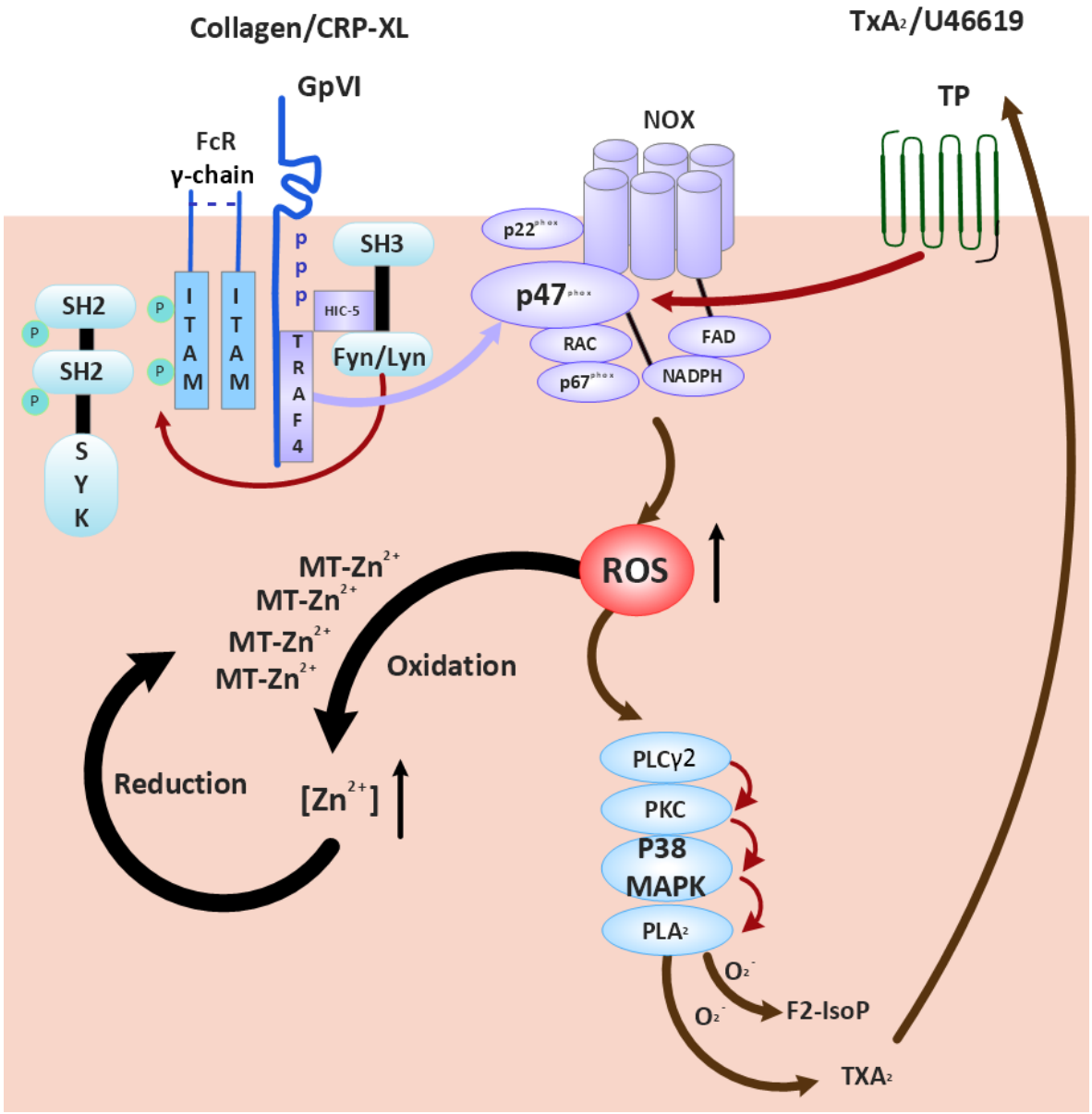

Figure 7.1. General schematic illustrating agonist-evoked intracellular Zn^{2+} elevation upon changes in redox states in platelets. Glycoprotein VI **(**GpVI) or thromboxane A2 receptor (TP) stimulation evokes elevation of reactive oxygen species (ROS). Stimulation of GpVI results in TRAF4 mediated ROS generation via the NADPH oxidase (NOX) pathway. The NOX pathway is activated by the NOX subunit $p47^{phox}$ which is associated with TRAF4 and interacts with GpVI. The NOX complex generates ROS. ROS elevation is able to mediate the PLCγ2/PKC/MAPKp38 signalling cascade resulting in PLA_2 activation. PLA_2 is then able to induce the synthesis of thromboxane A_2 (TXA_2), where F2 isoprostane (F2-IsoP) can also form as a result of oxidation by peroxides. TxA_2 and F2-IsoP can both bind to TP. Stimulation of TP also evokes ROS generation via the NOX pathway. Upon GpVI stimulation, the HIC-5 protein which is associated with TRAF4 is associated with the Src Kinase Lyn and propagates GpVI induced signalling. Elevation of ROS via the NOX pathway upon GpVI and stimulation results in the oxidation of metallothionines (MTs) which then liberate Zn^{2+} from its thiols. Therefore, resulting in increased intracellular Zn^{2+} concentrations. In a reducing environment, Zn^{2+} is sequestered by the MTs via reduction, thus reducing the intracellular Zn^{2+} concentration.

Modest increases in ROS were observed upon thrombin stimulation, which was sensitive to TPEN-mediated chelation of Zn^{2+}. Whilst these data indicate that fluctuations in ROS induced by thrombin were attributable to Zn^{2+}, this is inconsistent with an absence in $[Zn^{2+}]_i$ increases in response to thrombin. It is possible that obligate Zn^{2+}-bound proteins are functionally implicated in ROS regulation. In this scheme, such proteins would not be influenced by changes in $[Zn^{2+}]_i$, but would be affected by Zn^{2+} chelation via TPEN. The nature of such proteins, and whether this mechanism occurs is currently speculative. Recent studies demonstrate that thrombin-evoked ROS increases are dependent on both PAR4 and the membrane protein GPIbα although the exact mechanism and the relationship between ROS and thrombin evoked activation is yet to be elucidated (Carrim et al., 2015).

The findings from this thesis provide evidence to suggest the mechanism that evokes activatory increases in $[Zn^{2+}]_i$ involves GpVI and TP-induced ROS increases within platelets, which culminate in the oxidation of Zn^{2+} sequestering redox-sensitive proteins, resulting in the release of Zn^{2+} into the cytosol. Confirmation of this scheme (illustrated in Figure 7.1) would require significant experimentation, such as examination of changes of the oxidation state of platelet MTs following agonist stimulation. Such experiments are interesting but beyond the scope of the current work.

Investigation of the effects of increased $[Zn^{2+}]_i$ on platelet activatory processes

The influence of $[Zn^{2+}]_i$ on the platelet activation was examined by using membrane permeable Zn^{2+}-specific ionophores, Py and Cq, which have been widely used to model increases in $[Zn^{2+}]_i$ in various cell types (Ding et al., 2005; Franklin et al., 2016; Kim et al., 1999, 1999; Rodríguez-Santiago et al., 2015; Schimmer et al., 2012; Seo et al., 2015). Cq and Py both induced significant increases in $[Zn^{2+}]_i$, where Cq was found to induce a greater elevation than Py (Figure 4.1), suggesting differences between these ionophores. Whilst these are yet to be investigated, one potential difference could be how these ionophores enter platelets, determining whether they could efficiently access Zn^{2+} stores Cq and Py differ structurally. Cq contains halogen groups (which are not present in Py) which increase lipophilicity enabling increases absorption in the cell as shown in neurons (Bush, 2003; Prachayasittikul et al., 2013). Thus Cq may be able to enter the cells more readily than Py and target storage sites. This may explain why Cq was able to induce a greater elevation of $[Zn^{2+}]_i$ than Py. Both of these ionophores only resulted in increases in FZ-3 fluorescence and did not evoke any fluctuations in FL-4, thus demonstrating the specificity of these ionophores to Zn^{2+} and not Ca^{2+}. In contrast, a non-specific effect was seen following application of the Ca^{2+} ionophore A23187. A23187 stimulation resulted in rapid increases $[Ca^{2+}]_i$, but also a modest increase in $[Zn^{2+}]_i$. This is not unexpected because A23187

has also previously shown to be able to bind to Zn^{2+}, and therefore may not be as specific to Ca^{2+} as previously thought (Sakanashi et al., 2009). However, A23187 was able to evoke a greater effect in terms of platelet activation such as aggregation and granule release (discussed below) than Cq and Py, indicating the greater contribution of Ca^{2+} compared to Zn^{2+} in platelet activation. Experimental differentiation of the effects of the cations is difficult, as the role of Ca^{2+} cannot be solely assessed due to chelators such as BAPTA, which has a high affinity for Zn^{2+} than Ca^{2+}. Therefore, chelating Ca^{2+} to determine if the effects seen were due to Ca^{2+} would also chelate Zn^{2+}. Chelation of Zn^{2+} via the highly specific $[Zn^{2+}]_i$ chelator TPEN would assess the role of Zn^{2+} and enable the effect of Ca^{2+} to be observed in the absence of Zn^{2+}. However, the use of chelators may also result in the stripping of cations from proteins that are always bound to cations which may disrupt the effect seen. Thus, the development of methodologies to assess cation induced activity is required, which may involve the development of more specific probes and chelators which could target specific sites of interest.

In contrast to agonist-induced $[Zn^{2+}]_i$ elevation, ionophore-induced $[Zn^{2+}]_i$ elevation was not redox-sensitive. Additionally, Zn^{2+} ionophore-induced $[Zn^{2+}]_i$ elevation was far greater than that induced by the CRP-XL. This indicates that ionophores can access Zn^{2+} stores that are otherwise inaccessible to conventional agonists. Whilst the existence of an accessible Zn^{2+} store in platelets is yet to be confirmed, a number of potential storage mechanisms are known to exist. These include redox-sensitive Zn^{2+} binding proteins and α-granules which are known to contain Zn^{2+} (Marx et al., 1993b). A potential drawback with the use of ionophores to model $[Zn^{2+}]_i$ elevation is that the level of $[Zn^{2+}]_i$ increases is higher than for conventional agonists. This suggests that ionophore use may not fully represent the physiological situation. Despite this, Zn^{2+} ionophores are a suitable tool to explore Zn^{2+}-dependent mechanisms and the functional role of Zn^{2+}.

The work described in Chapter 5 was designed to examine the functional role of increased $[Zn^{2+}]_i$ in different aspects of platelet behaviour. Elevation of $[Zn^{2+}]_i$ following ionophore stimulation induced upregulation of $\alpha_{IIb}\beta_3$, which is required for platelet aggregation (Bennett et al., 1999; Chari-Turaga and Naik, 2011; Nieswandt et al., 2009). This correlates well with aggregation data which shows that elevation of $[Zn^{2+}]_i$ evokes sub-maximal platelet aggregation (submaximal relative to the full aggregation evoked by agonist and a23187). Furthermore, this is consistent with data showing ionophore-induced aggregation was sensitive to the $\alpha_{IIb}\beta_3$ antagonist, GR144053 (Figures 5.1-2, 5.4).

Interestingly Cq, but not Py was able to induce an aggregatory response. However, Py was still able to induce increases in PAC-1 binding which is consistent with $\alpha_{IIb}\beta_3$ upregulation. This finding is difficult to reconcile, as upregulation of $\alpha_{IIb}\beta_3$ is associated with platelet aggregation. Py was found to induce a lower increase in $[Zn^{2+}]_i$ than Cq, which may not be enough to elicit a comparable response. This finding

indicates that high increases $[Zn^{2+}]_i$ are required for platelet aggregation. Differences in effects of the Zn^{2+} ionophores warrants further investigation to determine the differences in the mechanism of these two Zn^{2+} ionophores; however, it is worth noting that neither ionophore was supplemented with exogenous Zn^{2+}. A23187, which induced full platelet aggregation induced a reduction in PAC-1 binding in platelets that had been subjected to Zn^{2+} chelation with TPEN. This was again difficult to reconcile as chelation of $[Zn^{2+}]_i$ had no influence on the aggregatory response evoked by A23817 (Figure 5.1). However, it is probable that TPEN may also be stripping of Zn^{2+} from proteins that Zn^{2+} would bind in an obligate manner (i.e. always bound), results in a loss of function of proteins that would be independent of $[Zn^{2+}]_i$ fluctuations. Furthermore, Since A23187 also evoked a modest increase in $[Zn^{2+}]_i$ in a similar manner to Py, it can also be suggested that low increases in $[Zn^{2+}]_i$ may not elicit an aggregatory response but may potentiate this response instead. This was shown in previous work where low concentrations of exogenous Zn^{2+} potentiated agonist-evoked aggregatory responses (Watson et al., 2016). Further work carried out in Chapter 5 elucidated the role of $[Zn^{2+}]_i$ in platelet aggregation which further coincided with the work by Watson et al., (2016), as chelation of $[Zn^{2+}]_i$ reduced the level of PAC-1 binding induced by the conventional agonists (CRP-XL, U46619 and thrombin, Figure 5.12). Therefore, further outlining the importance that Zn^{2+} has on platelet aggregation, although the exact mechanism by which Zn^{2+} mediates platelet aggregation response is yet to be confirmed.

Elevation of $[Zn^{2+}]_i$ resulted in increases tyrosine phosphorylation of proteins, further indicating the potential of Zn^{2+} to modulate platelet behaviour. Tyrosine phosphorylation is a major signalling event in platelets, that can lead to full activation. Zn^{2+}-dependent Increases in tyrosine phosphorylation may indicate Zn^{2+}-dependent changes to the activatory state of phosphatases or kinases, some of which have previously been shown to be sensitive to Zn^{2+}. For example, protein tyrosine phosphatases such as SHP-1 (Src homology 2 (SH2) domain-containing tyrosine phosphatases) and SHP-2 have IC_{50} values of 93nM and 1-2µM respectively for Zn^{2+} thus may be modulated upon $[Zn^{2+}]_i$ elevation. These phosphatases are known to be activated upon GpVI stimulation, where SHP-1 is a positive regulator of platelet activation via $\alpha_{IIb}\beta_3$ activation, and SHP-2 negatively regulates platelet activation. Since GpVI has also been demonstrated to evoke increases in $[Zn^{2+}]_i$ in this thesis, these phosphatases which are modulated upon GpVI stimulation may be as a result of increased $[Zn^{2+}]_i$. Therefore, it can be suggested that GpVI induced regulation of platelet activation may be mediated by Zn^{2+}. Increases in redox dependant GpVI induced $[Zn^{2+}]_i$ elevation may regulate SHP-2 thus resulting in enhanced GpVI induced activity. Furthermore, SHP-2 phosphatase was found to regulate GpVI signalling in a redox-sensitive manner (Jang et al., 2014) as discussed above. Elevation of ROS upon GpVI stimulation may result in increased $[Zn^{2+}]_i$ which may also regulate SHP-2 in addition to increased ROS. Thus the relationship between ROS and Zn^{2+}

upon elevation via GpVI stimulation could play a key role in further mediating GpVI induced signalling and platelet activation further. Further assessment would be required to determine the activity of these phosphatases in response to Zn^{2+} and provides a platform to assess a potential new regulatory signalling pathway in platelets. Kinases such as protein kinase C (PKC) and Ca^{2+}/calmodulin dependent kinase II (CaMKII) have been shown to be influenced by Zn^{2+} (Csermely et al., 1988; Hubbard et al., 1991b; Lengyel et al., 2000). However, whether this occurs in platelets is not known. It could be speculated that increases in Zn^{2+} could lead to the activation of PKC, (which plays a central role in platelets in mediating a wide range of activatory processes in platelets such as aggregation and granule release, (Yacoub et al., 2006),) and CaMKII which plays a significant role in Ca^{2+} signalling, Millon-Frémillon et al., 2013; Vostal et al., 1991). This would result in increased platelet activity, suggesting a mechanism by which Zn^{2+} is able to evoke platelet activity. Thus, these findings provide initial reports demonstrating that these kinases may also be influenced in platelet activity which plays major roles in evoking platelet activation in response to increased $[Zn^{2+}]_i$. Further work is required to determine the role of Zn^{2+} in influencing kinases in additions to phosphatases, which may serve to elucidate novel mechanism in platelet physiology.

Platelet shape change is mediated by cytoskeletal rearrangement in the initial steps of upon platelet activation. $[Zn^{2+}]_i$ elevation via ionophore stimulation resulted in shape change, which could be inhibited by Cyt-D treatment, verifying the shape-changing response as biological and not a non-specific chemical, response (Figure 5.5). Chelation of $[Zn^{2+}]_i$ also inhibited the spreading of platelet spreading on fibrinogen, indicating a key role for $[Zn^{2+}]_i$ in platelet shape change, which may be attributable to outside-in signalling (Figure 1.7). These data implicate Zn^{2+} in the functional regulation of cytoskeletal rearrangement. The extent and significance of the role of Zn^{2+} is currently unknown. It is possible that increases in $[Zn^{2+}]_i$ are an absolute requirement for the initiation or propagation of shape change. However, specific targets of Zn^{2+} are as yet unknown. $[Zn^{2+}]_i$ has been found play a major role in regulating cytoskeletal changes in nucleated cells (Perrin et al., 2017b; Rudolf et al., 2008b). Chelation of $[Zn^{2+}]_i$ using TPEN in HeLa and prostate cancer (PC)-3 cell lines suppresses the formation of filopodia and stress fibres as a result of actin rearrangement in repose to H_2O_2. H_2O_2 stimulation results in the elevation of FZ-3 fluorescence, which is consistent with increases in $[Zn^{2+}]_i$, which was associated with activation of the TRP channel TRMP2 in these cell types (Li et al., 2016). Furthermore, in this study, application of the Zn^{2+} ionophore Py increased cell migration, which was inhibited upon TPEN pretreatment. This study confirms a role for Zn^{2+} in actin rearrangement that mediates filopodia and stress fibre formation and cellular migration. The mechanism by which Zn^{2+}

regulates cytoskeletal changes is yet to be confirmed. Cellular cytoskeletal arrangement involves Rho family GTPases such as RhoA. It is possible that Zn^{2+} may influence this process via interaction with these proteins, however again this yet to be studied and serves as a platform to assess the role of Zn^{2+} in cytoskeletal changes in these cells which have been shown play a major role thus far (Li et al., 2016a).

Zn^{2+} has also been shown to regulate tubulin polymerisation in neurons, as incubation of neuronal cells in Zn^{2+} deficient media results in impaired transport of the transcription factor NFAT (nuclear factor of activated T cells) due to a loss of tubulin polymerisation (Mackenzie and Oteiza, 2007; Perrin et al., 2017a). The mechanism by which Zn^{2+} regulates tubulin polymerisation in neurons is yet to be elucidated. However previous work in rodent neurons has shown the association of Zn^{2+} and tubulin and the ability of Zn^{2+} to stimulate tubulin polymerisation (Hesketh, 1982). These studies further illustrate the role that Zn^{2+} has on cytoskeletal rearrangement in cells.

In Chapter 5 it was found that chelation of $[Zn^{2+}]_i$ in mouse embryonic fibroblasts (MEF) resulted in a loss of attachment and cellular spreading. Zn^{2+} may be involved in regulating the affinity state of integrins in these cells since chelation of $[Zn^{2+}]_i$ in MEF prevented adhesion. Inside out signalling evokes the activation of integrins which is essential for adhesion (Calderwood, 2004), thus $[Zn^{2+}]_i$ may play a key role in regulating inside out activation of these MEF cells. This correlates with showing that TPEN also inhibits platelet adhesion and spreading, which suggested that Zn^{2+} may play a role in regulating integrins via the outside in and inside out signalling process in platelets (Figure 1.5-6). These findings support published work from in nucleated cells illustrate the importance of Zn^{2+} in regulating cytoskeletal changes as Zn^{2+} has been shown to regulate a number of processes induced upon cytoskeletal rearrangement including filopodia and stress fibre formation, tubulin polymerisation, adhesion and spread and are suggestive of conserved mechanisms. Identification of a reported role of Zn^{2+} in regulating cytoskeletal rearrangement in nucleated cells further implicates a similar role for Zn^{2+} in platelets as shown in this thesis and discussed above. However, the mechanism by which Zn^{2+} mediates changes in the cytoskeletal in platelets is currently unknown, however, may involve the regulation of signalling process including Rho GTPases such as RhoA and integrins which are known to evoke actin rearrangement during cytoskeletal remodelling and adhesion in nucleated cells (Chauhan et al., 2011).

One potential mechanism for Zn^{2+} induced cytoskeletal derangement in platelets involves the regulation of cytoskeletal proteins. Here, $[Zn^{2+}]_i$ elevation was found to induce increased phosphorylation of MLC. MLC phosphorylation occurs in response to activated MLCK and is able to induce changes actin dynamics. Published work has shown that platelet shape change occurs in a Ca^{2+}-

dependent manner that involves activation of the Ca^{2+}-binding protein calmodulin, which then enables activation of MLCK resulting in MLC phosphorylation (Kamiya et al., 2014; Shin et al., 2017). Additionally, platelet shape change involves the Rho-associated coiled-coil-containing kinases (ROCK) which regulate phosphorylation of MLC by inhibiting MLC phosphatases (MLC-P) (Paul et al., 1999). The data discussed in Chapter 5 indicates that $[Zn^{2+}]_i$-induced shape change occurs via a signalling pathway independent of calmodulin and was found to be mediated by a Ca^{2+}-independent signalling pathway which involves Rho-associated coiled coil-containing kinases (Figure 5.16). This is an interesting finding because it indicates that Zn^{2+} is not simply substituting for Ca^{2+}, for example, EF hands of calmodulin to regulated canonical downstream responses. The target of increased Zn^{2+} here is not known. The association of Zn^{2+} and ROCK serves as the major mechanism by which Zn^{2+} induced shape change occurs, however, the role for Zn^{2+} in ROCK signalling is yet to be confirmed. Although previous studies in endothelium cells have shown that ROCK consists of a Zn^{2+} binding motif (Bernal et al., 2011) suggests a potential role for Zn^{2+} in ROCK, as the binding of Zn^{2+} to this motif in ROCK may regulate the activity of ROCK. However, this relationship between Zn^{2+} and ROCK is still to be confirmed and warrants further investigation.

$[Zn^{2+}]_i$ did not induce phosphorylation of VASP, which indicated that $[Zn^{2+}]$ signalling was independent of cyclic nucleotide-dependent kinases such as PKG or PKA which have previously been shown to regulate platelet shape change (Aburima et al., 2013).

The elevation of $[Zn^{2+}]_i$ induced externalisation of dense granules but not α-granules. This was apparent upon chelation of $[Zn^{2+}]_i$ on experiments which measure granule release in response to conventional agonists. The signalling pathways that contribute to the differential release of α and dense granules are not fully understood. However, the work carried out this thesis provides a novel avenue which involves Zn^{2+} to further investigate the degranulation mechanisms (Golebiewska and Poole, 2015; Heijnen and Sluijs, 2015). Current understanding of signalling that evoked granule release in platelets involves several signalling events some of which include Ca^{2+} signalling, PKC dependent phosphorylation, integrin signalling, TxA2 generation and GTPase signalling. Granule release mediates enhanced platelet activation and also facilitates the recruitment of nearby platelets to the growing thrombus. All of these signalling pathways interlink during platelet activation and may potentially have Zn^{2+} implicated as a regulatory cation. The relationship between Zn^{2+} and Ca^{2+} is central to the work described in this thesis. The interplay between the two cations may have implications for intracellular signalling. For example, PKC, which is known to play a central role in platelet activation, is influenced by Zn^{2+} (Csermely et al., 1988). Therefore Zn^{2+} might be affecting platelet activity via direct PKC

activation. Integrin outside in and inside out signalling has also been suggested to be regulated by Zn^{2+}. Redox-sensitive GpVI signalling which is mediated by Zn^{2+} is also involved in TxA_2 generation (Figure 7.1). Here, GTPase signalling in particular ROCK signalling during platelet shape change was shown to be regulated by Zn^{2+}. Thus the potential regulatory role of Zn^{2+} in these signalling events suggests a potential regulatory role for Zn^{2+} inducing granule release. Further work is required to investigate each of these signalling events further to investigate the finding that $[Zn^{2+}]_i$ elevation only evoked dense granule and not α- granule release.

Differential regulation of cytoskeletal elements may serve as a mechanism to determine the $[Zn^{2+}]$-dependent differential granule release. *In vitro* studies have shown that granule secretion is accompanied by centralisation of the granules which is driven by actin and myosin-driven contractile forces (Gerrard and White, 1976; Morgenstern et al., 1984). Since Zn^{2+} regulates cytoskeletal rearrangement in platelets, Zn^{2+}-induced cytoskeletal rearrangement during platelet shape change may evoke centralisation of granules. This may explain the mechanism as to how Zn^{2+} mediated dense granule release but does not correlate with the absence of α granule release in response to Zn^{2+}. Interestingly previous work shows that the exposure of high concentrations of actin-disrupting agents (cytochalasins) inhibit α-granule release in response to agonists whereas dense granule release is enhanced in response to agonists (Flaumenhaft et al., 2005). These findings illustrated that the platelet cytoskeleton serves as a regulator of granule release and since Zn^{2+} has been found to potentially play a regulatory role in cytoskeletal remodelling in this thesis, these findings from this previous study (Flaumenhaft et al., 2005) provide a mechanism by which $[Zn^{2+}]_i$ elevation is inducing dense granule secretion but not α-granule secretion. Without knowing more about differential granule secretion in platelets, it is difficult to reconcile these observations, and further work is required. Interestingly whilst α granules have been shown to contain Zn^{2+} (Marx et al., 1993b),modulation of $[Zn^{2+}]_i$ had no effect on α granule release. This is also difficult to reconcile but could highlight mechanistic differences in differential granule release.

$[Zn^{2+}]_i$ elevations induce PS exposure, in a manner that is partially mediated by caspases. This is consistent with previous work which has shown that apoptosis which is measured by PS exposure is evoked by Zn^{2+} , particularly in nucleated cells such (Eron et al., 2018; Hamatake et al., 2000; Iitaka et al., 2001; Treves et al., 1994). Although the exact mechanism by which Zn^{2+} does this is yet to be confirmed, as Zn^{2+} regulates apoptosis in caspase independent and dependent manners, and remains an area with much scope to investigate (Hamatake et al., 2000; Zhang et al., 2014). Thus, these findings from previous work in nucleated cells, further strengthen a role for Zn^{2+} in inducing PS exposure in platelets, as illustrated by the findings in this thesis. This implicates a role for Zn^{2+} in mediating

initiation or propagation of the pro-coagulant pathway (Figure 1.1). Whilst the mechanism by which Zn^{2+} induced PS exposure in platelets is yet to be confirmed, a potential mechanism may involve the Ca^{2+} dependent scarambalase which has been identified as TMEM16F (transmembrane protein 16F) in platelets (Suzuki et al., 2013; van Kruchten et al., 2013; Yang et al., 2012). Scramblase facilitates the translocation of PS from the inner to the outer membrane in a Ca^{2+}-dependent manner (Figure 1.7). The scramblase protein, TMEMF16 protein may also be sensitive to activation by other cations such as Zn^{2+}. Furthermore, TMEMF proteins consist of a Ca^{2+} binding site which coordinates the activity of the protein (Brunner et al., 2014), which in the case of TMEMF16 would be PS exposure which. This binding site may also serve as a binding site for Zn^{2+}, as Ca^{2+} binding bindings sites such as the EF-hand domain have also been shown to occupy Zn^{2+} for example in calmodulin (Mills and Johnson, 1985; Warren et al., 2007b). Therefore, Zn^{2+} may also occupy the Ca^{2+} binding site in TMEMF16, which provides a potential mechanism by which Zn^{2+} mediates PS exposure. Interestingly, TMEM16F behaves as a non-selective cation channel during lipid scrambling. Its mechanism of action may, therefore, relate to Zn^{2+} translocation (Yang et al., 2012).

Whilst the mechanism by which TMEMF16 mediates PS exposure is still unclear, significant data are presented here to hypothesis an as yet unstudied role for Zn^{2+} in this process.

The interplay between Zn^{2+} and Ca^{2+} during platelet activation

Finally, the work described in Chapter 6 addressed the interplay between Zn^{2+} and Ca^{2+} signalling in platelets. The conclusions from this work are that Zn^{2+} signalling works independently of Ca^{2+}, as exogenous Ca^{2+} at physiological levels had no influence on agonist-evoked $[Zn^{2+}]_i$ increases. This demonstrates that these two cations may independently regulate platelet activity. This is an important observation, as it further indicates that platelet activity in response to Zn^{2+} reagents is not an artefact of Ca^{2+}-dependent processes. Furthermore, data from Chapter 6 suggests that whilst Zn^{2+} is released from intracellular stores in a similar manner to Ca^{2}+, it potentially involves ZIP7, perhaps working synergistically with IP_3R on the DTS. A novel mechanism termed SOZE (Store-Operated Zn^{2+} Entry) was proposed from this work, as agonists were able to evoke Zn^{2+} entry upon activation (Figure 6.12). In this scheme, reduction of Ca^{2+} stores following platelet activation results in the opening of cation channels on the platelet membrane surface (such as Orai or TRPC6). This leads to Zn^{2+} entry in a similar manner to Ca^{2+} entry. Zn^{2+} entering from the cytosol would then activate platelets in a similar manner to that previously shown with exogenously added Zn^{2+} (Watson et al., 2016). Whilst this is an intriguing possibility, further work is needed to confirm entry pathways, and to determine whether this system operates under conditions of physiological Ca^{2+}. Furthermore, whether membrane Zn^{2+}-

permeable channels or transporters are activated upon agonist stimulation is not known, but remains a possibility during platelet activation. Another possibility is of receptor-operated Zn^{2+} entry (ROZE), which may work in a similar manner to receptor mediates Ca^{2+} entry (ROCE) which occurs following agonist stimulation and results in cation entry via TPC6 channels (Gamberucci et al., 2002; Hassock et al., 2002; Varga-Szabo et al., 2009)].

7.1.1 Conclusion

In conclusion, the experiments described herein provide the first evidence for agonist-evoked increases of $[Zn^{2+}]_i$ in platelets, in a manner consistent with a secondary messenger. $[Zn^{2+}]_i$ elevations in response to GpVI or TP stimulation were found to be sensitive to the platelet redox state, indicative of a role for redox in agonist-evoked Zn^{2+} signalling. Modelling of $[Zn^{2+}]_i$ elevation using Zn^{2+}-specific ionophores demonstrates several functional roles for $[Zn^{2+}]_i$ in platelet activatory processes. $[Zn^{2+}]_i$ signalling was found to mediate key activatory platelet responses such as shape change, $\alpha_{IIb}\beta_3$ activation, dense granule release and PS exposure. The mechanism by which Zn^{2+} affects these platelet processes is yet to be determined, but modulation in the activity of Zn^{2+} binding enzymes could be one explanation. This work also provides the first evidence for SOZE upon agonist stimulation, which has been demonstrated to occur in a similar manner as SOCE in platelets.

The work described in this thesis has provided evidence to suggest a novel regulatory role for labile $[Zn^{2+}]_i$ during platelet activation. Figure 7.2 illustrates the speculative mechanism by which $[Zn^{2+}]_i$ elevation mediates platelet activation.

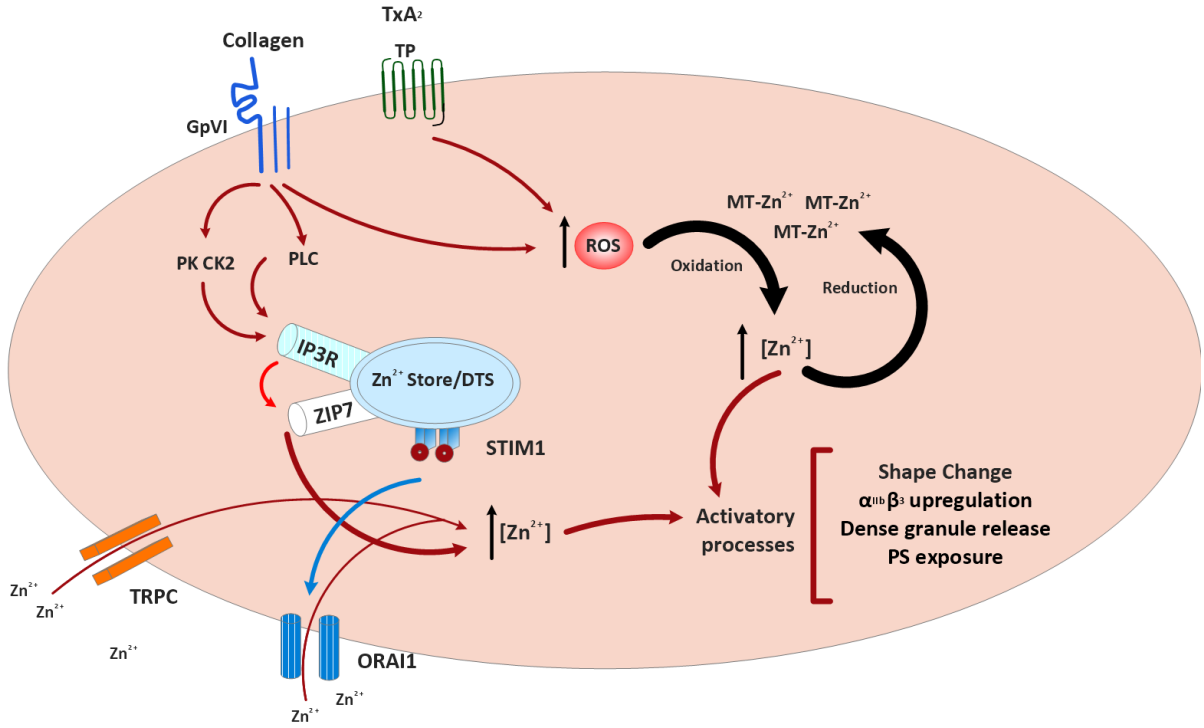

Figure 7.2. Schematic illustrating agonist evoked intracellular Zn^{2+} and its role in mediating platelet behaviour. GpVI and thromboxane A_2 receptor stimulation evoke reactive oxygen species (ROS) elevation. ROS elevation evokes oxidation of Zn^{2+} sequestered metallothioneins (MTs), resulting in the liberation of Zn^{2+} from the MTs and contributing to an increase in intracellular Zn^{2+} ($[Zn^{2+}]$). GpVI stimulation also results in phospholipase C (PLC)-mediated activation of the inositol-1,4,5-trisphosphate receptor (IP_3R activation) which contributes to Zn^{2+} release (whether this is due to conducting Zn^{2+} from the DTS, or from secondary regulation of $[Zn^{2+}]_i$ increases is not known. IP_3R activity contributes to $[Zn^{2+}]_i$ increases which may involve ZIP7. ZIP7 is also activated by the protein kinase CK2 via phosphorylation, which is activated upon GpVI stimulation via unknown mechanisms. Following store depletion (of Ca^{2+}, and possibly also Zn^{2+}), Zn^{2+} entry may occur from the extracellular space via the STIM1 which senses depletion of Zn^{2+} in the store, which then interacts with the cation channel, ORAI1 (Permeability of ORAI1 for Zn^{2+} has not been confirmed). This process is termed as store-operated Zn^{2+} entry (SOZE) and is analogous to store operates Ca^{2+} entry (SOCE). GpVI induced activation also evokes transient receptor channel (TRPC) mediated Zn^{2+} entry in a manner similar to receptor-operated Ca^{2+} entry (ROCE), termed as receptor-operated Zn^{2+} entry. SOZE and ROZE replenish Zn^{2+} stores and elevate $[Zn^{2+}]_i$. Elevated $[Zn^{2+}]_i$ regulates activatory process in platelets such as shape change, $\alpha_{IIb}\beta_3$ upregulation, dense granule release and phosphatidylserine exposure. Whilst this is a speculative model, it provides testable hypotheses to better understand the role of Zn^{2+} in platelet activation.

7.2 Future work

The work described in this thesis provides a number of potential avenues to explore for future work. Primarily, all of the experiments described here were performed in vitro. To understand whether Zn^{2+} is a significant modulator of platelet behaviour, it would be necessary to perform in vivo

work. However, the conclusions reached here that indicate that Zn^{2+} is an important mediator of platelet activation are consistent with previous reports that have shown reduced platelet activity in humans and rodent with dietary Zn^{2+} deficiency. Further *in vivo* studies could result in data being translated clinically to potentially contribute to the development of antithrombotics (Makris et al., 2013).

Quantitation of $[Zn^{2+}]_i$ concentrations

Due to a lack of suitable, commercially available reagents, it was not possible to accurately use ratiometric probes to reliably convert the increases in Zn^{2+} fluorescence to concentrations. Development of more Zn^{2+} probes may enable the determination of the level of $[Zn^{2+}]_i$ which would provide further information on the potential enzymes and thus processes that could be influenced by Zn^{2+}.

Zn^{2+} signalling is independent of PAR induced activation

Whilst U46619-dependent activation resulted in $[Zn^{2+}]_i$ fluctuations, PAR stimulation did not. This observation is difficult to reconcile, given that these receptors engage similar signalling pathways (Boknäs et al., 2014; Brass et al., 1993b; Chen et al., 2013; Zhou et al., 2017). Therefore, potential future work could aim to specifically target the signalling pathways of this agonist and try to differentiation and investigate the reasoning as to TP stimulation but not PAR stimulation results in $[Zn^{2+}]_i$ elevation.

Differences between the Zn^{2+} ionophores, clioquinol (Cq) and pyrithione (Py)

The differences between the Zn^{2+} ionophores Cq and Py could be further investigated as these ionophores were found to have a difference in platelet activity even tho they share the same purpose and approximate affinities to Zn^{2+}. The mechanism which attributes to $[Zn^{2+}]_i$ mediated modulations in platelet process is a major avenue to explore as if determined could potentially provide novel insights into the platelet physiology. Thus understanding and further development of reagents such as Cq and Py is imperative for further assessment of the role of Zn^{2+} in platelet behaviour.

Redox dependant Zn^{2+} signalling

The role of redox-sensitive proteins in platelets warrants further investigated, given that data from this thesis strongly implicated redox-sensitive proteins as a storage mechanism for Zn^{2+}. The expression and role of such proteins such as metallothioneins (MTs) have been shown in platelets.

MTs play an inhibitory role in platelet aggregation; however, its role in platelets is limited. Given that MTs are able to sequester Zn^{2+} (Hardyman et al., 2016; Krezel et al., 2007), MTs serve as a candidate to target to assess if Zn^{2+} storage in platelets is attributable to redox-sensitive proteins.

Further work could also be carried out to investigate the role of Zn^{2+} in NOX-mediated ROS generation, particular following GpVI stimulation. Data described here show that GpVI evokes the greatest increases in $[Zn^{2+}]_i$. This correlates with the potency of GpVI in terms of ROS production, relative to other agonists (Freedman, 2008; Walsh et al., 2014). The role of $[Zn^{2+}]_i$ in GpVI-induced ROS signalling via the NOX pathway is an interesting area to explore and would aid in further understanding the mechanistic link between GpVI induced $[Zn^{2+}]_i$ and intracellular ROS elevation in platelets. Since changes in redox are determined by ROS fluctuations, assessment of the relationship between this mechanistic link serves as a novel platform to determine redox dependant Zn^{2+} signalling.

The TRPM2 (transient receptor potential melastatin 2) which is expressed in platelets may be involved in evoking $[Zn^{2+}]_i$ elevation in platelets in a redox dependent manner. TRPM2 is gated by ROS and is permeable to Zn^{2+} as shown in pancreatic β cells (Manna et al., 2015). This mechanism of action of TRPM2 may also be applicable in platelets. Exogenous ROS may mediate exogenous Zn^{2+} entry and serves as a novel mechanism in platelets. Thus this provides another area to explore to elucidate further Zn^{2+} signalling which may be redox dependent.

The mobilisation of Zn^{2+} from intracellular stores

Identification of ZIP7 on platelets permits the further investigation of this protein in platelet function. The role and location of ZIP7 could be investigated as inhibition of ZIP7 activity via the inhibition of protein kinase CK2 was found to reduce agonist-evoked increases in $[Zn^{2+}]_i$. The investigation of Zn^{2+} in the DTS could also be explored since experiments described here showed that inhibition of IP_3R mediates Ca^{2+} mobilisation influenced ZIP7 activity. These findings are complex and difficult to understand, but allow the development of testable hypotheses. For example, the DTS may also contain Zn^{2+}, and that it may be released from the DTS along with Ca^{2+} albeit by different mechanisms (ZIP7 and IP3R). Pharmacological limitations prevented direct inhibition of ZIP7 activity. Thus indirect activation had to be carried out by targeting the protein kinase CK2 which mediates ZIP7 activity. However, inhibition of this kinase may also have an indirect effect on other processes in platelets which may complicate the conclusions reached. (Taylor et al., 2012, 2008). Thus the development of direct inhibitors of ZIP7 or knockout models of ZIP7 would provide further a way of further asses the role of ZIP7 and $[Zn^{2+}]_i$ release.

Store-operated Zn^{2+} entry (SOZE)

A major avenue of interest is the SOZE process which was proposed in chapter 6 as being analogous to SOCE. SOZE is a novel mechanism which may potentially be applicable in other cell types. SOCE involves STIM1 and ORAI1 which coordinate to detect store depletion and regulate Ca^{2+} entry (Guéguinou et al., 2016; Lang et al., 2013). The influence of Zn^{2+} on STIM1 and ORAI1 is yet to be studied but would be an easy initial target to test SOZE.

Another potential scheme to consider is ROZE, which is analogous the process of ROCE, where DAG mediated TRPC6 entry of Ca^{2+} occurs (Varga-Szabo et al., 2009). TRPC6 is expressed in platelets and is to be permeable to both Zn^{2}+ and Ca^{2+}. Therefore assessment of TRPC6 via pharmacological inhibition or knock out model studies would serve as a way to investigate the role of this channel in mediating Zn^{2+} entry. Furthermore the TRMP7 (transient receptor potential melastatin 7) cation channel may also evoke Zn^{2+} entry in a similar manner to TRPC6, as TRPM7 has been found to be a channel to be highly permeable to Zn^{2+}, even more so than Ca^{2+} in neurons (Inoue et al., 2010; Monteilh-Zoller et al., 2003). TRPM7 is expressed on platelet and megakaryocytes and has been implicated in the regulation of STIM1 activity (Leng et al., 2015; Mammadova-Bach et al., 2019). In previous studies, the deletion of the TRMP7 kinase in mice inhibits agonist-evoked $[Ca^{2+}]_i$ mobilisation as a result of a reduction in STIM1 activity during SOCE (2018). STIM1 activity is regulated via phosphorylation of its serine residues (Kawasaki et al., 2010; Pozo-Guisado and Martin-Romero, 2013). Thus TRPM7 kinase may be regulating STIM1 activity via phosphorylation of the serine residues of STIM1 , this may also apply to ORAI1 which is regulated in a similar manner to STIM1 (Kawasaki et al., 2010; Mammadova-Bach et al., 2019; Pozo-Guisado and Martin-Romero, 2013; Sanjeev K. et al., 2018). The findings from these studies suggest a potential mechanism by which Zn^{2+} may be implicated in the store-operated entry which may involve TRPM7. The function of TRPM7, Zn^{2+} and store-operated entry of cations are yet to be studied; however, TRP7 is another candidate in addition to ZIP7 that could be involved in mediating SOZE and is an area that warrants further investigation.

The mechanism by which Zn^{2+} affects functional responses in platelets

Here, canonical platelet functions, such as $\alpha_{IIb}\beta_3$ upregulation, shape change, dense granule release and PS exposure have been shown to be regulated by Zn^{2+}. Whilst the experiments described here have started to unravel the mechanisms by which Zn^{2+} regulates this mechanism; more work is needed.

In particular, the observation that Zn^{2+} differentially influences dense and alpha granule release provides an opportunity to better understand the differences in the regulation of

degranulation, which at present are poorly understood (Flaumenhaft, 2003; Golebiewska and Poole, 2015; Heijnen and van der Sluijs, 2015).

To summarise Zn^{2+} has been demonstrated to play a major role in platelets, and thus further understanding of the platelet physiology could be evoked by further investigation into the role that Zn^{2+} plays in platelets.

Bibliography

Abbate, V., Reelfs, O., Kong, X., Pourzand, C., Hider, R.C., 2016. Dual selective iron chelating probes with a potential to monitor mitochondrial labile iron pools. Chem. Commun. Camb. Engl. 52, 784–787. https://doi.org/10.1039/c5cc06170a

Abdelhalim, M.A.K., Alhadlaq, H.A., Moussa, S.A., 2010. Elucidation of the effects of a high fat diet on trace elements in rabbit tissues using atomic absorption spectroscopy. Lipids Health Dis. 9, 2. https://doi.org/10.1186/1476-511X-9-2

Abdollahi, A., Shoar, N., Shoar, S., Rasoulinejad, M., 2013. Extrinsic and intrinsic coagulation pathway, fibrinogen serum level and platelet count in HIV positive patients. Acta Med. Iran. 51, 472–476.

Aburima, A., Walladbegi, K., Wake, J.D., Naseem, K.M., 2017. cGMP signaling inhibits platelet shape change through regulation of the RhoA-Rho Kinase-MLC phosphatase signaling pathway. J. Thromb. Haemost. JTH 15, 1668–1678. https://doi.org/10.1111/jth.13738

Aburima, A., Wraith, K.S., Raslan, Z., Law, R., Magwenzi, S., Naseem, K.M., 2013. cAMP signaling regulates platelet myosin light chain (MLC) phosphorylation and shape change through targeting the RhoA-Rho kinase-MLC phosphatase signaling pathway. Blood 122, 3533–3545. https://doi.org/10.1182/blood-2013-03-487850

Achison, M., Joel, C., Hargreaves, P.G., Sage, S.O., Barnes, M.J., Farndale, R.W., 1996. Signals elicited from human platelets by synthetic, triple helical, collagen-like peptides. Blood Coagul. Fibrinolysis Int. J. Haemost. Thromb. 7, 149–152.

Alsted, T.J., Nybo, L., Schweiger, M., Fledelius, C., Jacobsen, P., Zimmermann, R., Zechner, R., Kiens, B., 2009. Adipose triglyceride lipase in human skeletal muscle is upregulated by exercise training. Am. J. Physiol. Endocrinol. Metab. 296, E445-453. https://doi.org/10.1152/ajpendo.90912.2008

Aman, A., Nguyen, M., Piotrowski, T., 2011. Wnt/β-catenin dependent cell proliferation underlies segmented lateral line morphogenesis. Dev. Biol. 349, 470–482. https://doi.org/10.1016/j.ydbio.2010.10.022

Ampofo, E., Müller, I., Dahmke, I.N., Eichler, H., Montenarh, M., Menger, M.D., Laschke, M.W., 2015. Role of protein kinase CK2 in the dynamic interaction of platelets, leukocytes and endothelial cells during thrombus formation. Thromb. Res. 136, 996–1006. https://doi.org/10.1016/j.thromres.2015.08.023

Andre, P., Delaney, S.M., LaRocca, T., Vincent, D., DeGuzman, F., Jurek, M., Koller, B., Phillips, D.R., Conley, P.B., 2003. P2Y12 regulates platelet adhesion/activation, thrombus growth, and thrombus stability in injured arteries. J. Clin. Invest. 112, 398–406. https://doi.org/10.1172/JCI17864

Andreini, C., Bertini, I., 2012. A bioinformatics view of zinc enzymes. J. Inorg. Biochem. 111, 150–156. https://doi.org/10.1016/j.jinorgbio.2011.11.020

Andrews, G.K., 2001. Cellular zinc sensors: MTF-1 regulation of gene expression. Biometals Int. J. Role Met. Ions Biol. Biochem. Med. 14, 223–237.

Aniksztejn, L., Charton, G., Ben-Ari, Y., 1987. Selective release of endogenous zinc from the hippocampal mossy fibers in situ. Brain Res. 404, 58–64.

Apgar, J., 1968. Effect of zinc deficiency on parturition in the rat. Am. J. Physiol. 215, 160–163.

Arman, M., Krauel, K., 2015. Human platelet IgG Fc receptor FcγRIIA in immunity and thrombosis. J. Thromb. Haemost. JTH 13, 893–908. https://doi.org/10.1111/jth.12905

Arslan, P., Di Virgilio, F., Beltrame, M., Tsien, R.Y., Pozzan, T., 1985a. Cytosolic Ca2+ homeostasis in Ehrlich and Yoshida carcinomas. A new, membrane-permeant chelator of heavy metals reveals that these ascites tumor cell lines have normal cytosolic free Ca2+. J. Biol. Chem. 260, 2719–2727.

Arslan, P., Di Virgilio, F., Beltrame, M., Tsien, R.Y., Pozzan, T., 1985b. Cytosolic Ca2+ homeostasis in Ehrlich and Yoshida carcinomas. J. Biol. Chem. 260, 2719–2727.

Arthur, J.F., Gardiner, E.E., Kenny, D., Andrews, R.K., Berndt, M.C., 2008. Platelet receptor redox regulation. Platelets 19, 1–8. https://doi.org/10.1080/09537100701817224

Arthur, J.F., Qiao, J., Shen, Y., Davis, A.K., Dunne, E., Berndt, M.C., Gardiner, E.E., Andrews, R.K., 2012. ITAM receptor-mediated generation of reactive oxygen species in human platelets occurs via Syk-dependent and Syk-independent pathways. J. Thromb. Haemost. 10, 1133–1141. https://doi.org/10.1111/j.1538-7836.2012.04734.x

Arthur, J.F., Shen, Y., Gardiner, E.E., Coleman, L., Murphy, D., Kenny, D., Andrews, R.K., Berndt, M.C., 2011. TNF receptor-associated factor 4 (TRAF4) is a novel binding partner of glycoprotein Ib and glycoprotein VI in human platelets. J. Thromb. Haemost. JTH 9, 163–172. https://doi.org/10.1111/j.1538-7836.2010.04091.x

Aschner, M., Cherian, M.G., Klaassen, C.D., Palmiter, R.D., Erickson, J.C., Bush, A.I., 1997. Metallothioneins in brain--the role in physiology and pathology. Toxicol. Appl. Pharmacol. 142, 229–242. https://doi.org/10.1006/taap.1996.8054

Aslan, J.E., Itakura, A., Gertz, J.M., McCarty, O.J.T., 2012. Platelet shape change and spreading. Methods Mol. Biol. Clifton NJ 788, 91–100. https://doi.org/10.1007/978-1-61779-307-3_7

Assaf, S.Y., Chung, S.-H., 1984. Release of endogenous Zn2+ from brain tissue during activity. Nature 308, 734–736. https://doi.org/10.1038/308734a0

Asselin, J., Gibbins, J.M., Achison, M., Lee, Y.H., Morton, L.F., Farndale, R.W., Barnes, M.J., Watson, S.P., 1997. A collagen-like peptide stimulates tyrosine phosphorylation of syk and phospholipase C gamma2 in platelets independent of the integrin alpha2beta1. Blood 89, 1235–1242.

Aster, R.H., 1967. Studies of the mechanism of “hypersplenic” thrombocytopenia in rats. J. Lab. Clin. Med. 70, 736–751.

Authi, K.S., 2007. TRP channels in platelet function. Handb. Exp. Pharmacol. 425–443. https://doi.org/10.1007/978-3-540-34891-7_25

Authi, K.S., Bokkala, S., Patel, Y., Kakkar, V.V., Munkonge, F., 1993. Ca2+ release from platelet intracellular stores by thapsigargin and 2,5-di-(t-butyl)-1,4-benzohydroquinone: relationship to Ca2+ pools and relevance in platelet activation. Biochem. J. 294 (Pt 1), 119–126.

Bachmann, C., Fischer, L., Walter, U., Reinhard, M., 1999. The EVH2 domain of the vasodilator-stimulated phosphoprotein mediates tetramerization, F-actin binding, and actin bundle formation. J. Biol. Chem. 274, 23549–23557.

Bailey, C.J., 2000. Potential new treatments for type 2 diabetes. Trends Pharmacol. Sci. 21, 259–265.

Bánsághi, S., Golenár, T., Madesh, M., Csordás, G., RamachandraRao, S., Sharma, K., Yule, D.I., Joseph, S.K., Hajnóczky, G., 2014. Isoform- and species-specific control of inositol 1,4,5-trisphosphate (IP3) receptors by reactive oxygen species. J. Biol. Chem. 289, 8170–8181. https://doi.org/10.1074/jbc.M113.504159

Bao, B., Prasad, A.S., Beck, F.W.J., Fitzgerald, J.T., Snell, D., Bao, G.W., Singh, T., Cardozo, L.J., 2010. Zinc decreases C-reactive protein, lipid peroxidation, and inflammatory cytokines in elderly

subjects: a potential implication of zinc as an atheroprotective agent. Am. J. Clin. Nutr. 91, 1634–1641. https://doi.org/10.3945/ajcn.2009.28836

Baranwal, S., Azad, G.K., Singh, V., Tomar, R.S., 2014. Signaling of chloroquine-induced stress in the yeast Saccharomyces cerevisiae requires the Hog1 and Slt2 mitogen-activated protein kinase pathways. Antimicrob. Agents Chemother. 58, 5552–5566. https://doi.org/10.1128/AAC.02393-13

Barceloux, D.G., 1999. Zinc. J. Toxicol. Clin. Toxicol. 37, 279–292.

Baudier, J., Glasser, N., Gerard, D., 1986. Ions binding to S100 proteins. I. Calcium- and zinc-binding properties of bovine brain S100 alpha alpha, S100a (alpha beta), and S100b (beta beta) protein: Zn2+ regulates Ca2+ binding on S100b protein. J. Biol. Chem. 261, 8192–8203.

Bearer, E.L., 1995. Cytoskeletal Domains in the Activated Platelet. Cell Motil. Cytoskeleton 30, 50–66. https://doi.org/10.1002/cm.970300107

Bearer, E.L., Prakash, J.M., Li, Z., 2002. Actin dynamics in platelets. Int. Rev. Cytol. 217, 137–182.

Beck, F., Geiger, J., Gambaryan, S., Veit, J., Vaudel, M., Nollau, P., Kohlbacher, O., Martens, L., Walter, U., Sickmann, A., Zahedi, R.P., 2014. Time-resolved characterization of cAMP/PKA-dependent signaling reveals that platelet inhibition is a concerted process involving multiple signaling pathways. Blood 123, e1–e10. https://doi.org/10.1182/blood-2013-07-512384

Beckman, J.S., Minor, R.L., White, C.W., Repine, J.E., Rosen, G.M., Freeman, B.A., 1988. Superoxide dismutase and catalase conjugated to polyethylene glycol increases endothelial enzyme activity and oxidant resistance. J. Biol. Chem. 263, 6884–6892.

Begonja, A.J., Gambaryan, S., Geiger, J., Aktas, B., Pozgajova, M., Nieswandt, B., Walter, U., 2005. Platelet NAD(P)H-oxidase–generated ROS production regulates αIIbβ3-integrin activation independent of the NO/cGMP pathway. Blood 106, 2757–2760. https://doi.org/10.1182/blood-2005-03-1047

Begonja, A.J., Teichmann, L., Geiger, J., Gambaryan, S., Walter, U., 2006. Platelet regulation by NO/cGMP signaling and NAD(P)H oxidase-generated ROS. Blood Cells. Mol. Dis. 36, 166–170. https://doi.org/10.1016/j.bcmd.2005.12.028

Bell, S.G., Vallee, B.L., 2009. The metallothionein/thionein system: an oxidoreductive metabolic zinc link. Chembiochem Eur. J. Chem. Biol. 10, 55–62. https://doi.org/10.1002/cbic.200800511

Bella, J., Hulmes, D.J.S., 2017. Fibrillar Collagens. Subcell. Biochem. 82, 457–490. https://doi.org/10.1007/978-3-319-49674-0_14

Bennett, J.S., Shattil, S.J., Power, J.W., Gartner, T.K., 1988. Interaction of fibrinogen with its platelet receptor. Differential effects of alpha and gamma chain fibrinogen peptides on the glycoprotein IIb-IIIa complex. J. Biol. Chem. 263, 12948–12953.

Bennett, J.S., Zigmond, S., Vilaire, G., Cunningham, M.E., Bednar, B., 1999. The platelet cytoskeleton regulates the affinity of the integrin alpha(IIb)beta(3) for fibrinogen. J. Biol. Chem. 274, 25301–25307.

Bernal, P.J., Bauer, E.M., Cao, R., Maniar, S., Mosher, M., Chen, J., Wang, Q.J., Glorioso, J.C., Pitt, B.R., Watkins, S.C., St Croix, C.M., 2011. A role for zinc in regulating hypoxia-induced contractile events in pulmonary endothelium. Am. J. Physiol. Lung Cell. Mol. Physiol. 300, L874-886. https://doi.org/10.1152/ajplung.00328.2010

Bernardi, B., Guidetti, G.F., Campus, F., Crittenden, J.R., Graybiel, A.M., Balduini, C., Torti, M., 2006. The small GTPase Rap1b regulates the cross talk between platelet integrin α2β1 and integrin αIIbβ3. Blood 107, 2728–2735. https://doi.org/10.1182/blood-2005-07-3023

Berndt, M.C., Metharom, P., Andrews, R.K., 2014. Primary haemostasis: newer insights. Haemoph. Off. J. World Fed. Hemoph. 20 Suppl 4, 15–22. https://doi.org/10.1111/hae.12427

Bernusso, V.A., Machado-Neto, J.A., Pericole, F.V., Vieira, K.P., Duarte, A.S.S., Traina, F., Hansen, M.D., Olalla Saad, S.T., Barcellos, K.S.A., 2015. Imatinib restores VASP activity and its interaction with Zyxin in BCR-ABL leukemic cells. Biochim. Biophys. Acta 1853, 388–395. https://doi.org/10.1016/j.bbamcr.2014.11.008

Beyersmann, D., Haase, H., 2001. Functions of zinc in signaling, proliferation and differentiation of mammalian cells. Biometals Int. J. Role Met. Ions Biol. Biochem. Med. 14, 331–341.

Bhatnagar, P., Wickramasinghe, K., Wilkins, E., Townsend, N., 2016. Trends in the epidemiology of cardiovascular disease in the UK. Heart Br. Card. Soc. 102, 1945–1952. https://doi.org/10.1136/heartjnl-2016-309573

Biagiotti, S., Menotta, M., Orazi, S., Spapperi, C., Brundu, S., Fraternale, A., Bianchi, M., Rossi, L., Chessa, L., Magnani, M., 2016. Dexamethasone improves redox state in ataxia telangiectasia cells by promoting an NRF2-mediated antioxidant response. FEBS J. 283, 3962–3978. https://doi.org/10.1111/febs.13901

Bochtler, T., Kirsch, M., Maier, B., Bachmann, J., Klingmüller, U., Anderhub, S., Ho, A.D., Krämer, A., 2012. Centrosomal targeting of tyrosine kinase activity does not enhance oncogenicity in chronic myeloproliferative disorders. Leukemia 26, 728–735. https://doi.org/10.1038/leu.2011.283

Bodie, S.L., Ford, I., Greaves, M., Nixon, G.F., 2001. Thrombin-Induced Activation of RhoA in Platelet Shape Change. Biochem. Biophys. Res. Commun. 287, 71–76. https://doi.org/10.1006/bbrc.2001.5547

Boknäs, N., Faxälv, L., Sanchez Centellas, D., Wallstedt, M., Ramström, S., Grenegård, M., Lindahl, T.L., 2014. Thrombin-induced platelet activation via PAR4: pivotal role for exosite II. Thromb. Haemost. 112, 558–565. https://doi.org/10.1160/TH13-12-1013

Bootman, M.D., Rietdorf, K., Collins, T., Walker, S., Sanderson, M., 2013. Converting fluorescence data into Ca2+ concentration. Cold Spring Harb. Protoc. 2013, 126–129. https://doi.org/10.1101/pdb.prot072827

Born, G.V., Dearnley, R., Foulks, J.G., Sharp, D.E., 1978. Quantification of the morphological reaction of platelets to aggregating agents and of its reversal by aggregation inhibitors. J. Physiol. 280, 193–212.

Born, G.V., Hume, M., 1967. Effects of the numbers and sizes of platelet aggregates on the optical density of plasma. Nature 215, 1027–1029.

Born, G.V.R., 1962. Aggregation of Blood Platelets by Adenosine Diphosphate and its Reversal. Nature 194, 927–929. https://doi.org/10.1038/194927b0

Born, G.V.R., Cross, M.J., 1963. The aggregation of blood platelets. J. Physiol. 168, 178–195.

Bouron, A., Oberwinkler, J., 2014. Contribution of calcium-conducting channels to the transport of zinc ions. Pflugers Arch. 466, 381–387. https://doi.org/10.1007/s00424-013-1295-z

Brass, L.F., Hoxie, J.A., Kieber-Emmons, T., Manning, D.R., Poncz, M., Woolkalis, M., 1993a. Agonist receptors and G proteins as mediators of platelet activation. Adv. Exp. Med. Biol. 344, 17–36.

Brass, L.F., Hoxie, J.A., Manning, D.R., 1993b. Signaling through G proteins and G protein-coupled receptors during platelet activation. Thromb. Haemost. 70, 217–223.

Brass, L.F., Manning, D.R., Cichowski, K., Abrams, C.S., 1997. Signaling through G proteins in platelets: to the integrins and beyond. Thromb. Haemost. 78, 581–589.

Brautigan, D.L., Bornstein, P., Gallis, B., 1981. Phosphotyrosyl-protein phosphatase. Specific inhibition by Zn. J. Biol. Chem. 256, 6519–6522.

Brondijk, T.H.C., Bihan, D., Farndale, R.W., Huizinga, E.G., 2012. Implications for collagen I chain registry from the structure of the collagen von Willebrand factor A3 domain complex. Proc. Natl. Acad. Sci. U. S. A. 109, 5253–5258. https://doi.org/10.1073/pnas.1112388109

Brüne, B., Ullrich, V., 1991. Calcium mobilization in human platelets by receptor agonists and calcium-ATPase inhibitors. FEBS Lett. 284, 1–4.

Brunner, J.D., Lim, N.K., Schenck, S., Duerst, A., Dutzler, R., 2014. X-ray structure of a calcium-activated TMEM16 lipid scramblase. Nature 516, 207–212. https://doi.org/10.1038/nature13984

Buitrago, L., Bhavanasi, D., Dangelmaier, C., Manne, B.K., Badolia, R., Borgognone, A., Tsygankov, A.Y., McKenzie, S.E., Kunapuli, S.P., 2013. Tyrosine phosphorylation on spleen tyrosine kinase (Syk) is differentially regulated in human and murine platelets by protein kinase C isoforms. J. Biol. Chem. 288, 29160–29169. https://doi.org/10.1074/jbc.M113.464107

Burkhart, J.M., Vaudel, M., Gambaryan, S., Radau, S., Walter, U., Martens, L., Geiger, J., Sickmann, A., Zahedi, R.P., 2012. The first comprehensive and quantitative analysis of human platelet protein composition allows the comparative analysis of structural and functional pathways. Blood 120, e73-82. https://doi.org/10.1182/blood-2012-04-416594

Bush, A.I., 2003. The metallobiology of Alzheimer's disease. Trends Neurosci. 26, 207–214. https://doi.org/10.1016/S0166-2236(03)00067-5

Bush, A.I., Tanzi, R.E., 2008. Therapeutics for Alzheimer's disease based on the metal hypothesis. Neurother. J. Am. Soc. Exp. Neurother. 5, 421–432. https://doi.org/10.1016/j.nurt.2008.05.001

Ca2+/Calmodulin-dependent Protein Kinases [WWW Document], n.d. URL https://www.ncbi.nlm.nih.gov/pmc/articles/PMC3617042/ (accessed 12.13.18).

Caen, J.P., Michel, H., 1972. Platelet Shape Change and Aggregation. Nature 240, 148–149. https://doi.org/10.1038/240148a0

Cai, Y., Biais, N., Giannone, G., Tanase, M., Jiang, G., Hofman, J.M., Wiggins, C.H., Silberzan, P., Buguin, A., Ladoux, B., Sheetz, M.P., 2006. Nonmuscle Myosin IIA-Dependent Force Inhibits Cell Spreading and Drives F-Actin Flow. Biophys. J. 91, 3907–3920. https://doi.org/10.1529/biophysj.106.084806

Calderwood, D.A., 2004. Integrin activation. J. Cell Sci. 117, 657–666. https://doi.org/10.1242/jcs.01014

Cangemi, R., Celestini, A., Del Ben, M., Pignatelli, P., Carnevale, R., Proietti, M., Calabrese, C.M., Basili, S., Violi, F., 2014. Role of platelets in NOX2 activation mediated by TNFα in heart failure. Intern. Emerg. Med. 9, 179–185. https://doi.org/10.1007/s11739-012-0837-2

Canton, J., Schlam, D., Breuer, C., Gütschow, M., Glogauer, M., Grinstein, S., 2016. Calcium-sensing receptors signal constitutive macropinocytosis and facilitate the uptake of NOD2 ligands in macrophages. Nat. Commun. 7, 11284. https://doi.org/10.1038/ncomms11284

Cao, J., Ehling, M., März, S., Seebach, J., Tarbashevich, K., Sixta, T., Pitulescu, M.E., Werner, A.-C., Flach, B., Montanez, E., Raz, E., Adams, R.H., Schnittler, H., 2017. Polarized actin and VE-cadherin dynamics regulate junctional remodelling and cell migration during sprouting angiogenesis. Nat. Commun. 8, 2210. https://doi.org/10.1038/s41467-017-02373-8

Capote, L.A., Mendez Perez, R., Lymperopoulos, A., 2015. GPCR signaling and cardiac function. Eur. J. Pharmacol. 763, 143–148. https://doi.org/10.1016/j.ejphar.2015.05.019

Carrim, N., Arthur, J.F., Hamilton, J.R., Gardiner, E.E., Andrews, R.K., Moran, N., Berndt, M.C., Metharom, P., 2015. Thrombin-induced reactive oxygen species generation in platelets: A novel role for protease-activated receptor 4 and GPIbα. Redox Biol. 6, 640–647. https://doi.org/10.1016/j.redox.2015.10.009

Carrim, N., Walsh, T.G., Consonni, A., Torti, M., Berndt, M.C., Metharom, P., 2014. Role of focal adhesion tyrosine kinases in GPVI-dependent platelet activation and reactive oxygen species formation. PloS One 9, e113679. https://doi.org/10.1371/journal.pone.0113679

Carter, R.N., Tolhurst, G., Walmsley, G., Vizuete-Forster, M., Miller, N., Mahaut-Smith, M.P., 2006. Molecular and electrophysiological characterization of transient receptor potential ion channels in the primary murine megakaryocyte. J. Physiol. 576, 151–162. https://doi.org/10.1113/jphysiol.2006.113886

Casella, J.F., Flanagan, M.D., Lin, S., 1981. Cytochalasin D inhibits actin polymerization and induces depolymerization of actin filaments formed during platelet shape change. Nature 293, 302–305.

Cerecedo, D., Stock, R., González, S., Reyes, E., Mondragón, R., 2002. Modification of actin, myosin and tubulin distribution during cytoplasmic granule movements associated with platelet adhesion. Haematologica 87, 1165–1176.

Chari-Turaga, R., Naik, U.P., 2011. Integrin αIIbβ3: a novel effector of Gα13. Cell Adhes. Migr. 5, 4–5.

Chauhan, B.K., Lou, M., Zheng, Y., Lang, R.A., 2011. Balanced Rac1 and RhoA activities regulate cell shape and drive invagination morphogenesis in epithelia. Proc. Natl. Acad. Sci. U. S. A. 108, 18289–18294. https://doi.org/10.1073/pnas.1108993108

Chausmer, A.B., 1998. Zinc, insulin and diabetes. J. Am. Coll. Nutr. 17, 109–115.

Chen, K., Craige, S.E., Keaney, J.F., 2009. Downstream targets and intracellular compartmentalization in Nox signaling. Antioxid. Redox Signal. 11, 2467–2480. https://doi.org/10.1089/ars.2009.2594

Chen, L., Wang, T., Wang, Y., Zhang, J., Qi, Y., Weng, H., Kang, Q., Guo, X., Baines, A.J., Mohandas, N., An, X., 2016. Protein 4.1G Regulates Cell Adhesion, Spreading, and Migration of Mouse

Embryonic Fibroblasts through the β1 Integrin Pathway. J. Biol. Chem. 291, 2170–2180. https://doi.org/10.1074/jbc.M115.658591

Chen, W.-F., Lee, J.-J., Chang, C.-C., Lin, K.-H., Wang, S.-H., Sheu, J.-R., 2013. Platelet protease-activated receptor (PAR)4, but not PAR1, associated with neutral sphingomyelinase responsible for thrombin-stimulated ceramide-NF-κB signaling in human platelets. Haematologica 98, 793–801. https://doi.org/10.3324/haematol.2012.072553

Chevallet, M., Jarvis, L., Harel, A., Luche, S., Degot, S., Chapuis, V., Boulay, G., Rabilloud, T., Bouron, A., 2014. Functional consequences of the over-expression of TRPC6 channels in HEK cells: impact on the homeostasis of zinc. Met. Integr. Biometal Sci. 6, 1269–1276. https://doi.org/10.1039/c4mt00028e

Chimienti, F., 2013. Zinc, pancreatic islet cell function and diabetes: new insights into an old story. Nutr. Res. Rev. 26, 1–11. https://doi.org/10.1017/S0954422412000212

Choudhury, A., Chung, I., Blann, A.D., Lip, G.Y.H., 2007. Platelet surface CD62P and CD63, mean platelet volume, and soluble/platelet P-selectin as indexes of platelet function in atrial fibrillation: a comparison of “healthy control subjects” and “disease control subjects” in sinus rhythm. J. Am. Coll. Cardiol. 49, 1957–1964. https://doi.org/10.1016/j.jacc.2007.02.038

Cimmino, G., Golino, P., 2013. Platelet biology and receptor pathways. J Cardiovasc. Transl. Res. 6, 299–309. https://doi.org/10.1007/s12265-012-9445-9

Clemetson, K.J., 2012. Platelets and primary haemostasis. Thromb. Res. 129, 220–224. https://doi.org/10.1016/j.thromres.2011.11.036

Cohen, J.J., 1999. Apoptosis: mechanisms of life and death in the immune system. J. Allergy Clin. Immunol. 103, 548–554.

Cohen, Z., Wilson, J., Ritter, L., McDonagh, P., 2004a. Caspase inhibition decreases both platelet phosphatidylserine exposure and aggregation: caspase inhibition of platelets. Thromb. Res. 113, 387–393. https://doi.org/10.1016/j.thromres.2004.03.020

Cohen, Z., Wilson, J., Ritter, L., McDonagh, P., 2004b. Caspase inhibition decreases both platelet phosphatidylserine exposure and aggregation: caspase inhibition of platelets. Thromb. Res. 113, 387–393.

Corbalán-García, S., Gómez-Fernández, J.C., 2006. Protein kinase C regulatory domains: the art of decoding many different signals in membranes. Biochim. Biophys. Acta 1761, 633–654. https://doi.org/10.1016/j.bbalip.2006.04.015

Corinaldesi, G., 2011. Platelet Activation in Cardiovascular Disease. Blood 118, 5242–5242.

Csermely, P., Szamel, M., Resch, K., Somogyi, J., 1988. Zinc can increase the activity of protein kinase C and contributes to its binding to plasma membranes in T lymphocytes. J. Biol. Chem. 263, 6487–6490.

Daaboul, D., Rosenkranz, E., Uciechowski, P., Rink, L., 2012. Repletion of zinc in zinc-deficient cells strongly up-regulates IL-1β-induced IL-2 production in T-cells. Met. Integr. Biometal Sci. 4, 1088–1097. https://doi.org/10.1039/c2mt20118f

Daleke, D.L., 2003. Regulation of transbilayer plasma membrane phospholipid asymmetry. J. Lipid Res. 44, 233–242. https://doi.org/10.1194/jlr.R200019-JLR200

Daly, M.E., 2011. Determinants of platelet count in humans. Haematologica 96, 10–13. https://doi.org/10.3324/haematol.2010.035287

Daniel, J.L., Molish, I.R., Rigmaiden, M., Stewart, G., 1984. Evidence for a role of myosin phosphorylation in the initiation of the platelet shape change response. J. Biol. Chem. 259, 9826–9831.

Davies, T.A., Drotts, D.L., Weil, G.J., Simons, E.R., 1989. Cytoplasmic Ca2+ is necessary for thrombin-induced platelet activation. J. Biol. Chem. 264, 19600–19606.

Dayananda, K.M., Singh, I., Mondal, N., Neelamegham, S., 2010. von Willebrand factor self-association on platelet GpIbalpha under hydrodynamic shear: effect on shear-induced platelet activation. Blood 116, 3990–3998. https://doi.org/10.1182/blood-2010-02-269266

Devergnas, S., Chimienti, F., Naud, N., Pennequin, A., Coquerel, Y., Chantegrel, J., Favier, A., Seve, M., 2004. Differential regulation of zinc efflux transporters ZnT-1, ZnT-5 and ZnT-7 gene expression by zinc levels: a real-time RT-PCR study. Biochem. Pharmacol. 68, 699–709. https://doi.org/10.1016/j.bcp.2004.05.024

Diaz-Ricart, M., Palomo, M., Fuste, B., Lopez-Vilchez, I., Carbo, C., Perez-Pujol, S., White, J.G., Escolar, G., 2008. Inhibition of tyrosine kinase activity prevents the adhesive and cohesive properties of platelets and the expression of procoagulant activity in response to collagen. Thromb. Res. 121, 873–883. https://doi.org/10.1016/j.thromres.2007.08.006

Ding, W.-Q., Lind, S.E., 2009. Metal ionophores - an emerging class of anticancer drugs. IUBMB Life 61, 1013–1018. https://doi.org/10.1002/iub.253

Ding, W.-Q., Liu, B., Vaught, J.L., Yamauchi, H., Lind, S.E., 2005. Anticancer activity of the antibiotic clioquinol. Cancer Res. 65, 3389–3395. https://doi.org/10.1158/0008-5472.CAN-04-3577

Diver, J.M., Sage, S.O., Rosado, J.A., 2001. The inositol trisphosphate receptor antagonist 2-aminoethoxydiphenylborate (2-APB) blocks Ca2+ entry channels in human platelets:

cautions for its use in studying Ca2+ influx. Cell Calcium 30, 323–329. https://doi.org/10.1054/ceca.2001.0239

Djillani, A., Nüße, O., Dellis, O., 2014. Characterization of novel store-operated calcium entry effectors. Biochim. Biophys. Acta 1843, 2341–2347. https://doi.org/10.1016/j.bbamcr.2014.03.012

Du, C., Zhang, X., Yao, M., Lv, K., Wang, J., Chen, L., Chen, Y., Wang, S., Fu, P., 2018. Bcl-2 promotes metastasis through the epithelial-to-mesenchymal transition in the BCap37 medullary breast cancer cell line. Oncol. Lett. 15, 8991–8898. https://doi.org/10.3892/ol.2018.8455

Dunster, J.L., Mazet, F., Fry, M.J., Gibbins, J.M., Tindall, M.J., 2015. Regulation of Early Steps of GPVI Signal Transduction by Phosphatases: A Systems Biology Approach. PLoS Comput. Biol. 11. https://doi.org/10.1371/journal.pcbi.1004589

Eide, D.J., 2004. The SLC39 family of metal ion transporters. Pflugers Arch. 447, 796–800. https://doi.org/10.1007/s00424-003-1074-3

Erdahl, W.L., Chapman, C.J., Taylor, R.W., Pfeiffer, D.R., 1995. Effects of pH conditions on Ca2+ transport catalyzed by ionophores A23187, 4-BrA23187, and ionomycin suggest problems with common applications of these compounds in biological systems. Biophys. J. 69, 2350–2363. https://doi.org/10.1016/S0006-3495(95)80104-9

Erdahl, W.L., Chapman, C.J., Taylor, R.W., Pfeiffer, D.R., 1994. Ca2+ transport properties of ionophores A23187, ionomycin, and 4-BrA23187 in a well defined model system. Biophys. J. 66, 1678–1693. https://doi.org/10.1016/S0006-3495(94)80959-2

Erdahl, W.L., Chapman, C.J., Wang, E., Taylor, R.W., Pfeiffer, D.R., 1996. Ionophore 4-BrA23187 transports Zn2+ and Mn2+ with high selectivity over Ca2+. Biochemistry 35, 13817–13825. https://doi.org/10.1021/bi961391q

Eron, S.J., MacPherson, D.J., Dagbay, K.B., Hardy, J.A., 2018. Multiple Mechanisms of Zinc-Mediated Inhibition for the Apoptotic Caspases-3, -6, -7, and -8. ACS Chem. Biol. 13, 1279–1290. https://doi.org/10.1021/acschembio.8b00064

Fägerstam, J.P., Whiss, P.A., Ström, M., Andersson, R.G., 2000. Expression of platelet P-selectin and detection of soluble P-selectin, NPY and RANTES in patients with inflammatory bowel disease. Inflamm. Res. Off. J. Eur. Histamine Res. Soc. Al 49, 466–472. https://doi.org/10.1007/s000110050618

Faller, P., Hureau, C., La Penna, G., 2014. Metal ions and intrinsically disordered proteins and peptides: from Cu/Zn amyloid-β to general principles. Acc. Chem. Res. 47, 2252–2259. https://doi.org/10.1021/ar400293h

Fasolato, C., Pozzan, T., 1989. Effect of membrane potential on divalent cation transport catalyzed by the “electroneutral” ionophores A23187 and ionomycin. J. Biol. Chem. 264, 19630–19636.

Faure, P., Durand, P., Blache, D., Favier, A., Roussel, A.M., 1995. Influence of a long-term zinc-deficient diet on rat platelet function and fatty acid composition. Biometals Int. J. Role Met. Ions Biol. Biochem. Med. 8, 80–85.

Feghhi, S., Tooley, W.W., Sniadecki, N.J., 2016. Nonmuscle Myosin IIA Regulates Platelet Contractile Forces Through Rho Kinase and Myosin Light-Chain Kinase. J. Biomech. Eng. 138. https://doi.org/10.1115/1.4034489

Feng, W., Benz, F.W., Cai, J., Pierce, W.M., Kang, Y.J., 2006. Metallothionein disulfides are present in metallothionein-overexpressing transgenic mouse heart and increase under conditions of oxidative stress. J. Biol. Chem. 281, 681–687. https://doi.org/10.1074/jbc.M506956200

Ferhat-Hamida, M.Y., Boukerb, H., Hariti, G., 2015. Contribution of the collagen binding activity (VWF:CB) in the range of tests for the diagnosis and classification of von Willebrand disease. Ann. Biol. Clin. (Paris) 73, 461–468. https://doi.org/10.1684/abc.2015.1050

Ferreira, T., Rasband, W., n.d. ImageJ User Guide 198.

Ferroni, P., Vazzana, N., Riondino, S., Cuccurullo, C., Guadagni, F., Davì, G., 2012. Platelet function in health and disease: from molecular mechanisms, redox considerations to novel therapeutic opportunities. Antioxid. Redox Signal. 17, 1447–1485. https://doi.org/10.1089/ars.2011.4324

Fiaturi, N., Russo, J.W., Nielsen, H.C., Castellot, J.J., 2018. CCN5 in alveolar epithelial proliferation and differentiation during neonatal lung oxygen injury. J. Cell Commun. Signal. 12, 217–229. https://doi.org/10.1007/s12079-017-0443-1

Finkenstaedt-Quinn, S.A., Ge, S., Haynes, C.L., 2015. Cytoskeleton dynamics in drug-treated platelets. Anal. Bioanal. Chem. 407, 2803–2809. https://doi.org/10.1007/s00216-015-8523-7

Flaumenhaft, R., 2003. Molecular basis of platelet granule secretion. Arterioscler. Thromb. Vasc. Biol. 23, 1152–1160. https://doi.org/10.1161/01.ATV.0000075965.88456.48

Flaumenhaft, R., Dilks, J.R., Rozenvayn, N., Monahan-Earley, R.A., Feng, D., Dvorak, A.M., 2005. The actin cytoskeleton differentially regulates platelet α-granule and dense-granule secretion. Blood 105, 3879–3887. https://doi.org/10.1182/blood-2004-04-1392

Flood, V.H., Schlauderaff, A.C., Haberichter, S.L., Slobodianuk, T.L., Jacobi, P.M., Bellissimo, D.B., Christopherson, P.A., Friedman, K.D., Gill, J.C., Hoffmann, R.G., Montgomery, R.R.,

Zimmerman Program Investigators, 2015. Crucial role for the VWF A1 domain in binding to type IV collagen. Blood 125, 2297–2304. https://doi.org/10.1182/blood-2014-11-610824

Fluo-4, AM, cell permeant - Thermo Fisher Scientific [WWW Document], n.d. URL https://www.thermofisher.com/order/catalog/product/F14201 (accessed 12.24.18).

Fontana, P., Zufferey, A., Daali, Y., Reny, J.-L., 2014. Antiplatelet therapy: targeting the TxA2 pathway. J Cardiovasc. Transl. Res. 7, 29–38. https://doi.org/10.1007/s12265-013-9529-1

Foote, J.W., Delves, H.T., 1984. Albumin bound and alpha 2-macroglobulin bound zinc concentrations in the sera of healthy adults. J. Clin. Pathol. 37, 1050–1054.

Foster, M., Samman, S., 2010. Zinc and redox signaling: perturbations associated with cardiovascular disease and diabetes mellitus. Antioxid. Redox Signal. 13, 1549–1573. https://doi.org/10.1089/ars.2010.3111

Fox, J.E., Lipfert, L., Clark, E.A., Reynolds, C.C., Austin, C.D., Brugge, J.S., 1993. On the role of the platelet membrane skeleton in mediating signal transduction. Association of GP IIb-IIIa, pp60c-src, pp62c-yes, and the p21ras GTPase-activating protein with the membrane skeleton. J. Biol. Chem. 268, 25973–25984.

Franklin, R.B., Zou, J., Zheng, Y., Naslund, M.J., Costello, L.C., 2016. Zinc Ionophore (Clioquinol) Inhibition of Human ZIP1-Deficient Prostate Tumor Growth in the Mouse Ectopic Xenograft Model: A Zinc Approach for the Efficacious Treatment of Prostate Cancer. Int. J. Cancer Clin. Res. 3.

Frederickson, C.J., 1989. Neurobiology of zinc and zinc-containing neurons. Int. Rev. Neurobiol. 31, 145–238.

Frederickson, C.J., Hernandez, M.D., Goik, S.A., Morton, J.D., McGinty, J.F., 1988. Loss of zinc staining from hippocampal mossy fibers during kainic acid induced seizures: a histofluorescence study. Brain Res. 446, 383–386.

Frederickson, C.J., Moncrieff, D.W., 1994. Zinc-containing neurons. Biol. Signals 3, 127–139.

Frederickson, C.J., Suh, S.W., Silva, D., Frederickson, C.J., Thompson, R.B., 2000. Importance of zinc in the central nervous system: the zinc-containing neuron. J. Nutr. 130, 1471S–83S. https://doi.org/10.1093/jn/130.5.1471S

Freedman, J.E., 2008. Oxidative stress and platelets. Arterioscler. Thromb. Vasc. Biol. 28, s11-16. https://doi.org/10.1161/ATVBAHA.107.159178

Frenette, P.S., Denis, C.V., Weiss, L., Jurk, K., Subbarao, S., Kehrel, B., Hartwig, J.H., Vestweber, D., Wagner, D.D., 2000. P-Selectin glycoprotein ligand 1 (PSGL-1) is expressed on platelets and can mediate platelet-endothelial interactions in vivo. J. Exp. Med. 191, 1413–1422.

Frontroth, J.P., 2013. Light transmission aggregometry. Methods Mol. Biol. Clifton NJ 992, 227–240. https://doi.org/10.1007/978-1-62703-339-8_17

Fujikawa, K., Fukumori, R., Nakamura, S., Kutsukake, T., Takarada, T., Yoneda, Y., 2015. Potential interactions of calcium-sensitive reagents with zinc ion in different cultured cells. PloS One 10, e0127421. https://doi.org/10.1371/journal.pone.0127421

Gachet, C., 2012. P2Y(12) receptors in platelets and other hematopoietic and non-hematopoietic cells. Purinergic Signal. 8, 609–619. https://doi.org/10.1007/s11302-012-9303-x

Gailit, J., Ruoslahti, E., 1988. Regulation of the fibronectin receptor affinity by divalent cations. J. Biol. Chem. 263, 12927–12932.

Gambaryan, S., Kobsar, A., Rukoyatkina, N., Herterich, S., Geiger, J., Smolenski, A., Lohmann, S.M., Walter, U., 2010. Thrombin and collagen induce a feedback inhibitory signaling pathway in platelets involving dissociation of the catalytic subunit of protein kinase A from an NFkappaB-IkappaB complex. J. Biol. Chem. 285, 18352–18363. https://doi.org/10.1074/jbc.M109.077602

Gamberucci, A., Giurisato, E., Pizzo, P., Tassi, M., Giunti, R., McIntosh, D.P., Benedetti, A., 2002. Diacylglycerol activates the influx of extracellular cations in T-lymphocytes independently of intracellular calcium-store depletion and possibly involving endogenous TRP6 gene products. Biochem. J. 364, 245–254.

Gammie, J.S., Zenati, M., Kormos, R.L., Hattler, B.G., Wei, L.M., Pellegrini, R.V., Griffith, B.P., Dyke, C.M., 1998. Abciximab and excessive bleeding in patients undergoing emergency cardiac operations. Ann. Thorac. Surg. 65, 465–469.

Gao, C., Xie, R., Yu, C., Wang, Q., Shi, F., Yao, C., Xie, R., Zhou, J., Gilbert, G.E., Shi, J., 2012. Procoagulant activity of erythrocytes and platelets through phosphatidylserine exposure and microparticles release in patients with nephrotic syndrome. Thromb. Haemost. 107, 681–689. https://doi.org/10.1160/TH11-09-0673

Gardiner, E.E., Andrews, R.K., 2014. Platelet receptor expression and shedding: glycoprotein Ib-IX-V and glycoprotein VI. Transfus. Med. Rev. 28, 56–60. https://doi.org/10.1016/j.tmrv.2014.03.001

Gardiner, E.E., Arthur, J.F., Kahn, M.L., Berndt, M.C., Andrews, R.K., 2004. Regulation of platelet membrane levels of glycoprotein VI by a platelet-derived metalloproteinase. Blood 104, 3611–3617. https://doi.org/10.1182/blood-2004-04-1549

Gartner, T.K., Bennett, J.S., 1985. The tetrapeptide analogue of the cell attachment site of fibronectin inhibits platelet aggregation and fibrinogen binding to activated platelets. J. Biol. Chem. 260, 11891–11894.

Gassmann, M., Grenacher, B., Rohde, B., Vogel, J., 2009. Quantifying Western blots: pitfalls of densitometry. Electrophoresis 30, 1845–1855. https://doi.org/10.1002/elps.200800720

Gavi, S., Shumay, E., Wang, H., Malbon, C.C., 2006. G-protein-coupled receptors and tyrosine kinases: crossroads in cell signaling and regulation. Trends Endocrinol. Metab. TEM 17, 48–54. https://doi.org/10.1016/j.tem.2006.01.006

GBD 2013 Mortality and Causes of Death Collaborators, 2015. Global, regional, and national age-sex specific all-cause and cause-specific mortality for 240 causes of death, 1990-2013: a systematic analysis for the Global Burden of Disease Study 2013. Lancet Lond. Engl. 385, 117–171. https://doi.org/10.1016/S0140-6736(14)61682-2

Ge, S., White, J.G., Haynes, C.L., 2012. Cytoskeletal F-actin, not the circumferential coil of microtubules, regulates platelet dense-body granule secretion. Platelets 23, 259–263. https://doi.org/10.3109/09537104.2011.620657

Gee, K.R., Zhou, Z.-L., Ton-That, D., Sensi, S.L., Weiss, J.H., 2002. Measuring zinc in living cells.: A new generation of sensitive and selective fluorescent probes. Cell Calcium 31, 245–251. https://doi.org/10.1016/S0143-4160(02)00053-2

Gerrard, J.M., White, J.G., 1976. The structure and function of platelets, with emphasis on their contractile nature. Pathobiol. Annu. 6, 31–59.

Gibbins, J., Asselin, J., Farndale, R., Barnes, M., Law, C.-L., Watson, S.P., 1996. Tyrosine Phosphorylation of the Fc Receptor γ-Chain in Collagen-stimulated Platelets. J. Biol. Chem. 271, 18095–18099. https://doi.org/10.1074/jbc.271.30.18095

Gibbins, J.M., 2004. Platelet adhesion signalling and the regulation of thrombus formation. J. Cell Sci. 117, 3415–3425. https://doi.org/10.1242/jcs.01325

Gibbins, J.M., Briddon, S., Shutes, A., van Vugt, M.J., van de Winkel, J.G., Saito, T., Watson, S.P., 1998. The p85 subunit of phosphatidylinositol 3-kinase associates with the Fc receptor gamma-chain and linker for activitor of T cells (LAT) in platelets stimulated by collagen and convulxin. J. Biol. Chem. 273, 34437–34443.

Gibbins, J.M., Mahaut-Smith, M.P. (Eds.), 2004. Platelets and Megakaryocytes: Volume 1: Functional Assays, Methods in Molecular Biology. Humana Press.

Gibbins, J.M., Okuma, M., Farndale, R., Barnes, M., Watson, S.P., 1997. Glycoprotein VI is the collagen receptor in platelets which underlies tyrosine phosphorylation of the Fc receptor gamma-chain. FEBS Lett. 413, 255–259.

Gibon, J., Tu, P., Bohic, S., Richaud, P., Arnaud, J., Zhu, M., Boulay, G., Bouron, A., 2011. The over-expression of TRPC6 channels in HEK-293 cells favours the intracellular accumulation of zinc. Biochim. Biophys. Acta 1808, 2807–2818. https://doi.org/10.1016/j.bbamem.2011.08.013

Glauner, H., Siegmund, D., Motejadded, H., Scheurich, P., Henkler, F., Janssen, O., Wajant, H., 2002. Intracellular localization and transcriptional regulation of tumor necrosis factor (TNF) receptor-associated factor 4 (TRAF4). Eur. J. Biochem. 269, 4819–4829.

Gofer-Dadosh, N., Klepfish, A., Schmilowitz, H., Shaklai, M., Lahav, J., 1997. Affinity modulation in platelet alpha 2 beta 1 following ligand binding. Biochem. Biophys. Res. Commun. 232, 724–727. https://doi.org/10.1006/bbrc.1997.6201

Gogia, S., Neelamegham, S., 2015. Role of fluid shear stress in regulating VWF structure, function and related blood disorders. Biorheology 52, 319–335. https://doi.org/10.3233/BIR-15061

Golebiewska, E.M., Poole, A.W., 2015. Platelet secretion: From haemostasis to wound healing and beyond. Blood Rev. 29, 153–162. https://doi.org/10.1016/j.blre.2014.10.003

Gordon, P.R., O'Dell, B.L., 1980. Rat platelet aggregation impaired by short-term zinc deficiency. J. Nutr. 110, 2125–2129. https://doi.org/10.1093/jn/110.10.2125

Gordon, P.R., Woodruff, C.W., Anderson, H.L., O'Dell, B.L., 1982. Effect of acute zinc deprivation on plasma zinc and platelet aggregation in adult males. Am. J. Clin. Nutr. 35, 113–119. https://doi.org/10.1093/ajcn/35.1.113

Görlach, A., Bertram, K., Hudecova, S., Krizanova, O., 2015. Calcium and ROS: A mutual interplay. Redox Biol. 6, 260–271. https://doi.org/10.1016/j.redox.2015.08.010

Gorog, P., Kovacs, I.B., 1995. Lipid peroxidation by activated platelets: a possible link between thrombosis and atherogenesis. Atherosclerosis 115, 121–128.

Gough, D.R., Cotter, T.G., 2011. Hydrogen peroxide: a Jekyll and Hyde signalling molecule. Cell Death Dis. 2, e213. https://doi.org/10.1038/cddis.2011.96

Gowland, E., Kay, H.E.M., Spillman, J.C., Williamson, J.R., 1969. Agglutination of platelets by a serum factor in the presence of EDTA. J. Clin. Pathol. 22, 460–464.

Grienberger, C., Konnerth, A., 2012. Imaging Calcium in Neurons. Neuron 73, 862–885. https://doi.org/10.1016/j.neuron.2012.02.011

Gryglewski, R.J., 1980. Prostaglandins, platelets, and atherosclerosis. CRC Crit. Rev. Biochem. 7, 291–338.

Gryglewski, R.J., Dembínska-Kieć, A., Korbut, R., 1978. A possible role of thromboxane A2 (TXA2) and prostacyclin (PGI2) in circulation. Acta Biol. Med. Ger. 37, 715–723.

Gryka, R.J., Buckley, L.F., Anderson, S.M., 2017. Vorapaxar: The Current Role and Future Directions of a Novel Protease-Activated Receptor Antagonist for Risk Reduction in Atherosclerotic Disease. Drugs RD 17, 65–72. https://doi.org/10.1007/s40268-016-0158-4

Guéguinou, M., Harnois, T., Crottes, D., Uguen, A., Deliot, N., Gambade, A., Chantôme, A., Haelters, J.P., Jaffrès, P.A., Jourdan, M.L., Weber, G., Soriani, O., Bougnoux, P., Mignen, O., Bourmeyster, N., Constantin, B., Lecomte, T., Vandier, C., Potier-Cartereau, M., 2016. SK3/TRPC1/Orai1 complex regulates SOCE-dependent colon cancer cell migration: a novel opportunity to modulate anti-EGFR mAb action by the alkyl-lipid Ohmline. Oncotarget. https://doi.org/10.18632/oncotarget.8786

Ha, K.-N., Chen, Y., Cai, J., Sternberg, P., 2006. Increased glutathione synthesis through an ARE-Nrf2-dependent pathway by zinc in the RPE: implication for protection against oxidative stress. Invest. Ophthalmol. Vis. Sci. 47, 2709–2715. https://doi.org/10.1167/iovs.05-1322

Haase, H., Maret, W., 2005. Fluctuations of cellular, available zinc modulate insulin signaling via inhibition of protein tyrosine phosphatases. J. Trace Elem. Med. Biol. Organ Soc. Miner. Trace Elem. GMS 19, 37–42. https://doi.org/10.1016/j.jtemb.2005.02.004

Haase, H., Maret, W., 2003. Intracellular zinc fluctuations modulate protein tyrosine phosphatase activity in insulin/insulin-like growth factor-1 signaling. Exp. Cell Res. 291, 289–298.

Haase, H., Ober-Blöbaum, J.L., Engelhardt, G., Hebel, S., Heit, A., Heine, H., Rink, L., 2008. Zinc signals are essential for lipopolysaccharide-induced signal transduction in monocytes. J. Immunol. Baltim. Md 1950 181, 6491–6502.

Hadfield, J., Plank, M.J., David, T., 2013. Modeling secondary messenger pathways in neurovascular coupling. Bull. Math. Biol. 75, 428–443. https://doi.org/10.1007/s11538-013-9813-x

Haeger, K., 1973. [Zinc and zinc deficiency--a clinical review]. Lakartidningen 70, 3243–3246.

Hallmans, G., Lasek, J., 1985. The effect of topical zinc absorption from wounds on growth and the wound healing process in zinc-deficient rats. Scand. J. Plast. Reconstr. Surg. 19, 119–125.

Halsted, J.A., 1971. Human zinc deficiency. Trans. Am. Clin. Climatol. Assoc. 82, 170–176.

Hamatake, M., Iguchi, K., Hirano, K., Ishida, R., 2000. Zinc induces mixed types of cell death, necrosis, and apoptosis, in molt-4 cells. J. Biochem. (Tokyo) 128, 933–939.

Hambidge, K.M., Walravens, P.A., 1982. Disorders of mineral metabolism. Clin. Gastroenterol. 11, 87–117.

Hambidge, M., 2000. Human zinc deficiency. J. Nutr. 130, 1344S–9S. https://doi.org/10.1093/jn/130.5.1344S

Hammond, J.W., Lu, S.-M., Gelbard, H.A., 2015. Platelet Activating Factor Enhances Synaptic Vesicle Exocytosis Via PKC, Elevated Intracellular Calcium, and Modulation of Synapsin 1 Dynamics and Phosphorylation. Front. Cell. Neurosci. 9, 505. https://doi.org/10.3389/fncel.2015.00505

Harburger, D.S., Calderwood, D.A., 2009. Integrin signalling at a glance. J. Cell Sci. 122, 159–163. https://doi.org/10.1242/jcs.018093

Hardyman, J.E.J., Tyson, J., Jackson, K.A., Aldridge, C., Cockell, S.J., Wakeling, L.A., Valentine, R.A., Ford, D., 2016. Zinc sensing by metal-responsive transcription factor 1 (MTF1) controls metallothionein and ZnT1 expression to buffer the sensitivity of the transcriptome response to zinc. Met. Integr. Biometal Sci. 8, 337–343. https://doi.org/10.1039/c5mt00305a

Harker, L.A., Finch, C.A., 1969. Thrombokinetics in man. J. Clin. Invest. 48, 963–974. https://doi.org/10.1172/JCI106077

Harper, M.T., Poole, A.W., 2010. Diverse functions of protein kinase C isoforms in platelet activation and thrombus formation. J. Thromb. Haemost. JTH 8, 454–462. https://doi.org/10.1111/j.1538-7836.2009.03722.x

Hartwig, J.H., 1992. Mechanisms of actin rearrangements mediating platelet activation. J. Cell Biol. 118, 1421–1442.

Hartwig, J.H., Barkalow, K., Azim, A., Italiano, J., 1999. The elegant platelet: signals controlling actin assembly. Thromb. Haemost. 82, 392–398.

Hashimoto, Y., Togo, M., Tsukamoto, K., Horie, Y., Watanabe, T., Kurokawa, K., 1994. Protein kinase C-dependent and -independent mechanisms of dense granule exocytosis by human platelets. Biochim. Biophys. Acta 1222, 56–62.

Hassock, S.R., Zhu, M.X., Trost, C., Flockerzi, V., Authi, K.S., 2002. Expression and role of TRPC proteins in human platelets: evidence that TRPC6 forms the store-independent calcium entry channel. Blood 100, 2801–2811. https://doi.org/10.1182/blood-2002-03-0723

Hathaway, D.R., Adelstein, R.S., 1979. Human platelet myosin light chain kinase requires the calcium-binding protein calmodulin for activity. Proc. Natl. Acad. Sci. U. S. A. 76, 1653–1657.

Hayes, J.M., Wormald, M.R., Rudd, P.M., Davey, G.P., 2016. Fc gamma receptors: glycobiology and therapeutic prospects. J. Inflamm. Res. 9, 209–219. https://doi.org/10.2147/JIR.S121233

Hechler, B., Léon, C., Vial, C., Vigne, P., Frelin, C., Cazenave, J.P., Gachet, C., 1998. The P2Y1 receptor is necessary for adenosine 5'-diphosphate-induced platelet aggregation. Blood 92, 152–159.

Heijnen, H., van der Sluijs, P., 2015. Platelet secretory behaviour: as diverse as the granules … or not? J. Thromb. Haemost. JTH 13, 2141–2151. https://doi.org/10.1111/jth.13147

Henrita van Zanten, G., Saelman, E.U., Schut-Hese, K.M., Wu, Y.P., Slootweg, P.J., Nieuwenhuis, H.K., de Groot, P.G., Sixma, J.J., 1996. Platelet adhesion to collagen type IV under flow conditions. Blood 88, 3862–3871.

Hesketh, J.E., 1982. Zinc-stimulated microtubule assembly and evidence for zinc binding to tubulin. Int. J. Biochem. 14, 983–990.

Heyns, A. du P., Eldor, A., Yarom, R., Marx, G., 1985. Zinc-induced platelet aggregation is mediated by the fibrinogen receptor and is not accompanied by release or by thromboxane synthesis. Blood 66, 213–219.

Higuchi, W., Fuse, I., Hattori, A., Aizawa, Y., 1999. Mutations of the platelet thromboxane A2 (TXA2) receptor in patients characterized by the absence of TXA2-induced platelet aggregation despite normal TXA2 binding activity. Thromb. Haemost. 82, 1528–1531.

Hodeify, R., Selvaraj, S., Wen, J., Arredouani, A., Hubrack, S., Dib, M., Al-Thani, S.N., McGraw, T., Machaca, K., 2015. A STIM1-dependent 'trafficking trap' mechanism regulates Orai1 plasma membrane residence and Ca2+ influx levels. J Cell Sci 128, 3143–3154. https://doi.org/10.1242/jcs.172320

Hogstrand, C., Kille, P., Ackland, M.L., Hiscox, S., Taylor, K.M., 2013. A mechanism for epithelial-mesenchymal transition and anoikis resistance in breast cancer triggered by zinc channel ZIP6 and STAT3 (signal transducer and activator of transcription 3). Biochem. J. 455, 229–237. https://doi.org/10.1042/BJ20130483

Holmsen, H., Weiss, H.J., 1970. Hereditary defect in the platelet release reaction caused by a deficiency in the storage pool of platelet adenine nucleotides. Br. J. Haematol. 19, 643–649.

Hou, X., Pedi, L., Diver, M.M., Long, S.B., 2012. Crystal structure of the calcium release-activated calcium channel Orai. Science 338, 1308–1313. https://doi.org/10.1126/science.1228757

Hoylaerts, M.F., 1997. Platelet-vessel wall interactions in thrombosis and restenosis role of von Willebrand factor. Verh. - K. Acad. Voor Geneeskd. Van Belg. 59, 161–183.

Huang, J., Sun, Y., Zhang, J.J., Huang, X.-Y., 2015. Pivotal role of extended linker 2 in the activation of Gα by G protein-coupled receptor. J. Biol. Chem. 290, 272–283. https://doi.org/10.1074/jbc.M114.608661

Hubbard, S.R., Bishop, W.R., Kirschmeier, P., George, S.J., Cramer, S.P., Hendrickson, W.A., 1991a. . Science 254, 1776–1779.

Hubbard, S.R., Bishop, W.R., Kirschmeier, P., George, S.J., Cramer, S.P., Hendrickson, W.A., 1991b. Identification and characterization of zinc binding sites in protein kinase C. Science 254, 1776–1779.

Huynh, K.C., Stoldt, V.R., Scharf, R.E., 2013. Contribution of distinct platelet integrins to binding, unfolding, and assembly of fibronectin. Biol. Chem. 394, 1485–1493. https://doi.org/10.1515/hsz-2013-0182

Hvas, A.-M., Favaloro, E.J., 2017. Platelet Function Analyzed by Light Transmission Aggregometry. Methods Mol. Biol. Clifton NJ 1646, 321–331. https://doi.org/10.1007/978-1-4939-7196-1_25

Hyun, T.H., Barrett-Connor, E., Milne, D.B., 2004a. Zinc intakes and plasma concentrations in men with osteoporosis: the Rancho Bernardo Study. Am. J. Clin. Nutr. 80, 715–721. https://doi.org/10.1093/ajcn/80.3.715

Hyun, T.H., Barrett-Connor, E., Milne, D.B., 2004b. Zinc intakes and plasma concentrations in men with osteoporosis: the Rancho Bernardo Study. Am. J. Clin. Nutr. 80, 715–721.

Iitaka, M., Kakinuma, S., Fujimaki, S., Oosuga, I., Fujita, T., Yamanaka, K., Wada, S., Katayama, S., 2001. Induction of apoptosis and necrosis by zinc in human thyroid cancer cell lines. J. Endocrinol. 169, 417–424.

Inoue, K., Branigan, D., Xiong, Z.-G., 2010. Zinc-induced neurotoxicity mediated by transient receptor potential melastatin 7 channels. J. Biol. Chem. 285, 7430–7439. https://doi.org/10.1074/jbc.M109.040485

International Zinc Nutrition Consultative Group (IZiNCG), Brown, K.H., Rivera, J.A., Bhutta, Z., Gibson, R.S., King, J.C., Lönnerdal, B., Ruel, M.T., Sandtröm, B., Wasantwisut, E., Hotz, C., 2004. International Zinc Nutrition Consultative Group (IZiNCG) technical document #1. Assessment of the risk of zinc deficiency in populations and options for its control. Food Nutr. Bull. 25, S99-203.

Islam, M.S., Berggren, P.O., 1993. Mobilization of Ca2+ by thapsigargin and 2,5-di-(t-butyl)-1,4-benzohydroquinone in permeabilized insulin-secreting RINm5F cells: evidence for separate uptake and release compartments in inositol 1,4,5-trisphosphate-sensitive Ca2+ pool. Biochem. J. 293 (Pt 2), 423–429.

Italiano, J.E., Lecine, P., Shivdasani, R.A., Hartwig, J.H., 1999. Blood Platelets Are Assembled Principally at the Ends of Proplatelet Processes Produced by Differentiated Megakaryocytes. J. Cell Biol. 147, 1299–1312. https://doi.org/10.1083/jcb.147.6.1299

Jackson, C.W., Edwards, C.C., 1977. Biphasic thrombopoietic response to severe hypobaric hypoxia. Br. J. Haematol. 35, 233–244.

Jakobsche-Policht, U., Bednarska-Chabowska, D., Sadakierska-Chudy, A., Adamiec-Mroczek, J., 2014. Expression of the PAR-1 protein on the surface of platelets in patients with chronic peripheral arterial insufficiency - preliminary report. Adv. Clin. Exp. Med. Off. Organ Wroclaw Med. Univ. 23, 159–167.

Jalagadugula, G., Mao, G., Kaur, G., Goldfinger, L.E., Dhanasekaran, D.N., Rao, A.K., 2010. Regulation of platelet myosin light chain (MYL9) by RUNX1: implications for thrombocytopenia and platelet dysfunction in RUNX1 haplodeficiency. Blood 116, 6037–6045. https://doi.org/10.1182/blood-2010-06-289850

Jang, J.Y., Min, J.H., Chae, Y.H., Baek, J.Y., Wang, S.B., Park, S.J., Oh, G.T., Lee, S.-H., Ho, Y.-S., Chang, T.-S., 2014. Reactive Oxygen Species Play a Critical Role in Collagen-Induced Platelet Activation via SHP-2 Oxidation. Antioxid. Redox Signal. 20, 2528–2540. https://doi.org/10.1089/ars.2013.5337

Jansen, J., Karges, W., Rink, L., 2009. Zinc and diabetes--clinical links and molecular mechanisms. J. Nutr. Biochem. 20, 399–417. https://doi.org/10.1016/j.jnutbio.2009.01.009

Jemiolo, D.K., Grisham, C.M., 1982. Divalent cation-nucleotide complex at the exchangeable nucleotide binding site of tubulin. J. Biol. Chem. 257, 8148–8152.

Jeng, A.Y., Ryan, T.E., Shamoo, A.E., 1978. Isolation of a low molecular weight Ca2+ carrier from calf heart inner mitochondrial membrane. Proc. Natl. Acad. Sci. U. S. A. 75, 2125–2129.

Jiang, L.J., Maret, W., Vallee, B.L., 1998. The glutathione redox couple modulates zinc transfer from metallothionein to zinc-depleted sorbitol dehydrogenase. Proc. Natl. Acad. Sci. U. S. A. 95, 3483–3488.

Jones, S., Solomon, A., Sanz-Rosa, D., Moore, C., Holbrook, L., Cartwright, E.J., Neyses, L., Emerson, M., 2010. The plasma membrane calcium ATPase modulates calcium homeostasis, intracellular signaling events and function in platelets. J. Thromb. Haemost. JTH 8, 2766–2774. https://doi.org/10.1111/j.1538-7836.2010.04076.x

Joseph, J.E., Harrison, P., Mackie, I.J., Machin, S.J., 1998. Platelet activation markers and the primary antiphospholipid syndrome (PAPS). Lupus 7 Suppl 2, S48-51.

Joshi, P., Riley, D.R.J., Khalil, J.S., Xiong, H., Ji, W., Rivero, F., 2018. The membrane-associated fraction of cyclase associate protein 1 translocates to the cytosol upon platelet stimulation. Sci. Rep. 8, 10804. https://doi.org/10.1038/s41598-018-29151-w

Judd, B.A., Myung, P.S., Obergfell, A., Myers, E.E., Cheng, A.M., Watson, S.P., Pear, W.S., Allman, D., Shattil, S.J., Koretzky, G.A., 2002. Differential requirement for LAT and SLP-76 in GPVI versus T cell receptor signaling. J. Exp. Med. 195, 705–717.

Kalev-Zylinska, M.L., Green, T.N., Morel-Kopp, M.-C., Sun, P.P., Park, Y.-E., Lasham, A., During, M.J., Ward, C.M., 2014. N-methyl-D-aspartate receptors amplify activation and aggregation of human platelets. Thromb. Res. 133, 837–847. https://doi.org/10.1016/j.thromres.2014.02.011

Kamiya, T., Nagaoka, T., Omae, T., Yoshioka, T., Ono, S., Tanano, I., Yoshida, A., 2014. Role of Ca2+ -dependent and Ca2+ -sensitive mechanisms in sphingosine 1-phosphate-induced constriction of isolated porcine retinal arterioles in vitro. Exp. Eye Res. 121, 94–101. https://doi.org/10.1016/j.exer.2014.01.011

Karim, M.R., Petering, D.H., 2016. Newport Green, a Fluorescent Sensor of Weakly Bound Cellular Zn2+: Competition with Proteome for Zn2+. Met. Integr. Biometal Sci. 8, 201–210. https://doi.org/10.1039/c5mt00167f

Kato, K., Omura, H., Ishitani, R., Nureki, O., 2017. Cyclic GMP-AMP as an Endogenous Second Messenger in Innate Immune Signaling by Cytosolic DNA. Annu. Rev. Biochem. 86, 541–566. https://doi.org/10.1146/annurev-biochem-061516-044813

Kawasaki, T., Ueyama, T., Lange, I., Feske, S., Saito, N., 2010. Protein kinase C-induced phosphorylation of Orai1 regulates the intracellular Ca2+ level via the store-operated Ca2+ channel. J. Biol. Chem. 285, 25720–25730. https://doi.org/10.1074/jbc.M109.022996

Kehrel, B., Wierwille, S., Clemetson, K.J., Anders, O., Steiner, M., Knight, C.G., Farndale, R.W., Okuma, M., Barnes, M.J., 1998. Glycoprotein VI is a major collagen receptor for platelet activation: it recognizes the platelet-activating quaternary structure of collagen, whereas CD36, glycoprotein IIb/IIIa, and von Willebrand factor do not. Blood 91, 491–499.

Kim, C.H., Kim, J.H., Moon, S.J., Chung, K.C., Hsu, C.Y., Seo, J.T., Ahn, Y.S., 1999. Pyrithione, a zinc ionophore, inhibits NF-kappaB activation. Biochem. Biophys. Res. Commun. 259, 505–509. https://doi.org/10.1006/bbrc.1999.0814

Kim, E.J., Lee, H.J., Lee, J., Youm, H.W., Lee, J.R., Suh, C.S., Kim, S.H., 2015. The beneficial effects of polyethylene glycol-superoxide dismutase on ovarian tissue culture and transplantation. J. Assist. Reprod. Genet. 32, 1561–1569. https://doi.org/10.1007/s10815-015-0537-8

Kim, G.-D., Das, R., Goduni, L., McClellan, S., Hazlett, L.D., Mahabeleshwar, G.H., 2016. Kruppel-like Factor 6 Promotes Macrophage-mediated Inflammation by Suppressing B Cell

Leukemia/Lymphoma 6 Expression. J. Biol. Chem. 291, 21271–21282. https://doi.org/10.1074/jbc.M116.738617

Kim, J.M., Koo, Y.K., Jin, J., Lee, Y.Y., Park, S., Yun-Choi, H.S., 2009. Augmentation of U46619 induced human platelet aggregation by aspirin. Platelets 20, 111–119. https://doi.org/10.1080/09537100802632282

Kimura, T., Kambe, T., 2016. The Functions of Metallothionein and ZIP and ZnT Transporters: An Overview and Perspective. Int. J. Mol. Sci. 17, 336. https://doi.org/10.3390/ijms17030336

Kirchhofer, D., Languino, L.R., Ruoslahti, E., Pierschbacher, M.D., 1990. Alpha 2 beta 1 integrins from different cell types show different binding specificities. J. Biol. Chem. 265, 615–618.

Kirkpatrick, J.P., McIntire, L.V., Moake, J.L., Cimo, P.L., 1980. Differential effects of cytochalasin B on platelet release, aggregation and contractility: evidence against a contractile mechanism for the release of platelet granular contents. Thromb. Haemost. 42, 1483–1489.

Kitajima, N., Numaga-Tomita, T., Watanabe, M., Kuroda, T., Nishimura, A., Miyano, K., Yasuda, S., Kuwahara, K., Sato, Y., Ide, T., Birnbaumer, L., Sumimoto, H., Mori, Y., Nishida, M., 2016. TRPC3 positively regulates reactive oxygen species driving maladaptive cardiac remodeling. Sci. Rep. 6, 37001. https://doi.org/10.1038/srep37001

Knappe, S., Gorczyca, M.E., Jilma, B., Derhaschnig, U., Hartmann, R., Palige, M., Scheiflinger, F., Dockal, M., 2013. Plasmatic tissue factor pathway inhibitor is a major determinant of clotting in factor VIII inhibited plasma or blood. Thromb. Haemost. 109, 450–457. https://doi.org/10.1160/TH12-07-0529

Koh, J.-Y., Suh, S.W., Gwag, B.J., He, Y.Y., Hsu, C.Y., Choi, D.W., 1996. The Role of Zinc in Selective Neuronal Death After Transient Global Cerebral Ischemia. Science 272, 1013–1016. https://doi.org/10.1126/science.272.5264.1013

Koo, Y.K., Kim, J.M., Koo, J.Y., Kang, S.S., Bae, K., Kim, Y.S., Chung, J.-H., Yun-Choi, H.S., 2010. Platelet anti-aggregatory and blood anti-coagulant effects of compounds isolated from Paeonia lactiflora and Paeonia suffruticosa. Pharm. 65, 624–628.

Kowalska, M.A., Juliano, D., Trybulec, M., Lu, W., Niewiarowski, S., 1994. Zinc ions potentiate adenosine diphosphate-induced platelet aggregation by activation of protein kinase C. J. Lab. Clin. Med. 123, 102–109.

Krebs, N.F., 2000. Overview of zinc absorption and excretion in the human gastrointestinal tract. J. Nutr. 130, 1374S–7S. https://doi.org/10.1093/jn/130.5.1374S

Krenn, B.M., Gaudernak, E., Holzer, B., Lanke, K., Van Kuppeveld, F.J.M., Seipelt, J., 2009. Antiviral activity of the zinc ionophores pyrithione and hinokitiol against picornavirus infections. J. Virol. 83, 58–64. https://doi.org/10.1128/JVI.01543-08

Krezel, A., Hao, Q., Maret, W., 2007. The zinc/thiolate redox biochemistry of metallothionein and the control of zinc ion fluctuations in cell signaling. Arch. Biochem. Biophys. 463, 188–200.

Krężel, A., Maret, W., 2017a. The Functions of Metamorphic Metallothioneins in Zinc and Copper Metabolism. Int. J. Mol. Sci. 18. https://doi.org/10.3390/ijms18061237

Krężel, A., Maret, W., 2017b. The Functions of Metamorphic Metallothioneins in Zinc and Copper Metabolism. Int. J. Mol. Sci. 18.

Krezel, A., Maret, W., 2007. Dual nanomolar and picomolar Zn(II) binding properties of metallothionein. J. Am. Chem. Soc. 129, 10911–10921. https://doi.org/10.1021/ja071979s

Kroll, M.H., Hellums, J.D., McIntire, L.V., Schafer, A.I., Moake, J.L., 1996. Platelets and shear stress. Blood 88, 1525–1541.

Krötz, F., Sohn, H.Y., Gloe, T., Zahler, S., Riexinger, T., Schiele, T.M., Becker, B.F., Theisen, K., Klauss, V., Pohl, U., 2002. NAD(P)H oxidase-dependent platelet superoxide anion release increases platelet recruitment. Blood 100, 917–924.

Krötz, F., Sohn, H.-Y., Pohl, U., 2004. Reactive oxygen species: players in the platelet game. Arterioscler. Thromb. Vasc. Biol. 24, 1988–1996. https://doi.org/10.1161/01.ATV.0000145574.90840.7d

Kumar, G., Tajpara, P., Bukhari, A.B., Ramchandani, A.G., De, A., Maru, G.B., 2014. Dietary curcumin post-treatment enhances the disappearance of B(a)P-derived DNA adducts in mouse liver and lungs. Toxicol. Rep. 1, 1181–1194. https://doi.org/10.1016/j.toxrep.2014.11.008

Kunicki, T.J., Orchekowski, R., Annis, D., Honda, Y., 1993. Variability of integrin alpha 2 beta 1 activity on human platelets. Blood 82, 2693–2703.

Kureishi, Y., Kobayashi, S., Amano, M., Kimura, K., Kanaide, H., Nakano, T., Kaibuchi, K., Ito, M., 1997. Rho-associated kinase directly induces smooth muscle contraction through myosin light chain phosphorylation. J. Biol. Chem. 272, 12257–12260.

Kuwahara, M., Sugimoto, M., Tsuji, S., Matsui, H., Mizuno, T., Miyata, S., Yoshioka, A., 2002. Platelet shape changes and adhesion under high shear flow. Arterioscler. Thromb. Vasc. Biol. 22, 329–334.

Lam, S., Tran, T., 2015. Vorapaxar: A Protease-Activated Receptor Antagonist for the Prevention of Thrombotic Events. Cardiol. Rev. 23, 261–267. https://doi.org/10.1097/CRD.0000000000000075

Lang, F., Münzer, P., Gawaz, M., Borst, O., 2013. Regulation of STIM1/Orai1-dependent Ca2+ signalling in platelets. Thromb. Haemost. 110, 925–930. https://doi.org/10.1160/TH13-02-0176

Lansdown, A.B., 1996. Zinc in the healing wound. Lancet Lond. Engl. 347, 706–707.

Lansdown, A.B.G., Mirastschijski, U., Stubbs, N., Scanlon, E., Agren, M.S., 2007. Zinc in wound healing: theoretical, experimental, and clinical aspects. Wound Repair Regen. Off. Publ. Wound Heal. Soc. Eur. Tissue Repair Soc. 15, 2–16. https://doi.org/10.1111/j.1524-475X.2006.00179.x

Latimer, P., 1983. Blood platelet aggregometer: predicted effects of aggregation, photometer geometry, and multiple scattering. Appl. Opt. 22, 1136–1143.

Lee, B.-K., Uprety, N., Jang, Y.J., Tucker, S.K., Rhee, C., LeBlanc, L., Beck, S., Kim, J., 2018. Fosl1 overexpression directly activates trophoblast-specific gene expression programs in embryonic stem cells. Stem Cell Res. 26, 95–102. https://doi.org/10.1016/j.scr.2017.12.004

Leng, T.-D., Lin, J., Sun, H.-W., Zeng, Z., O'Bryant, Z., Inoue, K., Xiong, Z.-G., 2015. Local anesthetic lidocaine inhibits TRPM7 current and TRPM7-mediated zinc toxicity. CNS Neurosci. Ther. 21, 32–39. https://doi.org/10.1111/cns.12318

Lengyel, I., Fieuw-Makaroff, S., Hall, A.L., Sim, A.T., Rostas, J.A., Dunkley, P.R., 2000. Modulation of the phosphorylation and activity of calcium/calmodulin-dependent protein kinase II by zinc. J. Neurochem. 75, 594–605.

Leung, T., Chen, X.Q., Manser, E., Lim, L., 1996. The p160 RhoA-binding kinase ROK alpha is a member of a kinase family and is involved in the reorganization of the cytoskeleton. Mol. Cell. Biol. 16, 5313–5327.

Lever, R.A., Hussain, A., Sun, B.B., Sage, S.O., Harper, A.G.S., 2015. Conventional protein kinase C isoforms differentially regulate ADP- and thrombin-evoked Ca^{2+} signalling in human platelets. Cell Calcium 58, 577–588. https://doi.org/10.1016/j.ceca.2015.09.005

Levy, J.V., 1983. Calmodulin antagonist W-7 inhibits aggregation of human platelets induced by platelet activating factor. Proc. Soc. Exp. Biol. Med. Soc. Exp. Biol. Med. N. Y. N 172, 393–395.

Li, B., Cui, W., Tan, Y., Luo, P., Chen, Q., Zhang, C., Qu, W., Miao, L., Cai, L., 2014. Zinc is essential for the transcription function of Nrf2 in human renal tubule cells in vitro and mouse kidney in vivo under the diabetic condition. J. Cell. Mol. Med. 18, 895–906. https://doi.org/10.1111/jcmm.12239

Li, F., Abuarab, N., Sivaprasadarao, A., 2016a. Reciprocal regulation of actin cytoskeleton remodelling and cell migration by Ca2+ and Zn2+: role of TRPM2 channels. J. Cell Sci. 129, 2016–2029. https://doi.org/10.1242/jcs.179796

Li, F., Abuarab, N., Sivaprasadarao, A., 2016b. Reciprocal regulation of actin cytoskeleton remodelling and cell migration by Ca2+ and Zn2+: role of TRPM2 channels. J. Cell Sci. 129, 2016–2029.

Li, N., Sul, J.-Y., Haydon, P.G., 2003. A calcium-induced calcium influx factor, nitric oxide, modulates the refilling of calcium stores in astrocytes. J. Neurosci. Off. J. Soc. Neurosci. 23, 10302–10310.

Li, Y.V., 2014. Zinc and insulin in pancreatic beta-cells. Endocrine 45, 178–189. https://doi.org/10.1007/s12020-013-0032-x

Li, Z., Delaney, M.K., O'Brien, K.A., Du, X., 2010. Signaling during platelet adhesion and activation. Arterioscler. Thromb. Vasc. Biol. 30, 2341–2349. https://doi.org/10.1161/ATVBAHA.110.207522

Lin, S., Cheng, M., Dailey, W., Drenser, K., Chintala, S., 2009. Norrin attenuates protease-mediated death of transformed retinal ganglion cells. Mol. Vis. 15, 26–37.

Lin, S.-Y., Raval, S., Zhang, Z., Deverill, M., Siminovitch, K.A., Branch, D.R., Haimovich, B., 2004. The protein-tyrosine phosphatase SHP-1 regulates the phosphorylation of alpha-actinin. J. Biol. Chem. 279, 25755–25764. https://doi.org/10.1074/jbc.M314175200

Liu, W., Wei, Z., Ma, H., Cai, A., Liu, Y., Sun, J., DaSilva, N.A., Johnson, S.L., Kirschenbaum, L.J., Cho, B.P., Dain, J.A., Rowley, D.C., Shaikh, Z.A., Seeram, N.P., 2017. Anti-glycation and anti-oxidative effects of a phenolic-enriched maple syrup extract and its protective effects on normal human colon cells. Food Funct. 8, 757–766. https://doi.org/10.1039/c6fo01360k

Lock, J.T., Sinkins, W.G., Schilling, W.P., 2012. Protein S-glutathionylation enhances Ca2+-induced Ca2+ release via the IP3 receptor in cultured aortic endothelial cells. J. Physiol. 590, 3431–3447. https://doi.org/10.1113/jphysiol.2012.232645

Lodish, H., Berk, A., Zipursky, S.L., Matsudaira, P., Baltimore, D., Darnell, J., 2000. Second Messengers. Mol. Cell Biol. 4th Ed.

Lood, C., Tydén, H., Gullstrand, B., Jönsen, A., Källberg, E., Mörgelin, M., Kahn, R., Gunnarsson, I., Leanderson, T., Ivars, F., Svenungsson, E., Bengtsson, A.A., 2016. Platelet-Derived S100A8/A9 and Cardiovascular Disease in Systemic Lupus Erythematosus: PLATELET S100A8/A9 AND CVD IN SLE. Arthritis Rheumatol. 68, 1970–1980. https://doi.org/10.1002/art.39656

Lopes Pires, M.E., Clarke, S.R., Marcondes, S., Gibbins, J.M., 2017. Lipopolysaccharide potentiates platelet responses via toll-like receptor 4-stimulated Akt-Erk-PLA2 signalling. PloS One 12, e0186981. https://doi.org/10.1371/journal.pone.0186981

Lopez, J.J., Salido, G.M., Gómez-Arteta, E., Rosado, J.A., Pariente, J.A., 2007. Thrombin induces apoptotic events through the generation of reactive oxygen species in human platelets. J. Thromb. Haemost. JTH 5, 1283–1291. https://doi.org/10.1111/j.1538-7836.2007.02505.x

Ltd, T.C. of B., 2011. Spectrin scaffold lets cells spread. J Cell Sci 124, e2306–e2306.

Lu, L., Zhu, M., 2014. Protein tyrosine phosphatase inhibition by metals and metal complexes. Antioxid. Redox Signal. 20, 2210–2224. https://doi.org/10.1089/ars.2013.5720

Ma, P., Cierniewska, A., Signarvic, R., Cieslak, M., Kong, H., Sinnamon, A.J., Neubig, R.R., Newman, D.K., Stalker, T.J., Brass, L.F., 2012. A newly identified complex of spinophilin and the tyrosine phosphatase, SHP-1, modulates platelet activation by regulating G protein-dependent signaling. Blood 119, 1935–1945. https://doi.org/10.1182/blood-2011-10-387910

Machlus, K.R., Italiano, J.E., 2013. The incredible journey: From megakaryocyte development to platelet formation. J Cell Biol 201, 785–796. https://doi.org/10.1083/jcb.201304054

Machtay, M., Scherpereel, A., Santiago, J., Lee, J., McDonough, J., Kinniry, P., Arguiri, E., Shuvaev, V.V., Sun, J., Cengel, K., Solomides, C.C., Christofidou-Solomidou, M., 2006. Systemic polyethylene glycol-modified (PEGylated) superoxide dismutase and catalase mixture attenuates radiation pulmonary fibrosis in the C57/bl6 mouse. Radiother. Oncol. J. Eur. Soc. Ther. Radiol. Oncol. 81, 196–205. https://doi.org/10.1016/j.radonc.2006.09.013

Mackenzie, G.G., Oteiza, P.I., 2007. Zinc and the cytoskeleton in the neuronal modulation of transcription factor NFAT. J. Cell. Physiol. 210, 246–256. https://doi.org/10.1002/jcp.20861

Mackman, N., Tilley, R.E., Key, N.S., 2007. Role of the extrinsic pathway of blood coagulation in hemostasis and thrombosis. Arterioscler. Thromb. Vasc. Biol. 27, 1687–1693. https://doi.org/10.1161/ATVBAHA.107.141911

Madan, M., Berkowitz, S.D., 1999. Understanding thrombocytopenia and antigenicity with glycoprotein IIb-IIIa inhibitors. Am. Heart J. 138, 317–326.

Mahaut-Smith, M.P., 2012. The unique contribution of ion channels to platelet and megakaryocyte function. J. Thromb. Haemost. JTH 10, 1722–1732. https://doi.org/10.1111/j.1538-7836.2012.04837.x

Maioli, E., Pacini, A., Viti, A., 1985. Microfilament organization in human platelets. Ric. Clin. Lab. 15, 105–112.

Makris, M., Van Veen, J.J., Tait, C.R., Mumford, A.D., Laffan, M., British Committee for Standards in Haematology, 2013. Guideline on the management of bleeding in patients on antithrombotic agents. Br. J. Haematol. 160, 35–46. https://doi.org/10.1111/bjh.12107

Mammadova-Bach, E., Nagy, M., Heemskerk, J.W.M., Nieswandt, B., Braun, A., 2019. Store-operated calcium entry in thrombosis and thrombo-inflammation. Cell Calcium 77, 39–48. https://doi.org/10.1016/j.ceca.2018.11.005

Mammadova-Bach, E., Ollivier, V., Loyau, S., Schaff, M., Dumont, B., Favier, R., Freyburger, G., Latger-Cannard, V., Nieswandt, B., Gachet, C., Mangin, P.H., Jandrot-Perrus, M., 2015. Platelet glycoprotein VI binds to polymerized fibrin and promotes thrombin generation. Blood 126, 683–691. https://doi.org/10.1182/blood-2015-02-629717

Manna, P.T., Munsey, T.S., Abuarab, N., Li, F., Asipu, A., Howell, G., Sedo, A., Yang, W., Naylor, J., Beech, D.J., Jiang, L.-H., Sivaprasadarao, A., 2015. TRPM2-mediated intracellular Zn2+ release triggers pancreatic β-cell death. Biochem. J. 466, 537–546. https://doi.org/10.1042/BJ20140747

Maret, W., 2000. The function of zinc metallothionein: a link between cellular zinc and redox state. J. Nutr. 130, 1455S–8S. https://doi.org/10.1093/jn/130.5.1455S

Marger, L., Schubert, C.R., Bertrand, D., 2014. Zinc: an underappreciated modulatory factor of brain function. Biochem. Pharmacol. 91, 426–435. https://doi.org/10.1016/j.bcp.2014.08.002

Marjoram, R.J., Li, Z., He, L., Tollefsen, D.M., Kunicki, T.J., Dickeson, S.K., Santoro, S.A., Zutter, M.M., 2014. α2β1 integrin, GPVI receptor, and common FcRγ chain on mouse platelets mediate distinct responses to collagen in models of thrombosis. PloS One 9, e114035. https://doi.org/10.1371/journal.pone.0114035

Marreiro, D. do N., Cruz, K.J.C., Morais, J.B.S., Beserra, J.B., Severo, J.S., de Oliveira, A.R.S., 2017. Zinc and Oxidative Stress: Current Mechanisms. Antioxidants 6. https://doi.org/10.3390/antiox6020024

Marx, G., Korner, G., Mou, X., Gorodetsky, R., 1993a. Packaging zinc, fibrinogen, and factor XIII in platelet alpha-granules. J. Cell. Physiol. 156, 437–442. https://doi.org/10.1002/jcp.1041560302

Marx, G., Korner, G., Mou, X., Gorodetsky, R., 1993b. Packaging zinc, fibrinogen, and factor XIII in platelet alpha-granules. J. Cell. Physiol. 156, 437–442.

Marx, G., Krugliak, J., Shaklai, M., 1991. Nutritional zinc increases platelet reactivity. Am. J. Hematol. 38, 161–165.

Masters, B.A., Quaife, C.J., Erickson, J.C., Kelly, E.J., Froelick, G.J., Zambrowicz, B.P., Brinster, R.L., Palmiter, R.D., 1994. Metallothionein III is expressed in neurons that sequester zinc in synaptic vesicles. J. Neurosci. Off. J. Soc. Neurosci. 14, 5844–5857.

Matias, C.M., Sousa, J.M., Quinta-Ferreira, M.E., Arif, M., Burrows, H.D., 2010a. Validation of TPEN as a zinc chelator in fluorescence probing of calcium in cells with the indicator Fura-2. J. Fluoresc. 20, 377–380. https://doi.org/10.1007/s10895-009-0539-y

Matias, C.M., Sousa, J.M., Quinta-Ferreira, M.E., Arif, M., Burrows, H.D., 2010b. Validation of TPEN as a zinc chelator in fluorescence probing of calcium in cells with the indicator Fura-2. J. Fluoresc. 20, 377–380.

Matowicka-Karna, J., 2016. Markers of inflammation, activation of blood platelets and coagulation disorders in inflammatory bowel diseases. Postepy Hig. Med. Doswiadczalnej Online 70, 305–312.

Maurer-Spurej, E., Devine, D.V., 2001. Platelet aggregation is not initiated by platelet shape change. Lab. Investig. J. Tech. Methods Pathol. 81, 1517–1525.

Maynard, D.M., Heijnen, H.F.G., Horne, M.K., White, J.G., Gahl, W.A., 2007. Proteomic analysis of platelet alpha-granules using mass spectrometry. J. Thromb. Haemost. JTH 5, 1945–1955. https://doi.org/10.1111/j.1538-7836.2007.02690.x

Mazharian, A., Mori, J., Wang, Y.-J., Heising, S., Neel, B.G., Watson, S.P., Senis, Y.A., 2013. Megakaryocyte-specific deletion of the protein-tyrosine phosphatases Shp1 and Shp2 causes abnormal megakaryocyte development, platelet production, and function. Blood 121, 4205–4220. https://doi.org/10.1182/blood-2012-08-449272

McCord, M.C., Aizenman, E., 2014. The role of intracellular zinc release in aging, oxidative stress, and Alzheimer's disease. Front. Aging Neurosci. 6. https://doi.org/10.3389/fnagi.2014.00077

Meers, P., Mealy, T., 1993. Calcium-dependent annexin V binding to phospholipids: stoichiometry, specificity, and the role of negative charge. Biochemistry 32, 11711–11721.

Merlini, P.A., Rossi, M., Menozzi, A., Buratti, S., Brennan, D.M., Moliterno, D.J., Topol, E.J., Ardissino, D., 2004. Thrombocytopenia caused by abciximab or tirofiban and its association with clinical outcome in patients undergoing coronary stenting. Circulation 109, 2203–2206. https://doi.org/10.1161/01.CIR.0000127867.41621.85

Michaëlsson, G., Ljunghall, K., Danielson, B.G., 1980. Zinc in epidermis and dermis in healthy subjects. Acta Derm. Venereol. 60, 295–299.

Michal, F., Born, G.V.R., 1971. Effect of the Rapid Shape Change of Platelets on the Transmission and Scattering of Light through Plasma. Nature. New Biol. 231, 220–222. https://doi.org/10.1038/newbio231220a0

Millon-Frémillon, A., Brunner, M., Abed, N., Collomb, E., Ribba, A.-S., Block, M.R., Albigès-Rizo, C., Bouvard, D., 2013. Calcium and Calmodulin-dependent Serine/Threonine Protein Kinase Type II (CaMKII)-mediated Intramolecular Opening of Integrin Cytoplasmic Domain-associated Protein-1 (ICAP-1α) Negatively Regulates β1 Integrins. J. Biol. Chem. 288, 20248–20260. https://doi.org/10.1074/jbc.M113.455956

Mills, J.S., Johnson, J.D., 1985. Metal ions as allosteric regulators of calmodulin. J. Biol. Chem. 260, 15100–15105.

Milne, D.B., Ralston, N.V., Wallwork, J.C., 1985. Zinc content of cellular components of blood: methods for cell separation and analysis evaluated. Clin. Chem. 31, 65–69.

Minashima, T., Kirsch, T., 2018. Annexin A6 regulates catabolic events in articular chondrocytes via the modulation of NF-κB and Wnt/ß-catenin signaling. PloS One 13, e0197690. https://doi.org/10.1371/journal.pone.0197690

Miskolczi, Z., Smith, M.P., Rowling, E.J., Ferguson, J., Barriuso, J., Wellbrock, C., 2018. Collagen abundance controls melanoma phenotypes through lineage-specific microenvironment sensing. Oncogene 37, 3166. https://doi.org/10.1038/s41388-018-0209-0

Mogami, H., Kishore, A.H., Word, R.A., 2018. Collagen Type 1 Accelerates Healing of Ruptured Fetal Membranes. Sci. Rep. 8, 696. https://doi.org/10.1038/s41598-017-18787-9

Moncada, S., Vane, J.R., 1980. Interrelationships between prostacyclin and thromboxane A2. Ciba Found. Symp. 78, 165–183.

Monroe, D.M., Hoffman, M., Roberts, H.R., 2002. Platelets and thrombin generation. Arterioscler. Thromb. Vasc. Biol. 22, 1381–1389.

Monteilh-Zoller, M.K., Hermosura, M.C., Nadler, M.J.S., Scharenberg, A.M., Penner, R., Fleig, A., 2003. TRPM7 provides an ion channel mechanism for cellular entry of trace metal ions. J. Gen. Physiol. 121, 49–60.

Mooberry, M.J., Key, N.S., 2016. Microparticle analysis in disorders of hemostasis and thrombosis. Cytom. Part J. Int. Soc. Anal. Cytol. 89, 111–122. https://doi.org/10.1002/cyto.a.22647

Morel, O., Morel, N., Freyssinet, J.-M., Toti, F., 2008. Platelet microparticles and vascular cells interactions: a checkpoint between the haemostatic and thrombotic responses. Platelets 19, 9–23. https://doi.org/10.1080/09537100701817232

Morgenstern, E., Korell, U., Richter, J., 1984. Platelets and fibrin strands during clot retraction. Thromb. Res. 33, 617–623.

Morrell, C.N., Sun, H., Ikeda, M., Beique, J.-C., Swaim, A.M., Mason, E., Martin, T.V., Thompson, L.E., Gozen, O., Ampagoomian, D., Sprengel, R., Rothstein, J., Faraday, N., Huganir, R., Lowenstein, C.J., 2008. Glutamate mediates platelet activation through the AMPA receptor. J. Exp. Med. 205, 575–584. https://doi.org/10.1084/jem.20071474

Murugappan, S., Shankar, H., Bhamidipati, S., Dorsam, R.T., Jin, J., Kunapuli, S.P., 2005. Molecular mechanism and functional implications of thrombin-mediated tyrosine phosphorylation of PKCdelta in platelets. Blood 106, 550–557. https://doi.org/10.1182/blood-2004-12-4866

Muylle, F.A.R., Adriaensen, D., De Coen, W., Timmermans, J.-P., Blust, R., 2006. Tracing of labile zinc in live fish hepatocytes using FluoZin-3. Biometals Int. J. Role Met. Ions Biol. Biochem. Med. 19, 437–450. https://doi.org/10.1007/s10534-005-4576-y

Naik, U.P., Patel, P.M., Parise, L.V., 1997. Identification of a Novel Calcium-binding Protein That Interacts with the Integrin αIIb Cytoplasmic Domain. J. Biol. Chem. 272, 4651–4654. https://doi.org/10.1074/jbc.272.8.4651

Nakashima-Kaneda, K., Matsuda, A., Mizuguchi, H., Sasaki-Sakamoto, T., Saito, H., Ra, C., Okayama, Y., 2013. Regulation of IgE-dependent zinc release from human mast cells. Int. Arch. Allergy Immunol. 161 Suppl 2, 44–51. https://doi.org/10.1159/000350359

Nakayama, S., Kretsinger, R.H., 1994. Evolution of the EF-hand family of proteins. Annu. Rev. Biophys. Biomol. Struct. 23, 473–507. https://doi.org/10.1146/annurev.bb.23.060194.002353

Nakeff, A., Maat, B., 1974. Separation of Megakaryocytes From Mouse Bone Marrow by Velocity Sedimentation. Blood 43, 591–595.

Newton, A.C., Bootman, M.D., Scott, J.D., 2016. Second Messengers. Cold Spring Harb. Perspect. Biol. 8, a005926. https://doi.org/10.1101/cshperspect.a005926

Nieswandt, B., Pleines, I., Bender, M., 2011. Platelet adhesion and activation mechanisms in arterial thrombosis and ischaemic stroke. J. Thromb. Haemost. JTH 9 Suppl 1, 92–104. https://doi.org/10.1111/j.1538-7836.2011.04361.x

Nieswandt, B., Varga-Szabo, D., Elvers, M., 2009. Integrins in platelet activation. J. Thromb. Haemost. JTH 7 Suppl 1, 206–209. https://doi.org/10.1111/j.1538-7836.2009.03370.x

Nieswandt, B., Watson, S.P., 2003. Platelet-collagen interaction: is GPVI the central receptor? Blood 102, 449–461. https://doi.org/10.1182/blood-2002-12-3882

Noleto Magalhães, R.C., Guedes Borges de Araujo, C., Batista de Sousa Lima, V., Machado Moita Neto, J., do Nascimento Nogueira, N., do Nascimento Marreiro, D., 2011. Nutritional status of zinc and activity superoxide dismutase in chronic renal patients undergoing hemodialysis. Nutr. Hosp. 26, 1456–1461. https://doi.org/10.1590/S0212-16112011000600037

Nonato, A.O., Olivon, V.C., Dela Justina, V., Zanotto, C.Z., Webb, R.C., Tostes, R.C., Lima, V.V., Giachini, F.R., 2016. Impaired Ca(2+) Homeostasis and Decreased Orai1 Expression Modulates Arterial Hyporeactivity to Vasoconstrictors During Endotoxemia. Inflammation. https://doi.org/10.1007/s10753-016-0354-y

Nurden, A.T., 2006. Glanzmann thrombasthenia. Orphanet J. Rare Dis. 1, 10. https://doi.org/10.1186/1750-1172-1-10

Nurden, A.T., Nurden, P., 2014. Congenital platelet disorders and understanding of platelet function. Br. J. Haematol. 165, 165–178. https://doi.org/10.1111/bjh.12662

O'Brien, J.R., Salmon, G.P., 1987. Shear stress activation of platelet glycoprotein IIb/IIIa plus von Willebrand factor causes aggregation: filter blockage and the long bleeding time in von Willebrand's disease. Blood 70, 1354–1361.

O'Dell, B.L., Emery, M., Xia, J., Browning, J.D., 1997. In vitro addition of glutathione to blood from zinc-deficient rats corrects platelet defects: Impaired aggregation and calcium uptake. J. Nutr. Biochem. 8, 346–350. https://doi.org/10.1016/S0955-2863(97)00020-X

O'Donoghue, M.L., Bhatt, D.L., Wiviott, S.D., Goodman, S.G., Fitzgerald, D.J., Angiolillo, D.J., Goto, S., Montalescot, G., Zeymer, U., Aylward, P.E., Guetta, V., Dudek, D., Ziecina, R., Contant, C.F., Flather, M.D., LANCELOT-ACS Investigators, 2011. Safety and tolerability of atopaxar in the treatment of patients with acute coronary syndromes: the lessons from antagonizing the cellular effects of Thrombin–Acute Coronary Syndromes Trial. Circulation 123, 1843–1853. https://doi.org/10.1161/CIRCULATIONAHA.110.000786

Oestreich, J.H., Ferraris, S.P., Steinhubl, S.R., Akers, W.S., 2013. Pharmacodynamic interplay of the P2Y(1), P2Y(12), and TxA(2) pathways in platelets: the potential of triple antiplatelet therapy with P2Y(1) receptor antagonism. Thromb. Res. 131, e64-70. https://doi.org/10.1016/j.thromres.2012.11.019

Offermanns, S., 2006. Activation of platelet function through G protein-coupled receptors. Circ. Res. 99, 1293–1304. https://doi.org/10.1161/01.RES.0000251742.71301.16

Ohlmann, P., Eckly, A., Freund, M., Cazenave, J.-P., Offermanns, S., Gachet, C., 2000. ADP induces partial platelet aggregation without shape change and potentiates collagen-induced aggregation in the absence of Gαq. Blood 96, 2134–2139.

Olas, B., Wachowicz, B., 2007. Role of reactive nitrogen species in blood platelet functions. Platelets 18, 555–565. https://doi.org/10.1080/09537100701504087

Olgar, Y., Ozdemir, S., Turan, B., 2018. Induction of endoplasmic reticulum stress and changes in expression levels of Zn2+-transporters in hypertrophic rat heart. Mol. Cell. Biochem. 440, 209–219. https://doi.org/10.1007/s11010-017-3168-9

Oliver, A.E., Tablin, F., Walker, N.J., Crowe, J.H., 1999. The internal calcium concentration of human platelets increases during chilling. Biochim. Biophys. Acta BBA - Biomembr. 1416, 349–360. https://doi.org/10.1016/S0005-2736(98)00239-9

Orem, B.C., Pelisch, N., Williams, J., Nally, J.M., Stirling, D.P., 2017. Intracellular calcium release through IP3R or RyR contributes to secondary axonal degeneration. Neurobiol. Dis. 106, 235–243. https://doi.org/10.1016/j.nbd.2017.07.011

Orford, J.L., Holmes, D.R., 2002. Abciximab readministration. Rev. Cardiovasc. Med. 3, 67–70.

Ornelas, A., Zacharias-Millward, N., Menter, D.G., Davis, J.S., Lichtenberger, L., Hawke, D., Hawk, E., Vilar, E., Bhattacharya, P., Millward, S., 2017. Beyond COX-1: the effects of aspirin on platelet biology and potential mechanisms of chemoprevention. Cancer Metastasis Rev. 36, 289–303. https://doi.org/10.1007/s10555-017-9675-z

Owens, A.P., Mackman, N., 2011. Microparticles in hemostasis and thrombosis. Circ. Res. 108, 1284–1297. https://doi.org/10.1161/CIRCRESAHA.110.233056

Ozaki, Y., Qi, R., Satoh, K., Asazuma, N., Yatomi, Y., 2000. Platelet activation mediated through membrane glycoproteins: involvement of tyrosine kinases. Semin. Thromb. Hemost. 26, 47–51.

Palmiter, R.D., Cole, T.B., Quaife, C.J., Findley, S.D., 1996. ZnT-3, a putative transporter of zinc into synaptic vesicles. Proc. Natl. Acad. Sci. U. S. A. 93, 14934–14939.

Palta, S., Saroa, R., Palta, A., 2014. Overview of the coagulation system. Indian J. Anaesth. 58, 515–523. https://doi.org/10.4103/0019-5049.144643

Pandya, C.D., Howell, K.R., Pillai, A., 2013. Antioxidants as potential therapeutics for neuropsychiatric disorders. Prog. Neuropsychopharmacol. Biol. Psychiatry 46, 214–223. https://doi.org/10.1016/j.pnpbp.2012.10.017

Paoletti, P., Vergnano, A.M., Barbour, B., Casado, M., 2009. Zinc at glutamatergic synapses. Neuroscience, Protein trafficking, targeting, and interaction at the glutamate synapse 158, 126–136. https://doi.org/10.1016/j.neuroscience.2008.01.061

Paredes, R.M., Etzler, J.C., Watts, L.T., Lechleiter, J.D., 2008. Chemical Calcium Indicators. Methods San Diego Calif 46, 143–151. https://doi.org/10.1016/j.ymeth.2008.09.025

Park, M.-H., Lee, S.-J., Byun, H.-R., Kim, Y., Oh, Y.J., Koh, J.-Y., Hwang, J.J., 2011. Clioquinol induces autophagy in cultured astrocytes and neurons by acting as a zinc ionophore. Neurobiol. Dis. 42, 242–251. https://doi.org/10.1016/j.nbd.2011.01.009

Park, M.K., Lee, K.K., Uhm, D.-Y., 2002. Slow depletion of endoplasmic reticulum Ca(2+) stores and block of store-operated Ca(2+) channels by 2-aminoethoxydiphenyl borate in mouse pancreatic acinar cells. Naunyn. Schmiedebergs Arch. Pharmacol. 365, 399–405. https://doi.org/10.1007/s00210-002-0535-0

Pasquet, J.M., Gross, B., Quek, L., Asazuma, N., Zhang, W., Sommers, C.L., Schweighoffer, E., Tybulewicz, V., Judd, B., Lee, J.R., Koretzky, G., Love, P.E., Samelson, L.E., Watson, S.P., 1999. LAT is required for tyrosine phosphorylation of phospholipase cgamma2 and platelet activation by the collagen receptor GPVI. Mol. Cell. Biol. 19, 8326–8334.

Paul, B.Z., Daniel, J.L., Kunapuli, S.P., 1999. Platelet shape change is mediated by both calcium-dependent and -independent signaling pathways. Role of p160 Rho-associated coiled-coil-containing protein kinase in platelet shape change. J. Biol. Chem. 274, 28293–28300.

Paz Matias, J., Costa e Silva, D.M., Clímaco Cruz, K.J., Gomes da Silva, K., Monte Feitosa, M., Oliveira Medeiros, L.G., do Nascimento Marreiro, D., do Nascimento Nogueira, N., 2014. Effect of zinc supplementation on superoxide dismutase activity in patients with ulcerative rectocolitis. Nutr. Hosp. 31, 1434–1437. https://doi.org/10.3305/nh.2015.31.3.8402

Pease, D.C., 1956. An Electron Microscopic Study of Red Bone Marrow. Blood 11, 501–526.

Pérez-Clausell, J., Danscher, G., 1986. Release of zinc sulphide accumulations into synaptic clefts after in vivo injection of sodium sulphide. Brain Res. 362, 358–361.

Perrin, L., Roudeau, S., Carmona, A., Domart, F., Petersen, J.D., Bohic, S., Yang, Y., Cloetens, P., Ortega, R., 2017a. Zinc and Copper Effects on Stability of Tubulin and Actin Networks in Dendrites and Spines of Hippocampal Neurons. ACS Chem. Neurosci. 8, 1490–1499. https://doi.org/10.1021/acschemneuro.6b00452

Perrin, L., Roudeau, S., Carmona, A., Domart, F., Petersen, J.D., Bohic, S., Yang, Y., Cloetens, P., Ortega, R., 2017b. Zinc and Copper Effects on Stability of Tubulin and Actin Networks in Dendrites and Spines of Hippocampal Neurons. ACS Chem. Neurosci. 8, 1490–1499.

Perry, D.K., Smyth, M.J., Stennicke, H.R., Salvesen, G.S., Duriez, P., Poirier, G.G., Hannun, Y.A., 1997. Zinc is a potent inhibitor of the apoptotic protease, caspase-3. A novel target for zinc in the inhibition of apoptosis. J. Biol. Chem. 272, 18530–18533.

Petersen, J., Hagan, I.M., 2005. Polo kinase links the stress pathway to cell cycle control and tip growth in fission yeast. Nature 435, 507–512. https://doi.org/10.1038/nature03590

Peyvandi, F., Garagiola, I., Baronciani, L., 2011. Role of von Willebrand factor in the haemostasis. Blood Transfus. Trasfus. Sangue 9 Suppl 2, s3-8. https://doi.org/10.2450/2011.002S

Pfeiffer, D.R., Taylor, R.W., Lardy, H.A., 1978. IONOPHORE A23187: CATION BINDING AND TRANSPORT PROPERTIES*. Ann. N. Y. Acad. Sci. 307, 402–423. https://doi.org/10.1111/j.1749-6632.1978.tb41965.x

Phillips, D.R., Baughan, A.K., 1983. Fibrinogen binding to human platelet plasma membranes. Identification of two steps requiring divalent cations. J. Biol. Chem. 258, 10240–10246.

Pietraforte, D., Vona, R., Marchesi, A., de Jacobis, I.T., Villani, A., Del Principe, D., Straface, E., 2014. Redox control of platelet functions in physiology and pathophysiology. Antioxid. Redox Signal. 21, 177–193. https://doi.org/10.1089/ars.2013.5532

Pignatelli, P., Pulcinelli, F.M., Lenti, L., Gazzaniga, P.P., Violi, F., 1998. Hydrogen peroxide is involved in collagen-induced platelet activation. Blood 91, 484–490.

Pitt, S.J., Stewart, A.J., 2015. Examining a new role for zinc in regulating calcium release in cardiac muscle. Biochem. Soc. Trans. 43, 359–363. https://doi.org/10.1042/BST20140285

Plow, E.F., Pierschbacher, M.D., Ruoslahti, E., Marguerie, G.A., Ginsberg, M.H., 1985. The effect of Arg-Gly-Asp-containing peptides on fibrinogen and von Willebrand factor binding to platelets. Proc. Natl. Acad. Sci. U. S. A. 82, 8057–8061.

Plum, L.M., Rink, L., Haase, H., 2010. The essential toxin: impact of zinc on human health. Int. J. Environ. Res. Public. Health 7, 1342–1365. https://doi.org/10.3390/ijerph7041342

Podoplelova, N.A., Sveshnikova, A.N., Kotova, Y.N., Eckly, A., Receveur, N., Nechipurenko, D.Y., Obydennyi, S.I., Kireev, I.I., Gachet, C., Ataullakhanov, F.I., Mangin, P.H., Panteleev, M.A., 2016. Coagulation factors bound to procoagulant platelets concentrate in cap structures to promote clotting. Blood 128, 1745–1755. https://doi.org/10.1182/blood-2016-02-696898

Pomorski, T.G., Menon, A.K., 2016. Lipid somersaults: Uncovering the mechanisms of protein-mediated lipid flipping. Prog. Lipid Res. 64, 69–84. https://doi.org/10.1016/j.plipres.2016.08.003

Poole, A., Gibbins, J.M., Turner, M., van Vugt, M.J., van de Winkel, J.G., Saito, T., Tybulewicz, V.L., Watson, S.P., 1997. The Fc receptor gamma-chain and the tyrosine kinase Syk are essential for activation of mouse platelets by collagen. EMBO J. 16, 2333–2341. https://doi.org/10.1093/emboj/16.9.2333

Poon, M.-C., 2007. Clinical use of recombinant human activated factor VII (rFVIIa) in the prevention and treatment of bleeding episodes in patients with Glanzmann's thrombasthenia. Vasc. Health Risk Manag. 3, 655–664.

Poon, M.-C., Di Minno, G., d'Oiron, R., Zotz, R., 2016. New Insights Into the Treatment of Glanzmann Thrombasthenia. Transfus. Med. Rev. 30, 92–99. https://doi.org/10.1016/j.tmrv.2016.01.001

Poon, M.-C., Zotz, R., Di Minno, G., Abrams, Z.S., Knudsen, J.B., Laurian, Y., 2006. Glanzmann's thrombasthenia treatment: a prospective observational registry on the use of recombinant human activated factor VII and other hemostatic agents. Semin. Hematol. 43, S33-36. https://doi.org/10.1053/j.seminhematol.2005.11.009

Pozo-Guisado, E., Martin-Romero, F.J., 2013. The regulation of STIM1 by phosphorylation. Commun. Integr. Biol. 6. https://doi.org/10.4161/cib.26283

Pozzan, T., Volpe, P., Zorzato, F., Bravin, M., Krause, K.H., Lew, D.P., Hashimoto, S., Bruno, B., Meldolesi, J., 1988. The Ins(1,4,5)P3-sensitive Ca2+ store of non-muscle cells: endoplasmic reticulum or calciosomes? J. Exp. Biol. 139, 181–193.

Prachayasittikul, Veda, Prachayasittikul, S., Ruchirawat, S., Prachayasittikul, Virapong, 2013. 8-Hydroxyquinolines: a review of their metal chelating properties and medicinal applications. Drug Des. Devel. Ther. 7, 1157–1178. https://doi.org/10.2147/DDDT.S49763

Pressman, B.C., 1976. Biological applications of ionophores. Annu. Rev. Biochem. 45, 501–530. https://doi.org/10.1146/annurev.bi.45.070176.002441

Prockop, D.J., Kivirikko, K.I., 1995. Collagens: molecular biology, diseases, and potentials for therapy. Annu. Rev. Biochem. 64, 403–434. https://doi.org/10.1146/annurev.bi.64.070195.002155

Pulcinelli, F.M., Pesciotti, M., Pignatelli, P., Riondino, S., Gazzaniga, P.P., 1998. Concomitant activation of Gi and Gq protein-coupled receptors does not require an increase in cytosolic calcium for platelet aggregation. FEBS Lett. 435, 115–118.

Qian, C., Colvin, R.A., 2016a. Zinc flexes its muscle: Correcting a novel analysis of calcium for zinc interference uncovers a method to measure zinc. J. Gen. Physiol. 147, 95–102.

Qian, C., Colvin, R.A., 2016b. Zinc flexes its muscle: Correcting a novel analysis of calcium for zinc interference uncovers a method to measure zinc. J. Gen. Physiol. 147, 95–102. https://doi.org/10.1085/jgp.201511493

Qiao, J., Arthur, J.F., Gardiner, E.E., Andrews, R.K., Zeng, L., Xu, K., 2018. Regulation of platelet activation and thrombus formation by reactive oxygen species. Redox Biol. 14, 126–130. https://doi.org/10.1016/j.redox.2017.08.021

Qiu, Y., Brown, A.C., Myers, D.R., Sakurai, Y., Mannino, R.G., Tran, R., Ahn, B., Hardy, E.T., Kee, M.F., Kumar, S., Bao, G., Barker, T.H., Lam, W.A., 2014. Platelet mechanosensing of substrate stiffness during clot formation mediates adhesion, spreading, and activation. Proc. Natl. Acad. Sci. U. S. A. 111, 14430–14435. https://doi.org/10.1073/pnas.1322917111

Radford, R.J., Lippard, S.J., 2013. Chelators for investigating zinc metalloneurochemistry. Curr. Opin. Chem. Biol. 17, 129–136. https://doi.org/10.1016/j.cbpa.2013.01.009

Rahman, K., Lowe, G.M., Smith, S., 2016. Aged Garlic Extract Inhibits Human Platelet Aggregation by Altering Intracellular Signaling and Platelet Shape Change. J. Nutr. 146, 410S–5S. https://doi.org/10.3945/jn.114.202408

Rahman, M.T., De Ley, M., 2008. Metallothionein in human thrombocyte precursors, CD61+ megakaryocytes. Cell Biol. Toxicol. 24, 19–25. https://doi.org/10.1007/s10565-007-9012-3

Rajpurkar, M., Chitlur, M., Recht, M., Cooper, D.L., 2014. Use of recombinant activated factor VII in patients with Glanzmann's thrombasthenia: a review of the literature. Haemoph. Off. J. World Fed. Hemoph. 20, 464–471. https://doi.org/10.1111/hae.12473

Ranasinghe, P., Wathurapatha, W.S., Galappatthy, P., Katulanda, P., Jayawardena, R., Constantine, G.R., 2018. Zinc supplementation in prediabetes: A randomized double-blind placebo-controlled clinical trial. J. Diabetes 10, 386–397. https://doi.org/10.1111/1753-0407.12621

Reed, G.L., Fitzgerald, M.L., Polgár, J., 2000. Molecular mechanisms of platelet exocytosis: insights into the "secrete" life of thrombocytes. Blood 96, 3334–3342.

Reininger, A.J., 2008. Function of von Willebrand factor in haemostasis and thrombosis. Haemoph. Off. J. World Fed. Hemoph. 14 Suppl 5, 11–26. https://doi.org/10.1111/j.1365-2516.2008.01848.x

Reséndiz, J.C., Kroll, M.H., Lassila, R., 2007. Protease-activated receptor-induced Akt activation--regulation and possible function. J. Thromb. Haemost. JTH 5, 2484–2493. https://doi.org/10.1111/j.1538-7836.2007.02769.x

Retzer, M., Essler, M., 2000. Lysophosphatidic acid-induced platelet shape change proceeds via Rho/Rho kinase-mediated myosin light-chain and moesin phosphorylation. Cell. Signal. 12, 645–648.

Richardson, J.L., Shivdasani, R.A., Boers, C., Hartwig, J.H., Italiano, J.E., 2005. Mechanisms of organelle transport and capture along proplatelets during platelet production. Blood 106, 4066–4075. https://doi.org/10.1182/blood-2005-06-2206

Rivera, J., Lozano, M.L., Navarro-Núñez, L., Vicente, V., 2009. Platelet receptors and signaling in the dynamics of thrombus formation. Haematologica 94, 700–711. https://doi.org/10.3324/haematol.2008.003178

Roberts, D.E., Matsuda, T., Bose, R., 2012. Molecular and functional characterization of the human platelet Na(+) /Ca(2+) exchangers. Br. J. Pharmacol. 165, 922–936. https://doi.org/10.1111/j.1476-5381.2011.01600.x

Rodríguez-Santiago, L., Alí-Torres, J., Vidossich, P., Sodupe, M., 2015. Coordination properties of a metal chelator clioquinol to Zn(2+) studied by static DFT and ab initio molecular dynamics. Phys. Chem. Chem. Phys. PCCP 17, 13582–13589. https://doi.org/10.1039/c5cp01615k

Roll, J.D., Reuther, G.W., 2012. ALK-activating homologous mutations in LTK induce cellular transformation. PloS One 7, e31733. https://doi.org/10.1371/journal.pone.0031733

Rollet-Labelle, E., Vaillancourt, M., Marois, L., Newkirk, M.M., Poubelle, P.E., Naccache, P.H., 2013. Cross-linking of IgGs bound on circulating neutrophils leads to an activation of endothelial cells: possible role of rheumatoid factors in rheumatoid arthritis-associated vascular dysfunction. J. Inflamm. Lond. Engl. 10, 27. https://doi.org/10.1186/1476-9255-10-27

Romero-Isart, N., Vasák, M., 2002. Advances in the structure and chemistry of metallothioneins. J. Inorg. Biochem. 88, 388–396.

Roohani, N., Hurrell, R., Kelishadi, R., Schulin, R., 2013. Zinc and its importance for human health: An integrative review. J. Res. Med. Sci. Off. J. Isfahan Univ. Med. Sci. 18, 144–157.

Rosenbaum, D.M., Rasmussen, S.G.F., Kobilka, B.K., 2009. The structure and function of G-protein-coupled receptors. Nature 459, 356–363. https://doi.org/10.1038/nature08144

Rotondo, S., Celardo, A., Evangelista, V., Cerletti, C., 1995. The endoperoxides/TxA2 analogue, U46619, inhibits human polymorphonuclear leukocyte function. J. Leukoc. Biol. 57, 72–79.

Rousseau, A., Rio, M.-C., Alpy, F., 2011. TRAF4, at the Crossroad between Morphogenesis and Cancer. Cancers 3, 2734–2749. https://doi.org/10.3390/cancers3022734

Rudolf, E., Klvacová, L., John, S., Cervinka, M., 2008a. Zinc alters cytoskeletal integrity and migration in colon cancer cells. Acta Medica (Hradec Kralove) 51, 51–57.

Rudolf, E., Klvacová, L., John, S., Cervinka, M., 2008b. Zinc alters cytoskeletal integrity and migration in colon cancer cells. Acta Medica 51, 51–57.

Rükgauer, M., Klein, J., Kruse-Jarres, J.D., 1997. Reference values for the trace elements copper, manganese, selenium, and zinc in the serum/plasma of children, adolescents, and adults. J. Trace Elem. Med. Biol. Organ Soc. Miner. Trace Elem. GMS 11, 92–98. https://doi.org/10.1016/S0946-672X(97)80032-6

Ryu, S.-Y., Kim, S., 2013. Evaluation of CK2 inhibitor (E)-3-(2,3,4,5-tetrabromophenyl)acrylic acid (TBCA) in regulation of platelet function. Eur. J. Pharmacol. 720, 391–400. https://doi.org/10.1016/j.ejphar.2013.09.064

Sakanashi, Y., Oyama, T.M., Matsuo, Y., Oyama, T.B., Nishimura, Y., Ishida, S., Imai, S., Okano, Y., Oyama, Y., 2009. Zn(2+), derived from cell preparation, partly attenuates Ca(2+)-dependent

cell death induced by A23187, calcium ionophore, in rat thymocytes. Toxicol. Vitro Int. J. Publ. Assoc. BIBRA 23, 338–345. https://doi.org/10.1016/j.tiv.2008.12.006

Sander, H.J., Slot, J.W., Bouma, B.N., Bolhuis, P.A., Pepper, D.S., Sixma, J.J., 1983. Immunocytochemical localization of fibrinogen, platelet factor 4, and beta thromboglobulin in thin frozen sections of human blood platelets. J. Clin. Invest. 72, 1277–1287. https://doi.org/10.1172/JCI111084

Sanjeev K., Chen Wenchun, Kraft Peter, Becker Isabelle C., Wolf Karen, Stritt Simon, Zierler Susanna, Hermanns Heike M., Rao Deviyani, Perraud Anne-Laure, Schmitz Carsten, Zahedi René P., Noy Peter J., Tomlinson Michael G., Dandekar Thomas, Matsushita Masayuki, Chubanov Vladimir, Gudermann Thomas, Stoll Guido, Nieswandt Bernhard, Braun Attila, 2018. TRPM7 Kinase Controls Calcium Responses in Arterial Thrombosis and Stroke in Mice. Arterioscler. Thromb. Vasc. Biol. 38, 344–352. https://doi.org/10.1161/ATVBAHA.117.310391

Santoro, S.A., Walsh, J.J., Staatz, W.D., Baranski, K.J., 1991. Distinct determinants on collagen support alpha 2 beta 1 integrin-mediated platelet adhesion and platelet activation. Cell Regul. 2, 905–913. https://doi.org/10.1091/mbc.2.11.905

Sargeant, P., Farndale, R.W., Sage, S.O., 1994. Calcium store depletion in dimethyl BAPTA-loaded human platelets increases protein tyrosine phosphorylation in the absence of a rise in cytosolic calcium. Exp. Physiol. 79, 269–272. https://doi.org/10.1113/expphysiol.1994.sp003762

Savi, P., Beauverger, P., Labouret, C., Delfaud, M., Salel, V., Kaghad, M., Herbert, J.M., 1998. Role of P2Y1 purinoceptor in ADP-induced platelet activation. FEBS Lett. 422, 291–295.

Savlov, E.D., Strain, W.H., Huegin, F., 1962. Radiozinc studies in experimental wound healing. J. Surg. Res. 2, 209–212. https://doi.org/10.1016/S0022-4804(62)80065-1

Schäfer, B.W., Fritschy, J.-M., Murmann, P., Troxler, H., Durussel, I., Heizmann, C.W., Cox, J.A., 2000. Brain S100A5 Is a Novel Calcium-, Zinc-, and Copper Ion-binding Protein of the EF-hand Superfamily. J. Biol. Chem. 275, 30623–30630. https://doi.org/10.1074/jbc.M002260200

Schimmer, A.D., Jitkova, Y., Gronda, M., Wang, Z., Brandwein, J., Chen, C., Gupta, V., Schuh, A., Yee, K., Chen, J., Ackloo, S., Booth, T., Keays, S., Minden, M.D., 2012. A phase I study of the metal ionophore clioquinol in patients with advanced hematologic malignancies. Clin. Lymphoma Myeloma Leuk. 12, 330–336. https://doi.org/10.1016/j.clml.2012.05.005

Schneider, C., 2009. An update on products and mechanisms of lipid peroxidation. Mol. Nutr. Food Res. 53, 315–321. https://doi.org/10.1002/mnfr.200800131

Schoenwaelder, S.M., Yuan, Y., Josefsson, E.C., White, M.J., Yao, Y., Mason, K.D., O'Reilly, L.A., Henley, K.J., Ono, A., Hsiao, S., Willcox, A., Roberts, A.W., Huang, D.C.S., Salem, H.H., Kile, B.T., Jackson, S.P., 2009. Two distinct pathways regulate platelet phosphatidylserine exposure and procoagulant function. Blood 114, 663–666. https://doi.org/10.1182/blood-2009-01-200345

Schrör, K., 1997. Aspirin and platelets: the antiplatelet action of aspirin and its role in thrombosis treatment and prophylaxis. Semin. Thromb. Hemost. 23, 349–356. https://doi.org/10.1055/s-2007-996108

Schumacher, M.A., Crum, M., Miller, M.C., 2004. Crystal structures of apocalmodulin and an apocalmodulin/SK potassium channel gating domain complex. Struct. Lond. Engl. 1993 12, 849–860. https://doi.org/10.1016/j.str.2004.03.017

Scott, B.J., Bradwell, A.R., 1983. Identification of the serum binding proteins for iron, zinc, cadmium, nickel, and calcium. Clin. Chem. 29, 629–633.

Seifert, J., Rheinlaender, J., Lang, F., Gawaz, M., Schäffer, T.E., 2017. Thrombin-induced cytoskeleton dynamics in spread human platelets observed with fast scanning ion conductance microscopy. Sci. Rep. 7, 4810. https://doi.org/10.1038/s41598-017-04999-6

Sekler, I., Sensi, S.L., Hershfinkel, M., Silverman, W.F., 2007. Mechanism and regulation of cellular zinc transport. Mol. Med. Camb. Mass 13, 337–343. https://doi.org/10.2119/2007–00037.Sekler

Selvadurai, M.V., Hamilton, J.R., 2018. Structure and function of the open canalicular system - the platelet's specialized internal membrane network. Platelets 29, 319–325. https://doi.org/10.1080/09537104.2018.1431388

Senis, Y.A., Mazharian, A., Mori, J., 2014. Src family kinases: at the forefront of platelet activation. Blood 124, 2013–2024. https://doi.org/10.1182/blood-2014-01-453134

Sensi, S.L., Canzoniero, L.M., Yu, S.P., Ying, H.S., Koh, J.Y., Kerchner, G.A., Choi, D.W., 1997. Measurement of intracellular free zinc in living cortical neurons: routes of entry. J. Neurosci. Off. J. Soc. Neurosci. 17, 9554–9564.

Sensi, S.L., Paoletti, P., Bush, A.I., Sekler, I., 2009. Zinc in the physiology and pathology of the CNS. Nat. Rev. Neurosci. 10, 780–791. https://doi.org/10.1038/nrn2734

Seo, B.-R., Lee, S.-J., Cho, K.S., Yoon, Y.H., Koh, J.-Y., 2015. The zinc ionophore clioquinol reverses autophagy arrest in chloroquine-treated ARPE-19 cells and in APP/mutant presenilin-1-transfected Chinese hamster ovary cells. Neurobiol. Aging 36, 3228–3238. https://doi.org/10.1016/j.neurobiolaging.2015.09.006

Sharir, H., Zinger, A., Nevo, A., Sekler, I., Hershfinkel, M., 2010. Zinc Released from Injured Cells Is Acting via the Zn2+-sensing Receptor, ZnR, to Trigger Signaling Leading to Epithelial Repair. J. Biol. Chem. 285, 26097–26106. https://doi.org/10.1074/jbc.M110.107490

Sharov, V.S., Dremina, E.S., Galeva, N.A., Williams, T.D., Schöneich, C., 2006. Quantitative mapping of oxidation-sensitive cysteine residues in SERCA in vivo and in vitro by HPLC-electrospray-tandem MS: selective protein oxidation during biological aging. Biochem. J. 394, 605–615. https://doi.org/10.1042/BJ20051214

Shastri, B.P., Sankaram, M.B., Easwaran, K.R., 1987. Carboxylic ionophore (lasalocid A and A23187) mediated lanthanide ion transport across phospholipid vesicles. Biochemistry 26, 4925–4930.

Shattil, S.J., Hoxie, J.A., Cunningham, M., Brass, L.F., 1985. Changes in the platelet membrane glycoprotein IIb.IIIa complex during platelet activation. J. Biol. Chem. 260, 11107–11114.

Shattil, S.J., Motulsky, H.J., Insel, P.A., Flaherty, L., Brass, L.F., 1986. Expression of fibrinogen receptors during activation and subsequent desensitization of human platelets by epinephrine. Blood 68, 1224–1231.

Sheu, J.R., Hsiao, G., Shen, M.Y., Wang, Y., Lin, K.H., Lin, C.H., Chou, D.S., 2003. Inhibitory mechanisms of metallothionein on platelet aggregation in in vitro and platelet plug formation in in vivo experiments. Exp. Biol. Med. Maywood NJ 228, 1321–1328.

Shin, E.-K., Park, H., Noh, J.-Y., Lim, K.-M., Chung, J.-H., 2017. Platelet Shape Changes and Cytoskeleton Dynamics as Novel Therapeutic Targets for Anti-Thrombotic Drugs. Biomol. Ther. 25, 223–230. https://doi.org/10.4062/biomolther.2016.138

Siegel-Axel, D., Langer, H., Lindemann, S., Gawaz, M., 2006. [Role of platelets in atherosclerosis and inflammation]. Med. Klin. Munich Ger. 1983 101, 467–475. https://doi.org/10.1007/s00063-006-1066-0

Sies, H., 2014. Role of Metabolic H2O2 Generation: Redox Signalling and Oxidative Stress. J. Biol. Chem. jbc.R113.544635. https://doi.org/10.1074/jbc.R113.544635

Sims, P.J., Wiedmer, T., Esmon, C.T., Weiss, H.J., Shattil, S.J., 1989. Assembly of the platelet prothrombinase complex is linked to vesiculation of the platelet plasma membrane. Studies in Scott syndrome: an isolated defect in platelet procoagulant activity. J. Biol. Chem. 264, 17049–17057.

Sinha, N., Dabla, P.K., 2015. Oxidative stress and antioxidants in hypertension-a current review. Curr. Hypertens. Rev. 11, 132–142.

Sloviter, R.S., 1985. A selective loss of hippocampal mossy fiber Timm stain accompanies granule cell seizure activity induced by perforant path stimulation. Brain Res. 330, 150–153.

Smethurst, P.A., Onley, D.J., Jarvis, G.E., O'Connor, M.N., Knight, C.G., Herr, A.B., Ouwehand, W.H., Farndale, R.W., 2007. Structural basis for the platelet-collagen interaction: the smallest motif within collagen that recognizes and activates platelet Glycoprotein VI contains two glycine-proline-hydroxyproline triplets. J. Biol. Chem. 282, 1296–1304. https://doi.org/10.1074/jbc.M606479200

Smith, I.F., Parker, I., 2009. Imaging the quantal substructure of single IP3R channel activity during Ca2+ puffs in intact mammalian cells. Proc. Natl. Acad. Sci. U. S. A. 106, 6404–6409. https://doi.org/10.1073/pnas.0810799106

Smith, J.B., Araki, H., Lefer, A.M., 1980. Thromboxane A2, prostacyclin and aspirin: effects on vascular tone and platelet aggregation. Circulation 62, V19-25.

Smith, J.B., Selak, M.A., Dangelmaier, C., Daniel, J.L., 1992. Cytosolic calcium as a second messenger for collagen-induced platelet responses. Biochem. J. 288 (Pt 3), 925–929.

Smith, J.B., Willis, A.L., 1971. Aspirin selectively inhibits prostaglandin production in human platelets. Nature. New Biol. 231, 235–237.

Smith, M.P., Cramer, E.M., Savidge, G.F., 1997. Megakaryocytes and platelets in alpha-granule disorders. Baillieres Clin. Haematol. 10, 125–148.

Smolina, K., Wright, F.L., Rayner, M., Goldacre, M.J., 2012. Determinants of the decline in mortality from acute myocardial infarction in England between 2002 and 2010: linked national database study. BMJ 344, d8059. https://doi.org/10.1136/bmj.d8059

Sonego, G., Abonnenc, M., Tissot, J.-D., Prudent, M., Lion, N., 2017. Redox Proteomics and Platelet Activation: Understanding the Redox Proteome to Improve Platelet Quality for Transfusion. Int. J. Mol. Sci. 18. https://doi.org/10.3390/ijms18020387

Sørensen, J.C., Mattsson, B., Andreasen, A., Johansson, B.B., 1998. Rapid disappearance of zinc positive terminals in focal brain ischemia. Brain Res. 812, 265–269.

Soulet, C., Hechler, B., Gratacap, M.-P., Plantavid, M., Offermanns, S., Gachet, C., Payrastre, B., 2005. A differential role of the platelet ADP receptors P2Y1 and P2Y12 in Rac activation. J. Thromb. Haemost. JTH 3, 2296–2306. https://doi.org/10.1111/j.1538-7836.2005.01588.x

Stadler Nadina, Stanley Naomi, Heeneman Sylvia, Vacata Vladimir, Daemen Mat J.A.P., Bannon Paul G., Waltenberger Johannes, Davies Michael J., 2008. Accumulation of Zinc in Human Atherosclerotic Lesions Correlates With Calcium Levels But Does Not Protect Against Protein

Oxidation. Arterioscler. Thromb. Vasc. Biol. 28, 1024–1030. https://doi.org/10.1161/ATVBAHA.108.162735

Stalker, T.J., Newman, D.K., Ma, P., Wannemacher, K.M., Brass, L.F., 2012. Platelet Signaling. Handb. Exp. Pharmacol. 59–85. https://doi.org/10.1007/978-3-642-29423-5_3

Stefanidou, M., Maravelias, C., Dona, A., Spiliopoulou, C., 2006. Zinc: a multipurpose trace element. Arch. Toxicol. 80, 1–9. https://doi.org/10.1007/s00204-005-0009-5

Stefanini, M., 1999. Cutaneous bleeding related to zinc deficiency in two cases of advanced cancer. Cancer 86, 866–870.

Steinckwich, N., Schenten, V., Melchior, C., Bréchard, S., Tschirhart, E.J., 2011. An essential role of STIM1, Orai1, and S100A8-A9 proteins for Ca2+ signaling and FcγR-mediated phagosomal oxidative activity. J. Immunol. Baltim. Md 1950 186, 2182–2191. https://doi.org/10.4049/jimmunol.1001338

Stork, C.J., Li, Y.V., 2016. Elevated Cytoplasmic Free Zinc and Increased Reactive Oxygen Species Generation in the Context of Brain Injury. Acta Neurochir. Suppl. 121, 347–353. https://doi.org/10.1007/978-3-319-18497-5_60

Stork, C.J., Li, Y.V., 2006. Intracellular Zinc Elevation Measured with a “Calcium-Specific” Indicator during Ischemia and Reperfusion in Rat Hippocampus: A Question on Calcium Overload. J. Neurosci. 26, 10430–10437. https://doi.org/10.1523/JNEUROSCI.1588-06.2006

Sugiura, T., Nakamura, H., 1994. Metallothionein in platelets. Int. Arch. Allergy Immunol. 103, 341–348. https://doi.org/10.1159/000236652

Suh, S.W., Listiack, K., Bell, B., Chen, J., Motamedi, M., Silva, D., Danscher, G., Whetsell, W., Thompson, R., Frederickson, C., 1999. Detection of pathological zinc accumulation in neurons: methods for autopsy, biopsy, and cultured tissue. J. Histochem. Cytochem. Off. J. Histochem. Soc. 47, 969–972. https://doi.org/10.1177/002215549904700715

Sun, L., Gorospe, J.R., Hoffman, E.P., Rao, A.K., 2007. Decreased platelet expression of myosin regulatory light chain polypeptide (MYL9) and other genes with platelet dysfunction and CBFA2/RUNX1 mutation: insights from platelet expression profiling. J. Thromb. Haemost. JTH 5, 146–154. https://doi.org/10.1111/j.1538-7836.2006.02271.x

Suzuki, J., Fujii, T., Imao, T., Ishihara, K., Kuba, H., Nagata, S., 2013. Calcium-dependent phospholipid scramblase activity of TMEM16 protein family members. J. Biol. Chem. 288, 13305–13316. https://doi.org/10.1074/jbc.M113.457937

Suzuki, Y., Yamamoto, M., Wada, H., Ito, M., Nakano, T., Sasaki, Y., Narumiya, S., Shiku, H., Nishikawa, M., 1999. Agonist-induced regulation of myosin phosphatase activity in human platelets through activation of Rho-kinase. Blood 93, 3408–3417.

Tainer, J.A., Getzoff, E.D., Richardson, J.S., Richardson, D.C., 1983. Structure and mechanism of copper, zinc superoxide dismutase. Nature 306, 284–287. https://doi.org/10.1038/306284a0

Takeda, A., Tamano, H., Ogawa, T., Takada, S., Nakamura, M., Fujii, H., Ando, M., 2014. Intracellular Zn(2+) signaling in the dentate gyrus is required for object recognition memory. Hippocampus 24, 1404–1412. https://doi.org/10.1002/hipo.22322

Tang, L., Qiu, R., Tang, Y., Wang, S., 2014. Cadmium-zinc exchange and their binary relationship in the structure of Zn-related proteins: a mini review. Met. Integr. Biometal Sci. 6, 1313–1323. https://doi.org/10.1039/c4mt00080c

Tang, W.H., Stitham, J., Gleim, S., Di Febbo, C., Porreca, E., Fava, C., Tacconelli, S., Capone, M., Evangelista, V., Levantesi, G., Wen, L., Martin, K., Minuz, P., Rade, J., Patrignani, P., Hwa, J., 2011. Glucose and collagen regulate human platelet activity through aldose reductase induction of thromboxane. J. Clin. Invest. 121, 4462–4476. https://doi.org/10.1172/JCI59291

Tapiero, H., Tew, K.D., 2003. Trace elements in human physiology and pathology: zinc and metallothioneins. Biomed. Pharmacother. Biomedecine Pharmacother. 57, 399–411.

Taub, R., Gould, R.J., Garsky, V.M., Ciccarone, T.M., Hoxie, J., Friedman, P.A., Shattil, S.J., 1989. A monoclonal antibody against the platelet fibrinogen receptor contains a sequence that mimics a receptor recognition domain in fibrinogen. J. Biol. Chem. 264, 259–265.

Tautz, L., Senis, Y.A., Oury, C., Rahmouni, S., 2015. Perspective: Tyrosine phosphatases as novel targets for antiplatelet therapy. Bioorg. Med. Chem. 23, 2786–2797. https://doi.org/10.1016/j.bmc.2015.03.075

Taylor, C.G., 2005. Zinc, the pancreas, and diabetes: insights from rodent studies and future directions. Biometals Int. J. Role Met. Ions Biol. Biochem. Med. 18, 305–312. https://doi.org/10.1007/s10534-005-3686-x

Taylor, K.A., Pugh, N., 2016. The contribution of zinc to platelet behaviour during haemostasis and thrombosis. Met. Integr. Biometal Sci. 8, 144–155. https://doi.org/10.1039/c5mt00251f

Taylor, K.M., Hiscox, S., Nicholson, R.I., Hogstrand, C., Kille, P., 2012. Protein kinase CK2 triggers cytosolic zinc signaling pathways by phosphorylation of zinc channel ZIP7. Sci. Signal. 5, ra11. https://doi.org/10.1126/scisignal.2002585

Taylor, K.M., Vichova, P., Jordan, N., Hiscox, S., Hendley, R., Nicholson, R.I., 2008. ZIP7-mediated intracellular zinc transport contributes to aberrant growth factor signaling in antihormone-

resistant breast cancer Cells. Endocrinology 149, 4912–4920. https://doi.org/10.1210/en.2008-0351

Tcheng, J.E., Ellis, S.G., George, B.S., Kereiakes, D.J., Kleiman, N.S., Talley, J.D., Wang, A.L., Weisman, H.F., Califf, R.M., Topol, E.J., 1994. Pharmacodynamics of chimeric glycoprotein IIb/IIIa integrin antiplatelet antibody Fab 7E3 in high-risk coronary angioplasty. Circulation 90, 1757–1764.

Tcheng, J.E., Kereiakes, D.J., Lincoff, A.M., George, B.S., Kleiman, N.S., Sane, D.C., Cines, D.B., Jordan, R.E., Mascelli, M.A., Langrall, M.A., Damaraju, L., Schantz, A., Effron, M.B., Braden, G.A., 2001. Abciximab readministration: results of the ReoPro Readministration Registry. Circulation 104, 870–875.

Tepel, M., Wischniowski, H., Zidek, W., 1994. Thapsigargin-induced [Ca2+]i increase activates sodium influx in human platelets. Biochim. Biophys. Acta BBA - Mol. Cell Res. 1220, 248–252. https://doi.org/10.1016/0167-4889(94)90145-7

Thiagarajan, P., Tait, J.F., 1990. Binding of annexin V/placental anticoagulant protein I to platelets. Evidence for phosphatidylserine exposure in the procoagulant response of activated platelets. J. Biol. Chem. 265, 17420–17423.

Tomaiuolo, M., Brass, L.F., Stalker, T.J., 2017. Regulation of platelet activation and coagulation and its role in vascular injury and arterial thrombosis. Interv. Cardiol. Clin. 6, 1–12. https://doi.org/10.1016/j.iccl.2016.08.001

Torti, M., Bertoni, A., Sinigaglia, F., Balduini, C., Payrastre, B., Plantavid, M., Chap, H., Mauco, G., 2000. The platelet cytoskeleton regulates the aggregation-dependent synthesis of phosphatidylinositol 3,4-bisphosphate induced by thrombin. FEBS Lett. 466, 355–358.

Treves, S., Trentini, P.L., Ascanelli, M., Bucci, G., Di Virgilio, F., 1994. Apoptosis is dependent on intracellular zinc and independent of intracellular calcium in lymphocytes. Exp. Cell Res. 211, 339–343. https://doi.org/10.1006/excr.1994.1096

Truong-Tran, A.Q., Ho, L.H., Chai, F., Zalewski, P.D., 2000. Cellular Zinc Fluxes and the Regulation of Apoptosis/Gene-Directed Cell Death. J. Nutr. 130, 1459S-1466S. https://doi.org/10.1093/jn/130.5.1459S

Trybulec, M., Kowalska, M.A., McLane, M.A., Silver, L., Lu, W., Niewiarowski, S., 1993. Exposure of platelet fibrinogen receptors by zinc ions: role of protein kinase C. Proc. Soc. Exp. Biol. Med. Soc. Exp. Biol. Med. N. Y. N 203, 108–116.

Tubek, S., Grzanka, P., Tubek, I., 2008. Role of zinc in hemostasis: a review. Biol. Trace Elem. Res. 121, 1–8. https://doi.org/10.1007/s12011-007-8038-y

Vaduganathan, M., Bhatt, D.L., 2016. Simultaneous Platelet P2Y12 and P2Y1 ADP Receptor Blockade: Are Two Better Than One? Arterioscler. Thromb. Vasc. Biol. 36, 427–428. https://doi.org/10.1161/ATVBAHA.115.307097

Vallee, B.L., Falchuk, K.H., 1993. The biochemical basis of zinc physiology. Physiol. Rev. 73, 79–118.

van Kruchten, R., Mattheij, N.J.A., Saunders, C., Feijge, M.A.H., Swieringa, F., Wolfs, J.L.N., Collins, P.W., Heemskerk, J.W.M., Bevers, E.M., 2013. Both TMEM16F-dependent and TMEM16F-independent pathways contribute to phosphatidylserine exposure in platelet apoptosis and platelet activation. Blood 121, 1850–1857. https://doi.org/10.1182/blood-2012-09-454314

Varga-Szabo, D., Braun, A., Nieswandt, B., 2009. Calcium signaling in platelets. J. Thromb. Haemost. JTH 7, 1057–1066. https://doi.org/10.1111/j.1538-7836.2009.03455.x

Verma, A., Bhatt, A.N., Farooque, A., Khanna, S., Singh, S., Dwarakanath, B.S., 2011. Calcium ionophore A23187 reveals calcium related cellular stress as “I-Bodies”: an old actor in a new role. Cell Calcium 50, 510–522. https://doi.org/10.1016/j.ceca.2011.08.007

Vines, A., McBean, G.J., Blanco-Fernández, A., 2010. A flow-cytometric method for continuous measurement of intracellular Ca(2+) concentration. Cytom. Part J. Int. Soc. Anal. Cytol. 77, 1091–1097. https://doi.org/10.1002/cyto.a.20974

Vinholt, P.J., Nielsen, C., Söderström, A.C., Brandes, A., Nybo, M., 2017. Dabigatran reduces thrombin-induced platelet aggregation and activation in a dose-dependent manner. J. Thromb. Thrombolysis 44, 216–222. https://doi.org/10.1007/s11239-017-1512-2

Violi, F., Pastori, D., Carnevale, R., Pignatelli, P., 2015. Nutritional and therapeutic approaches to modulate NADPH oxidase-derived ROS signaling in platelets. Curr. Pharm. Des. 21, 5945–5950.

Violi, F., Pignatelli, P., 2014. Platelet NOX, a novel target for anti-thrombotic treatment. Thromb. Haemost. 111, 817–823. https://doi.org/10.1160/TH13-10-0818

Vostal, J.G., Jackson, W.L., Shulman, N.R., 1991. Cytosolic and stored calcium antagonistically control tyrosine phosphorylation of specific platelet proteins. J. Biol. Chem. 266, 16911–16916.

Vostal, J.G., Shafer, B., 1996. Thapsigargin-induced Calcium Influx in the Absence of Detectable Tyrosine Phosphorylation in Human Platelets. J. Biol. Chem. 271, 19524–19529. https://doi.org/10.1074/jbc.271.32.19524

Vu, T.T., Fredenburgh, J.C., Weitz, J.I., 2013. Zinc: an important cofactor in haemostasis and thrombosis. Thromb. Haemost. 109, 421–430. https://doi.org/10.1160/TH12-07-0465

Walders-Harbeck, B., Khaitlina, S.Y., Hinssen, H., Jockusch, B.M., Illenberger, S., 2002. The vasodilator-stimulated phosphoprotein promotes actin polymerisation through direct binding to monomeric actin. FEBS Lett. 529, 275–280.

Walsh, T.G., Berndt, M.C., Carrim, N., Cowman, J., Kenny, D., Metharom, P., 2014. The role of Nox1 and Nox2 in GPVI-dependent platelet activation and thrombus formation. Redox Biol. 2, 178–186. https://doi.org/10.1016/j.redox.2013.12.023

Walter, U., Eigenthaler, M., Geiger, J., Reinhard, M., 1993. Role of cyclic nucleotide-dependent protein kinases and their common substrate VASP in the regulation of human platelets. Adv. Exp. Med. Biol. 344, 237–249.

Wang, E., Taylor, R.W., Pfeiffer, D.R., 1998. Mechanism and specificity of lanthanide series cation transport by ionophores A23187, 4-BrA23187, and ionomycin. Biophys. J. 75, 1244–1254. https://doi.org/10.1016/S0006-3495(98)74044-5

Wang, G.R., Zhu, Y., Halushka, P.V., Lincoln, T.M., Mendelsohn, M.E., 1998. Mechanism of platelet inhibition by nitric oxide: in vivo phosphorylation of thromboxane receptor by cyclic GMP-dependent protein kinase. Proc. Natl. Acad. Sci. U. S. A. 95, 4888–4893.

Wang, J., Song, J., An, C., Dong, W., Zhang, J., Yin, C., Hale, J., Baines, A.J., Mohandas, N., An, X., 2014. A 130-kDa protein 4.1B regulates cell adhesion, spreading, and migration of mouse embryo fibroblasts by influencing actin cytoskeleton organization. J. Biol. Chem. 289, 5925–5937. https://doi.org/10.1074/jbc.M113.516617

Wang, Y., Fang, C., Gao, H., Bilodeau, M.L., Zhang, Z., Croce, K., Liu, S., Morooka, T., Sakuma, M., Nakajima, K., Yoneda, S., Shi, C., Zidar, D., Andre, P., Stephens, G., Silverstein, R.L., Hogg, N., Schmaier, A.H., Simon, D.I., 2014. Platelet-derived S100 family member myeloid-related protein-14 regulates thrombosis. J. Clin. Invest. 124, 2160–2171. https://doi.org/10.1172/JCI70966

Warren, J.T., Guo, Q., Tang, W.-J., 2007a. A 1.3-A structure of zinc-bound N-terminal domain of calmodulin elucidates potential early ion-binding step. J. Mol. Biol. 374, 517–527. https://doi.org/10.1016/j.jmb.2007.09.048

Warren, J.T., Guo, Q., Tang, W.-J., 2007b. A 1.3-A structure of zinc-bound N-terminal domain of calmodulin elucidates potential early ion-binding step. J. Mol. Biol. 374, 517–527. https://doi.org/10.1016/j.jmb.2007.09.048

Watanabe, Y., Ito, M., Kataoka, Y., Wada, H., Koyama, M., Feng, J., Shiku, H., Nishikawa, M., 2001. Protein kinase C-catalyzed phosphorylation of an inhibitory phosphoprotein of myosin phosphatase is involved in human platelet secretion. Blood 97, 3798–3805.

Watson, B.R., White, N.A., Taylor, K.A., Howes, J.-M., Malcor, J.-D.M., Bihan, D., Sage, S.O., Farndale, R.W., Pugh, N., 2016. Zinc is a transmembrane agonist that induces platelet activation in a tyrosine phosphorylation-dependent manner. Met. Integr. Biometal Sci. 8, 91–100. https://doi.org/10.1039/c5mt00064e

Watson, S.P., Auger, J.M., McCARTY, O.J.T., Pearce, A.C., 2005. GPVI and integrin αIIbβ3 signaling in platelets. J. Thromb. Haemost. 3, 1752–1762. https://doi.org/10.1111/j.1538-7836.2005.01429.x

Watt, J., Ewart, M.-A., Greig, F.H., Oldroyd, K.G., Wadsworth, R.M., Kennedy, S., 2012. The effect of reactive oxygen species on whole blood aggregation and the endothelial cell-platelet interaction in patients with coronary heart disease. Thromb. Res. 130, 210–215. https://doi.org/10.1016/j.thromres.2012.03.024

Wauters, A., Esmaeilzadeh, F., Bladt, S., Beukinga, I., Wijns, W., van de Borne, P., Pradier, O., Argacha, J.-F., 2015. Pro-thrombotic effect of exercise in a polluted environment: a P-selectin- and CD63-related platelet activation effect. Thromb. Haemost. 113, 118–124. https://doi.org/10.1160/TH14-03-0251

Weber, A.A., Braun, M., Hohlfeld, T., Schwippert, B., Tschöpe, D., Schrör, K., 2001. Recovery of platelet function after discontinuation of clopidogrel treatment in healthy volunteers. Br. J. Clin. Pharmacol. 52, 333–336.

Wee, J.L.K., Jackson, D.E., 2006. Phosphotyrosine signaling in platelets: lessons for vascular thrombosis. Curr. Drug Targets 7, 1265–1273.

Wencel-Drake, J.D., Painter, R.G., Zimmerman, T.S., Ginsberg, M.H., 1985. Ultrastructural localization of human platelet thrombospondin, fibrinogen, fibronectin, and von Willebrand factor in frozen thin section. Blood 65, 929–938.

Weng, Z., Li, D., Zhang, L., Chen, J., Ruan, C., Chen, G., Gartner, T.K., Liu, J., 2010. PTEN regulates collagen-induced platelet activation. Blood 116, 2579–2581. https://doi.org/10.1182/blood-2010-03-277236

Wentworth, J.K.T., Pula, G., Poole, A.W., 2006. Vasodilator-stimulated phosphoprotein (VASP) is phosphorylated on Ser157 by protein kinase C-dependent and -independent mechanisms in thrombin-stimulated human platelets. Biochem. J. 393, 555–564. https://doi.org/10.1042/BJ20050796

White, J.G., Rao, G.H., 1983. Influence of a microtubule stabilizing agent on platelet structural physiology. Am. J. Pathol. 112, 207–217.

White, J.G., Rao, G.H., 1982. Effects of a microtubule stabilizing agent on the response of platelets to vincristine. Blood 60, 474–483.

Wijesekara, N., Chimienti, F., Wheeler, M.B., 2009. Zinc, a regulator of islet function and glucose homeostasis. Diabetes Obes. Metab. 11 Suppl 4, 202–214. https://doi.org/10.1111/j.1463-1326.2009.01110.x

Wingelhofer, B., Kreis, K., Mairinger, S., Muchitsch, V., Stanek, J., Wanek, T., Langer, O., Kuntner, C., 2016. Preloading with L-BPA, L-tyrosine and L-DOPA enhances the uptake of [18F]FBPA in human and mouse tumour cell lines. Appl. Radiat. Isot. Data Instrum. Methods Use Agric. Ind. Med. 118, 67–72. https://doi.org/10.1016/j.apradiso.2016.08.026

Woodier, J., Rainbow, R.D., Stewart, A.J., Pitt, S.J., 2015. Intracellular Zinc Modulates Cardiac Ryanodine Receptor-mediated Calcium Release. J. Biol. Chem. 290, 17599–17610. https://doi.org/10.1074/jbc.M115.661280

Woulfe, D., Yang, J., Brass, L., 2001. ADP and platelets: the end of the beginning. J. Clin. Invest. 107, 1503–1505. https://doi.org/10.1172/JCI13361

Wu, R.F., Xu, Y.C., Ma, Z., Nwariaku, F.E., Sarosi, G.A., Terada, L.S., 2005. Subcellular targeting of oxidants during endothelial cell migration. J. Cell Biol. 171, 893–904. https://doi.org/10.1083/jcb.200507004

Wu, Y.P., Vink, T., Schiphorst, M., van Zanten, G.H., IJsseldijk, M.J., de Groot, P.G., Sixma, J.J., 2000. Platelet thrombus formation on collagen at high shear rates is mediated by von Willebrand factor-glycoprotein Ib interaction and inhibited by von Willebrand factor-glycoprotein IIb/IIIa interaction. Arterioscler. Thromb. Vasc. Biol. 20, 1661–1667.

Wurster, T., May, A.E., 2012. Atopaxar. A novel player in antiplatelet therapy? Hamostaseologie 32, 228–233. https://doi.org/10.5482/HAMO-12-05-0009

Xia, W., Li, Y., Wang, B., Chen, J., Wang, X., Sun, Q., Sun, F., Li, Z., Zhao, Z., 2015. Enhanced Store-Operated Calcium Entry in Platelets is Associated with Peripheral Artery Disease in Type 2 Diabetes. Cell. Physiol. Biochem. Int. J. Exp. Cell. Physiol. Biochem. Pharmacol. 37, 1945–1955. https://doi.org/10.1159/000438555

Xiong, X., Arizono, K., Garrett, S.H., Brady, F.O., 1992. Induction of zinc metallothionein by calcium ionophore in vivo and in vitro. FEBS Lett. 299, 192–196.

Xue, J., Moyer, A., Peng, B., Wu, J., Hannafon, B.N., Ding, W.-Q., 2014. Chloroquine is a zinc ionophore. PloS One 9, e109180. https://doi.org/10.1371/journal.pone.0109180

Yacoub, D., Théorêt, J.-F., Villeneuve, L., Abou-Saleh, H., Mourad, W., Allen, B.G., Merhi, Y., 2006. Essential Role of Protein Kinase Cδ in Platelet Signaling, $\alpha_{IIb}\beta_3$ Activation, and Thromboxane A_2 Release. J. Biol. Chem. 281, 30024–30035. https://doi.org/10.1074/jbc.M604504200

Yamasaki, S., Sakata-Sogawa, K., Hasegawa, A., Suzuki, T., Kabu, K., Sato, E., Kurosaki, T., Yamashita, S., Tokunaga, M., Nishida, K., Hirano, T., 2007. Zinc is a novel intracellular second messenger. J. Cell Biol. 177, 637–645. https://doi.org/10.1083/jcb.200702081

Yang, H., Kim, A., David, T., Palmer, D., Jin, T., Tien, J., Huang, F., Cheng, T., Coughlin, S.R., Jan, Y.N., Jan, L.Y., 2012. TMEM16F Forms a Ca2+-Activated Cation Channel Required for Lipid Scrambling in Platelets during Blood Coagulation. Cell 151, 111–122. https://doi.org/10.1016/j.cell.2012.07.036

Ye, X., Sun, M., 2017. AGR2 ameliorates tumor necrosis factor-α-induced epithelial barrier dysfunction via suppression of NF-κB p65-mediated MLCK/p-MLC pathway activation. Int. J. Mol. Med. 39, 1206–1214. https://doi.org/10.3892/ijmm.2017.2928

Yin, H.Z., Weiss, J.H., 1995. Zn(2+) permeates Ca(2+) permeable AMPA/kainate channels and triggers selective neural injury. Neuroreport 6, 2553–2556.

Yokoyama, M., Koh, J., Choi, D.W., 1986. Brief exposure to zinc is toxic to cortical neurons. Neurosci. Lett. 71, 351–355.

Yu, H., Zhou, Y., Lind, S.E., Ding, W.-Q., 2009. Clioquinol targets zinc to lysosomes in human cancer cells. Biochem. J. 417, 133–139. https://doi.org/10.1042/BJ20081421

Zhang, K., Chen, J., 2012. The regulation of integrin function by divalent cations. Cell Adhes. Migr. 6, 20–29. https://doi.org/10.4161/cam.18702

Zhang, X., Zhao, Y., Chu, Q., Wang, Z.-Y., Li, H., Chi, Z.-H., 2014. Zinc modulates high glucose-induced apoptosis by suppressing oxidative stress in renal tubular epithelial cells. Biol. Trace Elem. Res. 158, 259–267. https://doi.org/10.1007/s12011-014-9922-x

Zhao, J., 2007. Interplay Among Nitric Oxide and Reactive Oxygen Species. Plant Signal. Behav. 2, 544–547.

Zhao, J., Bertoglio, B.A., Gee, K.R., Kay, A.R., 2008. The zinc indicator FluoZin-3 is not perturbed significantly by physiological levels of calcium or magnesium. Cell Calcium 44, 422–426. https://doi.org/10.1016/j.ceca.2008.01.006

Zhao, L., Wu, X., Si, Y., Yao, Z., Dong, Z., Novakovic, V.A., Guo, L., Tong, D., Chen, H., Bi, Y., Kou, J., Shi, H., Tian, Y., Hu, S., Zhou, J., Shi, J., 2017. Increased blood cell phosphatidylserine exposure and circulating microparticles contribute to procoagulant activity after carotid artery stenting. J. Neurosurg. 127, 1041–1054. https://doi.org/10.3171/2016.8.JNS16996

Zhao, Y., Xiao, Z., Chen, W., Yang, J., Li, T., Fan, B., 2015. Disulfiram sensitizes pituitary adenoma cells to temozolomide by regulating O6-methylguanine-DNA methyltransferase expression. Mol. Med. Rep. 12, 2313–2322. https://doi.org/10.3892/mmr.2015.3664

Zhou, X.E., Melcher, K., Xu, H.E., 2017. Understanding the GPCR biased signaling through G protein and arrestin complex structures. Curr. Opin. Struct. Biol. 45, 150–159. https://doi.org/10.1016/j.sbi.2017.05.004

Zorov, D.B., Juhaszova, M., Sollott, S.J., 2014. Mitochondrial reactive oxygen species (ROS) and ROS-induced ROS release. Physiol. Rev. 94, 909–950. https://doi.org/10.1152/physrev.00026.2013

Zwaal, R.F.A., Comfurius, P., Bevers, E.M., 1992. Platelet procoagulant activity and microvesicle formation. Its putative role in hemostasis and thrombosis. Biochim. Biophys. Acta BBA - Mol. Basis Dis. 1180, 1–8. https://doi.org/10.1016/0925-4439(92)90019-J

.